

# Functional Perturbation of the Gab2 Multiprotein Complex by High-affinity SH2-binding Monobodies in Chronic Myelogenous Leukemia

THÈSE N° 6538 (2015)

PRÉSENTÉE LE 30 MARS 2015

À LA FACULTÉ DES SCIENCES DE LA VIE  
CHAIRE FONDATION ISREC EN ONCOLOGIE TRANSLATIONNELLE  
PROGRAMME DOCTORAL EN BIOTECHNOLOGIE ET GÉNIE BIOLOGIQUE

ÉCOLE POLYTECHNIQUE FÉDÉRALE DE LAUSANNE

POUR L'OBTENTION DU GRADE DE DOCTEUR ÈS SCIENCES

PAR

**Emel Başak GENCER AKÇOK**

acceptée sur proposition du jury:

Prof. M. Dal Peraro, président du jury  
Prof. O. Hantschel, directeur de thèse  
Prof. C. Heinis, rapporteur  
Prof. S. Koide, rapporteur  
Prof. M. Thome-Miazza, rapporteuse



ÉCOLE POLYTECHNIQUE  
FÉDÉRALE DE LAUSANNE

Suisse  
2015



## Acknowledgements

I am grateful for having many amazing people throughout my doctoral studies for their friendship, support and sharing these past years with me.

First of all I want to thank to Prof. Oliver Hantschel for giving me the opportunity to work on such an exciting project and for his support during my doctoral studies. He was a great supervisor and he always motivated me to pursue this project and always motivated me to be ambitious for this sometimes-challenging project. I am grateful for your support and patience.

I would like to also thank to my mentor Prof. John McKinney and the members of my thesis committee Prof. Matteo Dal Peraro, Prof. Christian Heinis, Prof. Margot Thome Miazza and Prof. Shohei Koide for their evaluation and constructive feedback.

Especially I would like to thank to our collaborators Shohei Koide and Fern Sha. Performing this doctoral study would be impossible without your amazing contribution and fruitful discussions. I am glad that I met amazing people like you through our collaboration.

Acknowledgements to EPFL Proteomics Core facility, especially Dr. Romain Hamelin, to all present and previous members of Flow Cytometry Core Facility and Protein expression core facility.

I also want to thank to all the present and previous members of our neighbor laboratories in our floor, Gönczy lab, Lingner lab and Simanis lab. It was a great opportunity to get to know you all and spend the time during my PhD.

When we started our lab, it was only me, Sandrine Georgeon and Ines Kaupe. I am grateful that I met Ines such a hardworking person even if it was for a short period of time. Sandrine, the angel of our laboratory, is an irreplaceable colleague, friend for me. She is always encouraging, never lets you down when you ask for some help, always smiling and always in a good mood and she is my go-to person whenever I needed something. Then our group grew with Orest, Allan, Sina, Barbara, Tim and Nadine. Orest Kuzyk has been a great collaborator and his never-ending energy was always making me cheer-up. His enthusiasm for science and a happy life was always admirable. Allan Lamontanara, having

the Italian and Portugal blood and being raised up in France, he was always making my day and was always there to cheer me up. He is all I could ask for an office mate and it has been always great to share ideas on research and on life. Sina Reckel is our first post-doc and it is a great experience to be her colleague. She is such a rational, determined and friendly person one can imagine. Barbara Gerig, Tim Kükenschöner and Nadine Schmidt have been also great collaborators. Also I would like to thank our master students Nicholas, Delphine and intern Linda. I am grateful for your friendship and it has been a pleasure to work with you.

I would like to thank to my Turkish friends in Lausanne. They were my family in here and whenever I was with them, even in the lunch breaks, I felt like home. I would like to thank to Berker, Kerem, Cem, Ece, Gizem, Can, Buğra, Meltem especially Nariye, Meriç, Emre... Your presence was invaluable and the times we spent together was hilarious.

Most importantly, I would like to thank to my family. My mother Esen, father Musa and my brother Mustafa... Your support, your love carried me to here. I will be forever indebted to my parents. And my parents in law Mehmet Akçok, Kamuran Akçok and Ümran Turpçulu, I am glad that we are a big family and whenever I was talking to you, I felt so relieved and you always encouraged me.

Finally, I would like to thank to my husband Ismail Akçok. His support, kindness, generosity was invaluable for me. His energy, good mood, his patience were the very important factors that kept me straight. He was always next to me, listening to me even if we were in different countries for the first three years of my PhD. No matter it takes, I always felt his hands and support on my shoulders. It would have been impossible without you.

*Lausanne – December 16, 2014*



## Abstract

Chronic myeloid leukemia is a myeloproliferative disorder that is characterized by a reciprocal chromosomal translocation between chromosome 9 and 22. This translocation results in the expression of the Bcr-Abl protein, which is a constitutively active tyrosine kinase. Despite the great improvement in patient survival using tyrosine kinase inhibitors (TKI), resistance caused by point mutations in the Abl kinase domain is a major drawback in TKI therapy. Bcr-Abl forms a multi-protein complex and Gab2 (Grb2-associated binder 2) is one of the few functionally critical scaffold proteins and substrates of Bcr-Abl. The interaction of Gab2 with Bcr-Abl coordinates the activation of the MAP and PI3-kinase pathways and thus Bcr-Abl transformation. The goal of this thesis was to understand the contributions of the different pathways activated downstream of Gab2. In order to pursue this aim, we aimed at targeting the Gab2 protein complex with high-affinity and highly specific engineered fibronectin type III monobodies, which are recombinant single domain binding proteins that may act as protein interaction inhibitors, binding to the SH2 domains of Gab2 interactors.

Firstly, the Gab2 complex was studied in an unbiased way by using interaction proteomics in order to confirm the pre-defined interactors of Gab2 and find out new interactors that could be possibly targetable by monobodies. To this end, Gab2 and the known interactors were affinity-tagged and expressed in CML cells, and interacting proteins were identified after tandem affinity purification by protein mass spectrometry. Many known interactors were confirmed and possible novel interactors were identified.

Next, the SH2 domains of the Gab2 interactors SHP2 and PLC $\gamma$ 1 were targeted by monobodies and binding clones were functionally characterized. Initially, monobodies targeting the SH2 domains of SHP2, which is an oncogenic tyrosine phosphatase, were studied. Tandem affinity purification of the monobodies demonstrated that they are monospecific for their cognate target protein and no other SH2 domain-containing proteins were identified by mass spectrometric analysis. Upon monobody expression in cell lines, we were able to show a significant decrease of phosphorylation of tyrosine residues of SHP2 that are critical for its catalytic activity. Monobodies targeting the N-SH2 domain

disrupted the interaction of SHP2 with its upstream activator, the Gab2 scaffold protein, suggesting the decoupling of SHP2 from the Bcr-Abl protein complex by disrupting the phosphotyrosine-SH2 mediated interaction. Moreover, SHP2 downstream signaling was altered upon monoclonal antibody expression. HCC-1171 non-small cell lung cancer cell line was investigated for ERK phosphorylation due to its high ERK phosphorylation and the presence of a SHP2 activating mutation. Strikingly, ERK phosphorylation was abolished in the HCC-1171 cells upon monoclonal antibody expression. The physiological effects of monoclonal antibodies were investigated in an inducible expression system in HCC-1171 cells. However, we could not detect significant changes in cell proliferation or ERK phosphorylation when compared to the non-binding control monoclonal antibody. Furthermore, tandem monoclonal antibodies targeting both SH2 domains of SHP2 simultaneously resulted in decreased ERK phosphorylation in Bcr-Abl overexpressing cells. PLC $\gamma$ 1 targeting monoclonal antibodies were also monospecific for their target protein in cells. In addition, PLC $\gamma$ 1 phosphorylation was decreased upon monoclonal antibody expression in cells.

Although monoclonal antibodies against p85 subunit of PI3K remains to be evaluated and better monoclonal antibodies are required for PLC $\gamma$ 1 targeting, our results validate monoclonal antibodies as potent and specific antagonists of protein-protein interactions in cells and they could be powerful tools to investigate the participation of different signaling pathways in malignant transformation.

**Keywords:** Chronic myeloid leukemia, Gab2, SHP2, Bcr-Abl, monoclonal antibody, tandem affinity purification, interaction proteomics, tyrosine phosphatase, tyrosine kinase

## Résumé

La leucémie myéloïde chronique (CML) est un trouble myélo-prolifératif qui est caractérisé par une translocation chromosomique réciproque entre les chromosomes 9 et 22. Cette translocation entraîne l'expression de la protéine Bcr-Abl, qui est une tyrosine kinase constitutivement active. En dépit de l'amélioration de la survie des patients traités au moyen d'inhibiteurs de tyrosine kinase (TKI), l'apparition de résistances dues à des mutations ponctuelles dans le domaine kinase de Abl est un inconvénient majeur pour les thérapies utilisant les TKI. Bcr-Abl forme un complexe multi-protéique et GAB2 (Grb2-associated binder 2) est l'une des protéines adaptatrices critiques de ce complexe, ainsi qu'un substrat de Bcr-Abl. L'interaction de GAB2 avec Bcr-Abl coordonne l'activation des voies de signalisation MAP et PI3-kinase et par conséquent la transformation cellulaire. L'objectif de cette thèse est de comprendre les contributions des différentes voies activées en aval de la protéine GAB2. Afin de poursuivre cet objectif, nous avons cherché à cibler le complexe protéique GAB2 en utilisant des molécules de hautes affinités appelées « monobodies » (basés sur la fibronectine de type III) se liant aux domaines SH2 (Src Homology domain 2) des protéines interagissant avec GAB2. Les monobodies sont des protéines recombinantes qui peuvent agir comme inhibiteur des interactions protéines/protéines.

Tout d'abord, le complexe GAB2 a été étudié en utilisant la protéomique afin de confirmer les interacteurs connus et d'en trouver de nouveaux pouvant être ciblés avec des monobodies. Dans ce but, les interacteurs connus de GAB2 ont été marqués (affinity tag) et exprimés dans des cellules dérivées de patients atteints de CML. Les protéines interagissant ont été identifiées par spectrométrie de masse après purification en utilisant la technique de « tandem affinity purification ». Un nombre important d'interacteurs préalablement observés ainsi que de possibles nouveaux interacteurs ont été identifiés.

Ensuite, les domaines SH2 de deux interacteurs de GAB2 : SHP2 et PLC $\gamma$ 1 ont été ciblés par des monobodies. Initialement, des monobodies ciblant les domaines SH2 de SHP2, qui est une tyrosine-phosphatase oncogénique, ont été étudiés. Nous avons d'abord vérifié que ces monobodies soient bien

monospécifiques pour leur protéine cible : aucune autres protéines contenant des domaines SH2 n'ont été identifiées comme interagissant avec les monobodies (spectrométrie de masse). Lors de l'expression de ces monobodies dans des lignées cellulaires, une diminution significative de la phosphorylation des résidus tyrosines de SHP2, qui sont essentiels pour son activité catalytique, a été observée. Les monobodies ciblant le domaine N-SH2 de SHP2 ont empêché son interaction avec la protéine adaptatrice GAB2, suggérant un « découplage » de SHP2 du complexe protéique de Bcr-Abl. De plus, la signalisation en aval de SHP2 a été altérée lors de l'expression des monobodies.

Nous avons aussi étudié la phosphorylation de ERK dans la lignée cellulaire de cancer du poumon non à petites cellules HCC-1171, pour laquelle la protéine SHP2 est mutée et activée. La phosphorylation de ERK a été supprimée dans la lignée cellulaire HCC1171 après expression des monobodies. Les effets physiologiques des monobodies ont été étudiés en utilisant un système d'expression inductible dans les cellules HCC1171. Cependant, nous n'avons pas détecté dans ce contexte des changements significatifs dans la prolifération cellulaire ou de la phosphorylation de ERK. Des monobodies ciblant la protéine PLC $\gamma$ 1 ont aussi été étudié, et étaient également monospécifique pour leur protéine cible dans des cellules. En outre, une diminution de la phosphorylation de PLC $\gamma$ 1 a été observée après l'expression de ces monobodies.

Malgré que des monobodies dirigés contre la sous unité p85 de PI3K doivent encore être évalués et que des monobodies plus actifs contre PLC $\gamma$ 1 développés, nos résultats valident les monobodies comme des antagonistes puissants et spécifiques des interactions protéines-protéines dans des cellules. Les monobodies sont aussi des outils puissants pour comprendre l'importance des différentes voies de signalisation impliquées dans la formation de cancer.

**Mots-clés:** leucémie myéloïde chronique, GAB2, SHP2, Bcr-Abl, monobodies, la purification par « tandem affinity », proteomique, tyrosine phosphatase, tyrosine

# TABLE OF CONTENTS

Acknowledgements .....	iii
Abstract .....	v
Resume .....	vii
List of figures .....	xiii
List of tables .....	xv
<b>Chapter 1 – Introduction .....</b>	<b>1</b>
1.1 Chronic myelogenous leukemia .....	1
1.2 c-Abl kinase regulation and signaling .....	4
1.3 Bcr-Abl fusion protein and Bcr-Abl mediated malignant transformation ...	5
1.4 Targeted therapies and resistance .....	12
1.4.1 Imatinib as the gold standard therapy for CML .....	13
1.4.2 Second and third generation tyrosine kinase inhibitors .....	15
1.5 Gab2 scaffold protein as a “hub” of Bcr-Abl signaling .....	17
1.6 SHP2 and PLC $\gamma$ 1 signaling .....	20
1.6.1 SHP2 function and its role in cancer .....	20
<i>the role of SH2 domains in regulating the function of SHP2</i> .....	23
1.6.2 PLC $\gamma$ 1 function and its role in cancer .....	24
<i>the role of SH2 domains in regulating the function of PLC<math>\gamma</math>1</i> .....	26
1.7 Monobodies .....	27
1.8 Aim of the work .....	33
<b>Chapter 2 – Results .....</b>	<b>35</b>
2.1 Mapping of Gab2 interactome in K562 cells .....	35
2.1.1 Strep-HA purification of Gab2 and its interactors .....	36
2.2 Expression and purification of SH2 domains of SHP2, PLCg1 .....	42
2.3 SHP2 targeting monobodies .....	42
2.3.1 Selection of monobodies to the N- and C-SH2 domains of SHP2 .....	42
2.3.2 SHP2 targeting monobodies bind selectively to SHP2 in cells .....	46

2.3.3 SHP2 targeting monoclonal antibodies inhibit SHP2 activity in Bcr-Abl dependent signaling pathway .....	51
2.3.4 SHP2 targeting monoclonal antibodies inhibit the interaction of SHP2 with Gab2 .....	53
2.3.5 SHP2 targeting monoclonal antibodies inhibit the downstream signaling of SHP2 .....	55
2.3.6 Inducible expression system of SHP2 targeting monoclonal antibodies in HCC-1171 non small cell lung cancer cell line .....	60
2.3.7 Tandem monoclonal antibodies targeting SHP2 in Bcr-Abl signaling .....	67
2.4 PLC $\gamma$ 1 targeting monoclonal antibodies .....	70
2.4.1 PLC $\gamma$ 1 targeting monoclonal antibodies binds selectively to PLC $\gamma$ 1 in cells ....	70
2.4.2 Monoclonal antibody mediated modulation of PLC $\gamma$ 1 signaling .....	72
<b>Chapter 3 – Discussion .....</b>	<b>81</b>
3.1 Mapping of Gab2 interactome in K562 cells .....	81
3.2 SHP2 targeting monoclonal antibodies .....	84
3.3 PLC $\gamma$ 1 targeting monoclonal antibodies .....	92
3.4 Final conclusions .....	94
<b>Chapter 4 - Materials and Methods .....</b>	<b>99</b>
4.1 Cloning .....	99
4.2 Cell Culture and transfections .....	99
4.3 Immunoblotting and Immunoprecipitation .....	100
4.3.1 Preparation of total cell lysate .....	100
4.3.2 Immunoblotting analysis and antibodies .....	100
4.3.3 Immunoprecipitation .....	102
4.4 Stable cell line generation with retroviral infection .....	102
4.5 Flow cytometry analysis and cell sorting .....	103
4.6 Strep-HA affinity purification .....	103
4.7 Tandem affinity purification .....	104
4.8 LC-MS/MS analysis of the protein complexes .....	106
4.9 Expression and purification of recombinant SH2 domains .....	106

4.10 siRNA mediated knock down .....	106
4.11 Cell growth by CellTiter-Glo Luminescent cell viability assay .....	107
4.12 Lentiviral vector production .....	108
<b>Appendix</b> .....	<b>109</b>
<b>References</b> .....	<b>125</b>
<b>CV</b> .....	<b>147</b>





## LIST OF FIGURES

1.1. Discovery of Philadelphia chromosome .....	1
1.2. Disease initiation and progression in chronic myelogenous leukemia .....	3
1.3. Domain structure of c-Abl and Bcr-Abl .....	6
1.4. Bcr-Abl mediated activation of signaling pathways.....	11
1.5. A cartoon representation of the imatinib bound form of Abl kinase domain .....	13
1.6. Comparison of first and second generation TKI .....	16
1.7. SHP2 phosphatase structure and regulation .....	24
1.8. PLC $\gamma$ 1 domain structure and mechanism of activation upon RTK recruitment and binding.....	27
1.9. Structure and binding modes of monobodies .....	30
1.10 Representative cartoon models of the Bcr pY177 affinity clamp .....	32
1.11. Gab2 mediated activation of SHP2, PI3K and PLC $\gamma$ 1 .....	34
2.1. Schematic cartoon model of Strep-HA purification of a N-terminally tagged bait protein .....	36
2.2. Bait proteins followed in Strep-HA purification steps by anti-HA immunoblotting .....	38
2.3. Interactome of Gab2 scaffold protein and its interactors.....	40
2.4. The Gab2 protein network .....	41
2.5. Characterization of sequences and binding of SHP2 SH2-binding monobodies .....	44
2.6. Crystal structures of SHP2 SH2/monobody complexes .....	45
2.7. Expression levels of Strep-HA tagged N-SH2 targeting monobodies and affinity purification of NSa1 monobody in K562 and HEK293 cells .....	47
2.8. SHP2-targeting monobodies bind endogenous full-length SHP2 in transiently transfected HEK293 cells and TAP cell lines.....	48
2.9. Analysis of the SHP2-targeting monobody interactome .....	50
2.10. Monobodies inhibit SHP2 phosphorylation in cells .....	53
2.11. Expression of monobodies decouples Gab2 and SHP2 .....	54

2.12. Modulation and downstream signaling perturbation of SHP2 in HEK293 cells .....	56
2.13. ERK phosphorylation in HEK293 cells co-expressing SHP2 and monoclonal antibody upon EGF stimulation .....	57
2.14. Expression profile of solid tumor cell lines and mutated residues of SHP2 in H661 and HCC-1171 cell lines .....	58
2.15. ERK and SHP2 phosphorylation in stable HCC-1171 cells upon monoclonal antibody expression .....	59
2.16. Cell proliferation assay of stable HCC-1171 monoclonal antibody cell lines .....	60
2.17. Mode of action of the DOX-controllable transrepressor .....	61
2.18. FACS analysis of the lentivirus titration .....	63
2.19. Doxycycline concentration and induction time optimization and doxycycline withdrawal assay .....	64
2.20. FACS analysis and immunoblot detection of the SHP2 SH2 targeting monoclonal antibodies and ERK phosphorylation in inducible cells .....	65
2.21. Cumulative cell number of SHP2 SH2 targeting monoclonal antibodies in inducible cells .....	67
2.22. Tandem monoclonal antibodies targeting SHP2 N- and C-SH2 domains .....	69
2.23. Analysis of the PLC $\gamma$ 1-targeting monoclonal antibody interactome .....	71
2.24. PLC $\gamma$ 1 targeting monoclonal antibodies co-expressed with Bcr-Abl and PLC $\gamma$ 1 in HEK293 cells .....	73
2.25. Cytokine stimulation of cells to induce PLC $\gamma$ 1 phosphorylation and transfection reagent optimization .....	74
2.26. Buffer optimization of the immunoprecipitation assay of PLC $\gamma$ 1 and PLC $\gamma$ 1 targeting monoclonal antibodies in NIH3T3 cells .....	76
2.27. Comparison of overexpressed and endogenous PLC $\gamma$ 1 protein phosphorylation in the absence or presence of PDGF-bb .....	77
2.28. PLC $\gamma$ 1 targeting monoclonal antibodies decrease the site specific phosphorylation in NIH3T3 cells .....	78
2.29. PLC $\gamma$ 1 targeting monoclonal antibodies interfere with the binding of PLC $\gamma$ 1 to PDGFR $\alpha$ .....	79
2.30. siRNA mediated knock down of PLC $\gamma$ 1 protein and downstream signaling modulated by monoclonal antibodies .....	80

## LIST OF TABLES

2.1 Overview of mass spectrometry results from SHP2 monobody interactome analysis .....	51
2.2 Overview of mass spectrometry results from PLC $\gamma$ 1 monobody interactome analysis .....	72
A1. Interactor protein list of mass spectrometry results from Gab2 interactome analysis from K562 cells .....	109
A2. Complete protein list of mass spectrometry results from Gab2 interactome analysis from K562 cells .....	111
A3. Complete protein list of mass spectrometry results from PLC $\gamma$ 1 monobody interactome analysis from K562 cells .....	119
A4. Complete protein list of mass spectrometry results from PLC $\gamma$ 1 monobody interactome analysis from HEK293 cells .....	120



# CHAPTER 1

## INTRODUCTION

### 1.1 Chronic myelogenous leukemia

John Hughes Bennett was the first pathologist that described a report as “Case of Hypertrophy of the Spleen and Liver in which Death Took Place from Suppuration of the Blood” in 1845 (Piller, 2001). This was the first definition of chronic myelogenous leukemia (CML) and then a long journey started on the identification and discovery of molecular mechanisms of transformation in CML.

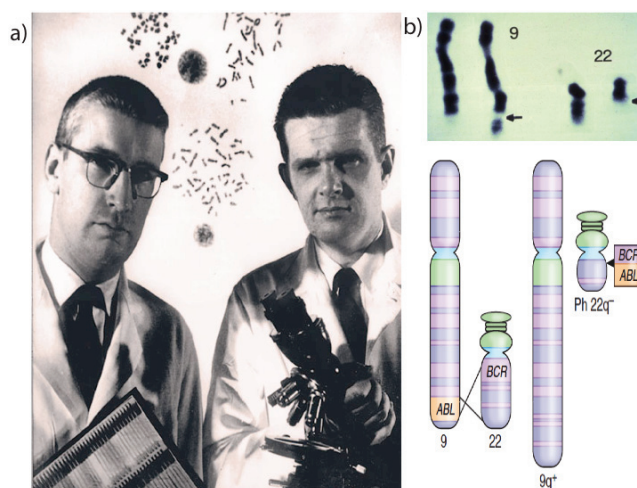


**Figure 1.1. Discovery of Philadelphia chromosome**

a) Peter Nowell (left) and David Hungerford (right) after the report of the discovery of Philadelphia chromosome.

b) Upper panel: The karyotype of a patient with CML. The translocation between chromosome 9 and 22 was imaged by Giemsa staining. Arrows show the breakpoint regions. Lower panel: A representative image of reciprocal translocation between chromosome 9 and 22, which contains ABL and BCR genes, respectively, on long arms. As a result of this translocation, the BCR-ABL oncogene is generated on chromosome 22, which is named as Philadelphia chromosome. Taken from (Lydon, 2009).

A long period of time after CMLs first description, cytogeneticists Peter Nowell and David Hungerford (Figure 1.1a) made a big discovery of the Philadelphia (Ph) chromosome and the critical importance of this translocation in the initiation of CML, which become as the hallmark of CML (Figure 1.1b) (Kurzrock, Gutterman, & Talpaz, 1988; Nowell & Hungerford, 1960). CML is a unique disease as it is the first malignancy that is described as a result of a

chromosomal abnormality. From the time of discovery of CML, many types of chemotherapeutic drugs were used to treat CML patients, like IFN $\alpha$ , hydroxyurea, busulphan treatments. However, these drugs caused insignificant rate of cytogenetic response and they did not have an effect on the rate of progression to blast crisis (Sawyers, 1999). In 1972, Janet Rowley had collected bone marrow samples from CML patients and studied the acute blastic phase. Then, in 1973, she has discovered that Ph chromosome arises from the translocation of chromosomes 9 and 22 (Rowley, 1973). After the discovery of the minute Ph chromosome by Nowell and Hungerford and Rowley's discovery upon the translocation, several papers were published and described the translocation of the c-ABL gene to the breakpoint cluster region gene through this reciprocal translocation (Groffen et al., 1984; Heisterkamp et al., 1983; Konopka, Watanabe, & Witte, 1984; Shtivelman, Lifshitz, Gale, & Canaani, 1985). As a result of this translocation, the Bcr-Abl oncogenic fusion protein is expressed (Figure 1.1b). c-Abl is a tyrosine kinase that has low activity but upon translocation, the resulted Bcr-Abl oncoprotein is a constitutively active tyrosine kinase and it is involved in many signaling pathways that in turn results in deregulated proliferation, growth factor independence, decreased cell differentiation and increased mitogenic signaling of myeloid cells (Cilloni & Saglio, 2012).

CML is a hematopoietic stem cell disorder that leads to the abnormal growth of myeloid cells and their accumulation in blood (Figure 1.2) (N. P. Shah, 2007). CML is composed of three stages; chronic phase, accelerated phase and blast crisis. Chronic phase is the early stage of CML and it is rarely diagnosed except by routine blood tests in which the peripheral blood shows leukocytosis. Immature white blood cells (blasts) are very low (5% or fewer) in the white blood cells. The clinical findings are enlarged spleen, fatigue, and weight loss. The second phase is accelerated phase in which the levels of immature white blood cells are higher than chronic phase (5-30%), and also an increase in spleen size, weight loss, poor appetite can be seen as symptoms. The most advanced phase is the blast crisis and many of the patients are diagnosed in this phase with some serious symptoms such as anemia, tiredness, fever, an increased spleen enlargement and recurring infections (Melo & Barnes, 2007).

CML serves as a model for other cancer types in several ways. It is defined as a multistep developed disease and genetically characterized by the reciprocal translocation. CML is considered a model disease also for targeted therapies to overcome the function of fusion oncogene product. Inhibition of Bcr-Abl is molecularly characterized with small molecule inhibitors. The first tyrosine kinase inhibitor that was developed for this purpose and it has very high specificity (Melo & Barnes, 2007). Targeted therapy strategies has gained further boost with the success of this specific small molecule inhibitor.

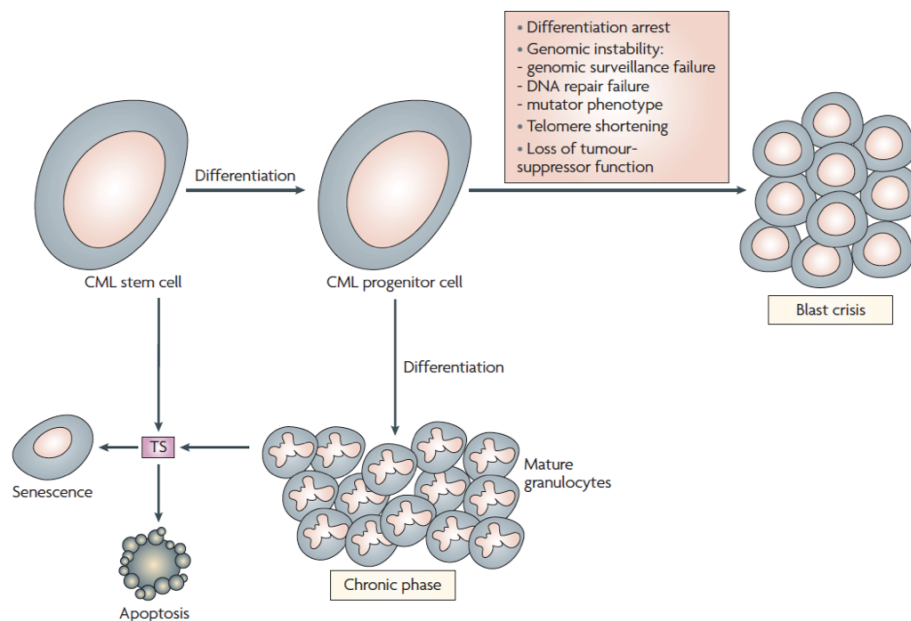


**Figure 1.2. Disease initiation and progression in chronic myelogenous leukemia**

a) CML is initiated with a Bcr-Abl positive hematopoietic stem cell. This stem cell can go under differentiation in order to give rise to progenitor cells for myeloid and lymphoid lineage, common myeloid progenitor (CMP) and common lymphoid progenitor (CLP), respectively. CML chronic phase (CP) can be defined as the differentiation of CMPs into granulocytes and accumulation of this mature granulocyte population. Tumor suppressor (TS) mechanisms can lead mature granulocytes either to apoptosis or senescence. CML blast crisis can be initiated as a result of a series of events like differentiation arrest, genomic instability, telomere shortening or loss of tumor suppressor functions. Blast crisis is the accumulation of genetically altered immature myeloid or lymphoid blast cells. Taken from (Melo & Barnes, 2007).

## 1.2 c-Abl kinase regulation and signaling

c-Abl is a member of Abl kinase family, it is expressed ubiquitously and the cellular activity of c-Abl is normally low. Nucleus, cytoplasm, mitochondria and the cell membrane are among the reported sites of this protein (Hantschel & Superti-Furga, 2004; Taagepera et al., 1998). In these compartments, c-Abl interacts with many proteins, thus has a wide range of cellular functions (Wong & Witte, 2004). Alternative splicing of the gene leads to two isoforms, c-Abl-1a and c-Abl-1b (Nagar et al., 2003). There is a 19-residue difference between the 1a and 1b (longer) isoform, which differ only at the N-terminal region. c-Abl 1b isoform contains a myristoylation site which is absent in 1a (Figure 1.3a) (Hantschel et al., 2003; Renshaw, Capozza, & Wang, 1988).

c-Abl consists of an N-terminal cap region, followed by an SH3 domain, an SH2 domain and finally a kinase domain (Hantschel & Superti-Furga, 2004). The C-terminal region of c-Abl is responsible for the interaction with other proteins and its subcellular localization. This region includes proline rich regions which provides binding sites for SH3 domain-containing proteins. Moreover, this region possesses nuclear localization signals, and an F-actin binding domain (Hantschel et al., 2005). The activity of the protein is tightly regulated by different aspects such as;

- 1) The presence and interaction of a unique N-terminal “cap” with the rest of the molecule (Hantschel et al., 2003; Pluk, Dorey, & Superti-Furga, 2002) and requirement of C-terminal part of the cap region for c-Abl autoinhibition as this region is thought to support the SH3-SH2 clamp inhibition of the kinase (Figure 1.3b) (Nagar et al., 2003).

- 2) The myristoylation of the glycine residue at position 2 at the N-terminus regulates docking of SH2 domain to the kinase domain and SH2 domain accessibility. (Figure 1.3b) (Hantschel et al., 2003).

- 3) The rigid SH2-SH3 connector is important for the autoinhibition, because this connector helps to stabilize the closed conformation in Src family kinases (Corbi-



Verge et al., 2013; Nagar et al., 2006; Young, Gonfloni, Superti-Furga, Roux, & Kuriyan, 2001).

4) Phosphorylation at Y245 (SH2-kinase linker region) and Y412 (activation loop) play a major role in the activation of abl kinase. c-Abl is normally not phosphorylated but upon phosphorylation of tyrosine residues such as Y412 and Y245 causes an increase in catalytic activity (Figure 1.5) (Brasher & Van Etten, 2000; Dorey et al., 2001; Van Etten, 1999).

5) SH2-kinase domain interface is important for the c-Abl regulation (Superti-Furga & Gonfloni, 1997) and for the maintenance of the autoinhibited state. Crystal structures showed that the SH2 domain is tightly bound to the C-terminal lobe of the kinase domain (Nagar et al., 2003). Upon activation of c-Abl, the SH2 domain locates to the tip of N-lobe of kinase domain and this conformation further activates the kinase. c-Abl could be activated by the binding of SH3 and SH2 domain ligands, which in turn causes a change in conformation and opening of the closed inhibitory clamp from the back of the kinase domain. Treatment of the kinase with phospholigands leads to an increase in activation of the kinase (Hantschel et al., 2003; Hantschel & Superti-Furga, 2004).

### **1.3 Bcr-Abl fusion protein and Bcr-Abl mediated malignant transformation**

*“Almost 50 years ago, David Hungerford and I noticed an abnormally small chromosome in cells from patients with chronic myelogenous leukemia (CML). This article is a personal perspective of the events leading to the discovery of this chromosome, which became known as the Philadelphia chromosome.”* (Quoted from a personal review from Peter C. Nowell (Nowell, 2007))

These results on the structure and regulation of c-Abl shed the light on the regulatory mechanisms of Bcr-Abl. Fusion with Bcr interrupts the autoinhibitory mechanism that keeps c-Abl in an inactive form. Therefore, tyrosine kinase activity of the Bcr-Abl protein is enhanced and results in the

initiation of CML (Pendergast, 2002; Smith & Mayer, 2002; Superti-Furga & Courtneidge, 1995). SH2 and SH3 domains are crucially involved in the leukomogenesis because of the interactions with other tyrosine-phosphorylated proteins and proline rich peptides, respectively (Hantschel, 2012).

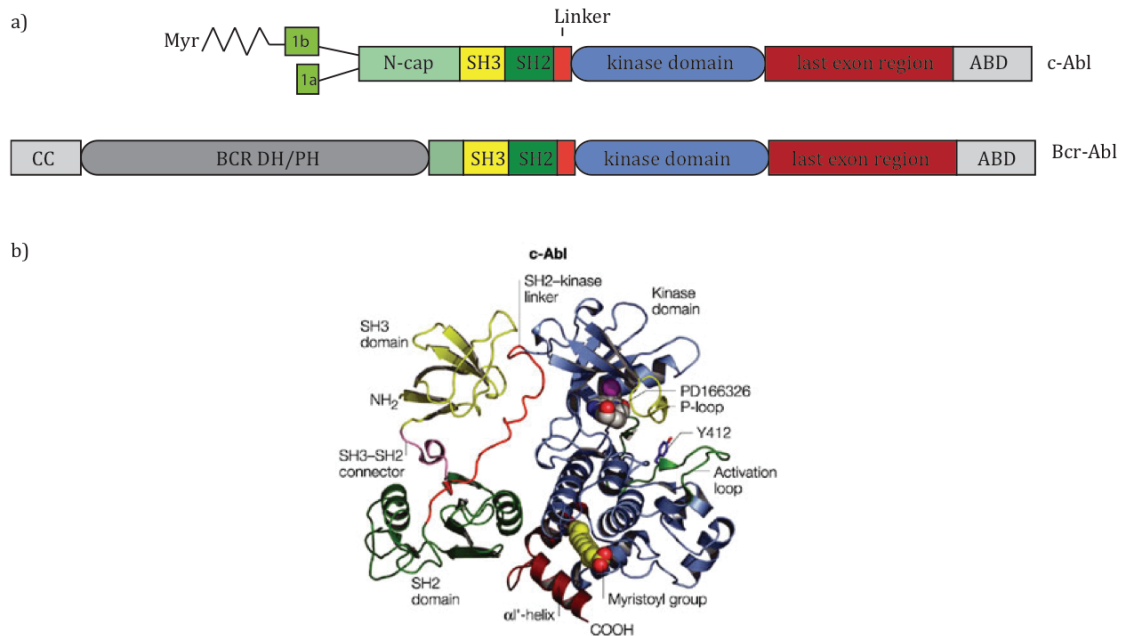


**Figure 1.3. Domain structure of c-Abl and Bcr-Abl**

a) c-Abl has 2 isoforms as 1a and 1b. 1b isoform is myristoylated while 1a does not have such a feature. Upon translocation, c-Abl loses the cap region and thus the myristoylation part. Since these two important autoinhibitory mechanisms are lost, Bcr-Abl becomes constitutively active. Domain structure of Bcr-Abl from N- to C-terminus; light gray: coiled-coil oligomerization domain, dark gray: Dbl and pleckstrin homology domains (DH/PH), green: Cap region, yellow: SH3 domain, dark green: SH2 domain, orange: SH2-kinase linker, blue: kinase domain, dark red: last exon region, light gray: C-terminal actin-binding domain (ABD).

b) The X-ray crystal structure of c-Abl-1b as ribbon which shows the compact packing of the kinase. N-cap, SH3, SH2 and the linker region are closed at the backside of the kinase domain. Taken from (Hantschel & Superti-Furga, 2004)

Also the Bcr part that is fused to c-Abl has important residues and domains that are crucial for transforming activity (Figure 1.3b) (Hantschel & Superti-Furga, 2004). For instance, the presence of the N-terminal coiled coil region is important for the oligomerization events which again disrupts the autoinhibited state of the protein. Thereby, this region contributes to the initiation of the autophosphorylation events of critical tyrosine residues in the activation loop or in the SH2-kinase linker region (McWhirter, Galasso, & Wang, 1993; Zhao, Ghaffari, Lodish, Malashkevich, & Kim, 2002). Moreover, the DH-PH

domain that lies within the Bcr protein is necessary for Bcr-Abl activity, because this domain might be important for Rho GTPase activation (Harnois et al., 2003; Sahay et al., 2008)

The BCR-ABL oncogene is present in three different isoforms as p185, p210 and p230 which depends on the length of BCR gene that is fused to c-ABL. They show different phenotypic properties, which were shown with the infection of primary mouse bone marrow cells. p185 Bcr-Abl isoform drives the expansion of lymphoid progenitors while p210 and p230 leads for the expansion of myeloid cells (Quackenbush et al., 2000). This demonstrates the fact that the different length isoforms are associated with different types of malignancies as, p185 is associated with 20–30% of B-cell acute lymphocytic leukemia (B-ALL), p210 with CML and 40% of Ph+ B-ALL, and the rare p230 isoform with a subset of patients with chronic neutrophilic leukemia (CNL) (Advani & Pendergast, 2002).

The mechanisms that are responsible for the Bcr-Abl mediated malignant transformation can be grouped as follows:

1) Genomic instability;

Transition from chronic phase to blast crisis is associated with increased genomic instability. In CML, Bcr-Abl affects genes that are responsible for genome stability, and as a result of some abnormalities transition to blast crisis occurs (Muvarak, Nagaria, & Rassool, 2012; Skorski, 2002). Some of these abnormalities can be listed as chromosome 8 trisomy, isochromosome I (17q), trisomy 19, trisomy 21 and monosomy 7 (Johansson, Fioretos, & Mitelman, 2002). Recently, Bolton-Gillespie showed that genomic instability may arise from CML stem cells that are irresponsive to imatinib (Bolton-Gillespie et al., 2013). Burke and Carroll reviewed the possible mechanisms in which it is proposed that Bcr-Abl leads to DNA damage and then the apoptotic pathways were inhibited which in turn cause the proliferation of cells without damage repair. This could be a result of Bcr-Abl being involved to the low-fidelity DNA repair mechanisms (Burke & Carroll, 2010). But yet, how does Bcr-Abl alter genomic instability is an incompletely answered question.

## 2) Constitutive activation of Abl tyrosine kinase;

The fusion of BCR sequences to the N-terminal region of c-Abl results in deletion and loss of the c-Abl cap region which contains the myristoylation site. Consequently, Bcr-Abl is able to shut down the autoinhibitory mechanism that is present in c-Abl. This event causes a dramatic increase in kinase activity, autophosphorylation, total tyrosine phosphorylation, and thus stimulation of many signalling events (Hantschel & Superti-Furga, 2004).

## 3) Activation of mitogenic signals;

Many pathways have been described to be activated by Bcr-Abl, such as mitogen-activated protein kinase (MAPK), Janus-activated kinase (JAK)/STAT, phosphoinositide 3-kinase (PI3K)/AKT pathway (reviewed in (Cilloni & Saglio, 2012; M. W. Deininger, Goldman, & Melo, 2000; Steelman et al., 2004). Furthermore, interacting with adaptor proteins through phosphotyrosine residues, Bcr-Abl can be involved in large multi-protein complexes (Pendergast et al., 1993; Puil et al., 1994; Uemura et al., 1997). For instance, a critical tyrosine residue (Y177) is described to be responsible for activation of MAPK pathway. Puil and colleagues found the evidence showing that Bcr-Abl forms a complex with Grb2 and Sos1, also with Grb2-Shc in order to stimulate Ras activity (Puil et al., 1994). Also, in this study, it was first suggested that Y177 is a possible autophosphorylation site where Grb2 first binds and then mediate the complex formation. The Grb2 binding site was shown to be necessary to induce a CML-like disease in mice by Bcr-Abl (Million & Van Etten, 2000; Pendergast et al., 1993). Afterwards, Sattler et al. also showed that Y177 residue is critical for Bcr-Abl mediated transformation. Moreover, they demonstrated that the Grb2 adaptor protein binds to phosphorylated Y177 residue and recruits Sos-1 and Gab2. Then Gab2 scaffold protein binds PI3K via its p85 regulatory subunit, PLC $\gamma$ 1 and SHP2 by SH2 mediated interactions (Sattler et al., 2002). PI3K recruitment to Bcr-Abl via its SH2 domain was shown in severe combined immunodeficiency (SCID) mice. By using PI3K specific inhibitors or an AKT dominant negative mutant, Skorski et al. showed that the PI3K/AKT pathway is necessary for Bcr-Abl induced leukemogenesis (Skorski et al., 1997). Moreover,

Kharas et al. demonstrated that PI3K targeting strongly blocked the transformation and leukemogenesis in mouse model of Ph<sup>+</sup> pre-B-ALL. In addition to this, inhibition of mTOR might be an attractive way of targeting mouse pre-B-ALL cells and Ph<sup>+</sup> CD19<sup>+</sup>CD34<sup>+</sup> cells (Kharas et al., 2008). Furthermore, Bcr-Abl affects autophagy regulation in cells through a PI3K/AKT/FOXO4 mediated signaling by upregulating ATF5, which is a negative regulator of autophagy (Sheng, Ma, Sun, Zhu, & Green, 2011). On the other hand, Crk and CrkL proteins interact with Bcr-Abl via PI3K and this interaction leads to increased proliferation (Hemmerlyckx et al., 2001; Sattler et al., 1996). CrkL binds to Bcr-Abl with its SH3 domain and afterwards phosphorylation of CrkL provides a binding site for c-Cbl via its SH2 domain. Then, PI3K can interact with phosphorylated c-Cbl and then the pathway could be activated (Sattler et al., 1996). Bcr-Abl also activates the JAK/STAT pathway (Cilloni & Saglio, 2012; Kisseleva, Bhattacharya, Braunstein, & Schindler, 2002; Shuai, Halpern, ten Hoeve, Rao, & Sawyers, 1996). Under normal conditions, STAT transcription factors require the cytokine-stimulated dimerization of JAK receptor kinases in order to get phosphorylated (Kisseleva et al., 2002). Shuai et al. first demonstrated a 91 kDa signal transducer and activator of transcription factor (STAT) present in the cytoplasm that is inactive and monomeric in unstimulated cells. But upon interferon alpha stimulation, STAT proteins form homodimers via SH2-phosphotyrosine mediated interactions and translocate into the nucleus (Shuai et al., 1994). Afterwards, studies demonstrated the activation of STAT proteins by Bcr-Abl in hematopoietic cells. Carlesso et al. showed that STAT1 and STAT5 is directly phosphorylated by Bcr-Abl and interestingly, JAK proteins are not consistently activated by Bcr-Abl, which suggests that activation of STATs maybe bypassing JAK kinase activity (Carlesso, Frank, & Griffin, 1996). In line with this study, it was also shown that both p185 and p210 Bcr-Abl is mediating the tyrosine phosphorylation and DNA binding function of STATs (Ilaria & Van Etten, 1996). Later on, STAT5/5A were shown to play an important role in CML-like disease in mice (A. Hoelbl et al., 2006; Ye, Wolff, Li, Zhang, & Ilaria, 2006). Warsch et al. showed that high STAT5 expression is in parallel with imatinib resistance in CML (Warsch et al., 2011), and moreover STAT5 is a key factor for the induction and maintenance of leukemia (Andrea Hoelbl et al., 2010).

Recently, Hantschel and his colleagues showed the indispensability of STAT5 and direct regulation by Bcr-Abl, rather than JAK2 activity (Hantschel, Warsch, et al., 2012). An additional protein important to Bcr-Abl mediated transformation is c-myc which has a vital importance to promote cell cycle progression, differentiation, cell death and angiogenesis (Cole & McMahon, 1999). Elevated and deregulated expression pattern of c-myc is observed in various types of cancer and sometimes c-myc can be a diagnostic marker for some cancer types (Pelengaris, Khan, & Evan, 2002). Sawyers et al showed that c-myc activity is required for Bcr-Abl transformation but the exact mechanism is not known (Sawyers, Callahan, & Witte, 1992). Fang et al. revealed that Bcr-Abl mediated survival is regulated at the transcriptional level via JAK2/PI3K signaling pathway that is activated by the c-myc transcription factor. In this study, shRNA mediated silencing of c-myc completely eliminated the colony formation of K562 cells on semi-solid culture system (Fang et al., 2009). Xie et al. also showed evidence on Bcr-Abl induced JAK2 mediated increase in c-myc expression (Xie, Lin, Sun, & Arlinghaus, 2002). In Bcr-Abl positive cells, Bcr-Abl and MAPK dependent phosphorylation and activation of HNRPK (heterogeneous nuclear ribonucleoprotein K) regulates myc mRNA translation (Notari et al., 2006).

Bcr-Abl affects many signalling pathways and it interacts with several binding proteins and substrates that were also identified (Figure 1.4). By having this much interactions with signalling proteins, Bcr-Abl leads to increased proliferation, decreased apoptosis and it gives rise to DNA defective cell population expansion and massive increase in myeloid cell population. Bcr-Abl also reduces the growth factor dependency of these cells. Targeting protein-protein interactions in Bcr-Abl mediated signalling could be an alternative way to inhibit the kinase signalling.

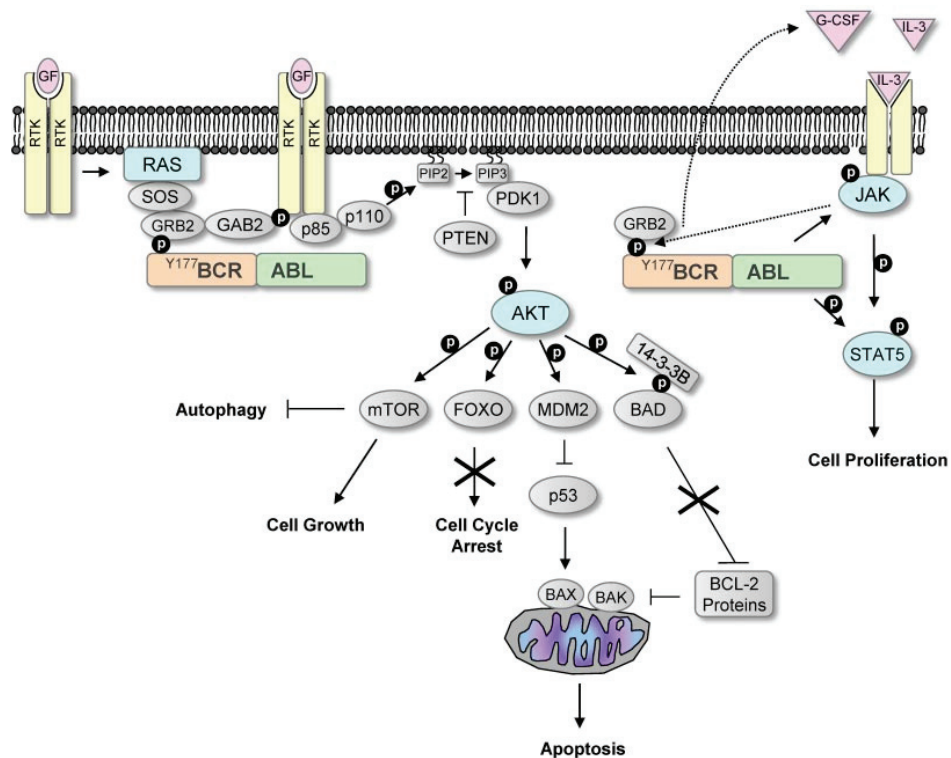


**Figure 1.4. Bcr-Abl mediated activation of signaling pathways**

Once bound to receptor tyrosine kinases, growth factor activate the receptors and leads to the activation of signaling pathways like RAS, PI3K/AKT, JAK pathways. Bcr-Abl expression mimics the growth factor activation. Phosphorylation of the tyrosine 177 residue is critical and this phosphosite interacts with Grb2 and Grb2 activates RAS via Son of Sevenless (SOS) protein. Also, Grb2 recruitment activates PI3K pathway through Gab2 adaptor protein and then binding of p85 regulatory subunit of PI3K provides the formation of phosphatidylinositol trisphosphate (PIP3) from phosphatidylinositol bisphosphate (PIP2). PIP3 provides the recruitment of the 3-phosphoinositide-dependent protein kinase-1 (PDK1) and then the serine/threonine kinases AKT which results in phosphorylation and activation of AKT. Activated AKT phosphorylates many proteins that effect proliferation and survival of the cell. JAK/STAT pathway is also a pathway that is activated by growth factors and frequently activated in myeloproliferative diseases. This pathway is activated in Bcr-Abl expressing cells and it has been also shown that Bcr-Abl bypass JAK2 activation and directly activates STAT5, which leads to proliferation. Taken from (Helgason, Karvela, & Holyoake, 2011)

#### 4) Inhibition of apoptosis;

Bcr-Abl shows anti-apoptotic effects (Amarante-Mendes et al., 1998; A. McGahon et al., 1994; McGahon, Cotter, & Green, 1994). Jaiswal et al demonstrated that myeloproliferative development could emerge from hematopoietic stem cells without Bcr-Abl expression and the additional mutations that inhibit apoptosis could be critical for transition to blast crisis. This is in agreement with enhanced expression levels of Bcl-2, which leads to the induction of blast crisis in their study. They hypothesize that the cooperative action between increased Bcl-2 expression and increased Bcr-Abl expression may be the key event of



transformation into blast crisis (Jaiswal et al., 2003). In another study, the Bcr-Abl oncogene inhibits apoptosis by inducing the expression levels of Bcl-2. Moreover, the Bcr-Abl expressing cells turn back to a state in which they show non-tumorigenicity when Bcl-2 expression is suppressed. These results help explaining the ability of Bcr-Abl oncogene to synergize with c-myc in cell transformation (Sanchez-Garcia & Grutz, 1995). Expression of anti-apoptotic Bcl-xL is induced by Bcr-Abl in a STAT5 dependent manner, which includes the binding of STAT5 to the Bcl-xL promoter region (Horita et al., 2000). Deming et al. demonstrated the inhibition of caspase activation after cytochrome c release that is mediated by Bcr-Abl (Deming et al., 2004). Bcr-Abl has the known above described roles in inhibition of apoptosis. It might be that Bcr-Abl causes the DNA-damaged cells to survive and increase the pool of cells with mis-repaired DNA. In this way, Bcr-Abl affects the apoptosis of cells.

## **1.4 Targeted therapies and resistance**

The development of targeted therapies for CML has been very important and vital step in molecular medicine (Melo & Barnes, 2007). CML is an extensively studied hematologic malignancy and its activation mechanisms are studied broadly, as already mentioned in section 1.1.

There is a highly conserved Asp-Phe-Gly (DFG) motif at the beginning of activation loop of Bcr-Abl which is essential for the orientation of ATP binding and thus kinase activity. Most of the kinase inhibitors are designed as ATP competitors and they are classified as type 1 and type 2 inhibitors. The type 1 inhibitors are bound around to the site that is occupied by adenine ring of ATP through mostly hydrophobic interactions but also hydrogen bonds. On the other hand, type 2 inhibitors which in addition bind to the hydrophobic site next to ATP binding pocket only available when the DGF motif is in a DFG-out conformation (Y. Liu & Gray, 2006).

In late 90s, imatinib was discovered from the screen of the selective protein kinase inhibitors from 2-phenylaminopyrimidine class with the help of discovery of Bcr-Abl fusion oncoprotein (Buchdunger et al., 1996). In 2001, FDA approved the drug imatinib (Gleevec) and Schindler et al. solved the kinase



domain of c-Abl in complex with imatinib, showing the binding of imatinib to the ATP-binding site of c-Abl only when the activation loop is in a closed conformation, and thus keeping the kinase in an inactive form (Schindler et al., 2000).

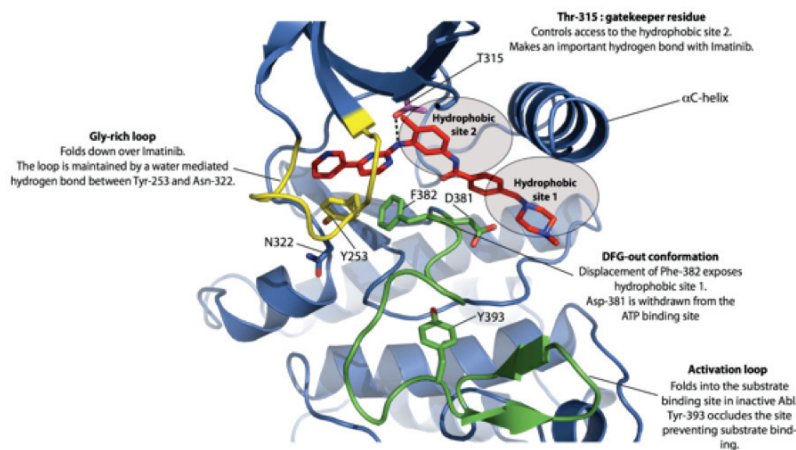


**Figure 1.5. A cartoon representation of the imatinib bound form of Abl kinase domain**  
 Imatinib (red sticks) binds to inactive conformation of Abl kinase and occupies substrate binding site, hindered by activation loop. The DFG motif is kept in “out” conformation, faces to hydrophobic site 1. The T315I gatekeeper residue keeps the control of access to active site. Taken from (Lamontanara, Gencer, Kuzyk, & Hantschel, 2013).

### 1.4.1 Imatinib as the gold standard therapy for CML

Imatinib (Gleevec, Novartis, Basel, Switzerland) was initially discovered as PDGFR, c-kit and abl inhibitor. This drug is the first tyrosine kinase inhibitor developed and approved for CML. Imatinib acts as an ATP-competitive inhibitor against Bcr-Abl fusion protein (Druker, Sawyers, et al., 2001; Druker, Talpaz, et al., 2001; Druker et al., 1996). This binding prevents the phosphorylation of substrate molecule and inhibits downstream signaling of Bcr-Abl (Capdeville, Buchdunger, Zimmermann, & Matter, 2002). Imatinib is able to bind to the inactive conformation of Bcr-Abl and keeps the activation loop in a closed conformation (Figure 1.3) (Nagar et al., 2002). Although imatinib achieved a remarkable success in clinical trials, cases of relapse via reactivation of Bcr-Abl kinase were reported after an initial response to imatinib in blast crisis (Branford et al., 2002; Gorre et al., 2001; Roche-Lestienne et al., 2002). One third of these patients had amplification of Bcr-Abl while half of them had a point

mutation in the c-Abl kinase domain that prevent inhibitor binding (von Bubnoff, Schneller, Peschel, & Duyster, 2002).

Resistance against imatinib occurs during treatment and most often encountered in accelerated phase and blast crisis (Gambacorti-Passerini, Piazza, & D'Incalci, 2003; N. Shah et al., 2002). There are two kinds of resistance mechanisms that could be developed against imatinib. The first one is intrinsic resistance, which is also termed as primary resistance while the other one is acquired resistance that is caused by point mutations (Bixby & Talpaz, 2010). The major acquired resistance mechanisms are mutations that occur in the kinase domain which cause a conformational change in the Bcr-Abl oncoprotein, which in turn prevents imatinib binding (T. O'Hare, Eide, & Deininger, 2007).

While increased expression of Bcr-Abl kinase through gene amplification is known as one of the Bcr-Abl dependent resistance mechanisms, point mutations are the most common mechanism of resistance. Among the point mutations that occur in the kinase domain, the T315I mutation is one of the most common and most efficient mechanisms of resistance (Lamontanara et al., 2013; Weisberg, Manley, Cowan-Jacob, Hochhaus, & Griffin, 2007). It was identified in imatinib-resistant patients and was called as “gatekeeper” mutation (Gorre et al., 2001). This mutation is suggested to lead resistance in two simultaneous means (Lamontanara et al., 2013). The first one is due to the absence of hydroxyl group in isoleucine. The switch to isoleucine prevents the formation of hydrogen bond between imatinib and the kinase domain. Secondly, isoleucine has a bulkier side chain than threonine which limits the binding of imatinib sterically (M. Deininger, Buchdunger, & Druker, 2005).

In addition to the point mutations, there are other resistance mechanisms against imatinib which could be described as Bcr-Abl independent mechanisms. Decreased intracellular imatinib concentrations caused by the expression changes in drug influx/efflux transporters (Mahon et al., 2000), imatinib binding by plasma proteins and overexpression of other kinases such as Src family kinases, like Lyn kinase (Donato et al., 2003; Wu et al., 2008) could be considered as Bcr-Abl independent mechanisms. On the other hand, imatinib fails to target CML stem cells. Since imatinib cannot target the quiescent stem cells, the insensitivity can cause relapse in the presence of mutations or after imatinib

therapy being stopped (Corbin et al., 2010; Hamilton et al., 2012; Kavalierchik, Goff, & Jamieson, 2008).

### **1.4.2 Second and third generation tyrosine kinase inhibitors**

As a result of common resistance cases against imatinib, second generation tyrosine kinase inhibitors were developed (Figure 1.6a,b) (Ramirez & DiPersio, 2008).

Nilotinib (AMN107, Tasisa, Novartis) is a highly selective and a potent inhibitor against Bcr-Abl (Weisberg et al., 2005). It is effective against a wide range of imatinib resistant mutants of Bcr-Abl, although the T315I gatekeeper mutant can not be inhibited with nilotinib (Saglio et al., 2010). Unfortunately, this molecule causes several side effects for newly diagnosed CML like rash, nausea, headaches, fatigue when compared to imatinib, (Saglio et al., 2010). Nilotinib is designed for a better fit into Bcr-Abl, and similar to imatinib, this inhibitor binds only to the inactive form of Bcr-Abl (Figure 1.6) (Weisberg et al., 2006) and reported to be 30 times more potent than imatinib (Rogers et al., 2012). Nilotinib is highly specific and mainly targets the same kinases as imatinib; named as ABL1/2, the receptor tyrosine kinases KIT, PDGFRA/B, DDR1/2 and the small oxidoreductase NQO2 (Rix et al., 2007)

Dasatinib (BMS354825, Sprycel, Bristol-Myers Squibb) is a dual Bcr-Abl/Src kinase inhibitor. It inhibits the majority of the imatinib-resistant mutations except the gatekeeper T315I mutation (N. P. Shah et al., 2004). Although its potency is 325 times higher than imatinib against the resistant mutants, dasatinib has a much broader target spectrum than imatinib and nilotinib (Hantschel, Rix, & Superti-Furga, 2008; Rix et al., 2007). It potently inhibits all Src kinases, most Tec kinases, almost the entire EphA/B family, several other tyrosine kinases, but also serine-threonine kinases in addition to the kinases inhibited by imatinib and nilotinib (Hantschel, Grebien, & Superti-Furga, 2012; Hantschel et al., 2008). Strikingly, crystal structure of dasatinib and Abl kinase domain demonstrated that, it binds to the active conformation of Bcr-Abl. The drug does not occupy the hydrophobic site 2 (Figure 1.5) and therefore does not need a DFG-out conformation to bind (Tokarski et al., 2006). Dasatinib

requires a less stringent conformational requirement which contributes to its high efficacy (Figure 1.5a,b) (Olivieri & Manzione, 2007).

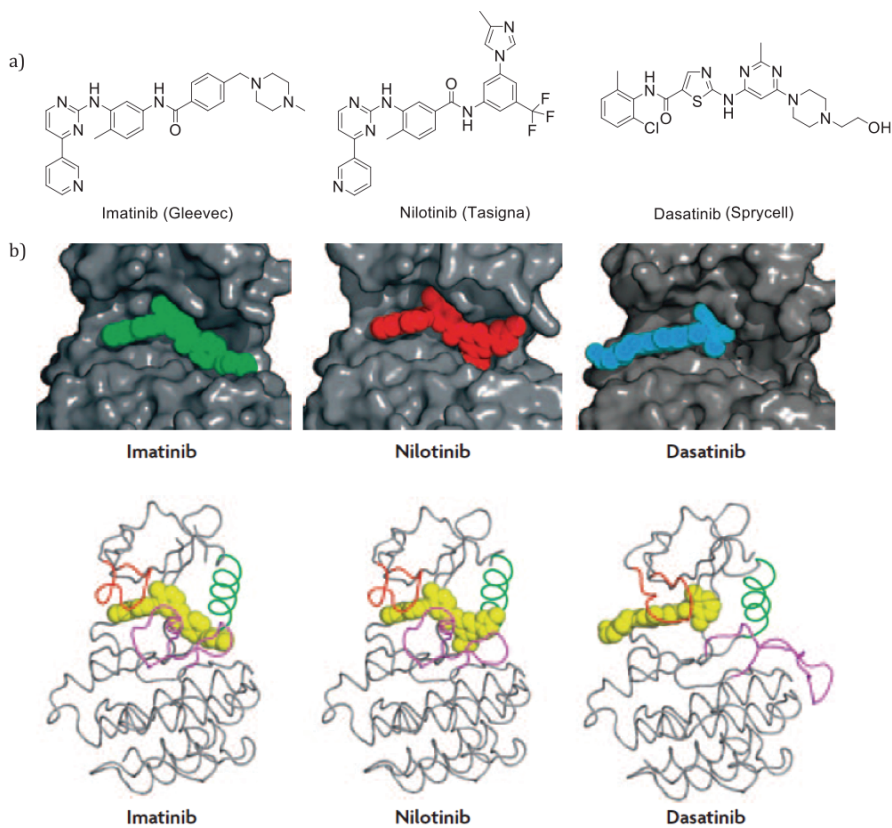


**Figure 1.6. Comparison of first and second generation TKI**

a) Chemical structures of imatinib, nilotinib and dasatinib

b) Binding properties of the tyrosine kinase inhibitor in Abl kinase domain. Upper panel: Crystal structure of the complex structure of inhibitors with Abl kinase. Lower panel: Binding modes of the inhibitors and the positioning of Glycine-rich loop (ATP-binding loop) in red, A-loop (activation loop, which is phosphorylated and leads to the full kinase activation) in magenta. In active form, the Glycine-rich loop has an extended conformation and the A-loop has DFG-in conformation, however in inactive conformation Glycine-rich loop closes over the inhibitor and DFG-out conformation is observed in A-loop. Imatinib and nilotinib keeps the kinase in an inactive conformation, while dasatinib binds it in an active conformation (Weisberg et al., 2007).

Bosutinib (SKI606, Pfizer) is another second-generation kinase inhibitor, which is approved for all stages of imatinib resistance/intolerance CML (Cortes et al., 2011). It has very similar properties like dasatinib in terms of inhibition type, potency and spectrum of kinase domain mutations being inhibited. This inhibitor is also insensitive for T315I mutation (Puttini et al., 2006). Since the T315I mutant is undruggable by the above-mentioned compounds and plays a major role in the development of resistance, third generation inhibitors were needed to be developed for this mutant.

Ponatinib (AP24534, ARIAD) is a type 2 third generation inhibitor inhibits not only imatinib-resistant mutants but also the gatekeeper T315I mutant. Its chemical structure allows for binding to the active site and also prevents the steric clash with the bulky isoleucine residue (Thomas O'Hare et al., 2009). Ponatinib has medium specificity for targeting SRC kinases but also receptor tyrosine kinases, such as KIT, RET, PDGFR, VEGFR, DDR1/2, EPH, TRK, and FGFR family members (Cortes et al., 2012; Hantschel, Grebien, et al., 2012). Its efficacy in patients carrying the T315I mutation led to FDA-approval in December 2012 (Frankfurt & Licht, 2013), although the tolerability of ponatinib may not be optimal because of a number of cardiovascular toxicity, like heart attacks, stroke or blood clots in legs or lungs.

Rebastinib (DCC2036, Deciphera) is also active against the T315I mutant. Upon binding, it induces and stabilizes the inactive conformation. In addition to Bcr-Abl, rebastinib also inhibits the SRC family kinases SRC, LYN, FGR, and HCK, and the receptors KDR, FLT3, and TIE2. It showed promising results in phase I clinical trials (W. W. Chan et al., 2011; Lamontanara et al., 2013).

Targeting of Bcr-Abl is necessary and using small molecules is a widely used treatment strategy. Despite the success of the small molecule inhibitors against Bcr-Abl in order to inhibit its activity, acquired point mutations and the ineffectiveness of these inhibitors against gatekeeper mutation let us to think about alternative targeting strategies. In my thesis, Gab2 protein was chosen to target as a critical scaffold downstream of Bcr-Abl and for being the mostly tyrosine phosphorylated protein in CML cells and thus provide the bridge between signaling proteins and Bcr-Abl. Selective inhibition of these interactors would enable defining the different contribution of Gab2 interacting proteins for signaling pathway activation.

## **1.5 Gab2 scaffold protein as a “hub” of Bcr-Abl signaling**

Scaffold proteins are very important players in signal transduction (Flynn, 2001). Even though these proteins have no enzymatic activity, their role is pivotal to maintain the interactions between different proteins and regulation of signaling pathways. These proteins can act as bridges between proteins thus

enabling the assembly and stabilization of protein complexes (T. Pawson & Scott, 1997). Scaffold proteins can act as transducers of the signals between proteins and as enhancers of these signals when they are overexpressed (Brummer, Schmitz-Peiffer, & Daly, 2010).

Grb2 associated binder (Gab) protein is an important scaffold protein. It harbors a protein interaction domain, protein interaction motifs or docking sites; an N-terminal PH domain, a central proline rich region which provides binding of SH3-containing proteins and also multiple tyrosine phosphorylation sites, respectively (Wöhrle, Daly, & Brummer, 2009). Gab proteins are conserved scaffold proteins and there are 3 mammalian paralogues which are Gab1, Gab2 and Gab3. Gab1 and Gab2 proteins are expressed ubiquitously, Gab3 also has an extensive expression distribution, although it is particularly highly expressed in lymphoid tissues (Haihua Gu & Neel, 2003).

Gab2 is located on chromosome 11q14.1 and amplified frequently in human cancers. Gab2 gains importance in terms of its role in carcinogenesis (Schwab, 1998). Gab2 proteins interact and act as amplifier of signals coming from RTKs, cytokine receptors, Fc receptors, T- and B-cell antigen receptors, G-protein coupled receptors or non-RTKs (Nishida & Hirano, 2003). Gab2 knock-out mice are viable and B- and T-cell development, blood counts and bone marrow found to be normal. This study showed that they have an impaired FcεRI signaling, which is highly dependent on PI3K pathway (H. Gu et al., 2001). Since Gab proteins have multiple tyrosine phosphorylation sites, it provides docking sites for SH2-domain containing proteins and orients protein-protein interactions (Tony Pawson, 2004; T. Pawson, Gish, & Nash, 2001). These important phosphotyrosine residues mediate the interaction of Gab2 with other downstream signaling proteins like SHP2 (an oncogenic tyrosine phosphatase), PLCγ1 (a phospholipase having critical role in activation of PKC and calcium signaling), p85 (regulatory subunit of PI3K), SHIP (phosphoinositid phosphatase) and Crk (adaptor protein) (H. Gu, Pratt, Burakoff, & Neel, 1998). In this way the Gab2 proteins have a determinant feature on cell proliferation, survival or differentiation.

As mentioned in section 1.3, Bcr-Abl contains multiple domains for protein-protein interactions, localization, and catalytic activity or for



oligomerization. Expression of constitutively active Bcr-Abl causes the phosphorylation of vast number of signaling proteins which then leads to the initiation of protein-protein interactions (Sattler & Griffin, 2003; Steelman et al., 2004). The striking study about Gab2 involvement in hematological malignancies was an important finding that Gab2<sup>-/-</sup> mice are resistant to transformation by Bcr-Abl (Sattler et al., 2002). This study, also, shows that phosphorylated Y177 on Bcr-Abl is critical for binding of Grb2 and recruiting Gab2. Mutation of Y177 into phenylalanine leads to decreased tyrosine phosphorylation of Gab2, decreased cell proliferation and migration. This study shows that Grb2 mediated recruitment of Gab2 is critical for the Bcr-Abl progression and induction of CML. Recently, Wohrle et al. showed the critical role of Gab2 in CML cells by using inducible expression or knockdown of Gab2. They discovered the resistance against tyrosine kinase inhibitors (imatinib, dasatinib, nilotinib and GNF-2) is connected to Gab2 expression and sensitivity against inhibitors were gained upon silencing of Gab2 (Wohrle et al., 2013). Moreover, with the help of quantitative mass spectrometry, Halbach et al. described comprehensively the response of CML cells against imatinib or dasatinib treatment. In this study, previous phosphosites were confirmed and new sites were identified and found that dasatinib is more efficient in downregulating the phosphorylation for Gab2 (Halbach et al., 2013).

Gab2 is not only important for hematological malignancies but also in solid tumors. It is well established that Gab2 is overexpressed in breast cancers (Bentires-Alj et al., 2006). Overexpression of this protein causes amplification of the signals that are received from tyrosine kinase receptors. Ke et al showed that Gab2 is also required for the metastasis of breast cancer (Ke et al., 2007). Overexpression of Gab2 was shown to have important functions in increased proliferation, independency of EGF and defective luminal clearance in MCF-10A cells, which displays the role of Gab2 in mammary tumorigenesis (Brummer et al., 2006).

Tyrosine phosphorylated Gab2, downstream of Bcr-Abl oncogenic kinase protein, recruits important signaling proteins to close proximity with Bcr-Abl. SHP2 oncogenic phosphatase and PLC $\gamma$ 1 phospholipase are among these interactors. We aimed to target the interaction of these proteins with Gab2 and

try to interfere with signaling in order to find out which pathway has more contribution on oncogenic transformation.

## **1.6 SHP2 and PLC $\gamma$ 1 signaling**

### **1.6.1 SHP2 function and its role in cancer**

Tyrosine phosphatases are a big family of proteins that consist of 107 genes and 81 active protein phosphatases that are being expressed from these genes (Alonso et al., 2004). In addition to the phosphatase domains, protein-protein interaction domains also contribute for the increased activity of these proteins (Cohen & Cohen, 1989).

For instance, SH2-domain containing phosphatases, so-called SHP proteins, have important roles in cancer development (G. Chan, Kalaitzidis, & Neel, 2008). There are 4 isoforms of SHP proteins. SHP1 is expressed mainly in lymphatic and hematopoietic cells while SHP2 is expressed ubiquitously (Poole & Jones, 2005). Interestingly, phenotypes differ in SHP2 knock-out and a dominant negative mutant. SHP2 knock-out mice is embryonically lethal, while the dominant negative SHP2, lacking the PTP domain, has been shown to have very mild phenotypes (Qu, Nguyen, Chen, & Feng, 2001; Qu et al., 1998; Zheng, Alter, & Qu, 2009). These results showed that, SHP2 can function in phosphatase dependent and independent manner. Without the phosphatase domain, SHP2 functions as a scaffold protein and it still has a role in signaling.

SHP2 has been shown to have role in diverse cytoplasmic signaling pathways that are activated by growth hormones, cytokines or extracellular matrix proteins (Neel, Gu, & Pao, 2003). Despite its phosphatase function, it plays a positive role in stimulating the epidermal growth factor receptor (EGFR) signals (Qu, Yu, Azzarelli, & Feng, 1999). SHP proteins are unique among phosphatases for having tandem SH2 domains located at the N-terminus of the protein, then followed by a phosphatase domain and C-terminus tail containing many tyrosine/serine residues that have major roles for the regulation of the protein's activity (Figure 1.7a,b) (Barford & Neel, 1998). SHP2 regulation is tightly controlled by the intramolecular interactions mediated by the SH2 and



PTP domains and also with the tyrosine residues at C-terminal tail (Figure 1.7a) (Poole & Jones, 2005). The phosphorylation of two important residues, tyrosine 542 and 580 has the intramolecular interaction with N-SH2 and C-SH2, respectively (Lu et al., 2001), and these phosphorylation events of the C-terminal tail have an activating role on SHP2.

SHP2 mutations are observed in human diseases which can lead to either activation or inactivation. Germline missense activating mutant of SHP2 is observed in Noonan Syndrome (NS), which is a developmental disorder characterized by malformations by facial dysmorphism, short stature, and congenital heart defects and increased risk of leukemia. PTPN11 (SHP2 encoding gene) is mutated in 50% of NS patients (Qiu et al., 2014). These mutations are present mostly in the N-SH2 and PTP domains, and mostly in the interface between these two domains (Tartaglia et al., 2001). On the other hand, somatic missense mutations of SHP2 are observed in 35% of patients with juvenile myelomonocytic leukemia (JMML) (Tartaglia et al., 2003).

Germline PTPN11 mutations are found in LEOPARD syndrome (LS) in nearly 90% of patients, which shares many common features than NS (Legius et al., 2002). But the striking fact about these mutations is that they are inactivating mutations of SHP2 and they act as dominant negative mutants in LS. On the other hand, another different feature of these mutations, unlike NS associated mutations, are that they mainly located in PTP domain only (Tartaglia & Gelb, 2005). After these findings, an important question remains to be answered: How activating or inactivating mutations cause two different syndromes with very similar clinical features? This question still needs an answer but this also proves that SHP2 is not acting only with its phosphatase activity but also with scaffold properties. SHP2 was also found mutated in solid tumors and other kinds of neoplasms (Bentires-Alj et al., 2004; Mohi & Neel, 2007). As an opposing role for SHP2 as a proto-oncogene in many types of leukemias, Bard-Chapeau et al showed that SHP2 is a tumor suppressor protein in hepatocellular carcinoma (Bard-Chapeau et al., 2011).

SHP2 was also described to be involved in CML. Scherr et al. demonstrated the involvement of SHP2, STAT5 and Gab2 in CD34<sup>+</sup> cells from CML patients. In this study, primary normal and CML CD34<sup>+</sup> cells were compared

and RNAi technology used to evaluate the functions of these proteins. It has been demonstrated that knock-down of these three proteins inhibit Bcr-Abl dependent proliferation but not cytokine dependent proliferation. SHP2 knock-down also showed the highest inhibitory effect on colony formation than STAT5 and Gab2 knock-down (Scherr et al., 2006). Furthermore, SHP-2 is required for hematopoietic cell transformation by Bcr-Abl. Primary yolk sac hematopoietic cells with wild type or SHP2 knock-out background were transduced with Bcr-Abl p210 retrovirally. The recipient mice with wild type SHP2 expression demonstrated myeloproliferative disease (MPD) while the SHP2 knock out mice did not manifest MPD (Chen et al., 2007).

In order to find out the SHP2 mediated dephosphorylated substrates, Agazie et al. developed and introduced “substrate trapping” mutants which are Asp to Ala in the WPD conserved loop and Cys to Ser in the active site. With the help of this double mutant, it has been shown that EGFR and Grb2 binder 1 proteins might be substrates of SHP2 (Agazie & Hayman, 2003a). On the other hand SHP2 was found to dephosphorylate the RasGAP docking sites on PDGFR (Klinghoffer & Kazlauskas, 1995), EGFR (Agazie & Hayman, 2003b) and HER2 (Zhou & Agazie, 2009). Timmerman et al. demonstrated that SHP2 demonstrates an important function in the recovery of disrupted endothelial cell-cell junctions by dephosphorylating  $\beta$ -catenin that is associated with VE-cadherin and improve further the mobility of VE-cadherin at the plasma membrane (Timmerman et al., 2012). Furthermore, SHP2 regulates the activity of Src family kinase (SFK). SFK activity is tightly regulated by tyrosine phosphorylation or dephosphorylation events. It is inhibited when phosphorylated from the tyrosine 529 (human Src) at C-terminal tail by C-terminal Src kinase (Csk) protein, and it is activated by the phosphorylation of tyrosine 416 (human Src) in the activation loop autophosphorylation. SHP2 regulates PAG phosphorylation, which is a transmembrane adaptor molecule found in lipid rafts, and the Csk recruitment. When PAG is dephosphorylated by SHP2, Csk activation is inhibited and then SFK gets activated (S. Q. Zhang et al., 2004). Also, SHP2 mediated dephosphorylation of paxillin causes the dissociation of Csk from paxillin-Src complex and leads to Src activation (Ren et al., 2004).

### *The role of SH2 domains in regulating the function of SHP2 |*

Deletion mutations showed that SH2 domains possess a great importance in regulating the phosphatase activity of the enzyme. In the closed conformation, the protein is autoinhibited and the N-SH2 domain forms extensive contacts with the catalytic domain. On the other hand, in the autoinhibited conformation, C-SH2 domain has little contact with the catalytic domain, but it interacts with the linker region between C-SH2 and the catalytic domain (Hof, Pluskey, Dhe-Paganon, Eck, & Shoelson, 1998). The opposite site of the phosphotyrosine binding pocket of the N-SH2 domain is in contact with the active site of catalytic domain. The N-SH2 domain occupies the catalytic pocket and thus, inhibits the binding of any substrate to the catalytic domain in the inactive form. The phosphotyrosine binding pockets of both SH2 domains are exposed to the solvent. In the active form the protein is in an open conformation. When the protein encounters a tyrosine-phosphorylated peptide, this causes structural rearrangements in the protein and the N-SH2 domain is removed from the catalytic domain (Figure 1.7b) (Barford & Neel, 1998). Both N- and C-SH2 domains have important role to maintain the closed, inactive conformation of the phosphatase or they lead to a switch to an open conformation where the active site of the PTP domain is free of the N-SH2 domain.

The importance of the SH2 domains was also shown by mutational analysis in the literature. Deletion mutation of 65 aminoacids in N-SH2 domain of SHP2 showed that the homozygous mutant mice died around day 9.5 due to some severe defects in the organization of axial mesodermal structures and posterior development during gastrulation and the mutant protein showed higher phosphatase activity (Qu et al., 1997). Dechert et al. demonstrated that the truncated form of SHP2 which lacks N-SH2 domain showed a higher catalytic activity than wild-type (Dechert, Adam, Harder, Clark-Lewis, & Jirik, 1994). These studies demonstrate the importance of the N-SH2 domain having an important role in regulating activity of SHP2.

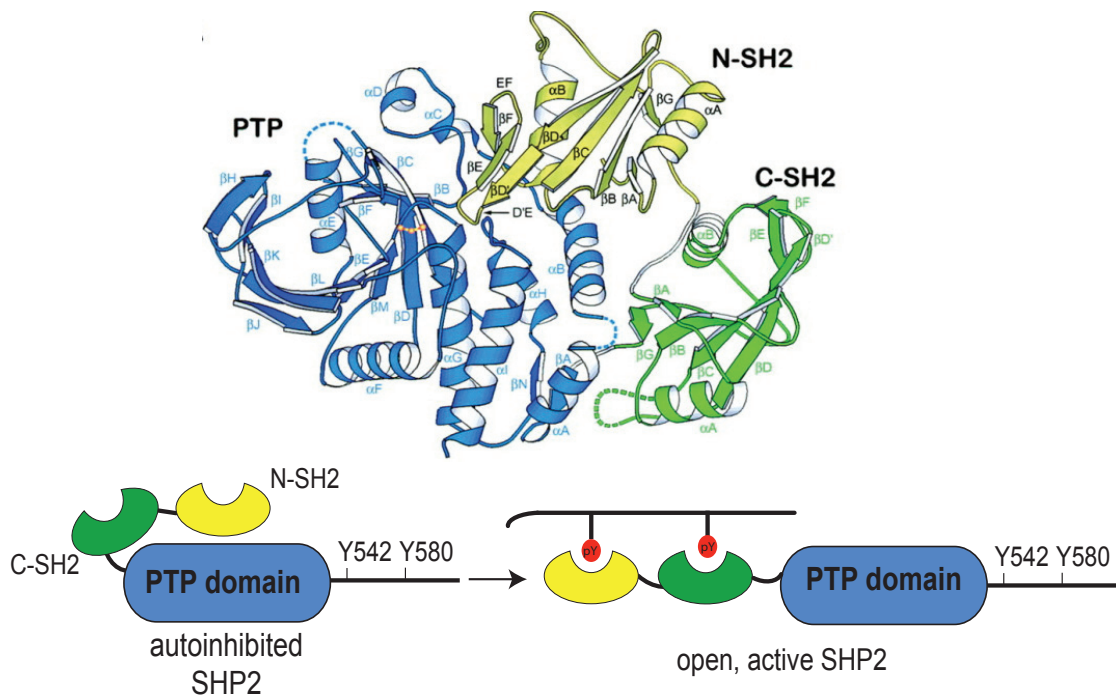


**Figure 1.7. SHP2 phosphatase structure and regulation**

Upper panel: Intramolecular SH2-domain mediated autoinhibition of SHP2 (ribbon structure). SHP2 tyrosine phosphatase is maintained in a closed conformation under normal conditions by intramolecular interactions between N-SH2 and protein tyrosine phosphatase (PTP) domain, since it blocks the substrate binding site of PTP domain. C-SH2 also binds to phosphatase domain but does not have a major role in inhibiting the phosphatase. Taken from (Hof et al., 1998).

Lower panel: Domain structure and a cartoon model of activation of SHP2. Crystal structure showed that in inactive conformation, SHP2 PTP domain is blocked by N-SH2, although the phosphotyrosine binding pockets of both SH2 domains are exposed to the solvent. When the protein encounters with a tyrosine phosphorylated binding partner, this binding event will release the autoinhibited state and activate SHP2.

### 1.6.2 PLC $\gamma$ 1 function and its role in cancer

Lipids are extensively involved in cell signaling serving as structural, scaffold elements and they possess functional diversities (Gallego et al., 2010). Phospholipases are enzymes that use phosphoinositides as substrates and they are divided into 3 main classes as A, C and D according to their specific reactions (Park et al., 2012). Phospholipase C (PLC) enzymes use phosphatidylinositol4,5-bisphosphate (PIP<sub>2</sub>) as substrate and generate two secondary messenger molecules, diacylglycerol (DAG) and inositol-1,4,5-triphosphate (IP<sub>3</sub>), by cleaving the bond between the glycerol and the phosphate. These signal molecules are responsible for the protein kinase C activation and Ca<sup>+2</sup> release from endoplasmic reticulum, respectively (Lattanzio, Piantelli, et al., 2013).

There are 13 mammalian PLC isoenzymes identified and these isoenzymes are divided into 6 subgroups, as PLC- $\beta$ , - $\gamma$ , - $\delta$ , - $\epsilon$ , - $\zeta$  and - $\eta$  (Suh et al., 2008). These subgroups have tissue/organ specific expression and mechanism of regulation and action (reviewed in Suh et al., 2008). PLC proteins have a multidomain structure with a characteristic PH domain (binding to phospholipids and proteins), EF-hand motifs (calcium binding), X-Y catalytic domain, and C2 domain (membrane targeting) (Rhee, 2001) (Katan, 2005).

Among the phospholipase C isoforms, PLC $\gamma$  is the most widely studied enzyme. PLC $\gamma$  enzymes have two isoforms; PLC $\gamma$ 1 and PLC $\gamma$ 2 (Katan, 1998). Although both isoforms are very similar to each other, in many studies they were shown to have distinct roles. They appear to be independent and do not compensate each other in the absence of the other (Kadamur & Ross, 2013) (Bonvini et al., 2003). PLC $\gamma$ 2 expression is restricted to hematopoietic system cells and regulates immune responses. PLC $\gamma$ 2 null mice show some defects in B-cell, platelet and natural killer cell functions (Regunathan et al., 2006; Wang et al., 2000). On the other hand, PLC $\gamma$ 1 is expressed ubiquitously and null mice die at embryonic day 9 because of improper vessel formation (Liao et al., 2002).

Unlike other isoforms, PLC $\gamma$  proteins have a unique domain structure in addition to the characteristic domains as mentioned above. Between the EF-hand motifs and the C2 domain, the X-Y catalytic domain is split by insertion of a linker. This linker comprises a split PH domain by two tandem SH2 domains and one SH3 domain, which is called X-Y linker (Figure 1.8a) (Park et al., 2012).

Phospholipases can be activated by many stimulants, including cytokines, growth factors or lipids (Suh et al., 2008). The presence of SH2 domains in the PLC $\gamma$  leads to the recruitment towards tyrosine phosphorylated receptor tyrosine kinase (RTK) and it transmits the signal coming from outside of the cell through the receptor, and then enhances this signal by generating secondary messengers (Bunney & Katan, 2011). Also the SH3 domain binds SOS1 and induces Ras activation as a result (Kim et al., 2000). PLC $\gamma$ 1 also has a role in cytoskeletal changes and migration of the cells. These changes are also facilitated by PI3K mediated activation of PLC $\gamma$ 1 by EGF mediated stimulation in breast cancer cells (Piccolo et al., 2002). PLC $\gamma$ 1 also showed an activating role for Rac1/CDC42 GTPases and with this, it induces the cell spreading by forming a

complex with  $\beta$ -Pix (Rac1/Cdc42 guanine exchange factor) and GIT adaptor protein (Jones & Katan, 2007). By using an RNAi dependent knockdown, Sala et al. showed that PLC $\gamma$ 1 regulates cell migration and metastasis and they observed a regression of metastasis upon PLC $\gamma$ 1 knockdown (Sala et al., 2008). An inducible dominant negative fragment of PLC $\gamma$ 1 was used to evaluate the role of PLC $\gamma$ 1 after tumor occurrence in mammary and prostate glands. They have observed a significant decrease in lung metastasis, and showed that PLC $\gamma$ 1 signaling pathways can prevent potential carcinomas (Shepard, Kassis, Whaley, Kim, & Wells, 2007). In order to evaluate the clinical significance of PLC, Lattanzio et al. analyzed the expression and phosphorylation levels of PLC $\gamma$ 1 in breast cancer patients. They generated valuable data on highly significant association between high expression of activated PLC $\gamma$ 1 and risk of metastatic relapse in a certain subpopulation of breast cancer patients treated with chemotherapy (Lattanzio, Marchisio, et al., 2013).

#### *The role of SH2 domains in regulating the function of PLC $\gamma$ 1*

Among all PLC isoforms, PLC $\gamma$  enzymes are unique for having two SH2 domains followed by one SH3 domain. These domains are important for its activity and protein-protein interactions. SH2 domains are necessary for the recruitment of PLC $\gamma$  to the tyrosine phosphorylated receptor tyrosine kinases which is located on the membrane (Bunney et al., 2012). The N-SH2 domain was shown to have the prior role to bind to the C-terminal tail of the FGF receptor, PDGFR or EGFR (Gresset, Hicks, Harden, & Sondek, 2010; Larose, Gish, Shoelson, & Pawson, 1993; Nishibe et al., 1990; Peters et al., 1992; Timsah et al., 2014). Once the protein is bound to the tyrosine phosphorylated kinase, the conformation changes and it is phosphorylated by the receptor tyrosine kinases at Y783 residue (Gresset et al., 2010). Afterwards, the C-SH2 domain binds to the phosphorylated Y783 residue and this event facilitates the full activation of PLC $\gamma$ . The C-SH2 domain was shown to have critical importance for the auto-inhibited form of PLC $\gamma$ 1 (Bunney et al., 2012). Deletion mapping showed that the X-Y linker possess a critical importance for the auto-inhibited state (Gresset et al., 2010). Phosphorylation of the Y783 residue leads to the activation of the lipase and binding of C-SH2 domain by intramolecular interactions is necessary for the



full activation of the enzyme (Figure 1.8b) (Poulin, Sekiya, & Rhee, 2005).

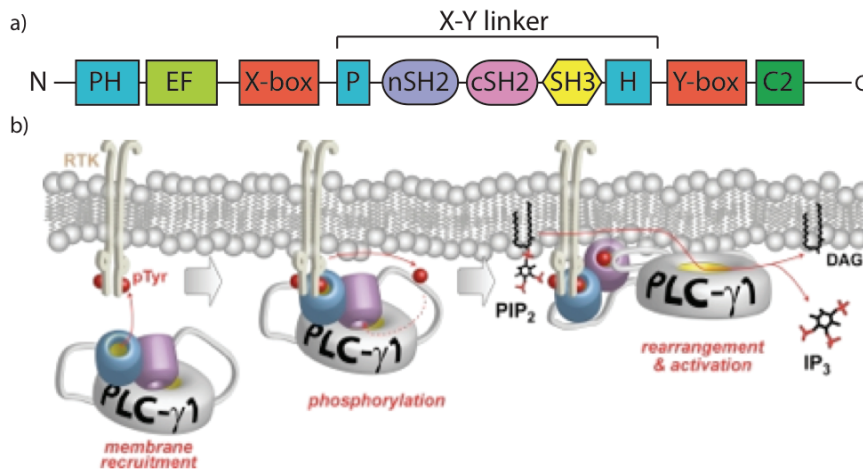


**Figure 1.8. PLC $\gamma$ 1 domain structure and mechanism of activation upon RTK recruitment and binding**

a) PLC $\gamma$ 1 has a multi-domain structure. It has a PH domain at the very N-terminus, which is followed by an EF-hand motif. Afterwards the X-Y catalytic domain is starting which is splitted into two, by a PH domain that is separated by a tandem SH2 domain and an SH3 domain. Lastly, at the C-terminus C2 domain is present.

b) PLC $\gamma$ 1 has a closed conformation in unstimulated cells. Upon stimulation, RTK autophosphorylation creates binding sites for PLC $\gamma$ 1. PLC $\gamma$ 1 is recruited to the membrane by its PH domain and bound to the tyrosine phosphorylated receptor with its N-SH2 domain. Upon binding, RTK phosphorylation occurs at the C-SH2-SH3 linker. Afterwards, full activation of the enzyme occurs with the intramolecular interaction between this tyrosine residue (Y783) and C-SH2 domain. Then, PLC $\gamma$ 1 catalyses the lysis of PIP<sub>2</sub> into DAG and IP<sub>3</sub>, which are important secondary messengers. Taken from (Gresset et al., 2010).

## 1.7 Monobodies

Monoclonal antibodies (mABs) are approved for clinical use and diversification of the antibody structures provide the development of new therapeutic antibodies. The field of mABs has become a rapidly processing research area in the past decades (Beck, Wurch, Bailly, & Corvaia, 2010). Their target specificity, low toxicity and ability to activate immune system make them promising reagents (Weiner, Surana, & Wang, 2010). Despite having some advantages, its large size causes a steric hindrance and prevents an efficient tissue penetration. They have a complex structure and properly formed disulfide bonds are necessary for their correct structure and function. On the other hand, the binding mode of mABs requires to fit in the shape of target epitope that confers the specificity, however their size might not be suitable for the grooves or pockets for the enzyme active sites, depending on the target epitope

properties and localization of the target (Skerra, 2000). Moreover, they are known to have cost-intensive production procedure. The global therapeutic mAB market is a multi-billion dollar market in contrast to non-antibody scaffolds and the global sale of mABs was 20.6 billion dollar in 2006 and it is expected to rise over 100 billion dollars by 2017 (Maggon, 2007). Since the production of full-length antibodies in bacteria is generally poor, antibody fragments, in particular single chain variable fragments (scFV) selection was commonly performed. The expression and production of these fragments does not require mammalian culture and could be promising candidates as therapeutic applications (C. M. Lee, Iorno, Sierro, & Christ, 2007).

As an alternative to mABs, small protein based drugs and diverse antibody fragments are being investigated. Combinatorial protein engineering has been increasingly utilized in order to generate new molecules with higher affinity and specificity than antibodies that could possibly interfere the protein-protein interaction (Wurch, Pierre, & Depil, 2012). For this purpose, non-antibody scaffolds are advantageous tools to use to develop new molecules.

Scaffold term defines a polypeptidic framework, contains a highly structured core and variable portions that are tolerable for modifications like insertion, deletion or substitutions (Hey, Fiedler, Rudolph, & Fiedler, 2005; Wurch et al., 2012). There are nearly 50 different scaffold-based affinity reagents and these scaffolds are being improved and the pharmacokinetic properties of these scaffold proteins are being investigated to overcome the limitations of the monoclonal antibodies. Flexible, small size and cleft penetrating properties of scaffolds makes them attractive pharmaceutical reagents (Nygren & Skerra, 2004) (Nuttall & Walsh, 2008). Their small size leads to improved tumor penetration which is provided by rapid blood clearance of scaffolds (Hey et al., 2005). In order to maintain high drug levels in serum, the renal clearance should be prevented and this could be achieved by choosing high molecular weight scaffolds or in some cases, increasing the molecular weight of the scaffold by attaching polyethylene glycol (PEG) prevents the kidney cut-off molecular weight (Caliceti & Veronese, 2003; Tolcher et al., 2011). The potential immunogenicity complications of the scaffolds are critical for the clinical use in order to prevent any unwanted effect. For this reason human protein based



scaffolds are more favorable (Tangri, LiCalsi, Sidney, & Sette, 2002).

FN type III (FN3), which consist of 94 residues, family proteins are involved in many specific ligand recognition like cell surface receptors, consisting of seven  $\beta$ -strands. There are 15 repeating units of FN3 in human fibronectin (Dickinson et al., 1994). FN3 is one of the most widely used non-antibody scaffold and it is similar to the immunoglobulin fold because of the global  $\beta$ -sandwich structure but it lacks disulfide bond which makes it more stable in the cytoplasm (Figure 1.9b) (Batori, Koide, & Koide, 2002). Koide et al. demonstrated FN3 domain as a molecular scaffold and especially the 10<sup>th</sup> repeat of FN3 is used to generate scaffold, now called the “monobodies” (A. Koide, Bailey, Huang, & Koide, 1998). Similar to complementarity-determining regions (CDRs) of antibodies, FN3 10<sup>th</sup> repeat has three surface loops at each end and the loop regions of monobodies could be diversified (Figure 1.9a,b) (A. Koide et al., 1998; A. Koide, Wojcik, Gilbreth, Hoey, & Koide, 2012; Wojcik et al., 2010). The wild-type FN3 domains possess a high thermal stability ( $T_m$  around 88°C) (A. Koide, Jordan, Horner, Batori, & Koide, 2001) and the FN3 domains are found to be very stable which was shown by the toleration to a variety of point mutations (Cota & Clarke, 2000). Combinatorial libraries could be generated by diversifying surface loops and  $\beta$ -sheets and then screening of these libraries yield high affinity and high specificity binders. In vitro selection of monobodies is widely performed by display techniques and these techniques allow the selection of antibodies at almost any specificity and affinity.

Monobodies have a lot of advantage over antibodies. They have small size (~95 residues), monomeric structure with no post-translational modifications. The absence of disulfide bond makes the molecule functional despite the reducing cellular environment. Moreover, their structural stability enables the high levels expression in bacteria (A. Koide et al., 1998).

Since highly specific recognition of the target is necessary for successful binding, wild-type FN3 needs to be diversified to generate new binding surfaces. Decision of the position and aminoacid identity makes library design a critical starting point. Usually, BC, DE and FG loops as well as  $\beta$ -strands are being modified by introducing random oligonucleotides or by a biased aminoacid composition which is usually be enriched in tyrosine residues. Batori et al. tested

whether the length of the loops play an important role or not for the maintenance of stability. Indeed, by inserting glycine residues into the loops, they demonstrated that loops have great importance for the stability of the monobody. They were also able to show that all loops except for EF loop can be modified without causing destabilization of the protein (Batori et al., 2002). The FN3 domain could be diversified as much as possible in order to achieve a notable number of possible high-affinity binders, but this much of diversified domain can result in constructs with poor biophysical properties. The constructs selected from a pre-selection can be used as a template for further affinity maturation library.

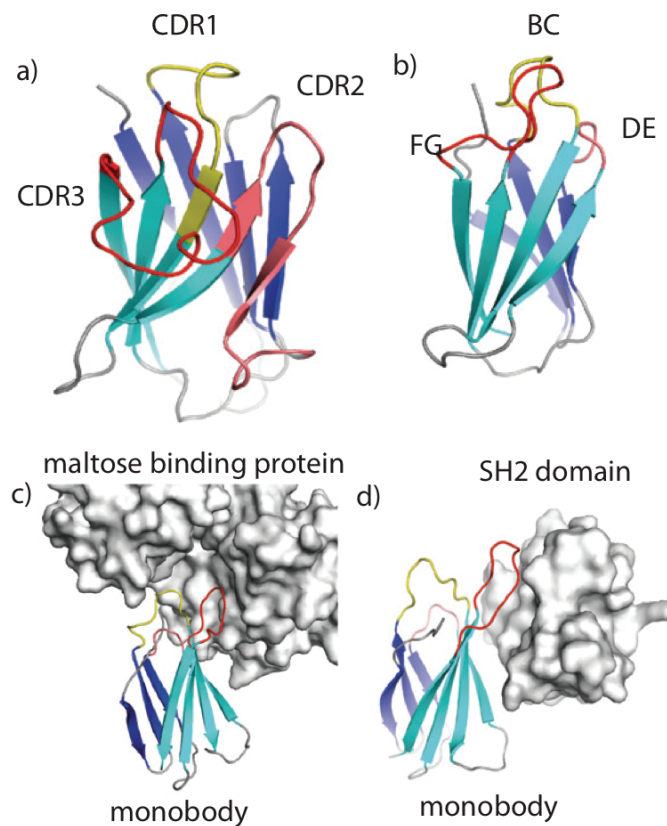


**Figure 1.9. Structure and binding modes of monobodies**

Structure comparison of variable light chain of the antibody showing the CDR region (a) and monobody structure demonstrating the b-sheets and loop structures (b). Different binding modes of monobodies were depicted. Monobodies can bind to their targets with the loop regions which is shown for maltose binding protein (c) or they can also bind to their target via  $\beta$ -sheet structures like in binding to SH2 domain (d) Taken from (A. Koide et al., 2012)

Wojcik et al. characterized a monobody, called HA4 that binds to Abl SH2 domain and successfully inhibits the interaction between Abl and phosphotyrosine ligands. This monobody binds to its target with high affinity and specificity; also, it is functional in cellular environment. Interactome analysis also demonstrated a successful recognition of Abl SH2 domain with high specificity. Moreover, HA4 blocks the processive phosphorylation of paxillin in cells, which was shown by a significant decrease in paxillin phosphorylation by Abl active form in the presence of HA4 wild type but not a non-binding mutant HA4. Furthermore, STAT5 phosphorylation was inhibited with HA4 expression (Wojcik et al., 2010). Grebien et al. showed that Abl SH2-kinase domain interface was disturbed with a tandem monobody called HA4-7c12. In this tandem monobody, HA4 binds to SH2 domain and 7c12 binds to the SH2-kinase domain interface and they are connected with a linker region (Grebien et al., 2011). By using this tandem monobody, they observed inhibition of leukemogenesis.

Recently, Koide lab developed new generation synthetic proteins by developing affinity-clamping technology that ensures an extremely high binding specificity. These affinity clamps are fusion proteins of a protein interaction domain with a monobody that enhances the specificity and affinity of the protein interaction domain and they are connected by a linker region that gives enough flexibility to bind to their target (S. Koide & Huang, 2013). Monobodies can be diversified and selected from combinatorial libraries against their target site. Such a strategy enables the direction of the affinity clamp against a peptide motif and enhances the affinity and specificity significantly when compared to a single protein interaction domain (Huang, Koide, Makabe, & Koide, 2008). In this way, for example, a target phosphotyrosine site could be clamped between the FN3 domain and a functional SH2 domain (Figure 1.10b).

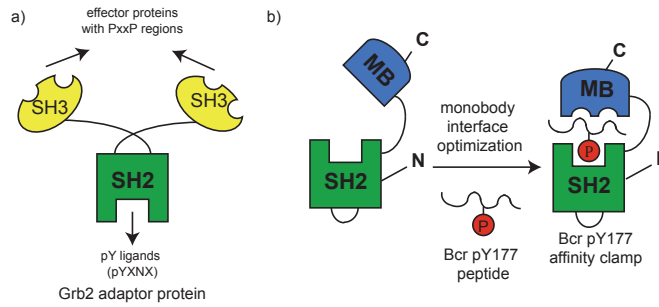


**Figure 1.10. Representative cartoon model of the Bcr pY177 affinity clamp (Figure provided by Oliver Hantschel)**

a) Grb2 adaptor protein domain structure showing a central SH2 domain which is flanked by two SH3 domains. The Grb2 SH2 domain binds tyrosine phosphorylated proteins with pYXNX motif where X is generally a hydrophobic aminoacid residue (Songyang et al., 1994).

b) Binding mode of Bcr pY177 affinity clamp. The SH2 domain of Grb2 is fused to monobodies and after optimization of the binding surface of monobody for the target region, Bcr pY177 phosphosite is clamped between two binding modules.

The first functional and structural characterization of the affinity clamps was investigated by using PDZ domain of human Erbin protein which binds to C-terminus of p120-related catenins with low micromolar affinity. The PDZ domain is covalently linked to FN3 domain, which is used as the enhancer domain of the interaction. In this study, different affinity clamps were compared and the affinity of these clamps was found to be significantly higher (at low nM range) than the parent PDZ domain. The crystal structures also revealed the different and improved binding of the affinity clamp when compared to parent PDZ domain (Huang, Makabe, Biancalana, Koide, & Koide, 2009). Yasui et al. developed chimeric Grb2 containing pY-clamps, introduced this to Grb2<sup>-/-</sup> mESCs and evaluate the phenotype of the engineered cells. SHP2 pY580 site was shown to be the key Grb2 ligand in these stem cells for the determination of the cell fate and it is sufficient for to drive primitive endoderm lineage statement (Yasui et al., 2014).

Due to outlined advantages and the above-mentioned studies, monobodies are advantageous tools that could be used to dissect the signaling networks. In my thesis, monobodies were used to target and interfere with SH2 domain interactions of phosphotyrosine residues of Gab2.

## 1.8 Aim of the Work

Gab2 is one of the major interactors and substrates of Bcr-Abl. The proline rich motif on Gab2 protein interacts with Bcr-Abl complex through the C-SH3 domain of the Grb2 adapter protein. Grb2, on the other hand, is bound to Bcr-Abl's phosphorylated Y177 with its SH2 domain. Through this interaction, Gab2 serves as a binding platform for SHP2, p85 (the regulatory subunit of PI3K) and PLC $\gamma$ 1. These proteins are bound to phosphotyrosine residues of Gab2 by their SH2 domains (Figure 1.11). The leukemogenesis of Bcr-Abl is highly dependent on the formation of this complex.

Presently, the essentiality or dispensability of Gab2 activated pathways for leukemogenesis are not known. Further understanding of this cascade is critical for the development of novel treatment strategies and to design further combinatorial therapies with TKIs. Having considered all these emerging roles of Gab2 in cancer and its critical interactions with many signaling proteins such as SHP2, PLC $\gamma$  and PI3K lead us to target the interaction between Gab2 and these signaling proteins. With the knowledge of SH2 domain-phosphotyrosine mediated interaction that forms this complex, we aimed to disrupt these interactions by using highly specific small protein inhibitors. Design and development of these inhibitors against SH2 domain is a challenging issue, because of the presence of 120 human SH2 domains that show high conservation and sequence homology in all species.

In order to confirm these interactions and find new interacting proteins that could be targeted by monobodies, we first aimed to reveal the interactors of Gab2 by performing tandem affinity purification. Expression of tandem affinity-tagged Gab2 and its interactors in cells will reveal the protein network around Gab2. Next, our aim is to develop monobodies against SH2 domains of the Gab2-binding proteins in order to interrupt the SH2 domain mediated interaction. Since the involvement of SHP2, p85 $\alpha$ , and PLC $\gamma$ 1 was shown before in Bcr-Abl mediated transformation, SH2 domains of these three proteins are used for screening of binding monobody constructs in Shohei Koides lab. Biophysical and structural characterization is also carried out in Koide lab. In order to investigate the specificity of monobodies in cells, we aim to express them in stable cell lines

and use tandem affinity purification of the monobodies, which gives an idea of the complexity of interactors.

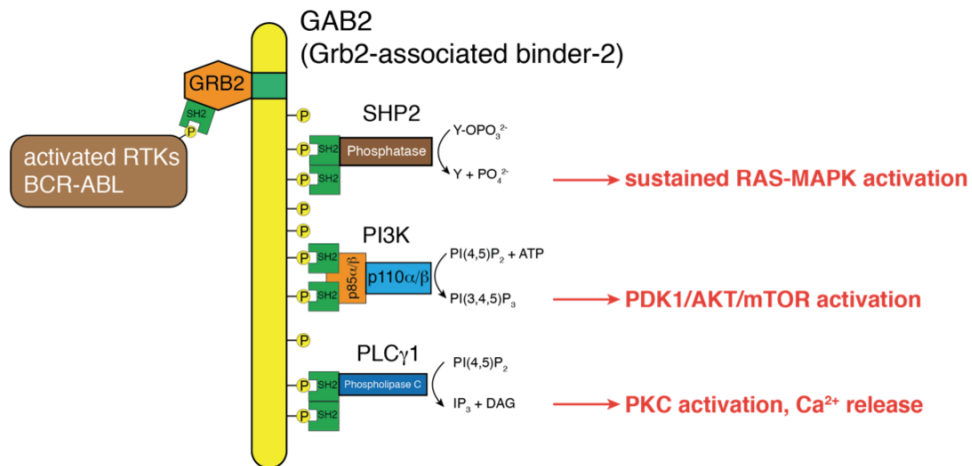


**Figure 1.11. Gab2 mediated activation of SHP2, PI3K and PLCγ1**

The Grb2 adaptor protein is bound to phosphotyrosine 177 residue of Bcr-Abl with its SH2 domain. Then, the Gab2 scaffold protein is recruited to complex by a proline rich region and bound to the SH3 domain of Grb2. Afterwards, SHP2, p85 regulatory subunits and PLCγ1 is bound to Gab2 through a SH2-phosphotyrosine mediated interaction. Figure provided by Oliver Hantschel

Afterwards the functionality of the monobodies to disrupt the targeted protein interactions and interference with the downstream signaling pathways are investigated in cells. In order to elucidate the physiological effect of SHP2 targeting monobodies and morphological outcomes, we aimed to use an inducible system to express them in lung cancer cell line, which possess an activating mutation in SHP2.

## CHAPTER 2

### RESULTS

#### 2.1 Mapping of the Gab2 interactome in K562 cells

In order to identify the endogenous interactor network of Gab2, we used an unbiased approach in Bcr-Abl positive K562 CML cell line, which is the tandem affinity purification method coupled to LC-MS/MS analysis. The Gab2 protein and its main interactors (Wöhrle et al., 2009), Gab1, Gab2, p85 $\alpha$ , p85 $\beta$ , PLC $\gamma$ 1, SHP1 and SHP2, were cloned into a pMIG vector, which is a mammalian expression vector with a retroviral 5' LTR promoter that is suitable for retroviral transductions.

In addition to the central hub, Gab2, we have chosen two out of five regulatory subunits of phosphatidyl inositol-3-kinase (PI3K), p85 $\alpha$  and p85 $\beta$ , Src-homology 2 domain containing phosphatases, SHP1 and SHP2, phospholipase C gamma, PLC $\gamma$ 1, and also Gab1 the closest paralogue of Gab2. The activation of PI3K was described by the indirect binding of PI3K to the activated receptor tyrosine kinases. Gu et al. investigated the role of Gab2 and showed that Gab2 phosphorylation is dependent on the binding to Grb2. Upon receptor activation with cytokine stimulation, Gab2 is phosphorylated and activated by these receptors (H. Gu et al., 2000). The interaction between Gab2 and PI3K is mediated with the SH2 domains of p85 regulatory subunits of the kinase. SHP1 and SHP2 are two phosphatases that contain two SH2 domains. Although SHP1 and SHP2 share high structural and primary sequence homology, they differ in some aspects (Hof et al., 1998). SHP1 is an accepted negative regulator of signaling events although SHP2 is thought to promote and positively regulate signaling. SHP2 is the first oncogenic tyrosine phosphatase that was identified (Reviewed in (Lorenz, 2009)). PLC $\gamma$ 1 is a multi-domain phospholipase and both SH2 domains are important for the catalytic activity. It was shown that N-SH2 domain is required for the receptor mediated activation of PLC $\gamma$ 1 and C-SH2 was necessary for intramolecular interactions which leads to full activation

(Bunney et al., 2012). The link between c-Abl was described and Plattner et al. demonstrated that PLC $\gamma$ 1 and c-Abl forms a complex in PDGFR activated cells. After the activation, PLC $\gamma$ 1 is negatively regulated via phosphorylation by c-Abl (Plattner et al., 2003).

### 2.1.1 Strep-HA purification of Gab2 and its interactors

The constructs were cloned as N- or C- terminal fusions for expression in a tandem Streptavidin binding peptide (Strep) and 3 consecutive hemagglutinin (HA) tagged (Strep-3xHA tag) pfMIG vector (Figure 2.1). All the constructs cloned as N-terminal fusion, except for Gab1, Gab2 and PLC $\gamma$ 1. These three proteins were cloned as C-terminal fusion because of the presence of a PH domain at the N-terminus, which is important for membrane recruitment. In this way, we avoided a possible disruption of the PH domain function by the tag. These vectors also have an IRES-GFP selective marker expression, which enable the identification of the positive cell population expressing the construct by FACS (fluorescence activated cell sorting). After the verification of the cloned construct by sequencing, stable K562 cell lines were generated for each protein by retroviral transduction.

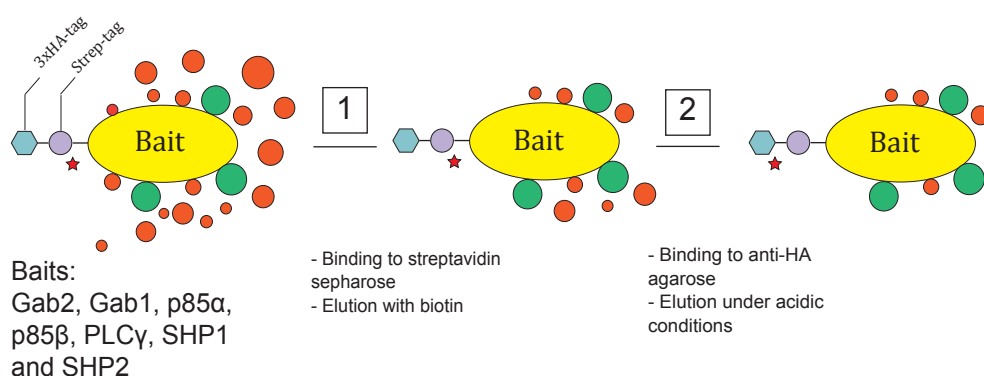


**Figure 2.1. Schematic cartoon model of Strep-HA purification of an N-terminally tagged bait protein**

K562 cells retrovirally transduced with the Strep-HA tagged bait proteins. Then the K562 cells expressing the Strep-HA-tagged bait proteins were lysed with lysis buffer and first purified with Streptactin beads. After washing the beads, the bound proteins were eluted by biotin solution for the following purification step. The eluate is then incubated with anti-HA beads and finally the protein complex was eluted with 0.150 M HCl in a tube with TEAB buffer to neutralize immediately (see Materials and Methods for detailed steps). The orange and green spheres indicate the interactors of the bait protein.



The tandem affinity purification (TAP) methods were widely used to purify and analyze the protein complexes that are interacting with the bait protein. Glatter et al. introduced a tandem purification method which uses Strep-3xHA (Strep-HA) affinity tag which consists of 48 aminoacid (Glatter, Wepf, Aebersold, & Gstaiger, 2009).

The expression levels of the bait proteins were revealed by anti-HA immunoblotting (Figure 2.2a). The stable K562 cell lines for Gab2 and its interactors were expanded to  $2 \times 10^8$  number of cells. After the tandem affinity purification of the bait proteins, the final eluate was snap-frozen in liquid nitrogen and then lyophilized overnight (Figure 2.1). Afterwards, the lyophilisate was resuspended and boiled in SDS sample buffer and then submitted for LC-MS/MS analysis. After receiving the MS results, the known contaminants were eliminated, like tubulin, keratin. Independent control purifications were performed by using an N-terminally tagged eGFP construct as bait protein that was used as a negative control. All purifications were done in triplicates. The proteins that have been identified in all replicates and detected with equal or more than 1 unique spectra were taken into consideration. We were able to identify the bait proteins in all the purifications. Moreover, we were able to confirm some of the known and identify novel interactors of bait proteins. Reciprocal co-finding of the interactions in affinity purifications is an important parameter to confirm and call a bait-prey interaction “true”. In our affinity purification, the reciprocal confirmation of the interactions was only observed between Gab2 with p85 $\alpha$ , p85 $\beta$  and SHP2 proteins. The interaction between SHP2 and Gab2 occurs through Grb2 scaffold protein, which is confirmed by our interactome study. SHP2 protein was identified in two out of three replicates in p85 $\alpha$  pull-down and in all replicates of p85 $\beta$  pull-down. However, in SHP2 pull-down neither of the p85 regulatory subunits were identified. Likewise, the reciprocal recovery of PLC $\gamma$ 1 and SHP1 with Gab2 was failed and the possible reasons are discussed in Section 3.1.

The purification efficiency was evaluated by following the bait protein from the purification steps by anti-HA immunoblotting. However, the purification of C-terminally fused Gab1 and Gab2 affinity purifications did not work, because after total extract (TE) and the flowthrough fraction from

Streptavidin beads (SN1), we could not identify the bait protein in the further steps of the purification by anti-HA immunoblotting (Figure 2.2b). Therefore, we tried to clone and express these two proteins as N-terminal fusions. Then when we have performed the Strep-HA purification of N-terminally fused Gab2, anti-HA immunoblotting revealed the presence of the bait protein in the last elution (E2) (Figure 2.2c).

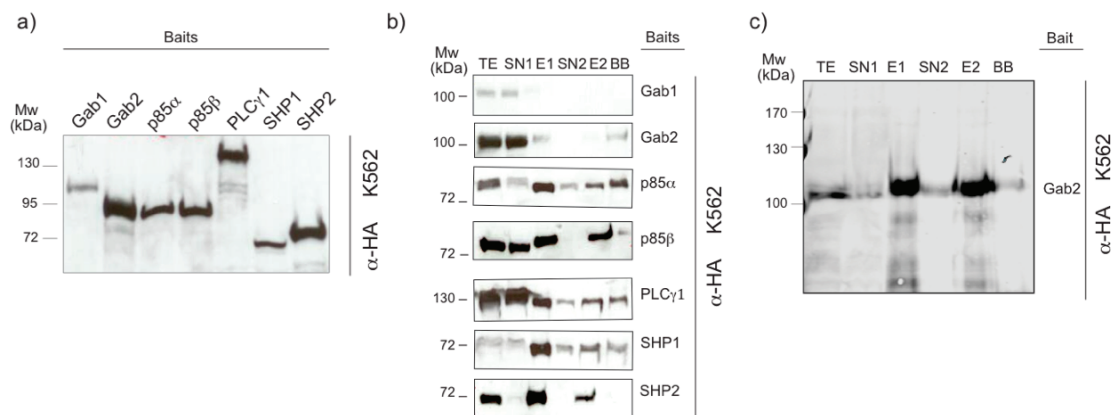


**Figure 2.2. Bait proteins followed in Strep-HA purification steps by anti-HA immunoblotting**

a) Expression levels of the bait proteins were detected by anti-HA immunoblotting. 100  $\mu$ g total cell lysate loaded in total volume of 20 $\mu$ L.

b) Representative purification steps for all bait proteins. In this purification set Gab1, Gab2 and PLC $\gamma$  were cloned as C-terminal and the other bait proteins were cloned as N-terminal fusion. The presence of the bait protein is followed by anti-HA immunoblotting.

c) Purification of N-terminally fused Strep-HA tagged Gab2. Abbreviations; TE: total eluate (0.33%), SN1: flowthrough after streptavidin beads (0.33%), E1: biotin eluate from Streptactin beads (2%), SN2: flowthrough after anti-HA beads (2%), E2: acidic elution from anti-HA beads (3.2%), BB: boiled anti-HA beads. (% of input indicated in brackets)

In all the cases the bait protein, except for C-terminally tagged Gab1, was identified abundantly in the E2 eluate fraction of Strep-HA purification by immunoblotting (Figure 2.2b,c) and MS analysis. Gab2 protein, as being the central hub for the interactors, was identified in p85  $\alpha/\beta$  isoforms, and in SHP2 affinity purifications, however in PLC $\gamma$ 1 and SHP1 pull-downs, Gab2 protein was not detected by MS analysis. In each affinity-purification, some of the known interactors were identified and also some novel interactors were detected (Figure 2.3). The most efficient pull-down was observed in 90kDa Gab2 scaffold protein in terms of the number of identified interactor proteins. Many of the known interactors were identified like PI3K p85 regulatory  $\alpha/\beta/\delta$  subunits, SHP2, CrkL, Grb2, and Cbl. In all Gab2 affinity purifications SHP2 was detected as

a high ranking interactor. The Grb2 adaptor protein was also detected, as it is a direct interactor of Gab2. In addition to the regulatory subunits, PI3K p110 catalytic  $\alpha/\beta/\delta$  subunits were detected. Moreover, Abl and Bcr peptides were detected. The previously known SHIP2 phosphatase and LRRK1 interaction was also confirmed by Gab2 pull-down in our experimental set up. SHIP2 phosphatase was shown to be a core interactor of Bcr-Abl (Brehme et al., 2009) and this protein was only detected in two of our replicates. Gab2 interacts also with other adaptor proteins like CrkL and Shc1/2 which was verified in our pull-downs. In literature, phosphorylated Shc was found to be recruiting Grb2 and Gab2, and the binding of Grb2 to Shc was provided as a complex with Gab2 (H. Gu et al., 1998). CrkL is also an adapter protein and the SH2 domain of CrkL binds to the phosphorylated protein such as Gab2 (Feller, 2001). The E3 ubiquitin-protein ligase Cbl was also detected in one of the replicates with low number of assigned spectra (Figure 2.3).

When p85 $\alpha$ , regulatory subunit of PI3K, was used as bait, the catalytic subunits, p110 $\alpha$ ,  $\beta$ ,  $\delta$  were pulled down in all three repeats with high ranking. Moreover, Gab2 was identified as a direct interactor, while Grb2 and SHP2 were identified as indirect interactors, which are the components of the Gab2 core network. As an unknown interactor, MARK3 (MAP/microtubule affinity-regulating kinase) was detected only in one of the replicates, PITPNB (Phosphatidylinositol transfer protein beta isoform), ARHGEF12 and 17 were detected as unknown interactors of p85 $\alpha$ . PITPNB was detected in the p85 $\alpha$  pull-down but not in p85 $\beta$  pull-down (Figure 2.3).

In p85 $\beta$  pull down, all the proteins identified in our affinity purification were known interactors (Figure 2.3). p85 $\beta$  pull-downs resulted the presence of p110 $\alpha/\beta/\delta$  catalytic subunits of PI3-kinase, as expected. Gab2 and Grb2 interactors were confirmed and SHP2 phosphatase was shown as a possibly indirect interactor of p85 $\beta$ . CrkL and Cbl were detected as an interactor of p85 $\beta$  showing that second or third shell proteins were also pulled down. Gab2 and p85 $\beta$  pull down identified overlapping set of proteins. p85 regulatory subunit of PI3-kinase is required to mediate the insulin-dependent recruitment of PI3-kinase to the plasma membrane (Luo, Field, Lee, Engelman, & Cantley,

2005). Insulin receptor substrate (IRS) 1 is phosphorylated on tyrosines after insulin receptor activation. In our affinity purifications, p85 $\beta$  was confirmed as an interactor of IRS1 and IRS2 as well. The interaction of p85 $\beta$  with IRS1/2 but not p85 $\alpha$  was identified in our pull downs (Figure 2.3).

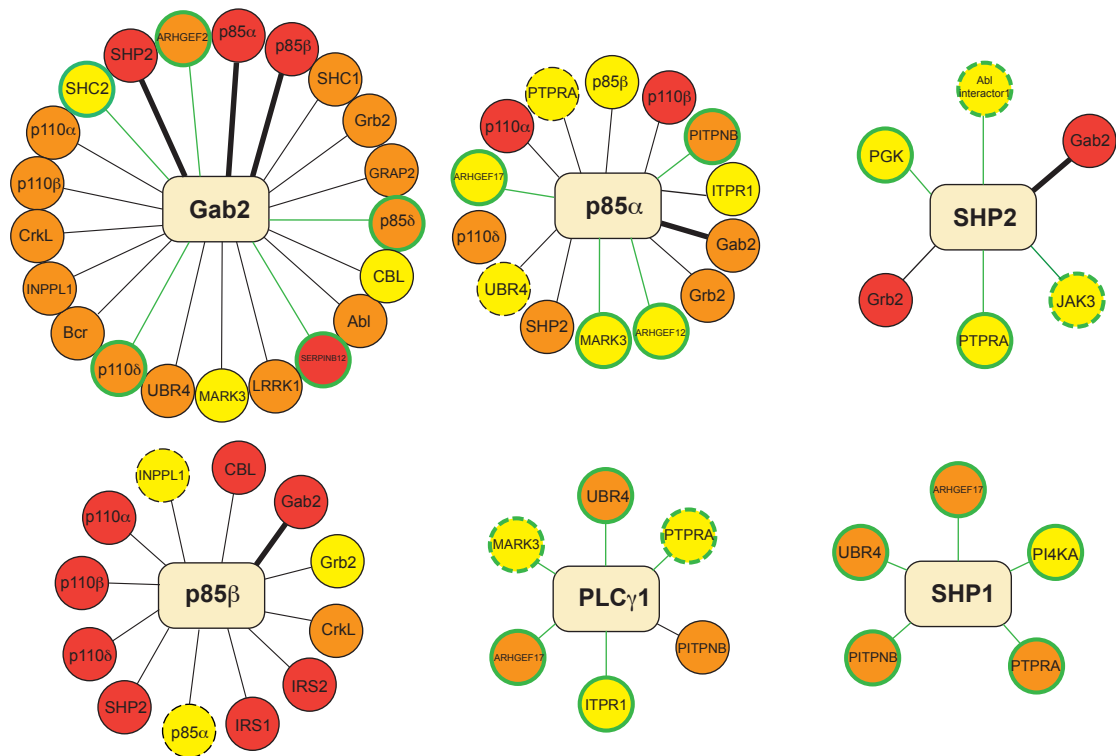


**Figure 2.3. Interactome of Gab2 scaffold protein and its interactors**

The Gab2 and the interactor proteins were subjected to Strep-HA purification. The bait protein is shown in the middle and the interactors were shown around the bait. Interactors shown as circles were annotated according to the HPRD, IntAct and BioGrid and the green-framed circles represent potential novel interactors. The reciprocal interactions are annotated as thick black edges. The proteins identified in three, two and one of the replicates are shown with red, orange and yellow colored circles, respectively. The dashed circles indicate the identification of the interactor with only 1 assigned spectra. The list of all interacting proteins identified with the numbers of spectra is shown in Appendix table A1, and the complete list of proteins was shown in Appendix table A2.

Strep-HA purifications of C-terminally tagged PLC $\gamma$ 1 were performed but yielded low number of spectral counts for the bait protein, and very few interactors were identified. In the first purification, no specific interactors were identified, but in the second and third purification, PITBN identified as a high ranking interactor which is a known interactor of PLC $\gamma$ 1. Furthermore, ARHGEF17, UBR4 ligase, PTPRA (Receptor-type tyrosine-protein phosphatase



## **2.2 Expression and purification of SH2 domains of SHP2, PLC $\gamma$ 1 and p85 $\alpha$**

Since the aim of the project is to disrupt the interaction of Gab2 with its critical interaction partners by using monobodies, the individual SH2 domain of SHP2, PLC $\gamma$ 1 and p85 $\alpha$  proteins were used as targets (Figure 1.9). These three proteins contain two SH2 domains and the SH2 domains are annotated as N-SH2 or C-SH2 according to their localization.

The N-SH2 and C-SH2 domains and tandem SH2 domains of SHP2 (Figure 2.5a, upper left panel) (PTPN11 gene name, residues 1-103, 97-217 and 1-217, respectively according to UniProt database entry Q06124), N- and C-SH2 domains of PLC $\gamma$ 1 (PLCG1 gene name, residues 537-666 and 655-763, UniProt database entry P19174) and p85 $\alpha$  (PIK3R1 gene name, residues 327-431 and 611-724, UniProt database entry P27986) were cloned into pHBT vector by Oliver Hantschel with 6xHis tag followed by Avidin (Avi) tag as N-terminal fusion and then the SH2 domains were expressed in E.coli BL21 cells. After expression the SH2 domains were purified with Nickel-NTA affinity chromatography with the 6xHis tag.

## **2.3 SHP2 targeting monobodies**

### **2.3.1 Selection of monobodies to the N- and C-SH2 domains of SHP2**

Purification of the SH2 domains followed by biotinylation and phage display selection of monobodies were performed by Fern Sha and Akiko Koide in Koide lab. In order to select the binding monobodies against the target domains, both the loop regions and  $\beta$ -sheet regions were mutated and diversified (Figure 2.5a, left lower and right panel). Three consecutive rounds of gradually decreased target concentrations were used as 200 nM, 100 nM, and 50 nM for phage display, respectively. Phages were captured onto biotinylated targets immobilized to streptavidin-coated magnetic beads. Afterwards, gene shuffling was performed to enrich the clones against N- and C-SH2 domains. Then yeast

surface display was performed in order to detect the competition of monobodies and this assay resulted with 4 unique clones for N-SH2 and 3 unique clones for C-SH2 domain (Figure 2.5a, right panel). At the end, NSa1 and NSa5 were selected against N-SH2 domain and Cs1 and Cs3 were selected against C-SH2 domain because of the higher solubility as a purified protein.

Surface plasmon resonance (SPR) was performed in the Koide lab in order to find out the binding affinity of monobodies for their target SH2 domains. It was shown that the monobodies were binding to their cognate SH2 domains with low nM  $K_D$  (dissociation constant) and no cross reactivity was detected with the other SH2 domain (Figure 2.5b). Furthermore, monobodies were also bound the tandem SH2 domains of SHP2, so the binding of monobodies was not inhibited with the nearby SH2 domain (Figure 2.5b). Strikingly the monobodies differentiated between SHP2 and tandem SH2 domains of SHP1, which is the closest homolog of SHP2 (Figure 2.5c). These data showed that both monobodies that were selected for both SH2 domains demonstrated high affinity and high specificity for their target SHP2 SH2 domains. On the other hand, the selected monobodies were also shown to interfere with the binding of SH2 domains to their natural ligands, which was shown with the help of phosphopeptides binding assay by using tandem SHP2 SH2 domains by the Koide lab. SHP2 is described to bind to phosphorylated Y614 and Y643 residues of Gab2 (Futami et al., 2011). NSa1 and NSa5 significantly inhibited the interaction between the tandem Gab2 phosphopeptide and SH2 domains of SHP2, although only Cs3 did not show an inhibitory effect when compared to no monobody condition (Figure 2.5d). Altogether, these data showed the potential of monobodies in terms of affinity, specificity and ability to interfere with phosphotyrosine ligands.

*Crystal structure of SHP2 SH2/monobody complexes shows that monobodies might act as pY competitors.* The recognition of SH2 domains by monobodies was investigated structurally and NSa1/N-SH2 and Cs1/C-SH2 crystal structures were solved at 2.3Å resolution by the Koide lab (Figure 2.6). Both monobodies were shown to occupy the phosphotyrosine binding pocket of their cognate SH2 domain which explains their ability to interfere with the binding of Gab2 phosphopeptide ligands (Figure 2.6a).



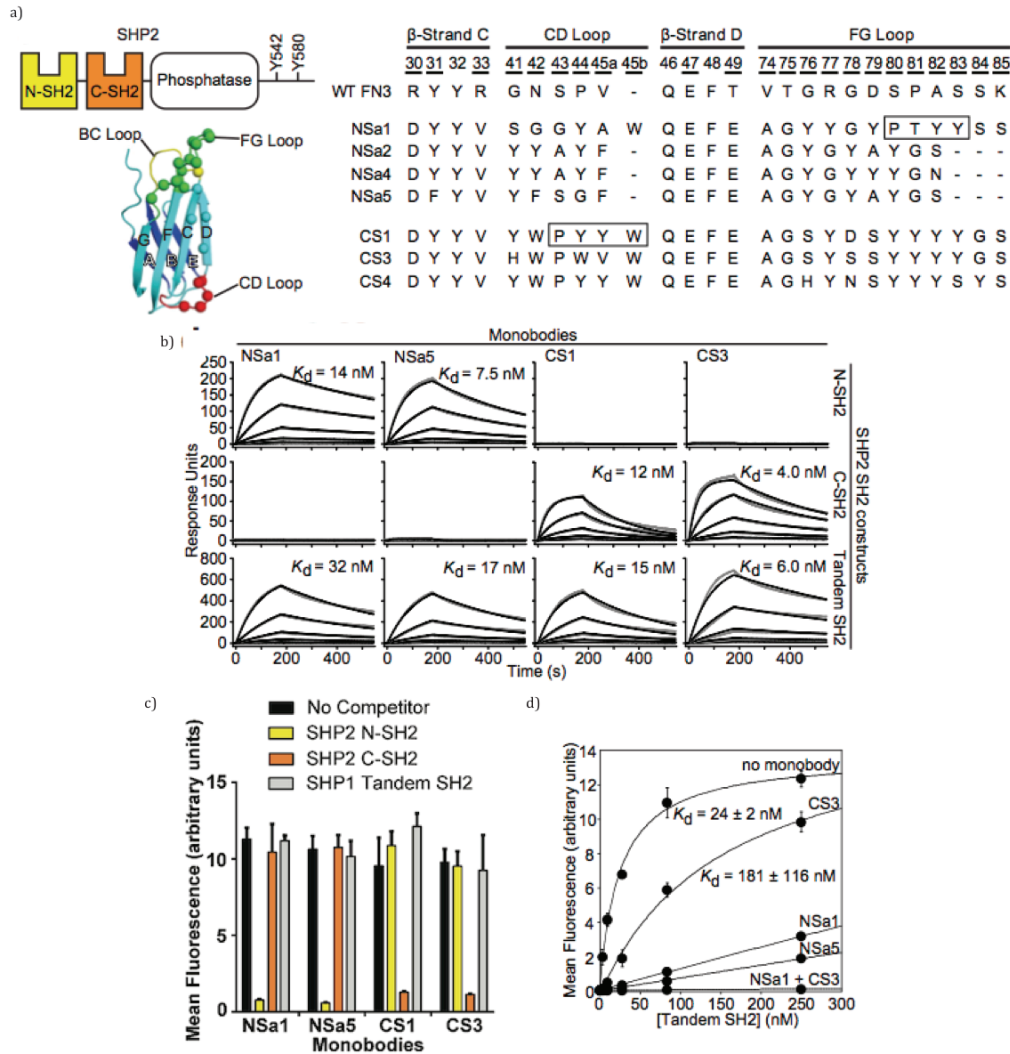


**Figure 2.5. Characterization of sequences and binding of SHP2 SH2-binding monobodies. Figure taken from (Sha et al., 2013)**

a) Left upper panel: Domain organization of SHP2. The N-SH2 and C-SH2 domains are shown in yellow and orange, respectively, and the phosphatase domain is colored in white. Phosphorylated tyrosine residues, Y542 and Y580, on the C-terminal tail were demonstrated. Left lower panel: Schematic figure of the FN3 monobody scaffold. The b-strands are labeled A-G and diversified residues are shown as colored spheres. Right panel: Amino acid sequences of selected SHP2 SH2-domain binding monobody clones were demonstrated. wild-type FN3 sequence was shown on above line and diversified sequence positions in the library were underlined in each loop region. The N- and C-SH2 targeting monobodies were selected against the isolated N-SH2 and C-SH2 domains of SHP2, respectively.

b) SPR sensorgrams for monobody binding to SHP2 SH2 domains. Kinetic parameters were calculated from the best fit of a 1:1 binding model (black traces) to the raw data (gray traces)

c) Competition experiments showed that there was no cross-reactivity between SHP2-targeting monobodies to SHP1. Binding signals of four monobodies (NSa1, NSa5, CS1 and CS3) to their respective cognate SH2 targets at 100 nM in the presence or absence of the indicated competitor proteins (SHP2 N-SH2, SHP2 C-SH2 and SHP1 tandem SH2) at 3  $\mu$ M were shown.

d) Inhibition of the interaction between tandem SHP2 SH2 domains with phosphotyrosine peptide containing a Gab2 fragment with tandem pY sites, Y614 and Y643. Binding titrations of the tandem SH2 domains to immobilized tandem pY peptide in the presence of saturating concentrations of the indicated monobodies were shown.



During the library design, 23 residues were diversified (Figure 2.5b) and in crystal structures, 20 and 13 residues were found to be located within NSa1/N-SH2 and Cs1/C-SH2 interface, respectively (Figure 2.6a,b). While the phosphopeptides were known to run perpendicular to the central  $\beta$ -sheet of the SH2 (Figure 2.6c), interestingly NSa1 and Cs1 were run in the opposite direction than phosphotyrosines in the contact region. This result shows the unique binding property of monobodies and might explain the high specificity (Figure 2.6c,d).

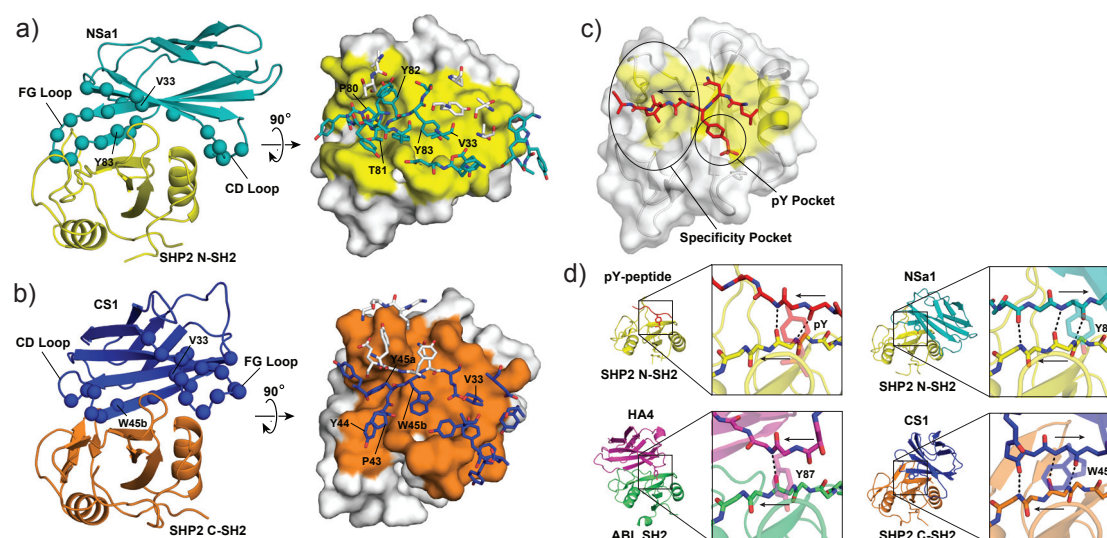


**Figure 2.6. Crystal structures of SHP2 SH2/monobody complexes. Figure taken from (Sha et al., 2013)**

Coordinates of the NSa1/N-SH2 and CS1/C-SH2 complexes have been deposited in the Protein Data Bank (PDB codes 4JE4 and 4JEG, respectively).

a) The interface of monobody NSa1 and SHP2 N-SH2. Left panel: a cartoon representation of the complex with monobody NSa1 shaded in teal, N-SH2 shaded in yellow, and residues diversified in the library are shown as spheres. Right panel: an orthogonal view of the interface, in which N-SH2 is represented as a surface model with the epitope shaded in yellow, and residues within the paratope of monobody NSa1 are represented by sticks. Residues that were not diversified in the library are shown as white sticks.

b) The interface of monobody CS1 with SHP2 C-SH2. Labeling scheme is similar as in panel (a) except monobody CS1 is shaded in blue and C-SH2 is shaded in orange.

c) The interface of the RLNpYAQLWHR peptide with SHP2 N-SH2 (PDB 3TL0) showing the typical positions of the pY-binding and specificity pockets of SH2. The orientation of the bound peptide is shown with an arrow.

d) Comparison of the binding modes of a pY-peptide, HA4, NSa1, and CS1 to their respective cognate SH2 domains. Intermolecular hydrogen bonds are shown as dashed lines and the orientations of the strands are labeled with arrows (expanded box).

### **2.3.2 SHP2 targeting monobodies bind selectively to SHP2 in cells**

A very important question was whether monobodies would show the similar specificity in a complex cellular environment as compared to the in vitro specificity. In order to answer this question, we benefitted from the tandem affinity purification methods followed by liquid chromatography coupled to tandem mass spectrometry (LC-MS/MS) to reveal the specificity of monobodies in cells. Because of the ease of cell line expansion and the high yield obtained after purification, we first tried to generate cell lines with Strep-HA-tagged monobodies in K562 and HEK293 cells with the 4 unique clones initially chosen for the N-SH2 domain. In spite of the success of this method in mapping the Gab2 interactome in terms of the expression of the bait protein (see section 2.1.1, Figure 2.2a), we failed to achieve high expression levels of monobodies when compared to a control cell line expressing Strep-HA-tagged Shc1 which was sorted and confirmed before to have a good expression level of the Shc1 bait protein (Figure 2.7a). The monobodies were expressed approximately 10-fold less than the control cell line. Nevertheless, we decided to do the Strep-HA purification for NSa1 stable cell line for K562 and HEK293 cells. The bait monobody protein was not detected in Strep-HA-purification in the last eluate fraction (E2) (Figure 2.7b). Anti-HA immunoblotting showed no or very low signal in total extract and the rest of the fractions, while the bait protein was detected in boiled beads (BB) fraction (Figure 2.7b).

We thought the low expression level and the unsuccessful purification might be because of the small size of Strep-HA tag and the monobody might get degraded in the cells. Afterwards, the monobodies were cloned in a tandem affinity purification tag vector as N-terminal fusion, whose tag size is bigger than the Strep-HA tag. This tag consists of two consecutive Protein G tag, which is followed by a TEV cleavage site and then a streptavidin binding peptide tag (SBP) and one myc tag, which will be called as TAP tag for the rest of the thesis (Figure 2.9a). HA4 monobody which was characterized previously to bind Abl SH2 domain was used as a positive control (Wojcik et al., 2010).

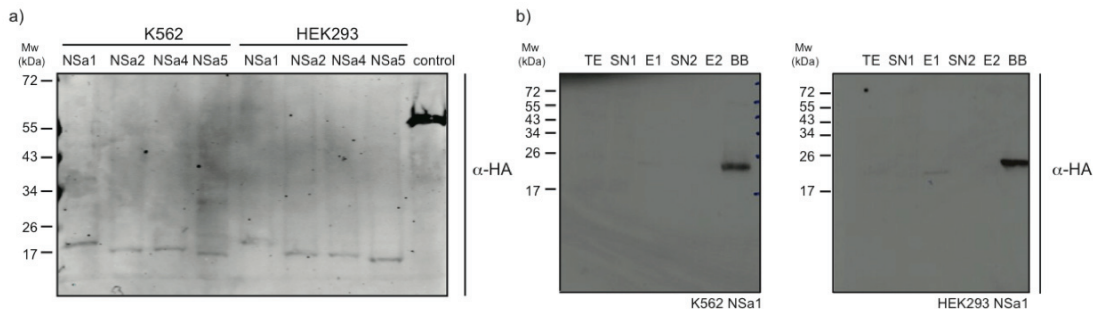


**Figure 2.7. Expression levels of Strep-HA tagged N-SH2 targeting monoclonal antibodies and affinity purification of NSa1 monoclonal antibody in K562 and HEK293 cells**

a) Expression levels of 4 monoclonal antibodies (NSa1, NSa2, NSa4, NSa5) in K562 and HEK293 cells for N-SH2 targeting monoclonal antibodies. pfMIG-Strep-3xHA-Shc1 K562 stable cell line used as an internal expression control. 100  $\mu$ g total cell lysate loaded in total volume of 20  $\mu$ L.

b) Strep-HA purification was performed in the same way as Figure 12. Abbreviations; TE: total extract (0.33%), SN1: flowthrough after streptavidin beads (0.33%), E1: biotin eluate from Streptactin beads (2%), SN2: flowthrough after anti-HA beads (2%), E2: acidic elution from anti-HA beads (3.2%), BB: boiled anti-HA beads. (% of input indicated in brackets)

TAP stable cell lines were generated in K562 and HEK293 cells by retroviral transduction, which was followed by tandem affinity purification. The binding of monoclonal antibodies to endogenous full length SHP2 was confirmed in both cell lines in a small-scale pull-down. IgG immunoprecipitation of monoclonal antibodies was performed with the use of protein G tag and then anti-SHP2 immunoblotting showed that NSa1, NSa5 and Cs3 were binding to full length endogenous SHP2, while Cs1 failed to bind to SHP2 (Figure 2.8a). We further confirmed that only the HA4 control monoclonal antibody pulled down c-Abl and Bcr-Abl in K562 stable cell lines, but the SHP2 targeting monoclonal antibodies did not interact neither with c-Abl nor Bcr-Abl (Figure 2.8b).

Moreover, when Bcr-Abl and monoclonal antibodies were transiently co-expressed in HEK293 cells, immunoprecipitation of anti-myc-tagged monoclonal antibodies (Figure 2.8c, lower panel) or anti-SHP2 (Figure 2.8c, middle panel) showed that NSa1, NSa5 and Cs3 were bound to SHP2 while Cs1 found to be bound to endogenous SHP2 to a lesser extent when compared with other monoclonal antibodies (Figure 2.8c).

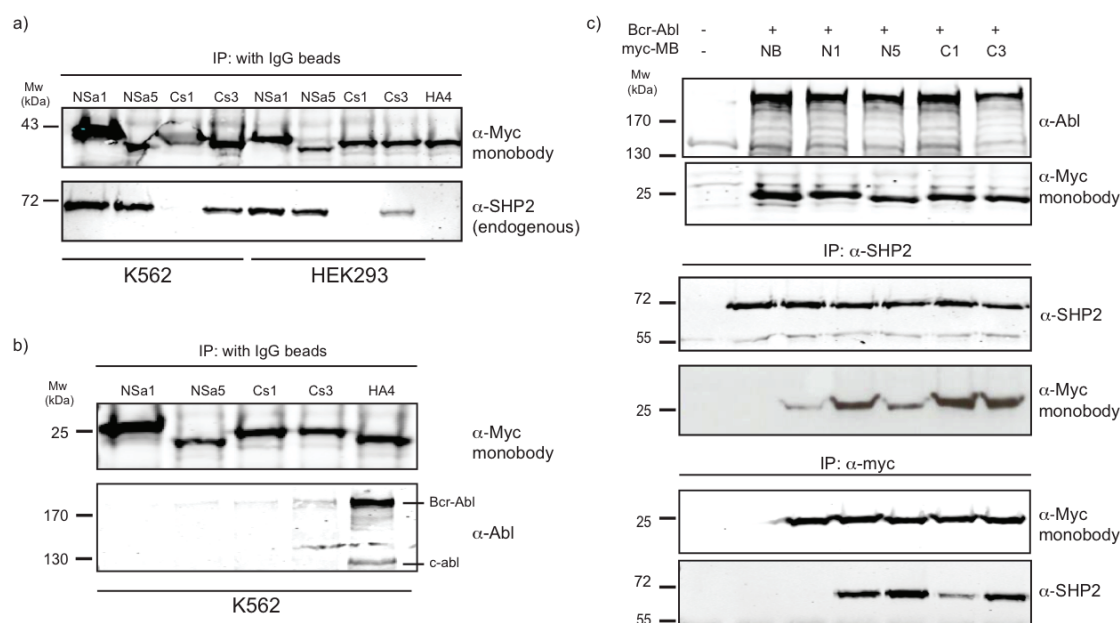


**Figure 2.8. SHP2-targeting monoclonal antibodies bind endogenous full-length SHP2 in transiently transfected HEK293 cells and TAP cell lines. Figure taken from (Sha et al., 2013)**

a) Immunoprecipitation of TAP-tagged monoclonal antibodies from HEK293 and K562 cell lines was performed by using IgG beads with 1 mg total cell lysate. Monoclonal antibodies were detected by using anti-myc-tag in the TAP construct (upper panel) and co-precipitated SHP2 was detected in both K562 and HEK293 cells using anti-SHP2 antibody (lower panel).

b) Immunoprecipitation of TAP-tagged monoclonal antibodies in K562 cell lines was performed by using IgG beads and binding of HA4 to c-Abl and Bcr-Abl was confirmed.

c) Myc-tagged monoclonal antibodies NSa1, NSa5, CS1 and CS3, as well as a non-binding (NB) control monoclonal body (HA4 Y87A) were transiently co-expressed in HEK293 cells along with Bcr-Abl (upper two panels). Immunoprecipitation of endogenous SHP2 showed binding of overexpressed monoclonal antibodies (middle panels). Immunoprecipitation of SHP2 targeting myc-tagged monoclonal antibodies showed co-immunoprecipitation of endogenous SHP2 (lower panels).

In stable monoclonal antibody expressing K562 and HEK293 cell lines, comparable expression levels of the monoclonal antibodies were obtained which was followed by anti-myc immunoblotting (Figure 2.9b). After affinity purification (Figure 2.9a), the bait monoclonal antibody was efficiently retrieved in the last elution fraction (Figure 2.9c). The presence of 1xmyc tag in the TAP vector construct enabled us to follow the expression of the protein by anti-myc immunoblotting. Despite the large amount of bait protein loss in the SN1 fraction, which is always the less efficient purification step, in the SN2 flowthrough fraction almost no bait protein was lost, which shows the efficiency of this method and a significant amount of bait protein was retrieved in the last elution fraction (E1), without any bound protein left on the streptactin beads (BB) in the last step (Figure 2.9c). The protein eluate was visualized by silver staining (Figure 2.9d, top panel). This data already shows that the purification yielded high amounts of bait protein around 17 kDa

and a prominent band around 70 kDa for NSa1, NSa5 and Cs3 but not for Cs1 monobody expressing cell lines, which is supposed to be SHP2 because of its molecular weight. There were also some additional bands weakly detected when compared to the band that was around 70 kDa. While NSa1, NSa5 and Cs3 were found to pull down this protein, Cs1 failed to co-immunoprecipitate with 70 kDa protein. Anti-SHP2 immunoblotting of the eluate sample also showed that NSa1, NSa5 and Cs3 were binding to SHP2 but not Cs1 (Figure 2.9d, lower panel). This result was in line with the pull downs that were made in one-step small scale purifications (Figure 2.8a). The TAP purifications were done in two biological replicates for both cell types and submitted for LC-MS/MS. SHP2 was by far the most abundant protein identified among the identified proteins from the affinity purification.

SHP2 was identified with high abundance in Nsa1, NSa5 and Cs3 monobody expressing cell lines. Around 1000 spectral count for N-SH2 targeting monobodies and more than 500 spectral counts for Cs3 targeting monobodies were detected for K562 and HEK293 cells. Even though Cs1 silver staining and immunoblotting did not result with a prominent signal for SHP2, more than 100 spectral counts were identified in both replicates for both cell lines. Strikingly, no other SH2 domain containing protein was found reproducibly in all eluates, for both replicates (Table 2.1). When the complexity of the cellular environment and the presence of approximately 120 expressed SH2 domains in cells is considered, this result quite strikingly showed the mono-specificity of monobodies for their targets.



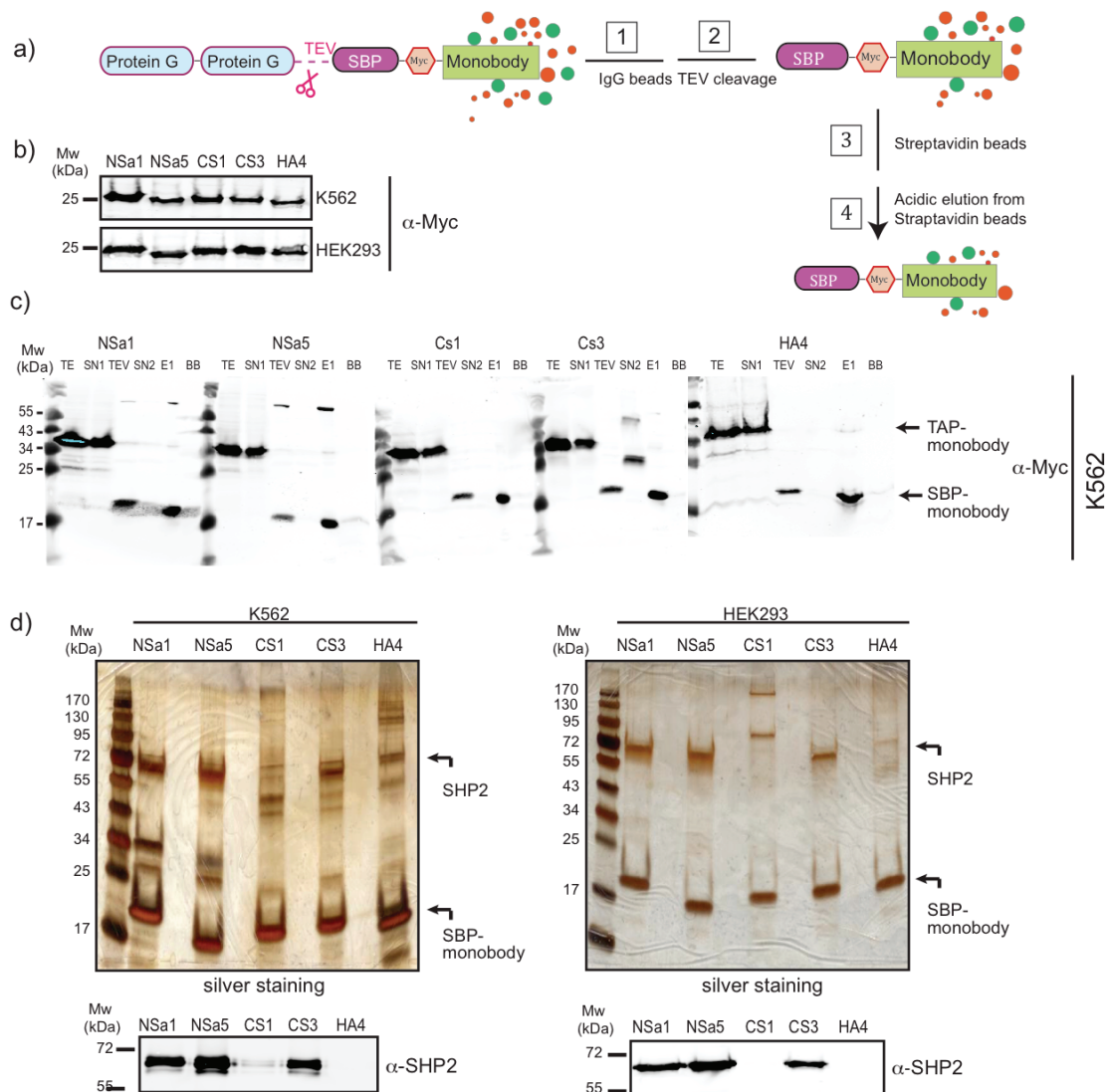


**Figure 2.9. Analysis of the SHP2-targeting monobody interactome** Figure taken from (Sha et al., 2013)

a) Schematic representation of TAP-tagged monobodies including the B1 domain of Staphylococcal protein G (Protein G), tobacco etch virus (TEV) protease recognition site, streptavidin-binding peptide (SBP) and myc-tag N-terminal to the monobody and the steps of tandem affinity purification.

b) Anti-Myc immunoblot analysis of total cell lysates of K562 and HEK293 stably expressing the TAP-tagged monobody clones. HA4 is a previously characterized monobody binding the SH2 domain of Abl and serves as an internal control.

c) Representative TAP of monobody complexes from K562 cells and anti-Myc immunoblotting performed to track the monobody expression. Abbreviations; TE: total extract (0.16%), SN1: supernatant IgG beads (0.16%), TEV: Eluate after TEV cleavage (2.5%), SN2: supernatant streptavidin beads (2.5), E1: eluate from Streptavidin beads (3.2%), BB: boiled Streptavidin beads to control efficiency of elution. The arrows on the blot show the molecular weight of monobodies before and after TEV cleavage (% of input indicated in brackets).

d) Visualization of the complexity of the final eluate by silver staining and immunoblotting against SHP2. Upper panel: Tandem affinity-purified monobody complexes (E1 fractions) from K562 and HEK293 cells were separated by SDS-PAGE and 10% of the eluate was used for silver staining. Lower panel: anti-SHP2 immunoblot analysis of 10% of the eluate.

Cell line	Bait	Total number of proteins identified*		Rank of SHP2 among all proteins**		Names and spectral counts (in brackets) of all identified SH2 domain-containing proteins in each sample	
		1st TAP	2nd TAP	1st TAP	2nd TAP	1st TAP	2nd TAP
		K562	NSa1	49	370	1	1
NSa5	53		256	1	1	SHP2 (1384)	SHP2 (1033)
CS1	119		275	6	8	SHP2 (210), TEC (74)	SHP2 (131)
CS3	112		285	1	1	SHP2 (800)	SHP2 (559), TYK2 (8)
HA4	74		106	33	8	ABL1 (159), SYK (107), INPPL1 (65), ABL2 (50), FYN (24), SHP2 (13), SHC1 (7), GRB2 (6)	ABL1 (90), SHP2 (76), INPPL1 (16), ABL2 (13), SYK (7), TYK2 (2)
HEK293	NSa1	201	527	2	1	SHP2 (768)	SHP2 (1583), GRB2 (5)
	NSa5	237	496	1	1	SHP2 (887)	SHP2 (2004), CSK (3), GRB2 (4)
	CS1	170	547	12	12	SHP2 (110)	SHP2 (258), TEC (8), INPPL1 (3), ABL2 (3)
	CS3	249	609	2	1	SHP2 (418)	SHP2 (1187), FYN (2)
	HA4	166	471	13	22	ABL2 (298), INPPL1 (244), SYK (37), ABL1 (31), FYN (20), SHP2 (12), ZAP70	ABL2 (533), INPPL1 (534), SYK (49), ABL1 (38), SHP2 (25), FYN (17), STAT5A (4), ZAP70 (2), CRKL (2)

**Table 2.1. Overview of mass spectrometry results from SHP2 monobody interactome analysis. Table taken from (Sha et al., 2013)**

\*Proteins were scored as identified if at least 2 unique peptides were detected. \*\*All identified proteins, including common contaminants, such as Keratin, were sorted by the number of assigned spectra from highest to lowest.

### 2.3.3 SHP2 targeting monobodies inhibit SHP2 activity in Bcr-Abl dependent signaling pathway

The specificity and affinity of the monobodies against their cognate SH2 domains were demonstrated in vitro (section 2.3.1). On the other hand, monobodies were shown to be mono-specific for their target SH2 domain in cells and the crystal structure demonstrated that monobodies occupy the phosphotyrosine binding site of SH2 domains. In order to further evaluate the effects of monobodies in cells, Bcr-Abl and SHP2 were co-expressed together with SHP2 targeting monobodies in HEK293 cells. The expression of the monobodies and SHP2 were followed anti-myc immunoblotting and all three proteins were expressed to similar levels, which has a critical importance for the evaluation of the results (Figure 2.10a, last 3 panels). Upon NSa1, NSa5 and Cs3 expression, a very strong decrease was observed in the intensity of a tyrosine phosphorylated band around 90 kDa when compared to non-binding control monobody (Figure 2.10a, upper panel). In the case of Cs1, we did not observe such a decrease of this 90 kDa phosphotyrosine band. The molecular weight of this band was in line with the 6xmyc-tagged SHP2 that we used in these experiments. Then, we wanted to find out whether this band is phosphorylated SHP2 or not. Anti-SHP2 immunoprecipitation followed by an anti-total phosphotyrosine immunoblotting showed that this band was indeed

phosphorylated SHP2, and phosphorylation was decreased in the presence of monobodies (Figure 2.10b). There are two important tyrosine residues that were previously described to have an important role in regulating SHP2 activity (Araki, Nawa, & Neel, 2003; Bennett, Hausdorff, O'Reilly, Freeman, & Neel, 1996). Lu et al. used nonhydrolyzable phosphotyrosine analogs and demonstrated that Y542 interacts with the N-SH2 domain to relieve the basal autoinhibited state of SHP2 and Y580 stimulates the activation of SHP2 by interacting with C-SH2 domain intramolecularly (Lu et al., 2001). These two residues, Y542 and Y580, were investigated by mutational analysis (Figure 2.10c). Upon co-expression with Bcr-Abl, SHP2 pull down and total phosphotyrosine immunoblotting showed that SHP2 Y542F single mutant showed tyrosine phosphorylation although for SHP2 Y580F single mutant, no total tyrosine phosphorylation was detected (Figure 2.10c, lower panels). In the double mutant SHP2, very low tyrosine phosphorylation was detected similar to single Y580F mutant. This result indicated that Y580 is the predominant site phosphorylated by Bcr-Abl. Interestingly, monobody expression significantly decreased the Y580 phosphorylation, however, Cs1 was not as effective as the other monobodies (Figure 2.10a, second panel). It is also noteworthy to mention that, monobodies were able to decrease the phosphorylation of the E76K mutant of SHP2, which is an activating mutation located in the N-SH2 domain and reported to have constitutive SHP2 activation (Keilhack, David, McGregor, Cantley, & Neel, 2005). NSa1 and NSa5 diminished the phosphorylation of SHP2 E76K when compared to a non-binding control monobody (Figure 2.10a, last 3 lanes in upper two panels). These data showed that SHP2 targeting monobodies decreased SHP2 phosphorylation at a critical tyrosine residue in Bcr-Abl expressing cells. The C-terminal tail tyrosine phosphorylation of SHP2 is important for increased SHP2 activity so we assumed that the significant decrease of phosphorylation of SHP2 might indicate a parallel decrease in activity.



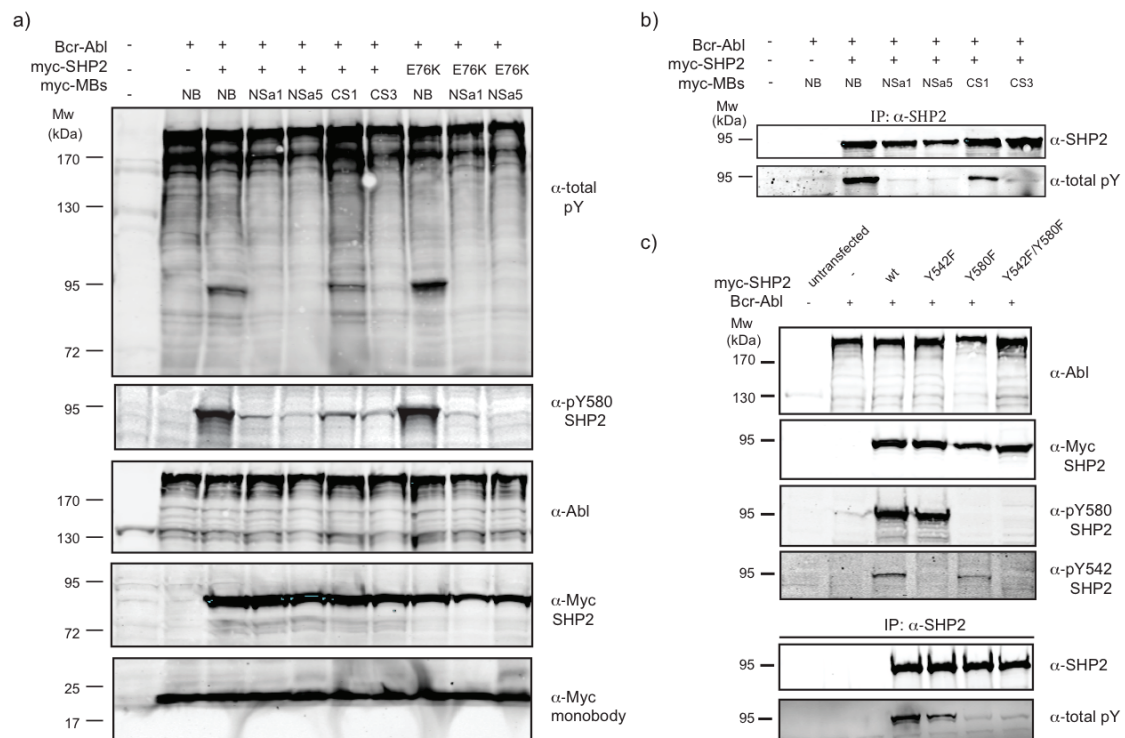


**Figure 2.10. Monobodies inhibit SHP2 phosphorylation in cells. Figure taken from (Sha et al., 2013)**

a) HEK293 cells were transiently transfected with the indicated expression constructs and total cell lysates immunoblotted with the indicated antibodies. E76K is an activating point mutation in SHP2, NB is a non-binding control monobody.

b) SHP2 was immunoprecipitated from HEK293 cell lysates that were transfected with the indicated expression constructs and immunoblotted with anti-SHP2 and anti-total phosphotyrosine antibody.

c) SHP2 Y580 is the predominant site affected by monobody expression and Y542 and Y580 are the two principal SHP2 phosphorylation sites in the conditions of the experimental set-up. myc-tagged SHP2 wt, single or double mutations in residues Y580 and Y542 into phenylalanine (Y580F and Y542F) were overexpressed with Bcr-Abl in HEK293 cells (upper two panels) and probed with phosphosite-specific antibodies for pY542 and pY580 (middle two panels). In the lower two panels, anti-SHP2 immunoprecipitated was performed with 1 mg total cell lysate and total tyrosine phosphorylation detected with a total anti-pY antibody (lower two panels).

### 2.3.4 SHP2 targeting monobodies inhibit the interaction of SHP2 with Gab2

SHP2 binding to the Gab2 scaffold protein is well described in the literature and the binding of its SH2 domains to Gab2 is an important mechanism of SHP2 activation (H. Gu et al., 1998). Monobodies already demonstrated an inhibitory effect between SHP2 SH2 domains and the Gab2 tandem phosphopeptide in vitro, so we were motivated to find out the cellular effects of monobodies in terms of the interference of SHP2-Gab2 interaction.

Immunoprecipitation experiments of endogenous SHP2 and Gab2 were performed in HEK293 cells that co-express Bcr-Abl and myc tagged monobodies. When NSa1 or NSa5 were expressed in cells, a strongly reduced Gab2-SHP2 interaction was observed upon immunoprecipitation of SHP2 or Gab2, whereas no reduction was observed with Cs1 or Cs3 expression (Figure 2.11a). This result was also confirmed by using a HEK293 cell line stably expressing HA-tagged Gab2.

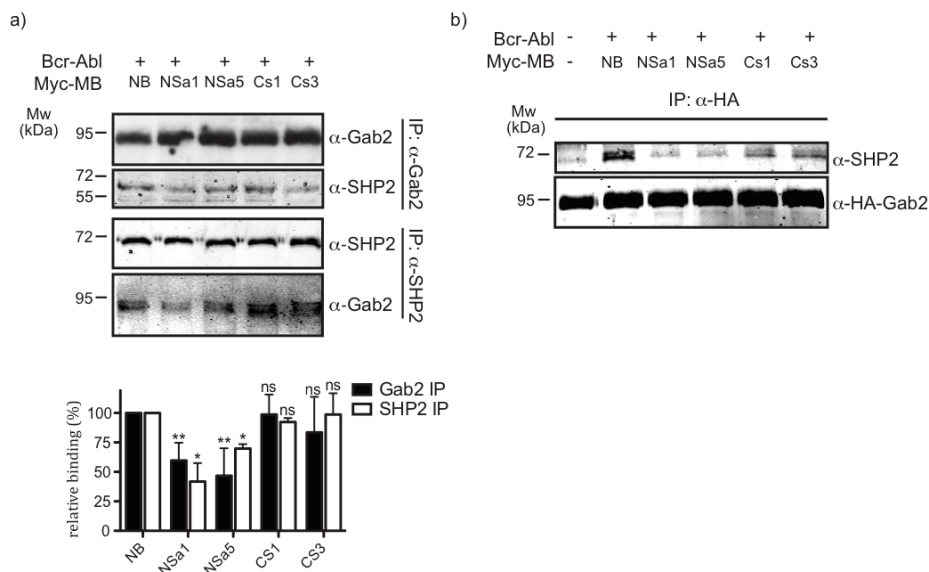


**Figure 2.11. Expression of monobodies decouples Gab2 and SHP2. Figure taken from (Sha et al., 2013)**

a) The interaction of endogenous SHP2 and Gab2 was monitored by reciprocal immunoprecipitation experiments upon overexpression of monobodies and Bcr-Abl. The bar graph shows the quantification of the SHP2-Gab2 interaction and its perturbation by monobody expression from six (for IP: Gab2) and two (for IP: SHP2) independent experiments (ns: not significant, \*:  $p < 0.05$ , \*\*:  $p < 0.005$ ).

b) The interaction of endogenous SHP2 with Gab2 in the presence of monobodies was studied in HEK293 cells that stably overexpress HA-tagged Gab2.

When Bcr-Abl and monobodies were overexpressed in this cell line, the interaction between endogenous SHP2 and overexpressed HA-tagged Gab2 was more prominently inhibited than the endogenous SHP2 and Gab2 interaction disruption when compared to non-binding monobody (Figure 2.11b). These results suggested that monobodies targeting the N-SH2, but not C-SH2 domain, might potently decouple SHP2 from Gab2 and thus the Bcr-Abl protein complex, thereby inhibit SHP2 activity.

### **2.3.5 SHP2 targeting monobodies inhibit downstream signaling of SHP2**

Since a decreased tyrosine phosphorylation and thus inactivation of SHP2 was observed in cells, the modulation of downstream signaling of SHP2 was investigated. STAT5 protein activity is positively regulated with SHP2 activity. Li et al. demonstrated that SHP2 has a critical role in regulating STAT5 activity in human CD34<sup>+</sup> cells (Li et al., 2011). The consequences of monobody expression on STAT5 phosphorylation was evaluated in Bcr-Abl overexpressed HEK293 cells. In this set of experiments, SHP2 wild type and the Y580F mutant were also compared where no phosphoband detected for Y580 site when specific phosphoantibody used (Figure 2.12a). STAT5 phosphorylation was decreased upon NSa5 monobody expression, although NSa1 had no inhibitory effect on STAT5 phosphorylation. Similarly, Cs3 decreased STAT5 phosphorylation although Cs1 also did not show inhibitory effect on the STAT5 phosphorylation (Figure 2.12a).

Paxillin is a multi-domain adapter protein located at the focal adhesions to the sites of cell adhesion to the extracellular matrix (Turner, 2000). It contains several motifs that enables protein-protein interaction, including SH3-domain binding site, SH2 domain binding sites which generates docking sites (Schaller, 2001). Ren et al. showed that paxillin is dephosphorylated by SHP2, which is recruited by Gab2 scaffold protein (Ren et al., 2004). When Bcr-Abl, myc-tagged monobodies and HA-tagged paxillin were overexpressed in HEK293 cells (Figure 2.12b, upper three panels), difference in the phosphorylation status of paxillin was observed. Upon NSa1 and Cs3 expression, anti-total phosphotyrosine immunoblotting showed an increased prominent phospho-band around 72 kDa which is in line with HA-tagged paxillin while NSa5 and Cs1 or the non-binding control monobody did not cause an increase in the phosphorylation (Figure 2.12b, fourth panel). In order to further confirm the paxillin phosphorylation, anti-HA immunoprecipitation was performed and indeed, paxillin showed an increased phosphorylation in response to NSa1 and Cs3 expression (Figure 2.12b, lower two panels).

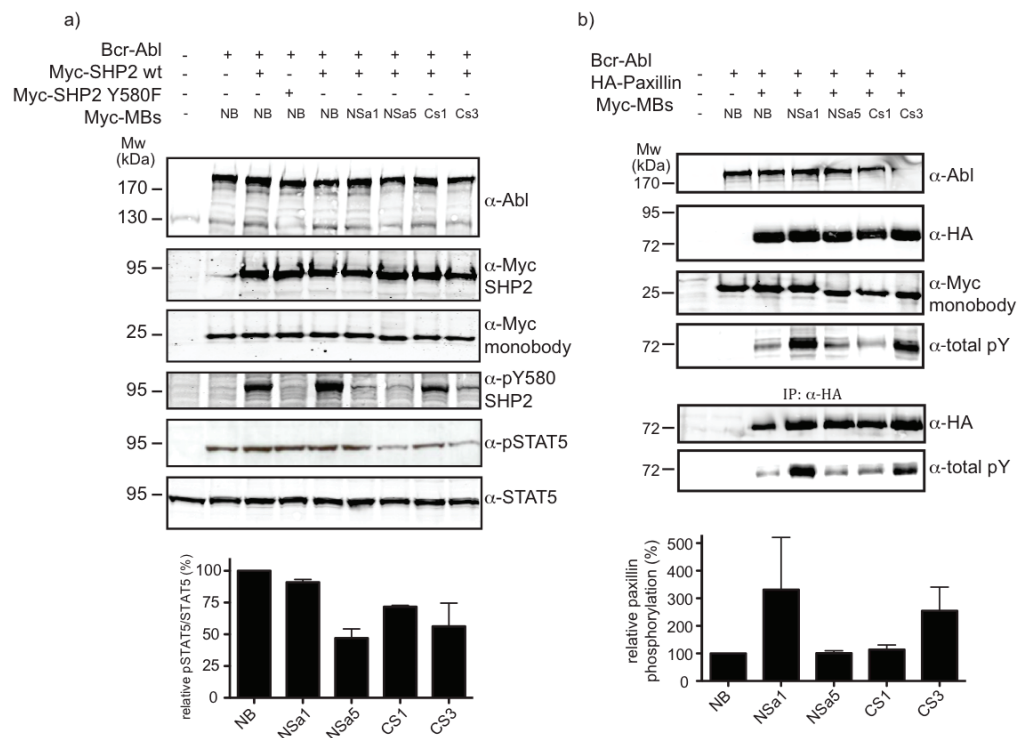


**Figure 2.12. Modulation and downstream signaling perturbation of SHP2 in HEK293 cells. Figure taken from (Sha et al., 2013)**

HEK293 cells were transiently transfected with the indicated expression constructs and total cell lysates immunoblotted with the indicated antibodies. The bar graphs show the quantification of the phosphorylation of STAT5 (a) and paxillin (b) and its perturbation by monobody expression from two representative independent experiments.

The MAPK pathway is known to be an important pathway that is positively regulated with increased SHP2 activity. SHP2 is an indirect activator of this pathway and thus increased SHP2 activity induces ERK phosphorylation (Araki et al., 2003; Dance, Montagner, Salles, Yart, & Raynal, 2008). First, ERK phosphorylation was investigated in response to EGF stimulation in HEK293 cells where SHP2 and monobodies were co-expressed. Upon stimulation with EGF, ERK phosphorylation was induced when compared to unstimulated cells (Figure 2.13). However, no difference was monitored in ERK phosphorylation upon monobodies expression (Figure 2.13, third panel).

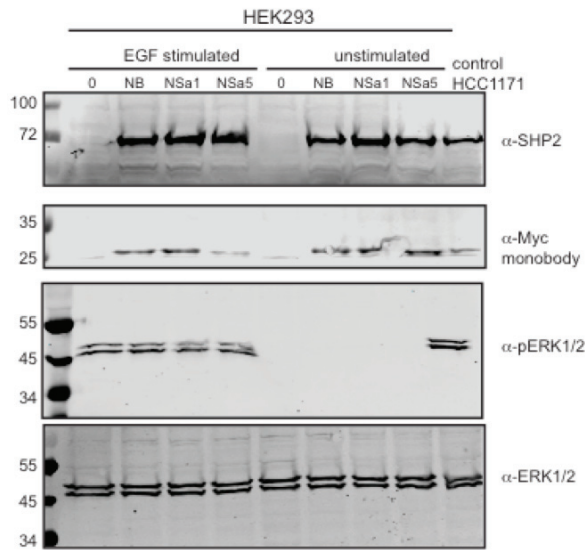


**Figure 2.13. ERK phosphorylation in HEK293 cells co-expressing SHP2 and monobody upon EGF stimulation**

The cells were co-transfected with 6xmyc-tagged SHP2 and monobodies (upper two panels). After 48 hours of post-transfection, the cells were stimulated with 1  $\mu\text{g}/\mu\text{L}$  EGF overnight in serum free medium and then lysed. The stimulated cells showed ERK phosphorylation when compared to unstimulated cells. HCC-1171 cells were loaded as an internal control cell line to detect ERK phosphorylation (third panel).

Then we decided to look into some solid tumor cell lines in order to have a good candidate cell line to evaluate the monobody effects on ERK phosphorylation (Figure 2.14). We were particularly interested in the H-661 and HCC-1171 cell lines, which were reported to possess activating point mutations in SHP2. The H-661 cell line has N58S mutation in the N-SH2/PTP domain interface and mutation of asparagine 58 into serine is an activating mutation. The HCC-1171 cell line possesses a V46L mutation, which is located on the N-SH2 domain, and mutation into leucine causes the constitutive activation of SHP2 (Figure 2.14, right panel) (Bentires-Alj et al., 2004).

The expression levels of Abl, SHP2, ERK, Gab2, and Gab1 proteins, and subsequently phosphorylation of SHP2 and ERK proteins were examined (Figure 2.14, left panel). All cell lines were shown to have comparable expression levels of total Abl, SHP2 and ERK. However, the expression levels of Gab1 and Gab2 were different in this set of cell lines, and when Gab2 was expressed high, the Gab1 protein was expressed low and vice versa. H1650 and H1975 cells have low Gab2 expression while they have high Gab1 expression. In similar manner, T-47D, H661, HCC-1171 and HCC-1954 cells have low Gab1 expression, in contrast,

they express high levels of Gab2 protein (Figure 2.14, left panel). Moreover, these cell lines only showed phosphorylation of Y542 but not Y580 residue, while Y580 was the dominant phosphorylated residue in Bcr-Abl stimulated cells. The Y542 residue phosphorylation also showed high correlation with Gab2 expression. Importantly, these cell lines demonstrated different levels of ERK phosphorylation (Figure 2.14, left panel). For instance, H1650 cells had almost no ERK phosphorylation while HCC-1171 cells have the highest ERK phosphorylation in this cell line panel. So we selected the HCC-1171 cell line because of its high Gab2 expression and ERK phosphorylation to further investigate the effects of monobodies (Figure 2.14, left panel).

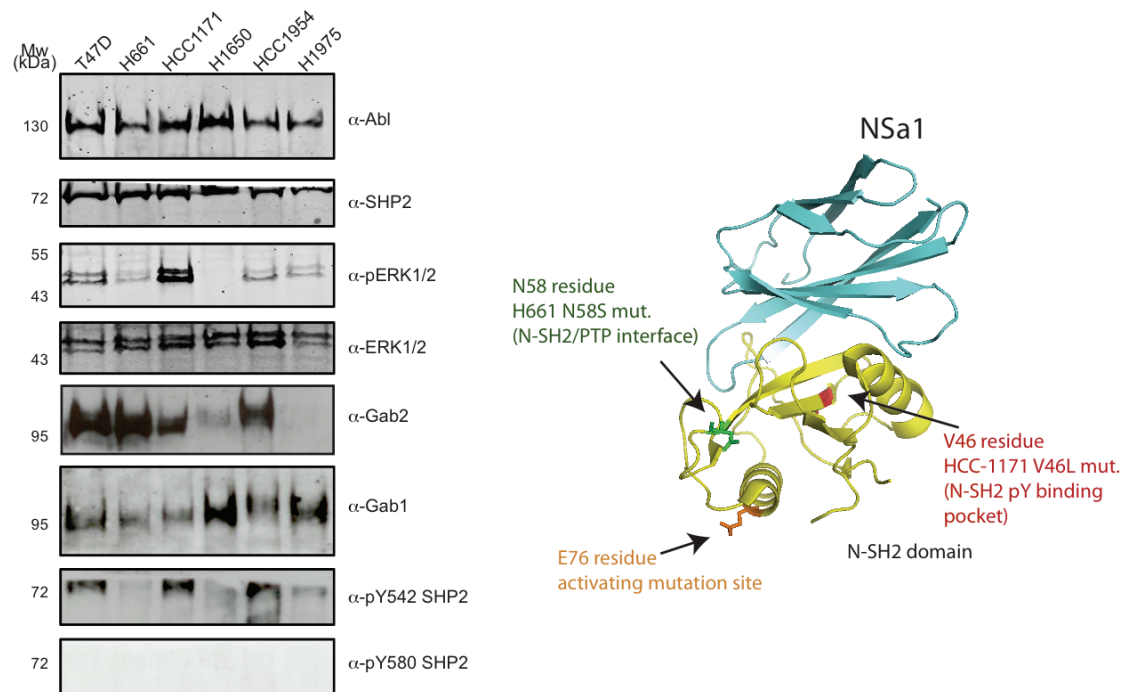


**Figure 2.14. Expression profile of solid tumor cell lines and mutated residues of SHP2 in H661 and HCC-1171 cell lines.**

Left: Parental solid tumor cell lines were subjected to immunoblotting with indicated antibodies. The definition of the cell lines are as follows; T-47D: ductal carcinoma, H-661: large cell lung cancer carcinoma, N58S mutation (N-SH2-PTP interface), HCC-1171: Epithelial cell, non-small cell carcinoma, V45L mutation (N-SH2 pY binding pocket), H1650: lung adenocarcinoma EGFR (DelE746A750), H1975: non-small cell lung cancer, EGFR (T790M/L858R), HCC1954: ductal carcinoma, ERBB2 amplification.. 100  $\mu$ g total cell lysate loaded in total volume of 20  $\mu$ L.

Right: Crystal structure of NSa1/N-SH2 complex showing the point mutations in H661, HCC-1171 and E76K constitutive activating mutation which is frequently seen in SHP2. This structure shows that these point mutations are not in the binding interface of monobody and N-SH2 domain.



Moreover the presence of a SHP2 activating point mutation makes this cell line even more interesting to investigate the roles of SHP2 SH2 domain targeting monobodies. The structural location of the V46 residue was checked and this residue was not in the N-SH2/NSa1 binding interface which eliminates the possibility of the V46L mutation to disrupt the binding of monobodies to the N-SH2 domain (Figure 2.14, right panel).

Transient transfection of these cells with monobodies did not result with high expression levels when compared to HEK293 cells, which is mostly used for transfection experiments because of the ease of transfection. Afterwards stable HCC-1171 cell lines expressing SHP2 SH2 domain targeting monobodies and non-binding control monobody were generated with retroviral transduction. After transduction of producer HEK293gp cells were performed by using the retroviral expression vector, HCC-1171 lung cancer cells were infected with the virus and then sorted by FACS.

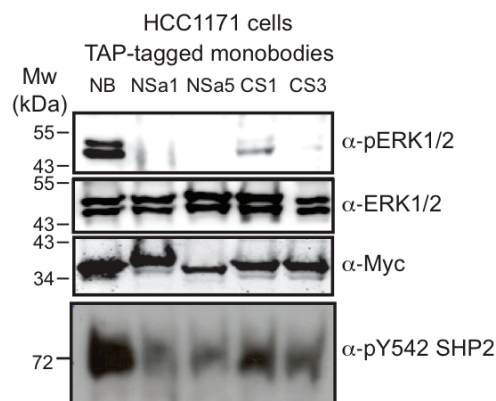


**Figure 2.15. ERK and SHP2 phosphorylation in stable HCC-1171 cells upon monobody expression. Upper figure panels taken from (Sha et al., 2013)**

HCC-1171 stably transduced with the TAP-tagged monobody clones and total cell lysates immunoblotted with the indicated antibodies.

Finally, the monobodies showed comparable expression levels (Figure 2.15, upper third panel). Strikingly, NSa1, NSa5 and CS3 almost completely abolished ERK phosphorylation although in Cs1 expressing cells, very mild ERK phosphorylation was detected (Figure 2.15, upper panel). Moreover, the SHP2 Y542 phosphorylation was also decreased significantly upon monobody expression while NB and Cs1 expressing cells still showed SHP2 phosphorylation (Figure 2.15, lower panel).

In spite of the fact that ERK activation is very important cell growth and proliferation (W. Zhang & Liu, 2002), abolishment of the ERK phosphorylation by monobodies did not result a change in growth of the cells when the proliferation of the stable HCC-1171 cell lines were analyzed in a time dependent manner (Figure 2.16).

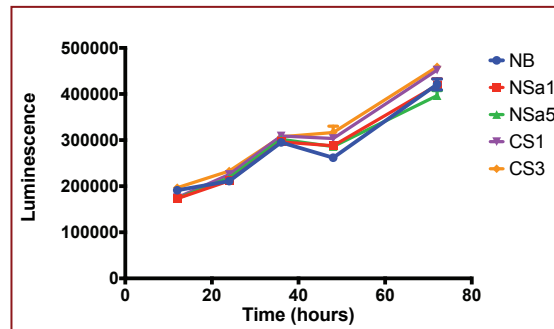


**Figure 2.16. Cell proliferation assay of stable HCC-1171 monobody cell lines**

Cells were seeded at  $5 \times 10^4$  per well as the starting cell number in 96-well plate with six replicates. Cell growth measured by Cell TiterGlo assay after 12-24-36 and 48 hours (see materials and methods for detailed protocol).

### **2.3.6 Inducible expression system of SHP2 targeting monobodies in HCC-1171 non-small cell lung cancer cell line**

As shown above, retrovirally transduced SHP2 targeting monobodies showed a significant reduction in ERK phosphorylation in HCC-1171 cells (Figure 2.15). Since MAPK is a very important pathway for the cell proliferation, we were motivated to see an effect on cell proliferation upon monobody expression. In the retroviral system, the possible adaptation of the cells for monobody expression might be a reason for not seeing any changes in cell proliferation.

In order to investigate the physiological roles of SHP2 targeting monobodies, we took advantage of an inducible expression system. Therefore, inducible expression of monobodies were investigated in order to get a sudden expression of monobodies and response from the cells. Unlike retroviral vector promoter, in the inducible lentiviral expression system a stronger promoter, which is EF-1 alpha, was utilized. HCC-1171 cells expressing a constitutive active mutant (V46L) of SHP2, as mentioned above, were used for this system.



We have adapted the system from Didier Trono's lab. The tetracycline controlled hybrid protein tTR-KRAB was used in this system in where a tetracycline repressor is (tTR) fused to the KRAB (Kruppel associated box) domain of human Kox1 zinc finger protein. KRAB is a transcriptional module in many types of zinc finger containing proteins that is thought to induce the formation of heterochromatin structure and thus suppress the expression of nearby genes up to 3kb from its binding site. Fusion to the tTR enables the modulation of the transcription from tet operator. In the absence of doxycycline, tTR-KRAB binds to tetO and suppress the promoter, while in the presence of doxycycline, the repressor is removed from the promoter and this facilitates a controllable expression or suppression (in case of siRNA) of genes (Figure 2.17) (Wiznerowicz & Trono, 2003).

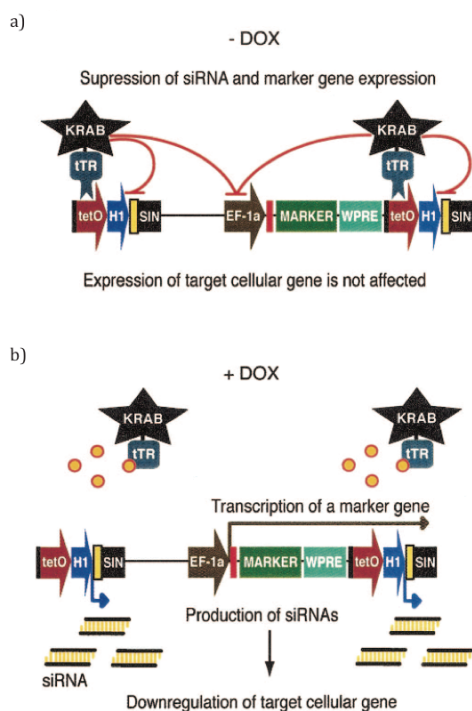


**Figure 2.17. Mode of action of the DOX-controllable transrepressor**

Activation mechanism of a gene in doxycycline controlled expression

In the absence of doxycycline (a), tTR-KRAB binds to tetO and the expression is suppressed. In the presence of doxycycline (b), tTR-KRAB is removed and the expression of the gene enabled.

Taken from (Wiznerowicz & Trono, 2003)

Firstly, large-scale tTR-KRAB lentivirus was produced in 293T cells by co-transfection of helper gene, envelope gene and the gene of interest, which is pLV-tTR-KRAB-IRES-dsRED. Following the transfection, the lentivirus was harvested from the supernatant of 293T virus producer cells and then concentrated by ultracentrifugation. Afterwards, parental HCC-1171 cells were infected with tTR-KRAB lentivirus and then sorted for dsRED expression. Following this, lentivirus

for the pLV-tTR-monobody-IRES-GFP constructs targeting SHP2 SH2 domains were also produced. An IRES-eGFP selection marker was cloned to the C-terminus of the monobody construct and thus the cells expressing this construct could be selected for eGFP expression. Stable sorted tTR-KRAB HCC-1171 cells were used to infect with monobody lentivirus. When the cells transduced first with the tTR-KRAB repressor and then with monobodies, in the absence of doxycycline, tTR-KRAB repressor mediated suppression of monobody construct expression was observed. Once the cells were induced with doxycycline, the tTR-KRAB repressor is removed from the promoter region of monobody-expressing vector and then the protein is expressed.

Following the production of the lentiviral monobody virus, we performed virus titration in parental HCC-1171 cells in order to find out the efficiency of the lentivirus preparation, which was performed by a serial dilution of the virus preparation. The expression of monobodies were followed by GFP selective marker. With increasing concentrations of lentivirus, increased GFP signal was followed by FACS by using parental cells as negative control (Figure 2.18a).

According to the titration data of the virus, 20  $\mu$ L of lentivirus for NSa1 and NSa5, 31  $\mu$ L for Cs1, 13  $\mu$ L for Cs3 and 14  $\mu$ L for non-binding (NB) monobody lentivirus were used in order to infect 100% of the HCC-1171-tTR-KRAB cells (Figure 2.18b). We have also optimized the doxycycline concentration and induction time for protein expression in small scale (Figure 2.19a). The HCC-1171-tTR-KRAB cells were infected with the NSa1 lentivirus and the cells were incubated with the indicated doxycycline concentrations and induction time points. The expression of the monobodies did not show significant differences with the different doxycycline concentrations. Therefore, we decided to use 4 $\mu$ g/mL for 48 hours of induction (Figure 2.19a).

Then, the HCC-1171-tTR-KRAB cells were incubated with the virus for 48 hours and then induced with doxycycline in order to check the induction efficiency of the cells. Nonetheless, FACS analysis of the induced cells showed that they were not 100% GFP positive. As a consequence, in order to have 100% GFP positive population, we infected the stable HCC-1171-tTR-KRAB cells again with the monobody lentivirus and then induced them with doxycycline. After

keeping the cells under doxycycline induction for 5 days. The cells were sorted for double positive population; dsRED (tTR-KRAB) and GFP (monobody).

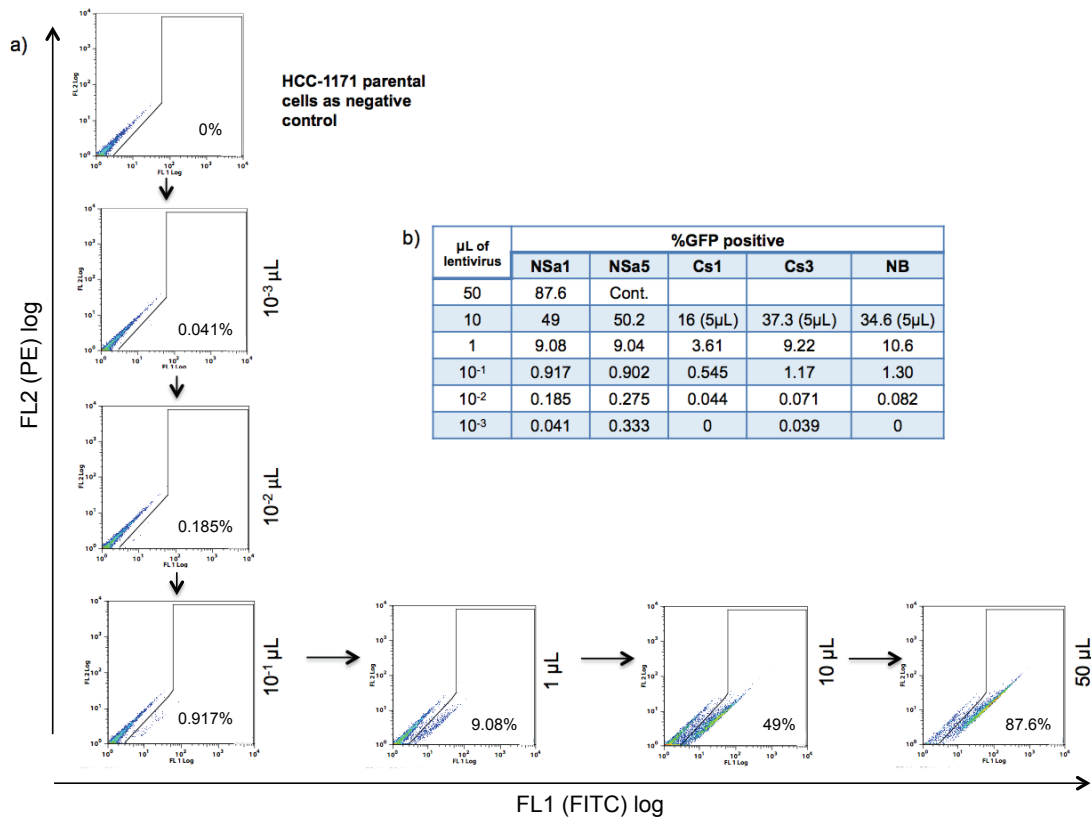


**Figure 2.18. FACS analysis of the lentivirus titration**

a) Representative FACS analysis of HCC1171 cells infected with NSa1 lentivirus with different amounts. The maximum virus amount used in the titration is 50 μL. Virus solution prepared with a serial dilution in medium. The cells were incubated with the lentivirus for 48 hours and then analyzed for the GFP expression. X axis of the graphs shows the FL2 (PE) log, Y axis of the graph shows the FL1 (FITC) log values.

b) The table showing the virus titration and the GFP positivity for all SHP2 SH2 targeting monobodies. For Nsa1 and Nsa5, the highest lentivirus amount used is 50 μL while for Cs1, Cs3 and NB monobody, the highest amount is 5 μL. NSa5 construct got contaminated when 50 μL lentivirus used (Cont.). With the lowest virus amount, Cs1 and NB showed 0% GFP positive cells.

Once we designed the experimental set-up described above which requires the induction and then sorting of the cells, we needed to remove doxycycline from the cells just after sorting because it is also important to have the cells in an uninduced-state which means no expression of the protein to start with. In order to achieve this, we needed to remove doxycycline from the cells to withdraw expression of monobody, but how much time is required to eliminate the protein expression? In order to find out the question, doxycycline withdrawal was performed in unsorted cells in which monobody-lentivirus-

infected tTR-KRAB cells were induced with doxycycline for 48 hours, then the doxycycline was removed from the cell medium and the cells were analyzed by anti-myc immunoblotting in every passage to track the expression of the monobody (Figure 2.19b). Between days 8-12, monobody expression was almost vanished (Figure 2.19b, lower panel). Following the sorting, the cells were cultured for 10 days without doxycycline in order to remove the protein expression.

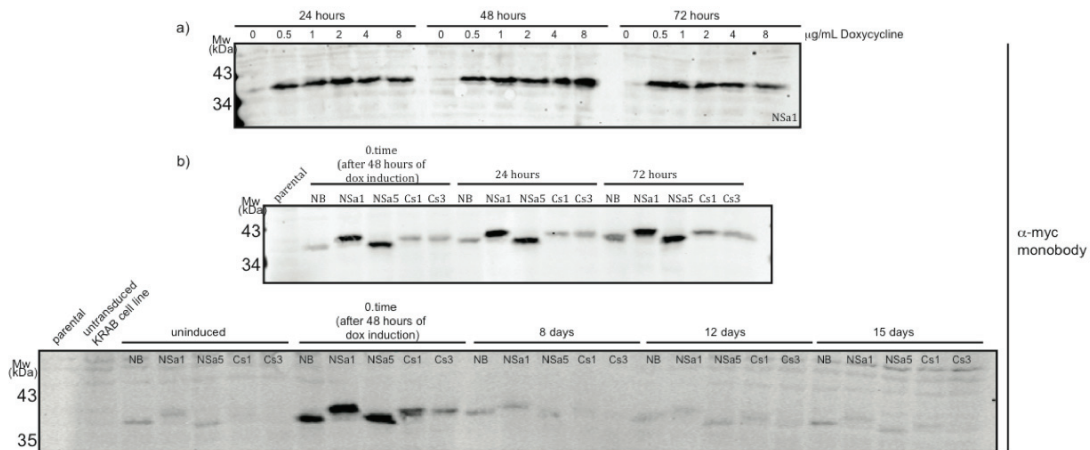


**Figure 2.19. Doxycycline concentration and induction time optimization and doxycycline withdrawal assay**

a)  $2 \times 10^5$  HCC-1171-tTR-KRAB cells were seeded in 6-well dishes and infected with NSa1 lentivirus. After 48 hours of infection, the cells were induced with doxycycline with the indicated concentrations and time periods. After the end of the time points the cells were lysed and subjected to anti-myc immunoblotting.

b)  $2 \times 10^5$  HCC-1171-tTR-KRAB cells seeded in 6-well dishes and infected with NB, NSa1, NSa5, Cs1 and Cs3 lentivirus. After 48 hours of infection, the cells were induced with 4 µg/mL doxycycline for 48 hours and at the end of this (0.time), the cells were washed and split without doxycycline. The cells were kept in culture without doxycycline for 15 days and in everytime point, samples spared for anti-myc immunoblotting. HCC-1171 parental and HCC-1171-tTR-KRAB untransduced cells loaded as controls.

After confirmation of protein expression depletion in the sorted cells, induction of the cells was started with doxycycline at 4 µg/µL. The cells were kept under doxycycline for 10 passages. The cells were split every three days. In every passage, the cells were counted, and cell samples spared for immunoblotting and as well as FACS analysis.

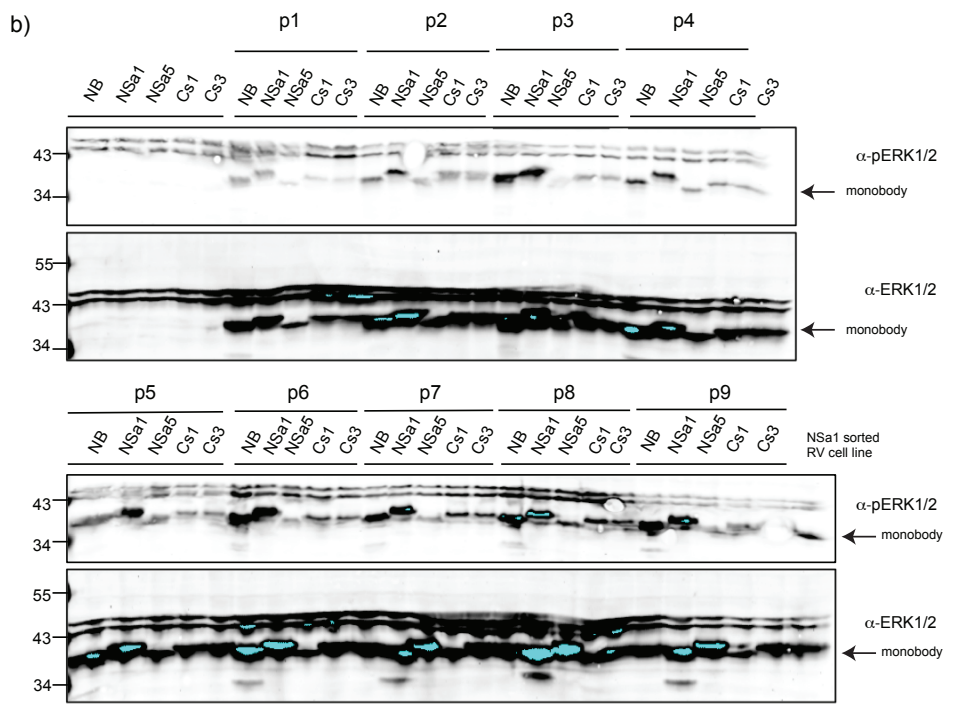
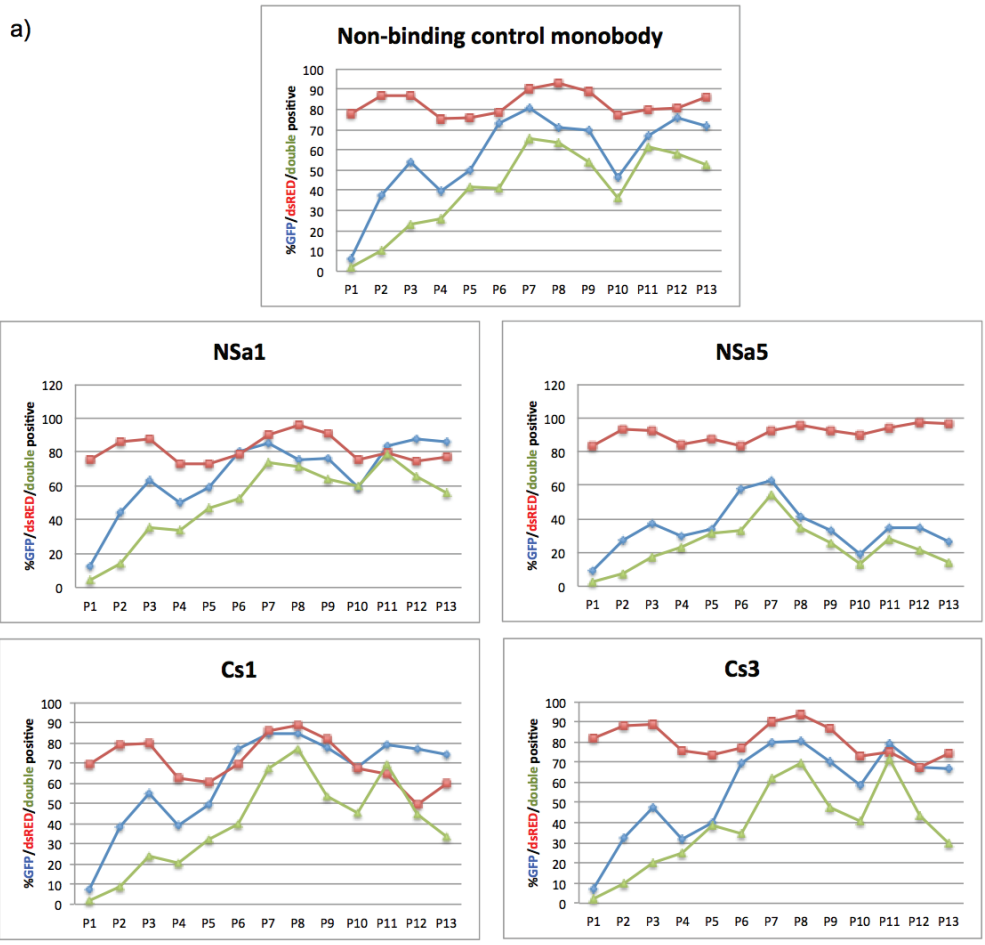


**Figure 2.20. FACS analysis and immunoblot detection of the SHP2 SH2 targeting monobodies and ERK phosphorylation in inducible cells.**

The stable cell line for each construct were seeded  $3 \times 10^5$  cell/mL and kept under doxycycline induction. Every passage, the cells were split to the same number of cells. Every splitting time,

cells were counted in triplicates, then half of the rest is analysed for FACS, the other half is centrifuged down, and snap frozen for WB.

a) FACS analysis of SHP2 SH2 targeting transduced cells HCC-1171-tTR-KRAB over 13 passages and the cells were split twice a week. The cells were analyzed for their dsRED and GFP expression. Single and double positive population was graphed and dsRED, GFP double positive population is graphed as red, blue and green bars, respectively.

b) The samples from every passage were lysed and analyzed for ERK phosphorylation and total ERK. Because of the presence of protein G tags, the monobody expression also detected with the secondary antibody that are indicated with arrows. Retrovirally transduced NSa1 stable cell line loaded as internal control.

The expression of the monobodies increased starting from the first passage when compared to the uninduced cells (Figure 2.20b). The expression of monobodies was not even and non-binding control monobody and NSa1 were expressed more than NSa5, Cs1 and Cs3 (Figure 2.20b). This was an unexpected observation because we were expecting to observe a similar level expression among monobodies. In the sixth passage, the expression levels of NB and NSa1 monobodies were comparable with the retrovirally transduced NSa1 control cell line. However, the FACS analysis of the cells were surprising, because even though the cells were sorted for double positivity and we were working with 100% positive monobody transduced cells, the first dose of doxycycline did not result in a high GFP positivity (Figure 2.20a). To our surprise, the population was even lower than 10% GFP positive. The comparable expression levels were observed with the sorted NSa1 retroviral stable cell line at fifth passage which might be a consequence of the stronger promoter (Figure 2.20b). Moreover, when we keep the cells under doxycycline induction for 13 passages, we could not induce the whole population for monobody expression. Furthermore, the GFP signal started to decrease after passage 9 (Figure 2.20a). On the other hand, we could not observe a change in ERK phosphorylation when compared to non-binding monobody, unlike in our retroviral transduction system (Figure 2.20b).

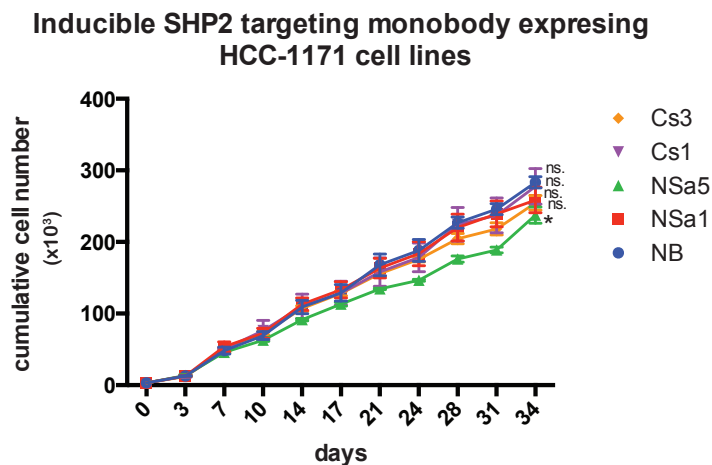


**Figure 2.21. Cumulative cell number of SHP2 SH2 targeting monoclonal antibodies in inducible cells**

The cells were counted in triplicates in each passage over 34 days and then splitted to the same cell number in every passage. Afterwards, the cumulative cell growth was calculated by multiplying the cell number with the dilution factor and by adding to the results on to the counts before.

The cells were counted every passage in triplicates. Then, the cumulative cell proliferation of the cells were calculated, however monoclonal antibody expression did not result a significant change of proliferation when compared to the non-binding monoclonal antibody control over 10 passages. Only NSa5 showed a decreased cell proliferation when compared to non-binding monoclonal antibody (Figure 2.21).

### 2.3.7 Tandem monoclonal antibodies targeting SHP2 in Bcr-Abl signaling

A model of full-length SHP2 once bound to NSa1 and Cs1 was generated by Fern Sha from Koide lab and enabled us to demonstrate that the accessibility of N- and C-SH2 domains by monoclonal antibodies were not hindered by each other (Figure 2.22a). After this observation, we wanted to investigate whether targeting SHP2 with tandem monoclonal antibodies would give a better inhibitory effect than the single monoclonal antibody in terms of downstream signaling modulation and blocking the interaction with Gab2. Tandem monoclonal antibodies were generated by connecting NSa1-Cs3 and NSa5-Cs3 with an 18 amino acid GS-linker region by the Koide lab that would bind N- and C-SH2 domains simultaneously. The SHP2 targeting tandem monoclonal antibodies were co-expressed with Bcr-Abl in HEK293 cells. The tandem HA4-7c12 monoclonal antibody that binds to Abl SH2 domain and SH2-kinase domain N-lobe interface (Grebien et al., 2011), respectively, was used as a control and a triple mutated HA4-7c12 was used as non-binding control monoclonal antibody (Figure 2.22b). The Bcr-Abl and 6xmyc-tagged tandem monoclonal antibody constructs were expressed to similar levels (Figure 2.22b, upper two panels).



Interestingly, we have observed a significant decrease in ERK phosphorylation upon expression of SHP2 targeting tandem monobodies when compared to the nonbinding control (Figure 2.22b). Since increased ERK phosphorylation is a critical read-out indicating the high SHP2 activity, inhibition of ERK phosphorylation showed that the signaling through the SH2 domains of SHP2 was blocked with the tandem monobodies in HEK293 cells. In order to show the binding of monobodies to endogenous SHP2, we performed reciprocal co-immunoprecipitations with myc tagged tandem monobodies and endogenous SHP2 (Figure 2.22c). With both ways of immunoprecipitation, we demonstrated the binding of tandem monobodies to endogenous SHP2, while no binding was detected in the non-binding control tandem monobody. Previously, we showed disruption of interaction between endogenous Gab2 and SHP2 proteins upon Bcr-Abl and single SHP2 targeting monobody expression in HEK293 cells (Results section 2.3.4). We further investigated the effects of SHP2 targeting tandem monobodies and when endogenous Gab2 protein was pulled down. We showed that the interaction with endogenous SHP2 protein was decreased upon tandem monobody expression when compared to the non-binding control (Figure 2.22d). We established already that single monobodies targeting the SH2 domains were potent in terms of inhibiting the SHP2 activity, thus inhibiting the protein-protein interactions and the downstream signaling pathways in HE293 cells and furthermore ERK phosphorylation was inhibited by SHP2 targeting single monobodies in HCC-1171 cells.



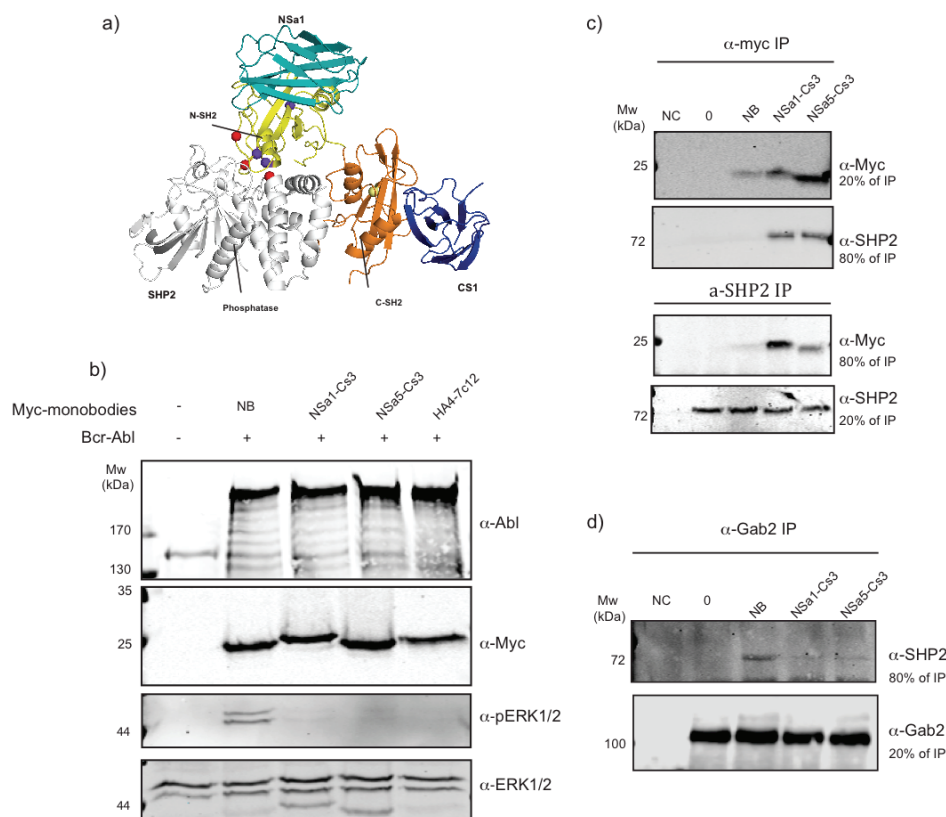


**Figure 2.22. Tandem monobodies targeting SHP2 N- and C-SH2 domains**

a) Monobodies NSa1 and CS1 were positioned by superimposing the SH2 domains of the NSa1/N-SH2 and CS1/C-SH2 complexes with their counterparts in full-length SHP2 (PDB 2SHP). N-SH2 is colored in yellow and C-SH2 is colored in orange. The spheres were gain-of-function mutations of SHP2 identified from solid tumors. The model was provided by Fern Sha.

b) HEK293 cells were transiently transfected with the indicated constructs. HA4-7c12 Y88A/Y172E/F197K was used as non-binding (NB) control monobody. After lysis, the total cell extract was subjected to immunoblotting with the indicated antibodies.

c) 1 mg total cell lysate was subjected to anti-myc immunoprecipitation by using anti-myc agarose beads (upper two panels) and anti-SHP2 immunoprecipitation (lower two panels). The IPs were split into two for anti-myc and anti-SHP2 immunoblotting. NC is the negative control without any protein lysate.

d) 1 mg total cell lysate was subjected to anti-Gab2 immunoblotting and then the IP was split into two for anti-Gab2 and anti-SHP2 immunoblotting.

In here, tandem monobodies targeting both SH2 domains of SHP2 were shown to be more potent in inhibiting SHP2 activity in HEK293 cells overexpressing Bcr-Abl which was evaluated by the decrease in ERK phosphorylation. In addition to targeting single SH2 domains, blocking of both SH2 domains simultaneously by tandem monobodies might be a better way of targeting a protein.

## 2.4 PLC $\gamma$ 1 targeting monobodies

### 2.4.1 PLC $\gamma$ 1 targeting monobodies bind selectively to PLC $\gamma$ 1 in cells

Selection of monobodies against PLC $\gamma$ 1 protein was performed in the Koide lab. After the selection of two clones against N-SH2 and 1 clone against C-SH2 domain, these monobodies were cloned into TAP vector as N-terminal fusions (Figure 2.23a) and stable cell lines for K562 and HEK293 cells were generated. We observed similar levels of expression levels in both cell lines for all monobody constructs and comparable expression levels as compared to the NSa1 monobody targeting the SHP2 N-SH2 domain that was characterized previously (Figure 2.23b). During the TAP purification, the presence of the bait monobody construct was tracked by anti-myc immunoblotting and the purification was shown to be efficient despite the large amount of bait protein loss in the SN1 fraction, which is always the less efficient purification step. We were able to retrieve significant amount of bait protein in the last elution fraction (E1), without any bound protein left on the streptactin beads (BB) in the last step (Figure 2.23c). The final E2 elution fraction was subjected to silver staining as well as anti-PLC $\gamma$ 1 immunoblotting. After silver staining, the monobodies were detected very abundantly and a clear single band around 130 kDa was also detected in both cell lines for NLa4 and NLa7, but not for CLa4 expressing cells which is in line with PLC $\gamma$ 1 molecular weight. Other bands were also detected around 70 kDa strongly for K562 and but weakly in HEK293 (Figure 2.23d, upper panel). Moreover, anti-PLC $\gamma$ 1 immunoblotting revealed the pull down of endogenous PLC $\gamma$ 1 with N-SH2 targeting monobodies but not with C-SH2 targeting monobody (Figure 2.23d, lower panel).

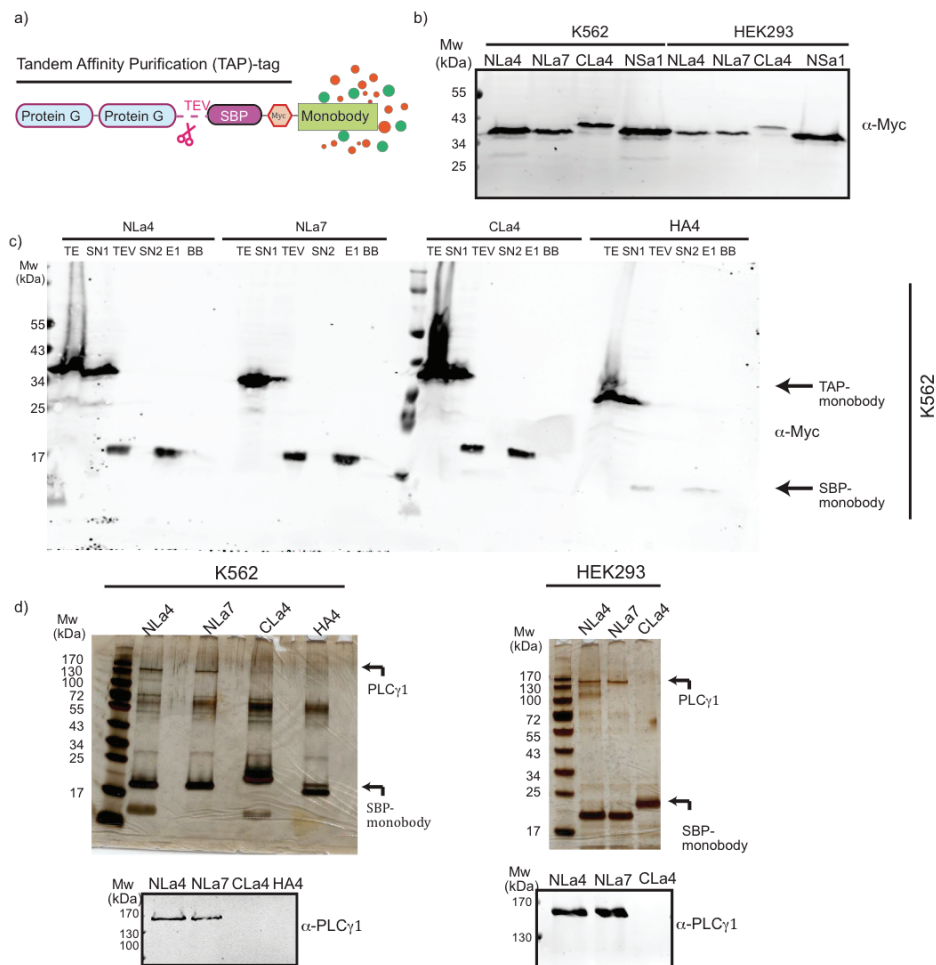


**Figure 2.23. Analysis of the PLC $\gamma$ 1-targeting monobody interactome**

a) Schematic representation of TAP-tagged monobodies including the B1 domain of Staphylococcal protein G (Protein G), tobacco etch virus (TEV) protease recognition site, streptavidin-binding peptide (SBP) and myc-tag N-terminal to the monobody.

b) Immunoblot analysis of total cell lysates of K562 and HEK293 stably expressing the TAP-tagged monobody clones. NSa1 is a previously characterized monobody binding the N-SH2 domain of SHP2 and serves as an internal control.

c) Representative TAP of monobody complexes from K562 cells and anti-myc immunoblotting was performed to track the monobody expression. Abbreviations; TE: total extract (0.16%), SN1: supernatant IgG beads (0.16%), TEV: Eluate after TEV cleavage (2.5%), SN2: supernatant streptavidin beads (2.5%), E1: eluate from Streptavidin beads (3.2%), BB: boiled Streptavidin beads to control efficiency of elution. The arrows on the blot show the molecular weight of monobodies before and after TEV cleavage. (% of input indicated in brackets)

d) Visualization of the complexity of the final eluate by silver staining and immunoblotting against PLC $\gamma$ 1. Upper panel: Tandem affinity-purified monobody complexes (E1 fractions) from K562 and HEK293 cells were separated by SDS-PAGE and 10% of the eluate was used for silver staining. Lower panel: 10% of E1 fraction was analyzed by an anti-PLC $\gamma$ 1 immunoblotting.

The two biological replicates of tandem affinity purification for both cell lines were submitted for LC-MS/MS analysis and PLC $\gamma$ 1 was identified with high abundance for both cell lines. In K562, PLC $\gamma$ 1 was identified as the only protein having an SH2 domain and no other SH2-domain containing protein was

detected in both replicates. In HEK293 cells, PLC $\gamma$ 1 was identified with high abundance and ranking, although PLC $\gamma$ 2 isoform was also detected in CLa4 monobody purification, and no other SH2 domain containing proteins were detected (Table 2.2). Silver staining and anti-PLC $\gamma$ 1 immunoblotting did not reveal binding of CLa4 to PLC $\gamma$ 1 (Figure 2.23d), however, with the MS data, we were able to identify PLC $\gamma$ 1 as an interactor in CLa4 expressing cell lines but with low spectral counts when compared to N-SH2 targeting monobodies (Table 2.2).

Cell line	Bait	Total number of proteins identified*		Rank of PLC $\gamma$ 1 among all proteins**		Names and spectral counts (in brackets) of all identified SH2 domain-containing proteins in each sample	
		1st TAP	2nd TAP	1st TAP	2nd TAP	1st TAP	2nd TAP
K562	NLa4	31	28	4	3	PLC $\gamma$ 1 (87)	PLC $\gamma$ 1 (131)
	NLa7	20	28	7	3	PLC $\gamma$ 1 (22)	PLC $\gamma$ 1 (139)
	CLa4	33	25	33	10	PLC $\gamma$ 1 (1)	PLC $\gamma$ 1 (19)
HEK293	NLa4	84	107	1	1	PLC $\gamma$ 1 (501)	PLC $\gamma$ 1 (374)
	NLa7	91	127	1	1	PLC $\gamma$ 1 (699)	PLC $\gamma$ 1 (432)
	CLa4	109	124	7	8	PLC $\gamma$ 1 (39), PLC $\gamma$ 2 (6)	PLC $\gamma$ 1 (24), PLC $\gamma$ 2 (12)

**Table 2.2. Overview of mass spectrometry results from PLC $\gamma$ 1 monobody interactome analysis.**

\* Proteins were scored as identified if at least 2 unique peptides were detected. \*\* All identified proteins, including common contaminants, such as Keratin, were sorted by the exclusive spectrum count from highest to lowest.

(see Appendix Table A3 and A4 for the complete list of proteins identified for K562 and HEK293, respectively)

## 2.4.2 Monobody mediated modulation of PLC $\gamma$ 1 signaling

In order to determine the effects of PLC $\gamma$ 1 targeting monobodies in Bcr-Abl mediated signaling, we co-expressed Bcr-Abl together with C-terminally V5-tagged-PLC $\gamma$ 1 and N-terminally 6xmyc tagged monobodies in HEK293 cells. Since full activation of PLC $\gamma$ 1 requires the phosphorylation of tyrosine 783, the phosphorylation of this residue was used as a read-out to evaluate the degree of activation of PLC $\gamma$ 1 (Bunney et al., 2012). When we co-expressed these three constructs in HEK293 cells, a decrease in PLC $\gamma$ 1 phosphorylation was demonstrated with a phosphosite-specific antibody when normalized to the total PLC $\gamma$ 1 levels which was detected with anti-V5 immunoblotting. The phosphorylation of PLC $\gamma$ 1 was decreased with NLa7 and CLa4 monobodies and to a lesser extent with NLa4 monobody (Figure 2.24).

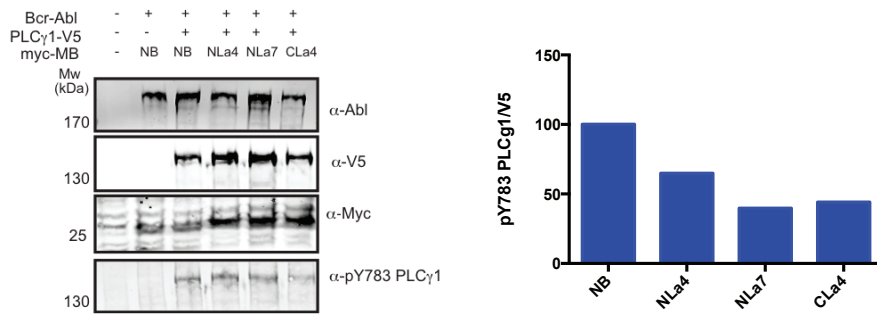


**Figure 2.24. PLCγ1 targeting monobodies co-expressed with Bcr-Abl and PLCγ1 in HEK293 cells**

HEK293 cells were transiently transfected with the indicated expression constructs and total cell lysates were subjected to immunoblotting with indicated antibodies. Tyrosine 783 phosphorylation was quantified and normalized to total PLCγ1 levels that are detected by anti-V5 signal.

The receptor tyrosine kinase mediated phosphorylation of PLCγ1 is a well-defined mechanism for activation. As discussed in introduction section 1.6.2, upon stimulation of the cells with growth factors, PLCγ1 is recruited to the membrane and bound to the RTK phosphorylated tyrosine site with N-SH2 domain, then PLCγ1 is further activated. We wanted to evaluate the functional role of PLCγ1 targeting monobodies upon growth factor stimulation. For this purpose, initially, NIH3T3 cells were used as control cell line to study PLCγ1 activation upon PDGF-bb stimulation. When 50 ng/mL PDGF-bb was used to stimulate the cells, PLCγ1 phosphorylation was stimulated, when compared to unstimulated control (Figure 2.25a). Next, K562 and HEK293 cells were stimulated with a set of growth factors including PDGF-bb, as an internal control, which were described to induce PLCγ1 activation (Bunney et al., 2012; Diaz-Flores et al., 2013; Margolis et al., 1990; Obermeier, Tinhofer, Grunicke, & Ullrich, 1996). However, we were not able to detect PLCγ1 phosphorylation in response to the growth factors in neither K562 nor HEK293 cells, in contrast to control NIH3T3 cells where we observed a single phosphotyrosine band for PLCγ1 (Figure 2.25b). Therefore, we decided to use NIH3T3 cells as the model system to investigate the roles of PLCγ1 targeting monobodies.

Next, NIH3T3 parental cells were used to optimize concentration- and time-dependent stimulation by PDGF-bb. First 50 ng/mL PDGF-bb was utilized to determine the optimum time point where PLCγ1 phosphorylated at the maximum level. After 10 minutes of stimulation, the cells showed increased phosphorylation of endogenous PLCγ1. The cells were stimulated for 6 hours

and the maximum phosphorylation of PLC $\gamma$ 1 was obtained after 30 minutes (Figure 2.25c, upper two panels).

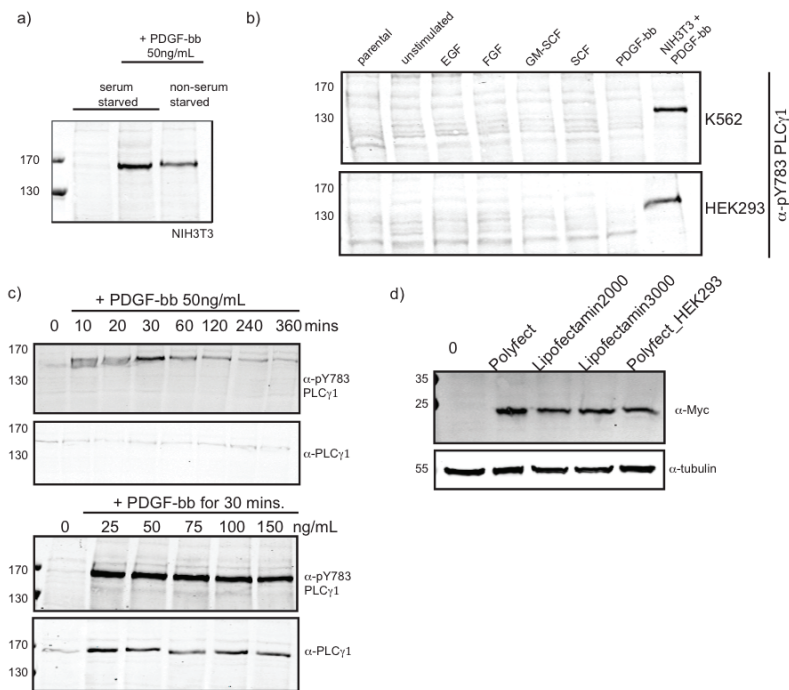


**Figure 2.25. Growth factor stimulation of cells to induce PLC $\gamma$ 1 phosphorylation and transfection reagent optimization**

a) NIH3T3 cells were seeded in 6 well plates and then incubated with and without serum in the absence or presence of PDGF-bb overnight. 50 ng/mL PDGF-bb was used to stimulate the cells, then the cells were lysed in IP buffer and probed with anti-pY783 PLC $\gamma$ 1 antibody.

b) K562 and HEK293 cells were seeded in 6 well plates and serum starved overnight. Next day, the cells were stimulated with the indicated growth factors for 15 minutes. NIH3T3 cells treated with PDGF-bb were used as an internal control for phosphorylated PLC $\gamma$ 1.

c) Upper panels: NIH3T3 cells were seeded in 6 cm dishes for each different condition. Next day, the medium of the cells were changed and then the cells were washed with PBS to remove any traces of medium and serum. Then serum free medium (SFM) was added on the cells then the cells were stimulated all at the same time. After each time points, the SFM with PDGF-bb was removed from the cells immediately and the cells were washed twice with PBS. At the end of the last time point, 6 hours, the cells were lysed and subjected to total and anti-pY783 PLC $\gamma$ 1 immunoblotting. Lower panels: The day before transfection, NIH3T3 cells were seeded in 6 cm dishes and on the day of transfection, the medium was removed and the cells were washed with PBS. Then, the cells were stimulated with different concentrations of PDGF-bb for 30 minutes.

d) The day before transfection, NIH3T3 cells were seeded in 6 cm dishes. On the day of transfection, the cells were transfected with 2  $\mu$ g 6xmyc tagged NLa4 monobody DNA with the indicated transfection reagents according to manufacturers instructions. HEK293 cells were transfected with 6xmyc tagged NLa4 as an internal control. At the end of incubation time, the cells were lysed and subjected to anti-myc and tubulin immunoblotting.

Subsequently, 30 minutes of stimulation time was used with different concentrations of PDGF-bb. We always compared to the unstimulated control, and the highest PLC $\gamma$ 1 phosphorylation was observed with 75 ng/mL PDGF-bb,



when normalized to the total PLC $\gamma$ 1 protein levels (Figure 2.25c, lower two panels). According to this optimization result, we decided to use 75 ng/mL PDGF-bb concentration and 30 minutes of stimulation for NIH3T3 cells.

Afterwards, the choice of the optimum transfection reagent for NIH3T3 cells was investigated by using a set of transfection reagents with NLa4 transfection (Figure 2.25d). When Polyfect transfection reagent was used, NIH3T3 cells expressed NLa4 monoclonal antibody to higher levels than the other reagents (Figure 2.25d)

Next, we sought to further confirm the interaction of monoclonal antibodies with endogenous PLC $\gamma$ 1. First, we ran the transfection experiment by transfecting the NIH3T3 cells with the PLC $\gamma$ 1 SH2 targeting monoclonal antibodies together with the non-binding control monoclonal antibody which is HA4 monoclonal antibody with Y87A mutation. When co-immunoprecipitation experiments were performed by using TAP (tandem affinity purification) buffer, we were able to recover all monoclonal antibodies pulled down with PLC $\gamma$ 1, although unexpectedly non-binding control monoclonal antibody was also pulled down with PLC $\gamma$ 1 (Figure 2.26a). TAP buffer is a mild buffer with low detergent concentration, so we used the IP (immunoprecipitation) buffer which is a more stringent buffer than TAP buffer (Figure 2.26b). The cells were cotransfected with NB and NLa4 monoclonal antibodies and then IP and TAP buffers were compared for co-immunoprecipitation assay. Similar expression levels of monoclonal antibodies were obtained (Figure 2.26b, upper panel) and when PLC $\gamma$ 1 pull down was performed, NB monoclonal antibody was still bound to PLC $\gamma$ 1 with IP buffer. Since the unspecific binding of the control monoclonal antibody was not eliminated with TAP or IP buffer, RIPA (radioimmunoprecipitation assay) buffer was compared with IP buffer, which is even more stringent than IP buffer with higher detergent concentration (Figure 2.26c). The monoclonal antibody constructs were expressed to similar levels (Figure 2.26c, upper panel) and IP buffer could not eliminate the interaction between non-binding monoclonal antibody and PLC $\gamma$ 1, while RIPA buffer eliminated the unspecific binding of the non-binding control monoclonal antibody and still NLa4 was bound to PLC $\gamma$ 1 (Figure 2.26c, lower two panels).

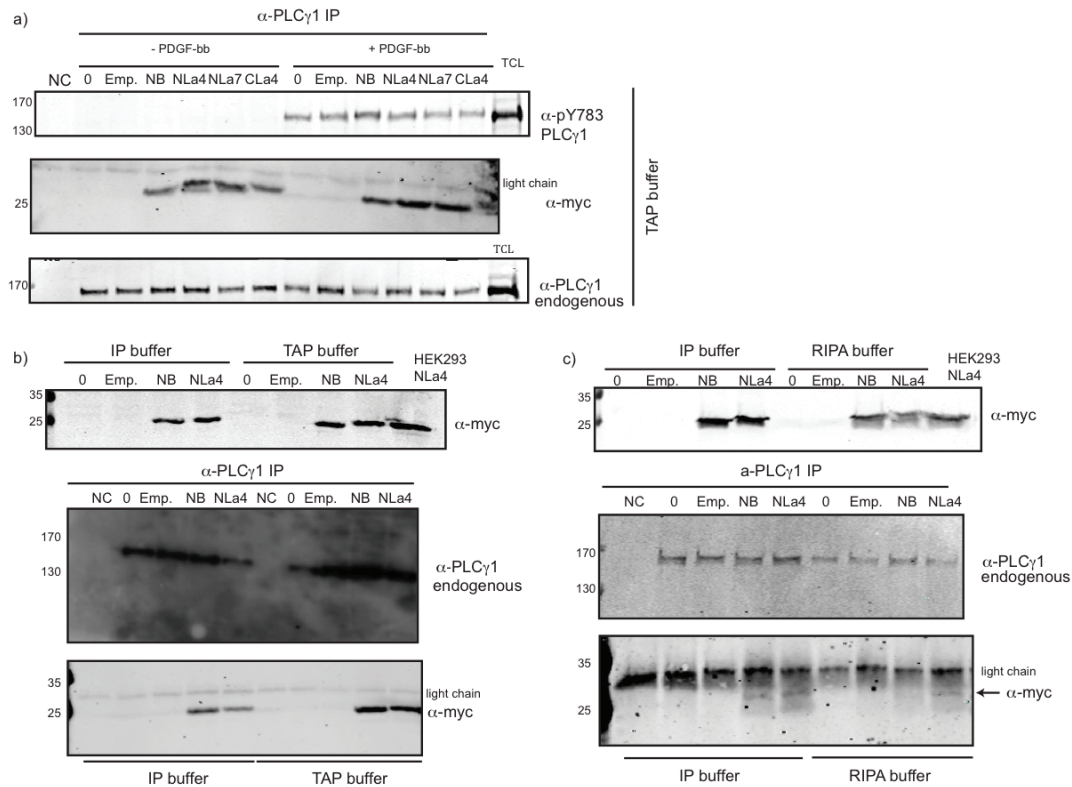


**Figure 2.26. Buffer optimization of the immunoprecipitation assay of PLC $\gamma$ 1 and PLC $\gamma$ 1 targeting monoclonal antibodies in NIH3T3 cells**

a) The endogenous PLC $\gamma$ 1 immunoprecipitation was performed by using 500  $\mu$ g total cell lysate and 1  $\mu$ L PLC $\gamma$ 1 antibody for each sample. After incubation with the PLC $\gamma$ 1 antibody and protein G beads, the IP was split into three in order to have the 10 % of IP for anti-PLC $\gamma$ 1, 45% of IP for myc-tagged monoclonal antibody and 45% of IP for anti-pY783 PLC $\gamma$ 1 immunoblotting by using TAP buffer. NC: negative control, no lysate, only TAP buffer with PLC $\gamma$ 1 antibody and the protein G beads. TCL: total cell lysate

b) Upper panel: In order to compare TAP buffer and IP buffer, NIH3T3 cells were transfected with the indicated constructs in 6 cm dishes and the expression levels were similar and comparable levels with HEK293 cells transfected with NLa4. Lower two panels: Lysates were prepared with the indicated buffers and 500  $\mu$ g total cell lysate was used for endogenous PLC $\gamma$ 1 immunoprecipitation. 20% of IP was subjected to anti-PLC $\gamma$ 1, 80% of IP was subjected to anti-myc immunoblotting.

c) Upper panel: In order to compare RIPA buffer and IP buffer, NIH3T3 cells were transfected with the indicated constructs in 6 cm dishes and the expression levels were to similar and comparable levels with HEK293 cells transfected with NLa4. Lower two panels: Lysates were prepared with the indicated buffers and 500  $\mu$ g total cell lysate was used for endogenous PLC $\gamma$ 1 immunoprecipitation. 20% of IP was subjected to anti-PLC $\gamma$ 1, 80% of IP was subjected to anti-myc immunoblotting.

Next, we wondered whether overexpression of PLC $\gamma$ 1 would be sufficient for its activation without PDGF-bb stimulation. If this would be the case, it was also important to figure out the different phosphorylation levels of overexpressed or endogenous PLC $\gamma$ 1 protein in the presence or absence of PDGF-bb and whether PDGF-bb stimulation has a different effect on



overexpressed or endogenous PLC $\gamma$ 1 protein. Since our aim was to find a condition where we obtain the highest phosphorylation of PLC $\gamma$ 1, we set an experiment to compare all these different conditions (Figure 2.27).

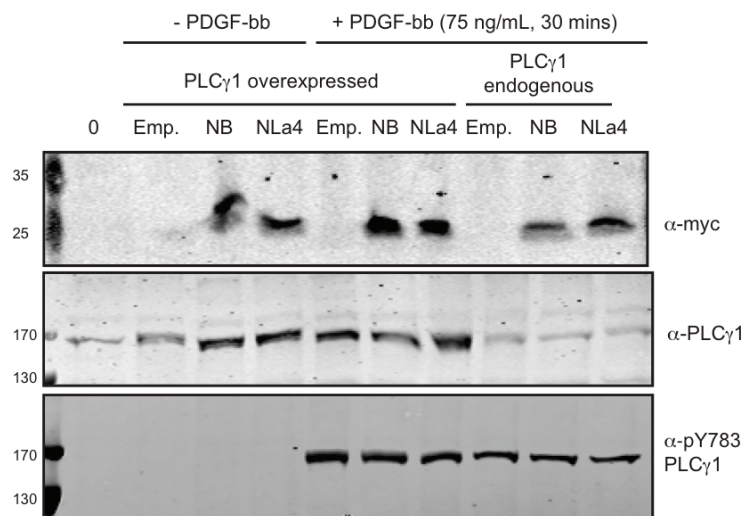


**Figure 2.27. Comparison of overexpressed and endogenous PLC $\gamma$ 1 protein phosphorylation in the absence or presence of PDGF-bb**

NIH3T3 cells were transiently transfected with the indicated constructs and total cell lysates were subjected to immunoblotting with the indicated antibodies. Emp: Empty vector control.

In this set up, the cells were transfected with empty vector, non-binding control monobody and NLa4 with and without overexpressed PLC $\gamma$ 1. We showed that PLC $\gamma$ 1 overexpression without PDGF-bb is not sufficient to induce its phosphorylation (Figure 2.27). When PLC $\gamma$ 1 was overexpressed without PDGF-bb stimulation, there was no PLC $\gamma$ 1 Y783 phosphorylation observed, so PDGF-bb was necessary for stimulating PLC $\gamma$ 1 phosphorylation. On the other hand, when overexpressed or endogenous PLC $\gamma$ 1 conditions were compared in the presence of PDGF-bb, we demonstrated that overexpressed PLC $\gamma$ 1 was phosphorylated more than endogenous PLC $\gamma$ 1 (Figure 2.27). We concluded that PLC $\gamma$ 1 overexpression was not sufficient for its activation in the absence of PDGF-bb and PDGF-bb stimulation is necessary for inducing the phosphorylation of PLC $\gamma$ 1. Furthermore, when the phosphorylation levels of overexpressed and endogenous PLC $\gamma$ 1 were compared, overexpressed PLC $\gamma$ 1 phosphorylation was stimulated more in response to PDGF-bb.

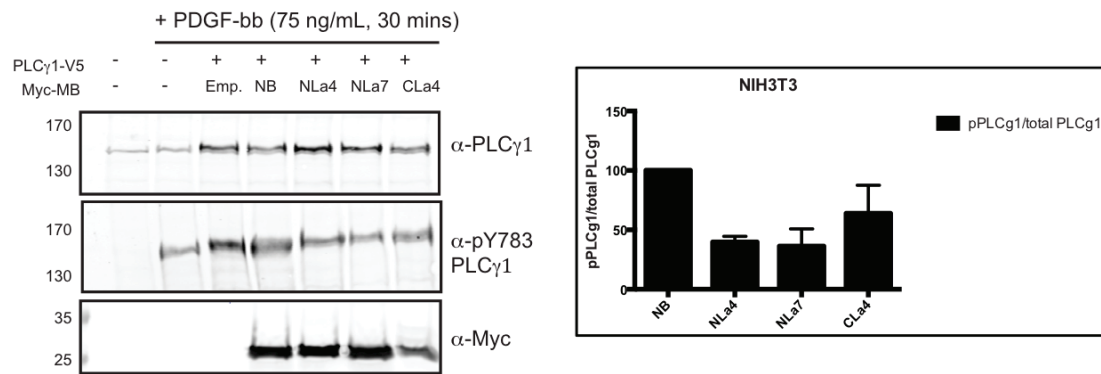


**Figure 2.28. PLCγ1 targeting monobodies decrease the site specific phosphorylation in NIH3T3 cells**

The NIH3T3 cells are co-transfected with 4 μg C-terminally V5 tagged PLCγ1 and 8 μg N-terminally 6xmyc tagged monobody DNA and then the cells were stimulated with 75ng/mL PDGF-bb for 30 minutes in serum free medium just before lysis. The cells were transiently transfected in 10 cm dishes and total cell lysates were subjected to immunoblotting with the indicated antibodies. The bar graph shows the quantification of the PLCγ1 phosphorylation upon monobody expression from two independent transfection sets and two technical replicates by using this transfection set. Emp: Empty vector control.

Up to this point, PDGF-bb stimulation was demonstrated to be necessary for stimulating the activation of PLCγ1 and overexpression of PLCγ1 showed more impact on phosphorylation-mediated activation of PLCγ1. Also, the concentration and time dependent stimulation by PDGF-bb were optimized. Following these optimizations, co-expression experiments were started by using NIH3T3 cells. When PLCγ1 and monobodies were co-expressed in cells, a decrease in PLCγ1 Y783 phosphorylation was observed in response to N-SH2 targeting monobodies when normalized to the non-binding control monobody. Upon NLa4 and NLa7 expression, PLCγ1 phosphorylation was decreased. CLa4 also decreased the PLCγ1 phosphorylation but not as efficient as N-SH2 targeting monobodies (Figure 2.28).

Then co-immunoprecipitation assay was performed in order to reveal the interaction between PLCγ1 and PDGFRα upon monobody expression. PLCγ1 and monobodies were co-expressed in NIH3T3 cells. When PLCγ1 was pulled down, the IP was split into three for immunoblotting in order to detect the interaction with endogenous PDGFRα and anti-myc tagged monobodies. Consistent with our interactome studies, we were able to detect N-SH2 targeting monobodies bound to PLCγ1 although C-SH2 targeting CLa4 monobody was failed to co-immunoprecipitate with PLCγ1 (Figure 2.29, upper panel). Moreover,

immunoprecipitation of PLC $\gamma$ 1 demonstrated that the interaction between PLC $\gamma$ 1 and PDGFR $\alpha$  is mildly decreased upon monobody expression (Figure 2.29, second panel).

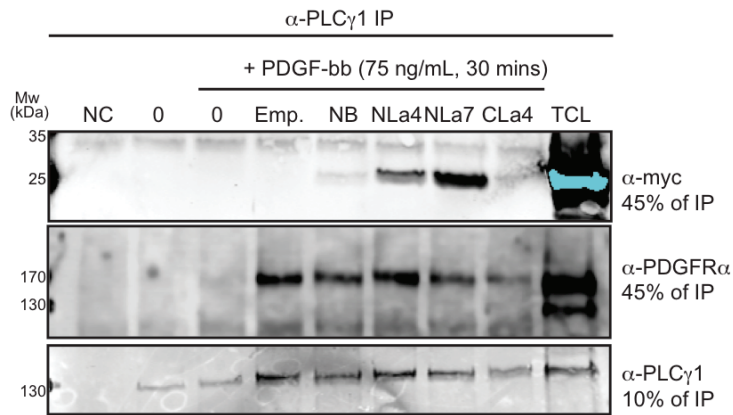


**Figure 2.29. PLC $\gamma$ 1 targeting monobodies interfere with the binding of PLC $\gamma$ 1 to PDGFR $\alpha$**   
 The NIH3T3 cells were cotransfected with C-terminally V5 tagged PLC $\gamma$ 1 and N-terminally 6xmyc tagged monobodies. Co-immunoprecipitation of PLC $\gamma$ 1 was performed by using 1 mg total protein lysate and then the IP split into three in order to have the 10 % of IP for anti-PLC $\gamma$ 1, 45% of IP for myc-tagged monobody and 45% of IP for anti-PDGFR $\alpha$  immunoblotting by using RIPA buffer.

In order to investigate the downstream signaling of PLC $\gamma$ 1, first knockdown of PLC $\gamma$ 1 in NIH3T3 cells were investigated to figure out the affected pathway by siRNA silencing (Figure 2.30). Lattanzio et al. discussed the effects of PLC $\gamma$ 1 under receptor tyrosine kinases and activation of the RAS/MAPK pathway through the increased protein kinase C (PKC) activity (Figure 2.30a) (Lattanzio, Piantelli, et al., 2013). siRNA mediated knockdown of PLC $\gamma$ 1 was performed and the modulation of downstream pathways were evaluated. Knockdown of PLC $\gamma$ 1 was performed in the absence or presence of PDGF-bb stimulation. We achieved an efficient knockdown of PLC $\gamma$ 1 in both conditions (Figure 2.30b, upper panel) and the Y783 phosphorylation was decreased upon knockdown of PLC $\gamma$ 1 (Figure 2.30b, middle panel). Upon silencing of PLC $\gamma$ 1 expression in NIH3T3 cells, we were able to see a decrease in ERK phosphorylation levels (Figure 2.30b, lower panel). Then we thought that MAPK pathway might be a good candidate to evaluate the signaling events in stimulated cells although it is not a pathway that is directly regulated by PLC $\gamma$ 1 (Figure 2.30a). Afterwards, with the motivation of the effects of monobodies on PLC $\gamma$ 1 phosphorylation, we wanted to find out

whether monobodies would show a similar effect than siRNA mediated knock down of the protein.

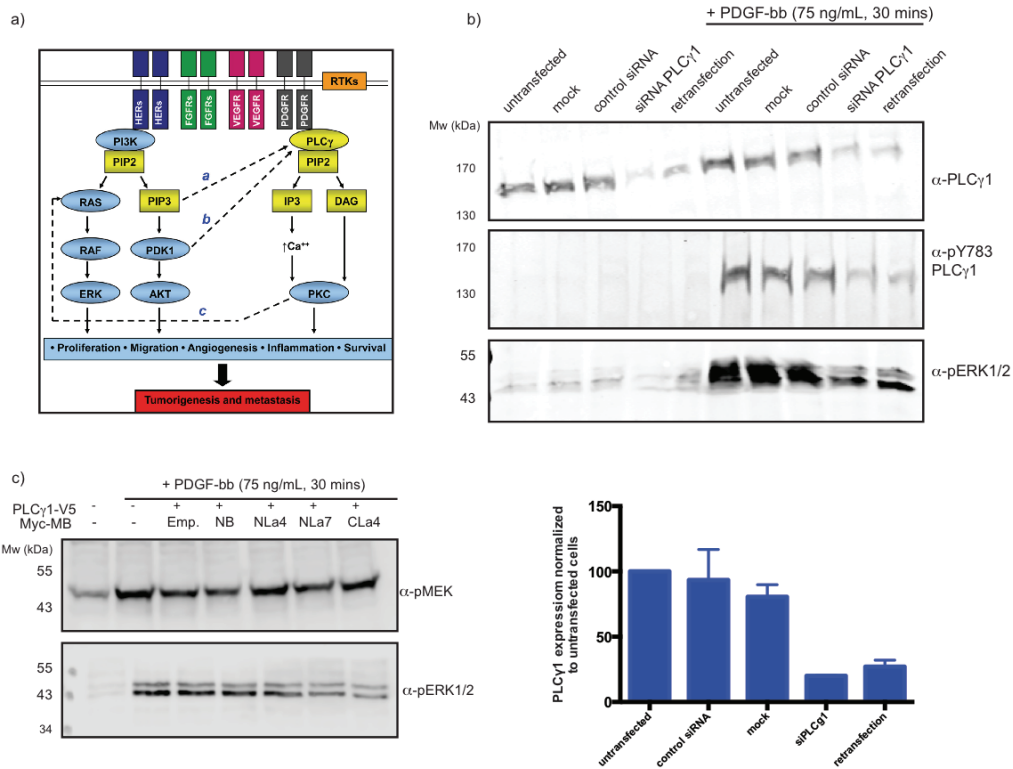


**Figure 2.30. siRNA mediated knock down of PLCγ1 protein and downstream signaling modulated by monobodies**

a) Figure showing the PLCγ1 signaling downstream of receptor tyrosine kinases. Taken from (Lattanzio, Piantelli, et al., 2013)

b) Upper: The knockdown of PLCγ1 in NIH3T3 cells was shown by anti-PLCγ1 immunoblotting. The first lane is untransfected sample, second lane is the mock sample and has been subjected to transfection reagent, third lane is control siRNA, fourth lane is the cells transfected only once, the last lane is retransfection sample which has been subjected to transfection twice. Lower panel: Quantification of total PLCγ1 levels normalized to untransfected control cell line.

c) NIH3T3 cells were co-transfected with PLCγ1 and monobodies and then immunoblotted with anti-pMEK and anti-pERK1/2.

When PLCγ1 and SH2 targeting monobodies were co-expressed in NIH3T3 cells, we were able to demonstrate ERK phosphorylation but not MEK phosphorylation was mildly affected upon monobody expression. No significant difference in MEK phosphorylation was detected, although ERK phosphorylation was decreased when compared to NB and empty vector (Figure 2.30c).

## CHAPTER 3

### DISCUSSION

Our interest in the Gab2 protein has led us to first map the interaction network of this protein by tandem affinity purification and secondly target the SH2 domain mediated interactions of Gab2 and with its critical interactors such as SHP2, p85 $\alpha$  and PLC $\gamma$ 1. We utilized monobodies, small antibody mimics in order to target and block the interaction between Gab2 and its interactor partners.

#### 3.1 Mapping of Gab2 interactome

We have used a small double-affinity tag (Strep-HA tag) consisting of a streptavidin-binding peptide and a three consecutive hemagglutinin (HA) epitope tag (Glatter et al., 2009). From the Strep-HA affinity purifications, we were able to confirm the known and identify some novel interactors of Gab2. However, C-terminally fused Gab1 and Gab2 pull down did not reveal the bait protein in immunoblotting. The reason of this might be the location of the tag, because when we performed the affinity purification of N-terminal fusion of Gab2, the pull-down yielded high amounts of bait protein and high number of specific interactors.

Since the Gab2 scaffold protein possesses many phosphorylated residues that in turn generate docking sites for other proteins, it is possibly not surprising that the Gab2 pull down resulted in the identification of many specific interactors. The Grb2 adaptor protein was identified in Gab2 pull down as expected. Furthermore, three out of five regulatory subunits of PI3K were also identified, p85 $\alpha$ , p85 $\beta$ , p85 $\delta$ . In addition to the regulatory subunits, catalytic subunits of PI3K (p110 $\alpha$ ,  $\beta$ ,  $\delta$ ) were also detected. This result showed us that second shell interactors were also pulled down with Gab2 bait protein. On the other hand, PI3K delta regulator and catalytic subunits were shown in here as an

interactor, which was not shown before. All the interactors that were identified in our Strep-HA pull-downs of p85 $\beta$  were all known interactors.

Gab2 was identified in all the purifications except for SHP1 and PLC $\gamma$ 1. However, Gab2 was shown to associate with SHP1 (Wheadon, Paling, & Welham, 2002; W. M. Yu, Hawley, Hawley, & Qu, 2002), in our setup neither Gab2 nor SHP1 pull down revealed a reciprocal interaction. The interaction between Gab2 and SHP1 in these literature papers was shown in IL-3 stimulated BaF3 cell line. This already suggests that the interaction between two proteins might be different cell lines and under different stimulants. K562 cells that we used for the interactome studies express the endogenous Bcr-Abl protein and the interaction between Gab2 and SHP1 might not be favored in these cells. SHP1 pull down did not result with any known interactors, not even Gab2, although in SHP2 purification, Gab2 and Grb2 were identified with high ranking. The interaction between Gab2 and SHP2 was shown in BaF3 cell line transduced with Bcr-Abl (Sattler et al., 2002) and our result confirms this interaction in K562 cells. Our results and the studies from literature confirmed the formation of Gab2-SHP2 complex in Bcr-Abl positive cells. According to our interactome study, the interaction between SHP2 and Gab2 is mediated via Grb2 scaffold protein which is in line with the data from literature (Figure 2.4).

PLC $\gamma$ 1 is activated through growth factor stimulated non-receptor or receptor tyrosine kinases (Rhee, 2001). Although Strep-HA purifications of C-terminally tagged PLC $\gamma$ 1 resulted in few interactors, some of these interactions might be specific interactions. For instance, MARK3 localize on the cell membrane and the presence of KA1 (kinase associated-1) domain leads MARK/PAR1 kinases to the membrane where it binds to the acidic phospholipids (Moravcevic et al., 2010). ITPR1 is a receptor for inositol 1,4,5-trisphosphate (IP3) and is involved in PIP2 hydrolysis and diacylglycerol, IP3 signaling (Yamada et al., 1994). Gab2, as being an interactor of PLC $\gamma$ 1, was not retrieved in PLC $\gamma$ 1 pull-down. As discussed above, the identification of few interactors might be due to the cell type and maybe K562 cells might not be a suitable system and do not facilitate the Gab2-PLC $\gamma$ 1 interaction. Nevertheless, the identification of possible specific interactors like MARK3, ITPR1 which have related functions and present in the similar cellular location and pathway with PLC $\gamma$ 1 shows that

the pull down is successful in this aspect. On the other hand, the reason of insufficient number of specific interactors identified in PLC $\gamma$ 1 pull down might be a technical issue which could be related to the size of the PLC $\gamma$ 1 bait protein, which is the highest molecular weight bait in our experimental set-up.

All the bait proteins selected for our Strep-HA purifications, Gab1, Gab2, p85 $\alpha$ , p85 $\beta$ , SHP1, SHP2 and PLC $\gamma$ 1, were expressed in K562 cells which was followed by anti-HA immunoblotting. The samples from the purifications showed us that N-terminally fused Gab2, SHP2 and p85 $\beta$  were the most efficient pull-downs because there was no protein loss in the flowthrough steps. In p85 $\alpha$ , PLC $\gamma$ 1 and SHP1 pull downs, the efficiency was lower. In the flowthrough fractions, especially in the first step, the bait protein was lost in big amounts. The efficient identification of the specific interactors by MS analysis was in parallel with the efficiency of the pull down. If we consider the amount of protein retrieved in pull-down and the small amount of protein loss during the protein purification, the small loss of bait protein could mean that most of the interactors of the bait protein would more possibly be pulled down. However the physiological environment of the protein should be also considered. The complexity of the proteome of a cell could be different and thus the interactome could vary for every protein that heavily depends on the expression levels of the interactors and the bait protein itself. While some proteins have few interactors, others have many interactors. In Gab2, SHP2 and p85 $\beta$  pull downs, we were able to confirm the known interactors and identify new ones, however p85 $\alpha$ , PLC $\gamma$ 1 and SHP1 pull downs yielded less identified proteins.

The identification of known interactors validated the Strep-HA affinity purification method and we were also able to identify possible novel interactors. We were expecting that mapping Gab2 interactome would also enable us to identify some additional SH2- or targetable-protein interaction domain containing proteins interacting with Gab2 in addition to SHP2, p85 $\alpha$  and PLC $\gamma$ 1. However, the interactome of Gab2 did not yield such a protein at the end. Although PLC $\gamma$ 1 was not identified as an interactor of Gab2 in our affinity purifications, the importance of the PLC $\gamma$ 1 pathway was demonstrated before in leukemia development of CML through PLC $\gamma$ 1 controlled activation of Bcr-Abl



downstream pathway mTOR/p70S6-kinase pathway (Markova et al., 2010). We have included PLC $\gamma$ 1 as a potential important player in Bcr-Abl signaling assuming that the failed detection of Gab2-PLC $\gamma$ 1 interaction was coming from the selection of a different cellular system or from a technical issue.

Finally, further experimental approaches are necessary to evaluate the interactors found in Gab2 interactome in terms of the interaction stoichiometry and abundance. This is necessary to find out the key components of the interactome. The reciprocal co-occurrence of the interactors and bi-directional interactions should be verified by western blotting. This would enable us to determine whether the interaction is true or not. Moreover, the Gab2 interactome studies should be also done in other Bcr-Abl positive cellular systems, either by using cells transduced with Bcr-Abl or express endogenous Bcr-Abl. Furthermore, comparison of these results in primary cells or in CML patient cells with different disease phases would enable us to observe the stability and conservation of the complex in different systems.

The challenge of the Gab2 interactome analysis is the identification of critical interactors of Gab2 in Bcr-Abl signaling that are beneficial to target together with Bcr-Abl pharmacologically. To figure out this issue, we used monoclonal antibodies to dissect the different signaling networks of Bcr-Abl. As a next step, we started to target SH2 protein interaction domain and our first interactor was SHP2.

### **3.2 SHP2 targeting monoclonal antibodies**

Our second aim was to target and inhibit the SH2 domain mediated interaction of tyrosine phosphorylated Gab2 and SH2-domain containing interaction partners in order to understand the contribution of different pathways involved in Bcr-Abl mediated transformation, signaling pathway activation and leukemogenesis. Such an intention requires the inactivation of individual pathways and dissection of the signaling networks through Gab2 protein. For this purpose, we aimed to develop highly specific protein inhibitors called monoclonal antibodies.

In order to assess the specificity of monobodies in cells, first, we have used the Strep-HA tag for the affinity purification, which is a 48 amino acid long tag. The Strep-HA tagged monobodies were not well expressed, moreover the affinity purification was unsuccessful. We argued that when a small tag fused to monobodies which is already a small size (15 kDa) protein, the degradation of monobodies would be more plausible. Then a bigger tag, which is around 20 kDa, consists of two Protein G tag, a TEV cleavage site and an SBP tag (this tag will be called TAP tag in the thesis). When the expression of monobodies were compared with the previous small Strep-HA tag, the TAP tag fused monobody expression was clearly better and using a bigger tag for small size monobodies was beneficial in our experimental set-up. The monobodies were expressed with this tag. When the affinity purification of the construct were followed by immunoblotting, one can see in the first flow through step, which was known to be a less efficient step, the bait protein was lost in big amounts. Burckstummer et al. showed that in the first step of the TAP purification, 40% of the bait was bound and 30% of the bait was retrieved after TEV-protease cleavage (Burckstummer et al., 2006). After similar results retrieved with this study, our data confirmed that the first step of TAP purification is the least efficient step. However, in the last elution fraction, the bait protein was identified successfully. This result also showed that the TAP-tag purification might be more useful for the small size bait proteins.

In addition to the MS analysis, monobodies were shown to be monospecific for SHP2 in cells. MS analysis showed the presence of SHP2 in Cs1 pull down with 5-10 fold less spectra counts when compared to other monobodies. The abundant bands observed in silver staining were appeared to be the metabolic enzymes in Cs1 pull-downs. Although similar affinities were retrieved for all four monobodies according to the SPR data and comparable specificity characteristics were observed in vitro, possible unspecific binding of Cs1 to metabolic enzymes or the abundance of the off-targets might have sequestered the binding of SHP2 to Cs1. This data already showed the importance of the evaluation of the specificity of monobodies in a cellular environment despite having similar affinities in vitro. Analyzing the specificity of the monobodies in

an unbiased way is important to assess the cellular specificity of binding monobodies.

Both monobodies occupy the pY-binding pockets of the N- and C-SH2 domains with larger interfaces than pY-SH2 domain interfaces. Binding to a large interface on SH2 domain explains the specificity of the monobodies and how they differentiate their target. Because the target domain is recognized with more residues which might differ in each SH2 domains. On the other hand, phosphotyrosine peptides generally run perpendicular to the central  $\beta$ -sheet of the SH2 domain (C. H. Lee et al., 1994) but SHP2 targeting monobodies bound within the peptide-binding site of SH2 run in the opposite direction to that of pY peptides. This binding represents a unique pY-independent mode of interaction with the SHP2 SH2 domains. This rare binding mode may contribute to the ability of these monobodies to discriminate their cognate targets from the other SH2 domains.

We have also evaluated the roles of monobodies in the context of CML signaling network. Y542 and Y580 residues are very important for the catalytic activity of SHP2 and get phosphorylated in response to many stimulants (Bennett, Tang, Sugimoto, Walsh, & Neel, 1994; Qu et al., 1997; Qu et al., 1999). N-SH2 domain of SHP2 binds to pY542 while C-SH2 domain binds to pY580 residue (Lu et al., 2001). Upon monobody expression, the Y580 phosphorylation was decreased significantly. The same effect was also observed when a constitutively active SHP2 E76K mutant was co-expressed with Bcr-Abl and monobodies. This result is promising and important because E76K mutation within the N-SH2 domain is the most commonly seen gain of function mutation in JMML (Tartaglia et al., 2003). With the E76K mutation, the closed autoinhibited conformation is not possible and SHP2 is constitutively active. These data demonstrated that targeting the peptide-binding interface of either SH2 domain of SHP2 with the monobodies inhibits the phosphorylation of SHP2 on critical tyrosine residues that are critical for its activation. Since the monobodies also inhibited the phosphorylation of SHP2 carrying the E76K mutation, this data suggests that they might be used as powerful tools to target SHP2 mutations. This result led us to think about the mechanism of inhibition of SHP2 phosphorylation. The disruption of the interaction between full length

endogenous SHP2 and Gab2 in cells was in line with the in vitro data where only NSa1 and NSa5 inhibited the binding of tandem SHP2 SH2 domains to tandem Gab2 phosphopeptide. Both data confirmed the similar results in where N-SH2 targeting monoclonal antibodies were able to decouple SHP2 SH2 domains from Gab2. The N-SH2 domain targeting monoclonal antibodies gain much more importance since the N-SH2 domain, but not C-SH2 domain, is the principal SH2 domain that regulates SHP2 activity (Barford & Neel, 1998).

Ras/MAPK pathway activation is promoted with enhanced SHP2 activity. There are different mechanisms that were suggested for SHP2 mediated activation of Ras/MAPK pathway. Bennett et al. demonstrated that SHP2 is phosphorylated from the Y542 residue by receptor tyrosine kinase, PDGFR, and then Grb2 protein is bound to this phosphotyrosine 542. In this way, SHP2 acts as an adaptor protein and recruits Grb2 to the cell membrane and then Ras/MAPK pathway gets activated (Bennett et al., 1994). Mutational analysis of the C-terminal tail tyrosine residues also showed that Y542 and Y580 phosphorylation upon PDGF or FGF stimulation, MAPK is activated. It was demonstrated that tyrosine phosphorylation is the important event rather than Grb2 binding (S. Q. Zhang et al., 2004). Alternatively, SHP2 can dephosphorylate many proteins which in turn results in the activation of MAPK pathway. For instance, by dephosphorylating Sprouty proteins that sequesters Grb2/SOS complex, SHP2 enables the recruitment of Grb2/SOS complex to the receptor (reviewed in (Mason, Morrison, Basson, & Licht, 2006)). Moreover SHP2 also dephosphorylates the RasGAP protein binding sites on the receptor and in this way SHP2 directs RasGAP to promote Ras/MAPK pathway activation (Cleghon et al., 1998). Also, SHP2 can dephosphorylate the Csk, a negative regulator of Src, adaptor proteins Csk/PAG and paxillin which enables the activation of Src and finally acts on Ras/MAPK pathway (Cunnick et al., 2002). The effect of the monoclonal antibodies on ERK phosphorylation was investigated upon EGF stimulation in HEK293 cells overexpressing SHP2 and monoclonal antibodies. However, we could not observe an effect of monoclonal antibodies on ERK phosphorylation. This result is not surprising if we assume that the hyperactivation of EGFR signaling might be a reason of ERK phosphorylation and inhibition of SHP2 activity was not sufficient. Subsequently, we screened a set of solid tumor cell lines in order to evaluate the

effects of monobodies. These cell lines demonstrated different expression levels of Gab2, and more interestingly showed different levels of ERK activation and SHP2 phosphorylation. The comparison of different cell lines was important because we wanted to test our monobodies in an environment where the ERK phosphorylation is high, which demonstrates an activated RAS/MAPK pathway. In addition to ERK, SHP2 phosphorylation was also a critical determinant for us to estimate the activation level of SHP2. What was interesting to see is that the Y542 residue was very well phosphorylated in some solid tumor cell lines, while Y580 residue was not phosphorylated at all. On the contrary, previously our results demonstrated that upon Bcr-Abl expression in HEK293 cells, Y580 of SHP2 was very well phosphorylated. We can argue that SHP2 C-terminal tail tyrosines were phosphorylated differently with different upstream kinases or stimulants. As a result, we chose HCC-1171 non-small cell lung cancer cell line expressing SHP2 with the activating V46L mutation to investigate the effects of monobodies on ERK phosphorylation in regards to the high Gab2 expression and high ERK and SHP2 phosphorylation. This cell line was even more interesting as it had the activating mutation in N-SH2 domain of SHP2. Upon transduction of the HCC-1171 cells with SHP2 targeting monobodies, a significant decrease in ERK phosphorylation was observed. Moreover, the Y542 phosphorylation was decreased upon monobody expression. Our findings for the SHP2 targeting monobodies indicated that targeting SHP2 with monobodies strongly reduces the phosphorylation of ERK and also SHP2 activity which was followed by the inhibition of Y542 phosphorylation. This results showed that monobodies have profound effects on SHP2 activity in both Bcr-Abl expressing cells and solid tumor cell lines. The promising data obtained from these cell lines opens the way of the usage of monobodies in a broad context. Since Ras/ERK pathway is important for the cell survival, using monobodies as small protein inhibitors might be beneficial for therapeutic aspect.

Although a significant decrease in ERK phosphorylation was observed in retrovirally stably/constitutively transduced HCC-1171 cells, this system did not allow us to see any changes on cell proliferation. We speculated that this effect might be due to the adaptation of the cells to monobody expression and this might be a reason for not detecting any profound effect on cell proliferation. If

the cells adapt themselves to the expression of monobody, the cells might get irresponsive for SHP2 inhibition and activate other pathways to proliferate. There are different types of promoters that have different degrees of control of gene expression. In mammalian expression vectors, cytomegalovirus immediate-early promoter (CMV), simian virus 40 early promoter (SV40), human Elongation Factor-1alpha (EF-1a), phosphoglycerate kinase 1 promoter (PGK) or chicken  $\beta$ -actin promoter (CAG) promoters are being widely used. Although most of the promoters have consistent strength for different cell lines, CMV is variable according to the cell line (Qin et al., 2010). CMV and EF-1alpha is always stronger than SV-40 promoter. In some cell lines CMV is stronger than EF-1alpha, but in others it is the other way around (C. I. Lee, Kohn, Ekert, & Tarantal, 2004; Teschendorf, Warrington, Siemann, & Muzyczka, 2002). In the retroviral expression system, we used retroviral gene transfer which facilitated the constitutive expression of the monobody under 5'LTR (long terminal repeat) retroviral promoter that results in a low and mild expression of the construct. As we were not able to find any difference in proliferation with retroviral transduced stable cells, we decided to use an inducible expression system in order to study the physiological effects of monobodies.

Therefore, HCC-1171 cells with doxycycline inducible expression of SHP2 targeting monobodies was investigated in order to get a sudden and strong expression of monobodies and response from the cells. Unlike retroviral vector promoter, the lentiviral vector that was used in the inducible expression system has a stronger promoter, EF-1alpha. HCC-1171 cells were used for this system that express a constitutive active mutant (V46L) of SHP2 as mentioned above. By performing the titration of the lentivirus, the amount of the virus was calculated in order to infect 100% of the population. We aimed at 100% infection efficiency because the effect on ERK phosphorylation was observed with the retroviral transduced cells which were sorted for monobody expression. In the inducible system, transduction of all the cells was required to observe an effect of monobodies when the expression was induced. After first doxycycline induction, unexpectedly we achieved only less than 10% of the population induced although we were expecting the population to be 100% GFP positive. Then we decided to keep the cells under induction over 13 passages. The induction of the

expression of monobodies were successful in this cell lines however not to a level that we expected. By the time we have observed an increased GFP positive population, which means that the system was working, but the increase in GFP signal was not as sudden as we expected. This time period might create a room for the cells to allow for adaptation to the expression of the monobodies and we had the similar kind of obstacle of adaptation in retrovirally transduced cells. Therefore, we were not able to find a difference neither in proliferation of the cells nor ERK phosphorylation. Although in retrovirally transduced cells, we observed a complete abolishment of ERK phosphorylation, we could not reproduce this result with inducible system, which is probably because of the reason that not all the cells were expressing the monobodies after induction. We have detected the expression of the monobodies but since the cell population was partly GFP positive, the expression was coming from the cells that were infected with lentivirus and induced with doxycycline. As no decrease in ERK phosphorylation was observed in the inducible system in contrast to the constitutive system, significant changes in cell proliferation can not be expected. Since we could not obtain a cell population that is fully infected and induced, the result we had from this system was only coming from a mixture of cell population; infected and non-infected cells or induced and uninduced cells. The failed result of not having 100% induction, thus 100% GFP positive cells might be a failure of either the lentiviral infection step which might result in insufficient infection efficiency or the doxycycline induction step which might be insufficient induction efficiency. Also the possible overgrowth of uninduced cells over induced cell population might prevent us to observe the effects of monobodies on cell proliferation and ERK phosphorylation. This could be also a reason why we observed a decrease in GFP positive population after reaching a maximum which was around 60-80% GFP positivity. On the other hand, when the monobodies reached to a maximum level of expression which was followed by FACS, the monobodies might have showed a toxic effect on cells and this might explain the decrease in GFP positive population. Although, we had comparable levels of expression of monobodies when compared to the retrovirally transduced and sorted cell line, this is probably because of the strength of the promoter that we used in lentiviral vector. In the retroviral



vector, the promoter was weaker than in the inducible lentiviral vector. So, despite having less cells expressing monoclonal antibody than the sorted retrovirally transduced cells, the expression of the monoclonal antibody under doxycycline inducible promoter yielded a similar level of protein level.

However, in HCC-1171 lung cancer cell line where the pathways are activated with different proteins other than Bcr-Abl, a complete abolishment of ERK phosphorylation was observed with single monoclonal antibodies. By using tandem monoclonal antibodies, we observed an inhibitory effect of SHP2 on ERK phosphorylation in HEK293 cells which overexpress Bcr-Abl. We can argue that using tandem monoclonal antibodies could be beneficial to block both signaling domains at the same time and obtain superior effect than single monoclonal antibodies.

The data obtained in this study indicate that monoclonal antibodies were able to block SHP2 downstream signaling through inhibiting the activation of SHP2. The inhibitory effect on ERK phosphorylation was observed in a solid tumor cell line and tandem monoclonal antibodies inhibit the phosphorylation in HEK293 cells which overexpress Bcr-Abl. This would argue the broad efficacy of monoclonal antibodies in both solid tumors and hematological malignancies. The lack of progress in PTP targeting is because they were considered as tumor suppressors with opposing roles to tyrosine kinases. With the developing knowledge of tyrosine phosphatases in cancer or in other diseases, the effort on the drug development is increasing against PTPs. The PTP active site is highly conserved and highly positively charged and the screening of drug libraries end up with negatively charged compounds or oxidizing groups that react with the catalytic cysteine. The charged molecules have limiting cell membrane penetration (R. J. He et al., 2014). However the importance of PTPs in cancer, diabetes, autoimmunity and tuberculosis makes them very attractive targets (R. He, Zeng, He, Zhang, & Zhang, 2013). Despite the effort of the industry, there are no commercialized protein tyrosine phosphatase (PTP) inhibitors on the market (R. J. He et al., 2014). Targeting the phosphatases by monoclonal antibodies might be beneficial because the regulation of phosphatase activity is highly dependent on protein interaction domains like SH2 domain. Targeting such domains with monoclonal antibodies could be an alternative way of targeting PTPs rather than phosphatase domain.

### 3.3 PLC $\gamma$ 1 targeting monobodies

In this part of the thesis, we focused on PLC $\gamma$ 1 and targeting its SH2 domains with monobodies. After the selection of binders, we evaluated the specificity of the binder monobodies in cells and found that they are monospecific for their target protein. When the monobodies were tested in Bcr-Abl overexpressing cells, a decrease in PLC $\gamma$ 1 phosphorylation was observed but *in vitro* data, by Fern Sha, showed us that the monobodies were not acting as phosphotyrosine competitors when tested against Gab2 tandem phosphotyrosine peptide. SH2 domains of PLC $\gamma$ 1 have been reported to bind the activated receptor tyrosine kinases which are auto-phosphorylated. PLC $\gamma$ 1 is recruited to the phosphorylated tyrosine of the receptors by its SH2 domains. When PDGF is bound to PDGF receptor (PDGFR)  $\beta$  subunit, receptor tyrosine phosphorylation is triggered and association with signal transduction molecules, including PLC $\gamma$  occurs (Valius, Bazenet, & Kazlauskas, 1993). Characterization of PDGFR $\beta$  mutants showed that Y1021 phosphorylation is required for the association of PLC $\gamma$ 1 to the carboxy terminal of the receptor. On the other hand, Eriksson et al. demonstrated that PLC $\gamma$ 1 binds to PDGFR $\alpha$  from the Y1018 residue that is in the same motif with PDGFR $\beta$  Y1021 (NH<sub>2</sub>-YIPLPD-COOH). It is suggested that the complex between PLC $\gamma$  and the PDGFR $\alpha$  is more stable than that of PLC $\gamma$  and the PDGFR $\beta$  (Eriksson et al., 1995). Next, PDGFR $\beta$  pY1021 site containing peptide was used for the binding characterization of PLC $\gamma$ 1 targeting monobodies. NLa4 did not inhibit the N-SH2 to phosphopeptide binding, while CLa4 showed an inhibition of C-SH2 to phosphopeptide binding. Monobodies showed more inhibitory effect on PDGFR phosphopeptide than tandem Gab2 phosphopeptide. Then we investigated the roles of monobodies in PDGF induced environment and showed that monobodies decreased the phosphorylation of PLC $\gamma$ 1 upon PDGF stimulation. They were able to decrease the interaction between PDGFR $\alpha$  and modulate the ERK phosphorylation mildly in cells.

In cells, we showed that N-SH2 targeting monobodies inhibited Y783 phosphorylation better than CLa4. This might be due to the additional factors in the complex cellular environment and when the low specificity of the CLa4

against PLC $\gamma$ 1 is considered, this result is not surprising. On the other hand, this does not eliminate the fact that C-SH2 targeting might be also necessary for PLC $\gamma$ 1 activation inhibition.

When the interaction of PLC $\gamma$ 1 with PDGFR $\alpha$  under PDGF-bb stimulation was investigated, CLa4 demonstrated decrease the interaction between PLC $\gamma$ 1 and the receptor. This result was unexpected because it has been described that mainly N-SH2 domains of PLC $\gamma$ 1 was responsible for the binding to the receptor tyrosine kinases and C-SH2 was mostly responsible for the intramolecular interactions. The interaction of PLC $\gamma$ 1 with PDGFR $\alpha$  should be investigated more in detail and further analysis of the binding should be elucidated by comparing the tyrosine 1021 mutant which is deficient in binding PLC $\gamma$ 1 together with wild type receptor in the presence of monobodies. In this way, one can evaluate whether monobodies are as effective as Y1021F mutant PDGFR $\alpha$  in terms of the disruption of interaction. Furthermore, the activation of PLC $\gamma$ 1 under FGFR could be also investigated upon FGF stimulation.

The comparison of different receptor stimulation and the effects of monobodies on PLC $\gamma$ 1 activation is beneficial.

The evaluation of ERK phosphorylation showed a decrease in ERK phosphorylation but not in MEK phosphorylation. This result might indicate that monobodies might affect the PLC $\gamma$ 1 activation status although we need to consider that the effect of PLC $\gamma$ 1 on ERK phosphorylation is indirect. The phosphorylation of the upstream kinase of ERK, MEK, was not affected by monobody expression so the modulation of this pathway should be investigated more in detail.

From in vitro data, when Gab2 tandem phosphopeptide was tested, neither of the PLC $\gamma$ 1 targeting monobodies were found to be as phosphotyrosine inhibitors and when PDGFR $\alpha$  phosphopeptide was used, CLa4 found to be a possible phosphotyrosine inhibitor. However, cellular interactome data showed that CLa4 failed to bind PLC $\gamma$ 1 in K562 and HEK293 cells. Since the in vitro and cellular data contradicts in terms of being phosphotyrosine inhibitor, a new set of PLC $\gamma$ 1 targeting monobodies should be developed and tested. In order to further evaluate monobodies on PLC $\gamma$ 1 catalytic activity, a radioactivity-based

assay could be used in a PIP2 hydrolysis assay. This is a widely used assay to measure the PLC $\gamma$ 1 catalytic activity although the specific measurement of PLC $\gamma$ 1 activity in this assay is not definitive. Also, a calcium assay could be done for the activity measurement by measuring the fluorescently labeled calcium levels but again the result of this assay could be due to not only PLC $\gamma$ 1 activity but also some other factors that could change the levels of intracellular calcium.

### **3.5 Final conclusions**

Proteins do not act isolated but they act as a component of complex molecular networks. When a complex disease is considered, cancer for instance, many signaling pathways are activated to promote the survival and proliferation of cancer cells. Stommel et al. demonstrated the multiple co-activation of RTK in glioblastoma multiforme and discussed that targeting single RTK might limit the efficacy of therapies (Stommel et al., 2007). The current understanding for the selection of pharmacological targets focus on a specific target in a specific signaling pathway, although when the complexity of the diseases are considered, these kind of single molecular targeting strategies are more likely to be problematic (Goh et al., 2007). Development of a drug candidate is delicate and costs over 850M USD (Wood, 2006). For this reason, the presence of a human interactome map would be greatly beneficial to provide insight into disease mechanisms and identifying the signaling networks more accurately as drug targets (Rual et al., 2005).

Bcr-Abl should be thought as a protein complex rather than a single kinase. By dissecting the network around Bcr-Abl and the critical interactors, combinatorial therapies should be considered by inhibiting the kinase activity in addition to the interactors by using protein inhibitors which monobodies might be good candidates. Combination of the multi-competent therapeutic reagents could be a better way to simultaneously target signaling pathways. The paradigm single drug for a single target should be reconsidered because of the off-target effects of these magic bullet drugs, which could possibly cause unwanted effects (Jaeger & Aloy, 2012). These effects can cause the remodeling of the protein complexes and could initiate the activation of other pathways, which was very

clearly demonstrated by Brehme et al. by using nilotinib and dasatinib remodeling in Bcr-Abl protein network (Brehme et al., 2009). This concept of Bcr-Abl biology and CML could be generalized to other oncogenic proteins in other malignancies.

The dissection of the signaling pathways is very important at this point because of the above-mentioned concepts. In this study, the effects of perturbing signaling nodes were investigated by using small protein inhibitors, monobodies. The investigation of the effects of the single signaling nodes by genetic knock-out or knock down strategies eliminate a single protein or causes the loss of protein expression. This elimination also removes the signaling domains and binding motifs at the same time. Using monobodies to selectively block the signaling nodes and define the participation of different signaling pathway activation could be an important brick to put on the network medicine concept. Furthermore, the combination of the signaling dissection by small protein inhibitors together with quantitative methods would enable the researchers to enhance and deepen the understanding of such signaling networks. There are some advances in drug discovery to target protein-protein interactions by using structure-based discovery approaches. In a recent review, the small molecule modulators were discussed and more than 12 small molecule modulators were in clinical development. However, the huge diversity and transient nature of protein-protein interactions and different binding modes, surfaces, makes it difficult to generalize these interactions. It is a generally accepted idea that the therapeutic class of "biologicals" has higher potency and affinity for their cognate target (Nero, Morton, Holien, Wielens, & Parker, 2014). Thus, these interactions between the biological and the targets are starting points for the drug discovery.

There are some other non-antibody protein scaffolds. Monobodies have similar properties but also some critical advantages over other intracellular binders like DARPins (designed ankyrin repeat proteins), Affibodies (designed based on the Z domain of protein A) or Anticalins (beta-barrel scaffold structures based on lipocalins) (Gebauer & Skerra, 2009). DARPins are derived from the natural ankyrin repeat proteins. In DARPins and monobodies, the shared properties are their small size, absence of disulphite bonds and the ease of production in bacterial systems with high yields (Gilbreth & Koide, 2012). On the

other hand, DARPins mostly bind to convex surfaces, while monobodies can bind to both convex and concave surfaces (Gilbreth & Koide, 2012). Monobodies have the antibody-like loops and characteristic fold of immunoglobulin domain while DARPins consists of a secondary structure. Moreover, monobodies have a highly biased library design and aromatic aminoacids, especially tyrosines, are enriched in the binding interface. DARPins, affibody and anticalin libraries use a largely unbiased set of aminoacids (Gilbreth & Koide, 2012). In monobodies, the diversified positions contribute an average of 80% of surface area and 68% of all contacting residues, while for DARPins, these values are 68% and 54%, respectively (Gilbreth & Koide, 2012). When the therapeutic potentials and immunogenicity of these scaffolds are considered, the choice of a scaffold with a human origin becomes very important. In this aspect monobodies are advantageous since their scaffold is human originated (Skerra, 2007). Tetranectin or avimer with human origin scaffold might be beneficial but they have three disulfide bridges which would be a drawback for these scaffold in the reducing cellular environment. Although having twice the size of monobodies, affilin has a human origin backbone and no disulfide bonds (Skerra, 2007).

A monobody based antibody mimetic, pegdinetanib (Angicept, CT-322) is in Phase II trials for the treatment of glioblastoma which is an antagonist of VEGFR-2 (Tolcher et al., 2011). As being an extracellular target, VEGFR-2 is bound and blocked by the FN3 based compound. However the challenging issue for monobodies as therapeutics is to target the intracellular targets and deliver them into the cell. To deliver the compound of interest has a wide range of strategies like viral delivery, immunoconjugates, liposomes. The maintenance of the drugs or proteins stability and potency is also critical. Cell penetrating peptides (CPP) are also used for the protein or peptide delivery although their tissue or cell specificity is still unanswered question. Transactivator of transcription (TAT) is one of the most widely studied CPP and some others are also investigated like AntP, CPP44, R9. Different types of cell penetrating peptides could be tested to deliver the monobodies into the cell. Moreover, the cell type specificity should be also elucidated in detail because the targeted delivery of monobodies would be essential for the pharmaceutical use.

The monoclonal antibodies could be used as a binder for various types of targets. We can argue that an extracellular target for monoclonal antibody would eliminate the obstacle for the delivery so it would be much more easier to target. Receptor–ligand interactions could be targeted, similar to CT-322 compound, but the binding surface also has a determinant criteria. For instance, IL2R and its ligand has a more planar surface binding interface which might be challenging for monoclonal antibody to target (Arkin, Tang, & Wells, 2014). Although, when we consider that monoclonal antibodies could bind both concave and convex areas, the targets that could be bound by monoclonal antibodies are in a large range. It is also noteworthy that the monoclonal antibodies preferably bind pockets or hinge regions that enable to target enzyme active sites by monoclonal antibodies.

However, some factors could hamper the monoclonal antibody activity and expression in the cell. Despite the high specificity and affinity of monoclonal antibodies to their cognate target in cells, some unspecific interactions also might occur. The SHP2 targeting Cs1 monoclonal antibody showed a similar affinity in vitro but in cells, the binding was hindered by abundant off-target interactions thus the specificity was less than the other monoclonal antibodies. Also, in our Strep-HA tagged monoclonal antibody expression, we were not able to detect a high level of monoclonal antibody expression which might argue the possibility of degradation because of the small size of tagged-monoclonal antibody. Because, a bigger tag solved this problem and the monoclonal antibody was expressed in cells. Moreover, if the target protein interaction domain undergoes post-translational modification, the binding of monoclonal antibodies might be interrupted. The intracellular and circulatory half-life of the monoclonal antibodies are still remains to be investigated (Hey et al., 2005). To conclude, there are still some challenges for monoclonal antibodies to be used therapeutically.





## CHAPTER 4

### MATERIALS AND METHODS

#### 4.1 Cloning

The Gateway cloning system (Invitrogen) was used to clone all the constructs into expression vectors. In order to clone the gene of interest in pDONR201 vector, the gene was first amplified by PCR by using primers compatible for gateway cloning. The primer sequence was designed as either N- or C-terminally fusion constructs. IMAGE fully sequenced cDNA clones for human GAB1, GAB2, PTPN6, PIK3R1 were obtained from Source Bioscience LifeSciences. Full-length cDNA of human PLCG1 including the Gateway cloning sites at 5' and 3' end was synthesized from GenScript.

For transient transfections, the pCS2-N-6xMyc-Gw (N-terminal fusion), pEF1-C-V5-Myc-Gw (C-terminal fusion), pcDNA3.1-Gw vectors were used. For retroviral transductions pfMIG-N-Strep-3xHA (N-terminal fusion), pfMIG-C-Strep-3xHA (C-terminal fusion) and pRVNTAP-GS-Gw (N-terminal fusion) vectors were used.

Point mutations were done using the Quick-change site directed mutagenesis kit (Stratagene). The sequences of all cDNAs and point mutations were confirmed by sequencing.

#### 4.2 Cell culture and transfections

The adherent cell lines HEK293, HEK293gp, NIH3T3, HCC1171 were maintained in Dulbecco's Modified Eagle's Medium (DMEM) GlutaMAX medium (Gibco, 31966-021) supplemented with 10% Fetal Calf Serum (Gibco, 10270-106) and 1% penicillin/streptomycin (AmiMed, 4-01F00-H) at 37°C in 5% CO<sub>2</sub>. The suspension cell line K562 was maintained in RPMI 1640 growth medium (Gibco, 61870-010) supplemented with 10% FCS and 1% penicillin streptomycin at 37°C in 5% CO<sub>2</sub>. Cells were transiently transfected with plasmids DNAs using

the Polyfect transfection reagent (Qiagen). 48 hours after transfection of the cells, cells were washed with 1x phosphate buffer saline (PBS). After the removal of the PBS, the cells were scraped from the dish into an Eppendorf tube by using ice-cold immunoprecipitation (IP) then lysed in IP buffer (50mM Tris-HCl, pH 7.5, 150 mM NaCl, 1% NP-40, 5 mM EDTA, 5 mM EGTA, 25 mM NaF, 1 mM orthovanadate, 1 mM PMSF (Sigma), 10 mg/ml TPCK (Applichem, A1801-0500) and Protease Inhibitor cocktail tablets (Roche, product number 04693116001). Then the lysate was centrifuged at 14000 rpm for 10 minutes in order to remove cell debris. The supernatants were transferred to a new Eppendorf tube. Total protein concentration was measured with the Bradford assay (Bio-Rad, catalog number 500-0006) and the lysates were subjected to SDS-PAGE, followed by immunoblot.

## **4.3 Immunoblotting and immunoprecipitation**

### **4.3.1 Preparation of total cell lysate**

Samples were prepared to obtain 100µg protein per 20 µL and boiled for 5 minutes in Laemmli buffer at 95°C then subjected to SDS-PAGE. Afterwards the SDS-PAGE samples stored at -20°C and the cell lysates were kept at -80°C.

### **4.3.2 Immunoblotting analysis and antibodies**

The samples were separated by SDS-PAGE and then transferred to a nitrocellulose membrane (Whatmann, Protran BA85, GE Healthcare) by using semi-dry blotting system (Hoefer Scientific Semi-phor TE70). The nitrocellulose membrane and the SDS-PAGE gel was sandwiched between three Whatman cellulose chromatography papers (3MM Chr sheets) that were pre-soaked with 1x western blot buffer (25 mM Tris, 192 mM Glycine, 10% (v/v) methanol). The transfer was done for 1.5 hours at 0.075mA/cm<sup>2</sup>. Afterwards, the membrane was blocked for 1 hour at room temperature with the blocking solution and then the membrane was incubated with the primary antibody overnight at 4°C which

was diluted in the solution recommended by the supplier. Next day, the membrane was washed three times for 5 minutes with TBS-T or PBS-T (TBS or 1xPBS supplemented with 0.1% Tween-20). Following the washing of the membrane, the primary antibody was detected with IRDye680 and IRDye800-coupled anti mouse or anti rabbit secondary antibody or HRP-conjugated IgG antibodies that were diluted 1:10000 in the washing buffer, PBS-T or TBS-T. Lastly, the secondary antibody was also washed three times 5 minutes washing. the following antibodies were used: Abl (Oncogene Science), total phosphotyrosine 4G10 (Millipore), HA (mouse, monoclonal, clone 16B12, Covance), and myc (anti tag)-IRDye800 (Rockland, catalog number 600-432-381), SHP2 (mouse, monoclonal, catalog number 610622, BD Transduction laboratories and rabbit, monoclonal, clone D50F2, Cell Signaling), pY580 SHP2 (rabbit, polyclonal, catalog number 3703, Cell Signaling), pY542 SHP2 (rabbit, polyclonal, catalog number 3751, Cell Signaling), Gab2 (rabbit, monoclonal, clone 26B6, Cell Signaling), STAT5 (rabbit, polyclonal, clone 06-968, Millipore) and pY694/699 STAT5 (mouse, monoclonal, clone 8-5-2, Millipore), paxillin (mouse, monoclonal, clone 5H11, Millipore), PLC $\gamma$ 1 (rabbit, polyclonal, catalog number 2822s, Cell Signaling), pY783 PLC $\gamma$ 1 (catalog number 2821, cell signaling), ERK (rabbit, polyclonal, catalog number 9102, Cell signaling), pT202/pY204 ERK (mouse, monoclonal, catalog number 9106, Cell signaling), V5 tag (mouse, monoclonal, clone SV5-Pk1, AbD Serotec), Grb2 (rabbit, clone C23, catalog number sc-255, Santacruz), myc tag (mouse, monoclonal, catalog number 9B11, Cell Signaling), tubulin (mouse, monoclonal, Clone DM1A, catalog number T9026, Sigma), pY177 Bcr (rabbit, polyclonal, catalog number 3901, cell signaling), AKT pan (rabbit, clone C67E7, catalog number 4691S, Cell signaling), pS473 AKT (rabbit, clone D9E, catalog number 4060S, Cell signaling), MEK1/2 (rabbit, polyclonal, catalog number 9122, Cell signaling), pS217/221 MEK (rabbit, monoclonal, catalog number 9154, Cell signaling), PDGFR $\alpha$  (rabbit, polyclonal, catalog number 3164, Cell Signaling).

We used IRDye680 and IRDye800-coupled anti mouse (Li-Cor, 926-32210) and anti-rabbit (Rockland, 611-732-127) secondary antibodies used for detection by using the Odyssey fluorescent imaging system (Li-Cor). For Licor secondary antibodies, Licor system used to develop the western blots. HRP-

conjugated IgG antibodies AffiniPure anti-mouse (Jackson ImmunoResearch, 115-035-003), AffiniPure anti-rabbit (Jackson ImmunoResearch, 111-035-003) were used to reveal primary antibodies and Amersham ECL Prime Western Blotting Detection Reagent (GE healthcare, RPN2232) substrate used for development and detection.

### **4.3.3 Immunoprecipitation**

0.5 to 1 mg of total protein was used for immunoprecipitations. The required volume of total cell lysate was calculated and then the volume was added up to 1 mL with IP buffer. Afterwards the required amount of antibody was added into diluted cell lysate and incubated on a rotating wheel for 2-3 hours at 4°C. Then 50 µl of Protein G sepharose (GE Healthcare, 17-0618-01-5ML) beads were added to each IP sample and incubated 1 hour on rotating wheel at 4°C. Subsequently, beads were washed 3 times with IP buffer and in the last wash 20% of the IP were spared to detect the bait protein. At the end, 20 µL of Laemmli buffer was added on the beads, boiled for 5 minutes at 95°C then subjected for western blot.

### **4.4 Stable cell line generation with retroviral infection**

The N-terminally cloned monobodies in pRV-N-TAP-GS-Gw and N- or C-terminally cloned Gab2 interactors in pFMIG-Strep-3xHA-Gw destination vectors were used to generate stable cell lines. TAP tag stands for 2xProtein G tag then a TEV cleavage site, followed by Streptavidin binding protein tag (SBP) and one myc tag. After the gene of interest, there is an internal ribosome entry site (IRES)-GFP to follow the expression of the construct by FACS. Stable cell lines were generated for HEK293 and K562 cells by retroviral infection using HEK293gp cells as virus producer cells which were derived from HEK293 cells. HEK293gp cells stably express MLV gag and pol proteins (Burns, Friedmann, Driever, Burrascano, & Yee, 1993). Following the co-transfection of VSV-G (vesicular stomatitis virus G) cDNA and the retroviral vector plasmid DNA in 293gp cells, pseudotyped retroviral vectors can be produced. The retroviral

vector plasmid constructs in addition to VSV-G cDNA which encodes for envelope protein were cotransfected by using the Polyfect transfection reagent. After 2 days, the virus was collected from the supernatant of the virus producing HEK293gp cells. Retrovirus was harvested twice with 12 hours of intervals and, afterwards the target cells were infected with the virus supernatant. Before treating the cells with retrovirus, cells were incubated with polybrene (Santa Cruz, sc-134220) to enhance the infection efficiency. Retrovirally infected cells were FACS-sorted according to GFP expression.

#### **4.5 Flow cytometry analysis and cell sorting**

Cell sorting was performed by FACS Aria II device (BD biosciences) at the EPFL Flow cytometry core facility. Parental cells were used as negative control and the cells were sorted according to their GFP or dsRED selective marker. Cells were harvested on the day of sorting and then washed with PBS. Afterwards the cells were resuspended in FACS buffer which is composed of 0.6% BSA in 1xPBS. Then the cells were submitted to the facility for sorting.

#### **4.6 Strep-HA affinity purification**

This method enables the improvement of yield, sensitive identification of protein complexes, high purity sample suitable for the LC-MS/MS analysis and requires relatively low amount of starting material. K562 CML cell line was used as model system because of the presence of endogenous Bcr-Abl expression, which is also a well characterized and most widely used CML cell line.

The stable cell lines were expanded to  $2 \times 10^8$  cells which corresponds to 5x15 cm dishes and the cell pellet snap frozen until the affinity purification was performed. Strep-HA buffer 1 (SH1 buffer) was prepared as follows: 50 mM, pH 8.0 HEPES, 150 mM NaCl, 5 mM EDTA, 0.5% NP-40 and the protease inhibitors were added freshly (50 mM NaF, 1 mM sodium orthovanadate, 1 mM PMSF, Roche cocktail protease inhibitors). The frozen cell pellet was thawed on ice for 5 minutes. 1 mL per 15 cm dish SH buffer 1 with 1  $\mu\text{g}/\text{mL}$  avidin (catalog number: 2-0204-015) was prepared and added to the cell pellet in order to bind and

remove the biotinylated carboxylases. Then the cell pellet was resuspended with the buffer and incubated on ice for 20 minutes. A sample was collected for immunoblotting (total extract (TE)). Following the incubation, the cell lysate was splitted into 2 mL eppendorf tubes and centrifuged at 13000 rpm for 15 minutes at 2°C. The concentration of the total protein was determined by Bradford assay. 400 µL StrepTactin sepharose was transferred to a fresh BioRad Biospin column and washed with 2 times with 1 mL SH1 buffer. After washing the beads, the protein lysate was applied on the column and allowed to enter resin by gravity flow (Sample saved from the flowthrough named as SN1). Streptactin sepharose was washed with 4 times with 1 mL SH1 buffer and then eluted into a fresh eppendorf with 2.5 mM biotin solution (sample was saved from the eluate named as E1). In the meantime, 200 µL anti-HA agarose beads (catalog number: 081M4865) were washed twice with 1 mL SH1 buffer. The anti-HA agarose beads were added to the biotin eluates and rotated on a spinning wheel for 1 hour at 4°C. Afterwards, the beads were centrifuged (sample saved from the supernatant named as SN2) and the beads were transferred to a fresh Biospin column, washed three times with 1 mL SH buffer 1, later the beads were washed with SH buffer 2 (50 mM pH 8.0 HEPES, 150 mM NaCl, 5 mM EDTA). At the last step, the proteins were eluted from the column directly with 2x250 µL 150 mM HCl into an eppendorf tube containing 125 µL TEAB (sample was saved from the eluate named as E2). The eluate snap was frozen in liquid nitrogen and lyophilized overnight. Anti-HA beads were left in the column was boiled by adding 75 µL Laemmli buffer at 95°C for 5 minutes (sample was named as boiled beads).

#### **4.7 Tandem affinity purification**

K562 cells and HEK293 cells were stably transduced with TAP-tagged monobodies and then they were sorted for GFP positivity. The Abl SH2-targeting monobody HA4 was used as control for the TAP purifications. Two biological repeats were done for the two different cell lines. Firstly, the cells were expanded to 2-3x10<sup>9</sup> cells and then centrifuged at 300 x g, 5 minutes at 4°C. After washing the cell pellet with PBS, the pellet was frozen in liquid nitrogen until



affinity purification. Then the cell pellet was lysed with 25 mL TAP buffer (50 mM Tris-HCl pH 7.5, 100 mM NaCl, 5% glycerol, 0.2% NP-40, 1.5 mM MgCl<sub>2</sub> and 25 mM NaF)) and incubated on ice for 15 minutes. Later, the cells were spun 15 minutes at 4500 x g at 4°C. Then, the supernatant was placed into Beckman Coulter Ultracentrifuge tubes (polycarbonate thick walls, 38mL, catalog number: 355631) and spun down at 100.000 x g for 1 hour at 4°C. Meanwhile, IgG beads (Sigma, product code: A2909-5ML) were washed and equilibrated with TAP buffer. At the end of centrifugation, 200 µL IgG beads were added to the lysate and incubated for 2-3 hours rotating at the cold room on a rotating wheel. Afterwards, the beads were recovered by centrifugation at 600 rpm for 3 minutes at 4°C, then transferred to Bio-Rad Bio-Spin columns (catalog number: 732-6008), and afterwards washed with 10 mL TAP buffer. After washing the beads, TEV protease was diluted 1:10 in TEV cleavage buffer (10 mM Tris-HCl pH 7.5, 100 mM NaCl, 0.5 M EDTA pH 8.0). The outlet of the columns were closed with its lid and carefully strengthened with parafilm, then TEV protease was added and incubated at 16°C shaking in the cold room in a thermoshaker (800 rpm). After cleaving the protein with TEV protease, the protein was eluted into a fresh tube. Streptavidin UltraLink Resin beads (Pierce, product code: 53114, 5mL) were washed with TEV cleavage buffer, then added and incubated with the eluate in order to bind with SBP tag for 1 hour on rotating wheel at cold room. Lastly, the beads were washed with 10 mL TAP buffer in Bio-Rad Bio-spin column to remove any unbound protein, then protein complexes were eluted using 2x250 µL 0.150 M hydrochloric acid and immediately neutralized with 125 µL 0.5 M triethyl-ammonium bicarbonate (TEAB). The eluate was snap-frozen in liquid nitrogen and lyophilized overnight. The efficiency of elution was checked by boiling the beads in SDS-PAGE sample buffer. The eluates were resolved by SDS-PAGE (any kD gel, Bio-rad, catalog number: 456-9033) and 10% were silver stained, 10% were immunoblotted, whereas the remaining eluate were prepared for mass spectrometric analysis.

## **4.8 LC-MS/MS analysis of the protein complexes**

The remaining part of each tandem affinity purification eluate were separated by SDS-PAGE in pre-cast gel and stained with R-250 Coomassie Blue Solution. Proteins were identified by LC/MS-MS in PCF of EPFL. Protein identifications were grouped according to shared peptides, and a single protein representing the group is said to be identified. Gel lanes were cut into pieces and subjected to in-gel digestion with trypsin. Extracted peptides were separated by reversed-phase chromatography on a Dionex Ultimate 3000 RSLC nano UPLC system (Dionex) on-line connected in-line either with an Orbitrap Elite or an Orbitrap Q-Exactive Mass Spectrometer (Thermo Fischer Scientific). Raw data were processed with Proteome Discoverer (v. 1.3) and searched with Mascot against a human database (UniProt release 2012\_04; 86747 sequences). Data were further processed, inspected and visualized using the Scaffold 3 software. Common contaminants were eliminated for the further analysis.

## **4.9 Expression and purification of recombinant SH2 domains**

The N-SH2 and C-SH2 domains were prepared as fusion proteins C-terminal to 6xHis, a biotin-acceptor tag, and a TEV cleavage site using an in-house vector termed pHBT. (A. Koide, Gilbreth, Esaki, Tereshko, & Koide, 2007; A. Koide et al., 2012). All proteins were purified using Ni-Sepharose columns (GE Healthcare).

## **4.10 siRNA mediated knock down**

siRNA mediated knock down was performed for PLC $\gamma$ 1 genes by using On-target plus Smart pool from Thermo Scientific Dharmacon, GE Healthcare. The catalog numbers for the siRNA for PLC $\gamma$ 1 is L-003559-00. HCC1171, K562 and NIH3T3 cells were seeded in 2 ml in 6-well plate with  $1 \times 10^6$  cells per well. The day after seeding, the medium was removed from the cells and 500  $\mu$ L fresh medium added then transfection was performed by HiperFect transfection

reagent. In total five samples were prepared as untransfected cells, control siRNA, mock (no siRNA, only transfection reagent added) and knockdown of the gene of interest was performed once and twice. Transfection mix was prepared by mixing 18  $\mu$ L HiperFect transfection reagent (Qiagen, catalog number: 301705) and 20  $\mu$ M 5  $\mu$ L siRNA in 500  $\mu$ L serum free medium (SFM). Then the transfection mix was vortexed and incubated for 10 minutes at room temperature. Afterwards, the mix was added on the cells. The next day, 500  $\mu$ L fresh medium was added on the all the cells except the retransfection sample. These cells were retransfected with the same procedure, and on next day 500  $\mu$ L fresh medium added to this sample. The cells were incubated at 37°C for 48 hours, then lysed and subjected to immunoblotting.

#### **4.11 Cell growth by CellTiter-Glo Luminescent cell viability assay**

CellTiter-Glo Luminescent cell viability assay is a very sensitive method that measures the viable cells in culture based on the quantitation of ATP amount which is a measure of the presence of metabolically active cells. The cells were seeded at  $5 \times 10^4$  cells in 100  $\mu$ L per well in a 96 well plate (opaque walled) per well in 100  $\mu$ L medium for each construct. Then the cells were incubated at different time points. After the incubation period, an equal volume, 100 $\mu$ L, of CellTiter-Glo reagent was added on the cells. Following the mixing of the 96-well plate on the shaker to induce cell lysis for 2 minutes, the plate was incubated in the dark for 10 minutes at room temperature to stabilize the luminescent signal. Then the luminescence signal was recorded by SpectraMax.

#### **4.12 Lentiviral vector production**

Lentiviral vectors for tTR-KRAB repressor, inducible monobody expression vectors were produced as previously described (Wiznerowicz & Trono, 2003). Briefly, the plasmids pMD2G (55  $\mu$ g), pCMVR8.74 (102  $\mu$ g) and pLV-N-TAP-monobody vectors were mixed for co-transfection of 5x 15 cm HEK293T using the calcium phosphate method (CalPhos Mammalian

Transfection Kit, Clontech). Transfected cells were incubated overnight and the supernatant was replaced after 8 hours by fresh DMEM medium containing 10% FCS and replaced by fresh medium for another 12 hours. The medium was harvested 3 times with 12 hours time intervals. The harvested supernatant was cleared using a 0.22  $\mu\text{m}$  filter (Stericup, Millipore) before virus concentration by ultracentrifugation for 2h at 50,000 x g, 16°C (Beckman Coulter: Ultra-Clear tubes No. 344058, Rotor SW32Ti). The supernatant was removed carefully and the virus pellet was resuspended in 20  $\mu\text{L}$  ice-cold 1xPBS for each tube and then finally the lentiviral particles were frozen at -80°C.

























Table A3. Complete protein list of mass spectrometry results from PLCγ1 monobody interactome analysis from K562 cells

#	Emel_GenCe	EmelSubDB_140407	Visible?	Started?/Identified Proteins (37)	Accession Ni	Molecular W	Protein Gro	ClA4	ClA4_2	NLa4	NLa4_1	NLa4_2	NLa7	NLa7_1	NLa7_2
1	TRUE	Empty	Empty	NLa7 Monobody	NLa7	18 kDa	TRUE	unknown	398	754	320	235	323	323	687
2	TRUE	Empty	Empty	Keratin, type II cytoskeletal 1 OS=Homo sapiens GN=KRT1 PE=1 SV=6	P04264	66 kDa	TRUE	unknown	369	102	161	59	119	115	115
3	TRUE	Empty	Empty	Sequence from Hantschellab	TEV	19 kDa	TRUE	unknown	17	161	13	222	22	206	206
4	TRUE	Empty	Empty	Keratin, type I cytoskeletal 9 OS=Homo sapiens GN=KRT9 PE=1 SV=3	P35527	62 kDa	TRUE	unknown	243	37	101	27	75	64	64
5	TRUE	Empty	Empty	Keratin, type I cytoskeletal 10 OS=Homo sapiens GN=KRT10 PE=1 SV=6	P13645	59 kDa	TRUE	unknown	157	56	83	33	69	61	61
6	TRUE	Empty	Empty	Isoform 2 of 1-phosphatidylinositol 4,5-bisphosphate phospholipase gamma-1 OS=Homo sapiens GN=PLCG1	P19174-2	149 kDa	TRUE	unknown	1	19	87	131	22	139	139
7	TRUE	Empty	Empty	Keratin, type II cytoskeletal 2 epidermal OS=Homo sapiens GN=KRT2 PE=1 SV=2	P35908	65 kDa	TRUE	unknown	108	48	59	27	32	36	36
8	TRUE	Empty	Empty	Epidermal growth factor receptor substrate 1S OS=Homo sapiens GN=EPS1S PE=1 SV=2	P42566	95 kDa	TRUE	unknown	4	1	85	114	0	4	4
9	TRUE	Empty	Empty	ClA4 Monobody	ClA4	19 kDa	TRUE	unknown	43	51	22	37	41	5	5
10	TRUE	Empty	Empty	Heat shock cognate 71 kDa protein OS=Homo sapiens GN=HSPA8 PE=1 SV=1	P11142	71 kDa	TRUE	unknown	28	24	23	38	17	32	32
11	TRUE	Empty	Empty	Isoform 2 of Epidermal growth factor receptor substrate 1S-like 1 OS=Homo sapiens GN=EPS1S1	QBUBC2-2	100 kDa	TRUE	unknown	2	0	57	113	0	4	4
12	TRUE	Empty	Empty	Isoform 4 of Titin OS=Homo sapiens GN=TTN	QBWZ42-4	3716 kDa	TRUE	unknown	11	0	0	0	0	0	0
13	TRUE	Empty	Empty	Stress-70 protein, mitochondrial OS=Homo sapiens GN=HSPA9 PE=1 SV=2	P38646	74 kDa	TRUE	unknown	43	17	26	12	7	10	10
14	TRUE	Empty	Empty	Keratin, type II cytoskeletal 5 OS=Homo sapiens GN=KRT5 PE=1 SV=3	P13647	62 kDa	TRUE	unknown	52	9	15	3	8	11	11
15	TRUE	Empty	Empty	Keratin, type I cytoskeletal 14 OS=Homo sapiens GN=KRT14 PE=1 SV=4	P02533	52 kDa	TRUE	unknown	49	13	23	1	10	10	10
16	TRUE	Empty	Empty	Hornerin OS=Homo sapiens GN=HRNR PE=1 SV=2	Q86Y23	282 kDa	TRUE	unknown	52	6	14	1	0	4	4
17	TRUE	Empty	Empty	Tubulin beta chain OS=Homo sapiens GN=TUBB PE=1 SV=2	P07437	50 kDa	TRUE	unknown	24	18	5	3	8	22	22
18	TRUE	Empty	Empty	Ubiquitin (Fragment) OS=Homo sapiens GN=RP27A PE=1 SV=1	J3QTR3 (+16)	12 kDa	TRUE	unknown	13	13	10	9	3	9	9
19	TRUE	Empty	Empty	40S ribosomal protein S3 OS=Homo sapiens GN=RPS3 PE=1 SV=2	P23396	27 kDa	TRUE	unknown	6	24	7	2	1	16	16
20	TRUE	Empty	Empty	Tubulin alpha-1C chain OS=Homo sapiens GN=TUBA1C PE=2 SV=1	F5H5D3 (+2)	58 kDa	TRUE	unknown	11	6	6	12	14	16	16
21	TRUE	Empty	Empty	Desmoplakin OS=Homo sapiens GN=DSP PE=1 SV=3	P15924	332 kDa	TRUE	unknown	22	0	2	0	5	0	0
22	TRUE	Empty	Empty	Putative elongation factor 1-alpha-like 3 OS=Homo sapiens GN=EEF1A3 PE=5 SV=1	Q5VTE0	50 kDa	TRUE	unknown	16	14	2	1	0	10	10
23	TRUE	Empty	Empty	Heat shock 70 kDa protein 1A/1B OS=Homo sapiens GN=HSPA1A PE=1 SV=5	P08107	70 kDa	TRUE	unknown	8	9	4	5	4	11	11
24	TRUE	Empty	Empty	Keratin, type II cytoskeletal 6A OS=Homo sapiens GN=KRT6A PE=1 SV=3	P02538	60 kDa	TRUE	unknown	17	7	7	0	2	6	6
25	TRUE	Empty	Empty	78 kDa glucose-regulated protein OS=Homo sapiens GN=GRP78 PE=1 SV=2	P11021	72 kDa	TRUE	unknown	7	8	8	7	1	6	6
26	TRUE	Empty	Empty	40S ribosomal protein S19 OS=Homo sapiens GN=RPS19 PE=1 SV=2	P39019	16 kDa	TRUE	unknown	6	11	4	1	0	9	9
27	TRUE	Empty	Empty	Serum albumin OS=Homo sapiens GN=ALB PE=1 SV=2	P02768	69 kDa	TRUE	unknown	5	5	3	5	2	13	13
28	TRUE	Empty	Empty	AP-2 complex subunit beta OS=Homo sapiens GN=AP2B1 PE=4 SV=1	K7E1T8	101 kDa	TRUE	unknown	0	0	10	19	0	0	0
29	TRUE	Empty	Empty	40S ribosomal protein S18 OS=Homo sapiens GN=RPS18 PE=1 SV=3	PG2269	18 kDa	TRUE	unknown	2	11	5	1	0	5	5
30	TRUE	Empty	Empty	Keratin, type I cytoskeletal 16 OS=Homo sapiens GN=KRT16 PE=1 SV=4	P08779	51 kDa	TRUE	unknown	13	6	3	0	5	2	2
31	TRUE	Empty	Empty	AP-2 complex subunit alpha-1 OS=Homo sapiens GN=AP2A1 PE=1 SV=3	O95782 (+1)	108 kDa	TRUE	unknown	0	0	5	15	0	0	0
32	TRUE	Empty	Empty	Desmoglein-1 OS=Homo sapiens GN=DSG1 PE=1 SV=2	Q02413	114 kDa	TRUE	unknown	10	1	2	0	1	0	0
33	TRUE	Empty	Empty	HLA-B associated transcript 3, isoform CRA_a OS=Homo sapiens GN=BAG6 PE=2 SV=1	BU0X83 (+3)	119 kDa	TRUE	unknown	7	1	0	0	1	0	0
34	TRUE	Empty	Empty	Keratin, type II cytoskeletal 4 OS=Homo sapiens GN=KRT4 PE=2 SV=1	F5H8K9 (+1)	54 kDa	TRUE	unknown	0	0	0	0	0	0	0
35	TRUE	Empty	Empty	Desmocollin-1 OS=Homo sapiens GN=DSCI1 PE=1 SV=2	Q08554 (+1)	100 kDa	TRUE	unknown	8	0	0	0	0	0	0
36	TRUE	Empty	Empty	AP-2 complex subunit alpha-2 OS=Homo sapiens GN=AP2A2 PE=1 SV=2	O94973 (+1)	104 kDa	TRUE	unknown	0	0	1	7	0	0	0
37	TRUE	Empty	Empty	Semonegelin-1 OS=Homo sapiens GN=SEMIG1 PE=1 SV=2	P04279	52 kDa	TRUE	unknown	6	0	0	0	0	0	0

\* SH2 domain containing proteins are highlighted.



Table A4. Complete protein list of mass spectrometry results from PLCγ1 monobody interactome analysis from HEK293 cells (continued)

61	TRUE	Empty	RNA-binding protein 14 OS=Homo sapiens GN=RBM14 PE=1 SV=2	Q9BPK6	69 kDa	unknown	6	8	4	4	5	10
62	TRUE	Empty	T-complex protein 1 subunit theta OS=Homo sapiens GN=CTC18 PE=1 SV=4	P50990	60 kDa	unknown	7	11	1	2	4	4
63	TRUE	Empty	Heterogeneous nuclear ribonucleoprotein K OS=Homo sapiens GN=HNRKPK PE=1 SV=1	P61978 (r3)	51 kDa	unknown	2	7	3	3	5	8
64	TRUE	Empty	Protein-L-isoaspartate O-methyltransferase OS=Homo sapiens GN=PCMT1 PE=2 SV=1	H7BY58 (r3)	30 kDa	unknown	5	9	1	3	4	4
65	TRUE	Empty	Actin, cytoplasmic 1 OS=Homo sapiens GN=ACTB PE=1 SV=1	P60709 (r1)	42 kDa	unknown	11	5	0	1	3	14
66	TRUE	Empty	ATP-dependent RNA helicase A OS=Homo sapiens GN=DM99 PE=1 SV=4	Q0R211	141 kDa	unknown	2	2	5	0	2	20
67	TRUE	Empty	RNA-binding protein EWS OS=Homo sapiens GN=EWSR1 PE=2 SV=1	BC02Y01 (r4)	65 kDa	unknown	4	6	6	3	4	9
68	TRUE	Empty	Probable ATP-dependent RNA helicase DDX17 OS=Homo sapiens GN=DDX17 PE=2 SV=1	H3BLZ8	80 kDa	unknown	2	3	3	2	3	10
69	TRUE	Empty	Epilakin OS=Homo sapiens GN=EPRK1 PE=1 SV=2	P58107	556 kDa	unknown	2	1	0	0	0	2
70	TRUE	Empty	Small nuclear ribonucleoprotein Sm D2 OS=Homo sapiens GN=SNRPD2 PE=1 SV=1	P11940 (r1)	71 kDa	unknown	1	5	0	3	4	16
71	TRUE	Empty	Small nuclear ribonucleoprotein Sm D2 OS=Homo sapiens GN=SNRPD2 PE=1 SV=1	P62316	14 kDa	unknown	4	5	6	5	4	16
72	TRUE	Empty	Keratinocyte proline-rich protein OS=Homo sapiens GN=KRRP PE=1 SV=1	Q51749	64 kDa	unknown	4	9	7	1	5	0
73	TRUE	Empty	Desmoglein OS=Homo sapiens GN=DSP PE=1 SV=3	P15924	332 kDa	unknown	2	1	9	3	0	0
74	TRUE	Empty	Keratin, type I cytoskeletal 16 OS=Homo sapiens GN=KRT16 PE=1 SV=4	P08779	51 kDa	unknown	6	7	5	0	5	1
75	TRUE	Empty	T-complex protein 1 subunit delta OS=Homo sapiens GN=CTD7 PE=2 SV=1	R72010 (r1)	52 kDa	unknown	4	9	0	1	4	5
76	TRUE	Empty	PREDICTED_405 ribosomal protein S4, X isoform [Mesocricetus auratus]	gi_524962683 ref ?	0	unknown	0	0	0	7	0	4
77	TRUE	Empty	PREDICTED_405 ribosomal protein S4, X isoform [Mesocricetus auratus]	P26373	24 kDa	unknown	3	3	1	5	3	6
78	TRUE	Empty	60S ribosomal protein L23a OS=Homo sapiens GN=RPL23A PE=2 SV=1	ABAU53 (r5)	22 kDa	unknown	3	3	2	4	2	7
79	TRUE	Empty	Cleavage and polyadenylation specificity factor subunit 5 OS=Homo sapiens GN=NJDT21 PE=1 SV=1	O43809	26 kDa	unknown	5	3	2	4	3	6
80	TRUE	Empty	T-complex protein 1 subunit zeta OS=Homo sapiens GN=CTC16A PE=2 SV=1	B4DP08 (r1)	55 kDa	unknown	3	7	1	2	4	4
81	TRUE	Empty	40S ribosomal protein S2 OS=Homo sapiens GN=RS2 PE=1 SV=2	P1E880	31 kDa	unknown	1	4	0	1	4	0
82	TRUE	Empty	Lys-63-specific deubiquitinase BRCC36 OS=Homo sapiens GN=BRCC3 PE=1 SV=2	P46736 (r1)	36 kDa	unknown	0	9	0	14	0	10
83	TRUE	Empty	40S ribosomal protein S4 OS=Homo sapiens GN=RS4P58 PE=2 SV=1	ABNE09 (r2)	33 kDa	unknown	1	5	0	7	6	4
84	TRUE	Empty	SWI/SNF complex subunit SMARCC1 OS=Homo sapiens GN=SMARCC1 PE=1 SV=3	Q39292	123 kDa	unknown	4	5	0	0	1	10
85	TRUE	Empty	Acyl-coenzyme A thioesterase 9, mitochondrial OS=Homo sapiens GN=ACOT9 PE=1 SV=2	Q39105 (r1)	50 kDa	unknown	0	2	18	0	0	0
86	TRUE	Empty	1-phosphatidylinositol 4,5-bisphosphate 3-ohospholipidase gamma 2, OS=Homo sapiens GN=PLCG2 PE=1 SV=4	P1E885	148 kDa	unknown	6	12	0	0	0	0
87	TRUE	Empty	40S ribosomal protein S3a OS=Homo sapiens GN=RS3A PE=1 SV=2	P61247	30 kDa	unknown	3	0	1	1	1	11
88	TRUE	Empty	T-complex protein 1 subunit beta OS=Homo sapiens GN=CTC2 PE=2 SV=2	F5GW16 (r2)	57 kDa	unknown	4	8	0	1	2	1
89	TRUE	Empty	T-complex protein 1 subunit eta OS=Homo sapiens GN=CTC7 PE=1 SV=2	Q99832 (r1)	59 kDa	unknown	3	9	0	2	1	2
90	TRUE	Empty	Clathrin heavy chain 1 OS=Homo sapiens GN=CLTC PE=1 SV=5	Q00610 (r1)	192 kDa	unknown	2	6	0	4	4	1
91	TRUE	Empty	T-complex protein 1 subunit alpha OS=Homo sapiens GN=TCP1 PE=1 SV=1	P17987	60 kDa	unknown	4	9	0	0	0	0
92	TRUE	Empty	Ras GTPase-activating-like protein IQGAP1 OS=Homo sapiens GN=IQGAP1 PE=1 SV=1	P46940	189 kDa	unknown	3	5	0	0	0	0
93	TRUE	Empty	ATP-dependent RNA helicase DDX1 OS=Homo sapiens GN=DDX1 PE=1 SV=2	Q392499	82 kDa	unknown	2	2	1	1	3	7
94	TRUE	Empty	Protein argonaute 2 OS=Homo sapiens GN=AGO2 PE=1 SV=3	Q9UKV8	97 kDa	unknown	2	0	1	1	3	12
95	TRUE	Empty	Heterogeneous nuclear ribonucleoprotein U OS=Homo sapiens GN=HNRNPU PE=1 SV=6	Q00859 (r1)	91 kDa	unknown	1	1	2	0	0	10
96	TRUE	Empty	APP-2 complex subunit beta OS=Homo sapiens GN=APP2B1 PE=4 SV=1	K7E1T8	101 kDa	unknown	0	0	5	7	0	0
97	TRUE	Empty	APP-2 complex subunit sigma OS=Homo sapiens GN=APP2S1 PE=4 SV=1	M0QY22 (r2)	19 kDa	unknown	0	0	10	14	0	0
98	TRUE	Empty	60S acidic ribosomal protein PO-like OS=Homo sapiens GN=RPLP0P6 PE=5 SV=1	Q8NHV5	34 kDa	unknown	1	3	3	1	7	0
99	TRUE	Empty	Dynein heavy chain 2, axonemal OS=Homo sapiens GN=DNAH2 PE=2 SV=3	G9P225	508 kDa	unknown	0	3	0	0	1	0
100	TRUE	Empty	Isoform 3 of Dystrorhin OS=Homo sapiens GN=DMD	P11532-4	426 kDa	unknown	1	0	0	0	0	0
101	TRUE	Empty	Ig gamma-1 chain, C region OS=Homo sapiens GN=IGHG1 PE=1 SV=1	P01857	36 kDa	unknown	4	1	0	0	0	5
102	TRUE	Empty	Small nuclear ribonucleoprotein-associated protein OS=Homo sapiens GN=SNRPN PE=2 SV=1	P62277	25 kDa	unknown	1	3	0	2	3	3
103	TRUE	Empty	40S ribosomal protein S13 OS=Homo sapiens GN=RP513 PE=1 SV=2	B3KVR1 (r5)	17 kDa	unknown	1	3	0	1	0	5
104	TRUE	Empty	60S ribosomal protein L12 OS=Homo sapiens GN=RPL12 PE=1 SV=1	P30050	18 kDa	unknown	0	1	1	5	0	8
105	TRUE	Empty	40S ribosomal protein S30 OS=Homo sapiens GN=FAU PE=1 SV=1	P26196	7 kDa	unknown	4	1	1	2	2	1
106	TRUE	Empty	Probable ATP-dependent RNA helicase DDX6 OS=Homo sapiens GN=DDX6 PE=1 SV=2	P62861	83 kDa	unknown	2	4	0	0	0	0
107	TRUE	Empty	Polymeric immunoglobulin receptor OS=Homo sapiens GN=PIGR PE=1 SV=4	P01833	84 kDa	unknown	4	1	0	0	0	0
108	TRUE	Empty	Dermodin OS=Homo sapiens GN=DDCD PE=1 SV=2	P81605 (r1)	11 kDa	unknown	1	5	2	1	4	1
109	TRUE	Empty	Heat shock protein HSP 90-beta OS=Homo sapiens GN=HSP90AB1 PE=1 SV=4	P08238	83 kDa	unknown	2	3	0	6	2	0
110	TRUE	Empty	T-complex protein 1 subunit epsilon OS=Homo sapiens GN=CTC5 PE=2 SV=1	E9PCA1	57 kDa	unknown	3	3	0	1	1	2
111	TRUE	Empty	Heterogeneous nuclear ribonucleoprotein M1 (Fragment) OS=Homo sapiens GN=HNRNPM PE=4 SV=1	M0R019 (r3)	77 kDa	unknown	2	3	0	2	1	1
112	TRUE	Empty	Nucleolin OS=Homo sapiens GN=NCL PE=1 SV=3	P19338	117 kDa	unknown	1	2	5	0	0	3
113	TRUE	Empty	Eukaryotic translation initiation factor 2 subunit 3 OS=Homo sapiens GN=EIF253 PE=1 SV=3	P41091	51 kDa	unknown	2	3	0	2	1	1
114	TRUE	Empty	UT small nuclear ribonucleoprotein 70 kDa OS=Homo sapiens GN=SNRP70 PE=1 SV=2	P06621 (r1)	52 kDa	unknown	1	9	0	2	1	0
115	TRUE	Empty	Fatty acid synthase OS=Homo sapiens GN=FASN PE=1 SV=3	Q9T230	273 kDa	unknown	2	3	1	3	1	0
116	TRUE	Empty	RuvB-like 2 OS=Homo sapiens GN=RVBL2 PE=1 SV=5	Q9T230	51 kDa	unknown	0	3	0	1	0	3
117	TRUE	Empty	Tubulin gamma-1 chain OS=Homo sapiens GN=TUBG1 PE=1 SV=2	P22258	51 kDa	unknown	0	0	0	1	0	3
118	TRUE	Empty	60S ribosomal protein L31 OS=Homo sapiens GN=RPL31 PE=1 SV=1	P62899	14 kDa	unknown	1	1	0	4	0	4
119	TRUE	Empty	Histone-arginine methyltransferase CBMT1 OS=Homo sapiens GN=CBMT1 PE=1 SV=3	Q08X53 (r1)	60 kDa	unknown	3	3	1	1	1	3
120	TRUE	Empty	Desmoglein-1 OS=Homo sapiens GN=DSG1 PE=1 SV=2	Q0Z413	114 kDa	unknown	3	3	1	1	0	0

\* SH2 domain containing proteins are highlighted.

**Table A4. Complete protein list of mass spectrometry results from PLC $\gamma$ 1 monobody interactome analysis from HEK293 cells (continued)**

121	TRUE	Empy	60S ribosomal protein L6 (Fragment) OS=Homo sapiens GN=RL6 PE=2 SV=1	26 kDa	0	0	0	2	0	0	3
122	TRUE	Empy	Purative adenosine/thymosinase 3 OS=Homo sapiens GN=AHCY2 PE=1 SV=1	67 kDa	0	0	0	0	0	0	2
123	TRUE	Empy	Glyceroldehyde-3-phosphate dehydrogenase OS=Homo sapiens GN=AHCY2 PE=1 SV=1	36 kDa	4	2	0	0	0	0	9
124	TRUE	Empy	Protein S100A8 OS=Homo sapiens GN=S100A8 PE=1 SV=1	11 kDa	1	4	2	0	0	0	1
125	TRUE	Empy	Sorting nexin-9 OS=Homo sapiens GN=SNX9 PE=1 SV=1	67 kDa	1	0	0	2	0	0	1
126	TRUE	Empy	Keratin, type I cytoskeletal 13 OS=Homo sapiens GN=KRT13 PE=1 SV=1	50 kDa	3	0	0	2	0	0	0
127	TRUE	Empy	Heterogeneous nuclear ribonucleoproteins A2/B1 OS=Homo sapiens GN=HNRNP2A2/B1 PE=1 SV=2	222.62 kDa	0	0	0	0	0	0	0
128	TRUE	Empy	Flagginn-2 OS=Homo sapiens GN=HLG2 PE=1 SV=1	248 kDa	0	2	0	0	0	0	0
129	TRUE	Empy	40S ribosomal protein S11 OS=Homo sapiens GN=RP311 PE=4 SV=1	14 kDa	1	0	0	0	0	0	1
130	TRUE	Empy	Cleavage and polyadenylation-specificity factor subunit 7 (Fragment) OS=Homo sapiens GN=CPSF7 PE=2 SV=1	41 kDa	2	2	0	0	0	0	1
131	TRUE	Empy	BRIS3 and BRCA1-A complex member 1 OS=Homo sapiens GN=BBAM1 PE=4 SV=1	36 kDa	0	0	0	4	7	0	0
132	TRUE	Empy	T-complex protein 1 subunit gamma OS=Homo sapiens GN=CGT3 PE=1 SV=4	61 kDa	1	4	0	0	2	0	1
133	TRUE	Empy	Heterogeneous nuclear ribonucleoprotein H2 OS=Homo sapiens GN=HNRHP2 PE=1 SV=1	49 kDa	1	0	0	1	2	0	1
134	TRUE	Empy	AT rich interactive domain 1B (SWI1-like), isoform CRA_1 OS=Homo sapiens GN=ARID1B PE=2 SV=1	237 kDa	2	3	0	0	0	0	3
135	TRUE	Empy	TRNA-splicing ligase RecB homolog OS=Homo sapiens GN=CZorf28 PE=1 SV=1	55 kDa	0	0	0	1	0	0	5
136	TRUE	Empy	60S ribosomal protein L23 OS=Homo sapiens GN=RL23 PE=1 SV=1	15 kDa	1	2	1	1	1	0	1
137	TRUE	Empy	60S ribosomal protein L7A OS=Homo sapiens GN=RL7A PE=1 SV=2	30 kDa	1	0	0	0	0	0	6
138	TRUE	Empy	60S ribosomal protein L7A OS=Homo sapiens GN=RL7A PE=2 SV=1	10 kDa	0	0	0	2	0	0	3
139	TRUE	Empy	Actin-like protein 6A OS=Homo sapiens GN=ACTL6A PE=1 SV=1	47 kDa	3	2	0	1	0	0	2
140	TRUE	Empy	Dihydrodipolysialic residue succinyltransferase component of 2-oxoglutarate dehydrogenase complex, mitochondrial OS=Homo sapiens GN=DLST PE=1 SV=1	16 kDa	0	0	0	2	0	0	4
141	TRUE	Empy	60S ribosomal protein L27 OS=Homo sapiens GN=RL27 PE=1 SV=2	257 kDa	1	2	0	0	0	0	0
142	TRUE	Empy	isoform 3 of Acetyl-CoA carboxylase 1 OS=Homo sapiens GN=ACACA	17 kDa	0	0	0	0	0	0	5
143	TRUE	Empy	40S ribosomal protein S9 OS=Homo sapiens GN=RP59 PE=2 SV=1	15 kDa	2	1	1	1	1	0	3
144	TRUE	Empy	Tubulin beta-4B chain OS=Homo sapiens GN=UBB4B PE=1 SV=1	50 kDa	1	1	0	0	0	0	2
145	TRUE	Empy	Protein transport protein Sec23A OS=Homo sapiens GN=SEC23A PE=2 SV=1	85 kDa	1	0	0	0	0	0	4
146	TRUE	Empy	isoform 2 of SWI/SNF-related matrix-associated actin-dependent regulator of chromatin subfamily E member 1 OS=Homo sapiens GN=SMARCE1	42 kDa	1	2	0	0	0	0	6
147	TRUE	Empy	isoform 2 of SWI/SNF-related matrix-associated actin-dependent regulator of chromatin subfamily E member 1 OS=Homo sapiens GN=SMARCE1	42 kDa	1	2	0	0	0	0	6
148	TRUE	Empy	isoform 2 of SWI/SNF-related matrix-associated actin-dependent regulator of chromatin subfamily E member 1 OS=Homo sapiens GN=SMARCE1	42 kDa	1	2	0	0	0	0	6
149	TRUE	Empy	isoform 2 of SWI/SNF-related matrix-associated actin-dependent regulator of chromatin subfamily E member 1 OS=Homo sapiens GN=SMARCE1	42 kDa	1	2	0	0	0	0	6
150	TRUE	Empy	isoform 2 of SWI/SNF-related matrix-associated actin-dependent regulator of chromatin subfamily E member 1 OS=Homo sapiens GN=SMARCE1	42 kDa	1	2	0	0	0	0	6
151	TRUE	Empy	isoform 2 of SWI/SNF-related matrix-associated actin-dependent regulator of chromatin subfamily E member 1 OS=Homo sapiens GN=SMARCE1	42 kDa	1	2	0	0	0	0	6
152	TRUE	Empy	isoform 2 of SWI/SNF-related matrix-associated actin-dependent regulator of chromatin subfamily E member 1 OS=Homo sapiens GN=SMARCE1	42 kDa	1	2	0	0	0	0	6
153	TRUE	Empy	isoform 2 of SWI/SNF-related matrix-associated actin-dependent regulator of chromatin subfamily E member 1 OS=Homo sapiens GN=SMARCE1	42 kDa	1	2	0	0	0	0	6
154	TRUE	Empy	isoform 2 of SWI/SNF-related matrix-associated actin-dependent regulator of chromatin subfamily E member 1 OS=Homo sapiens GN=SMARCE1	42 kDa	1	2	0	0	0	0	6
155	TRUE	Empy	isoform 2 of SWI/SNF-related matrix-associated actin-dependent regulator of chromatin subfamily E member 1 OS=Homo sapiens GN=SMARCE1	42 kDa	1	2	0	0	0	0	6
156	TRUE	Empy	isoform 2 of SWI/SNF-related matrix-associated actin-dependent regulator of chromatin subfamily E member 1 OS=Homo sapiens GN=SMARCE1	42 kDa	1	2	0	0	0	0	6
157	TRUE	Empy	isoform 2 of SWI/SNF-related matrix-associated actin-dependent regulator of chromatin subfamily E member 1 OS=Homo sapiens GN=SMARCE1	42 kDa	1	2	0	0	0	0	6
158	TRUE	Empy	isoform 2 of SWI/SNF-related matrix-associated actin-dependent regulator of chromatin subfamily E member 1 OS=Homo sapiens GN=SMARCE1	42 kDa	1	2	0	0	0	0	6
159	TRUE	Empy	isoform 2 of SWI/SNF-related matrix-associated actin-dependent regulator of chromatin subfamily E member 1 OS=Homo sapiens GN=SMARCE1	42 kDa	1	2	0	0	0	0	6
160	TRUE	Empy	isoform 2 of SWI/SNF-related matrix-associated actin-dependent regulator of chromatin subfamily E member 1 OS=Homo sapiens GN=SMARCE1	42 kDa	1	2	0	0	0	0	6
161	TRUE	Empy	isoform 2 of SWI/SNF-related matrix-associated actin-dependent regulator of chromatin subfamily E member 1 OS=Homo sapiens GN=SMARCE1	42 kDa	1	2	0	0	0	0	6
162	TRUE	Empy	isoform 2 of SWI/SNF-related matrix-associated actin-dependent regulator of chromatin subfamily E member 1 OS=Homo sapiens GN=SMARCE1	42 kDa	1	2	0	0	0	0	6
163	TRUE	Empy	isoform 2 of SWI/SNF-related matrix-associated actin-dependent regulator of chromatin subfamily E member 1 OS=Homo sapiens GN=SMARCE1	42 kDa	1	2	0	0	0	0	6
164	TRUE	Empy	isoform 2 of SWI/SNF-related matrix-associated actin-dependent regulator of chromatin subfamily E member 1 OS=Homo sapiens GN=SMARCE1	42 kDa	1	2	0	0	0	0	6
165	TRUE	Empy	isoform 2 of SWI/SNF-related matrix-associated actin-dependent regulator of chromatin subfamily E member 1 OS=Homo sapiens GN=SMARCE1	42 kDa	1	2	0	0	0	0	6
166	TRUE	Empy	isoform 2 of SWI/SNF-related matrix-associated actin-dependent regulator of chromatin subfamily E member 1 OS=Homo sapiens GN=SMARCE1	42 kDa	1	2	0	0	0	0	6
167	TRUE	Empy	isoform 2 of SWI/SNF-related matrix-associated actin-dependent regulator of chromatin subfamily E member 1 OS=Homo sapiens GN=SMARCE1	42 kDa	1	2	0	0	0	0	6
168	TRUE	Empy	isoform 2 of SWI/SNF-related matrix-associated actin-dependent regulator of chromatin subfamily E member 1 OS=Homo sapiens GN=SMARCE1	42 kDa	1	2	0	0	0	0	6
169	TRUE	Empy	isoform 2 of SWI/SNF-related matrix-associated actin-dependent regulator of chromatin subfamily E member 1 OS=Homo sapiens GN=SMARCE1	42 kDa	1	2	0	0	0	0	6
170	TRUE	Empy	isoform 2 of SWI/SNF-related matrix-associated actin-dependent regulator of chromatin subfamily E member 1 OS=Homo sapiens GN=SMARCE1	42 kDa	1	2	0	0	0	0	6
171	TRUE	Empy	isoform 2 of SWI/SNF-related matrix-associated actin-dependent regulator of chromatin subfamily E member 1 OS=Homo sapiens GN=SMARCE1	42 kDa	1	2	0	0	0	0	6
172	TRUE	Empy	isoform 2 of SWI/SNF-related matrix-associated actin-dependent regulator of chromatin subfamily E member 1 OS=Homo sapiens GN=SMARCE1	42 kDa	1	2	0	0	0	0	6
173	TRUE	Empy	isoform 2 of SWI/SNF-related matrix-associated actin-dependent regulator of chromatin subfamily E member 1 OS=Homo sapiens GN=SMARCE1	42 kDa	1	2	0	0	0	0	6
174	TRUE	Empy	isoform 2 of SWI/SNF-related matrix-associated actin-dependent regulator of chromatin subfamily E member 1 OS=Homo sapiens GN=SMARCE1	42 kDa	1	2	0	0	0	0	6
175	TRUE	Empy	isoform 2 of SWI/SNF-related matrix-associated actin-dependent regulator of chromatin subfamily E member 1 OS=Homo sapiens GN=SMARCE1	42 kDa	1	2	0	0	0	0	6
176	TRUE	Empy	isoform 2 of SWI/SNF-related matrix-associated actin-dependent regulator of chromatin subfamily E member 1 OS=Homo sapiens GN=SMARCE1	42 kDa	1	2	0	0	0	0	6
177	TRUE	Empy	isoform 2 of SWI/SNF-related matrix-associated actin-dependent regulator of chromatin subfamily E member 1 OS=Homo sapiens GN=SMARCE1	42 kDa	1	2	0	0	0	0	6
178	TRUE	Empy	isoform 2 of SWI/SNF-related matrix-associated actin-dependent regulator of chromatin subfamily E member 1 OS=Homo sapiens GN=SMARCE1	42 kDa	1	2	0	0	0	0	6
179	TRUE	Empy	isoform 2 of SWI/SNF-related matrix-associated actin-dependent regulator of chromatin subfamily E member 1 OS=Homo sapiens GN=SMARCE1	42 kDa	1	2	0	0	0	0	6
180	TRUE	Empy	isoform 2 of SWI/SNF-related matrix-associated actin-dependent regulator of chromatin subfamily E member 1 OS=Homo sapiens GN=SMARCE1	42 kDa	1	2	0	0	0	0	6

\* SH2 domain containing proteins are highlighted.





## REFERENCES

- Advani, A. S., & Pendergast, A. M. (2002). Bcr-Abl variants: biological and clinical aspects. *Leuk Res*, 26(8), 713-720.
- Agazie, Y. M., & Hayman, M. J. (2003a). Development of an efficient "substrate-trapping" mutant of Src homology phosphotyrosine phosphatase 2 and identification of the epidermal growth factor receptor, Gab1, and three other proteins as target substrates. *J Biol Chem*, 278(16), 13952-13958. doi: 10.1074/jbc.M210670200
- Agazie, Y. M., & Hayman, M. J. (2003b). Molecular mechanism for a role of SHP2 in epidermal growth factor receptor signaling. *Mol Cell Biol*, 23(21), 7875-7886.
- Alberts, B. (1998). The cell as a collection of protein machines: preparing the next generation of molecular biologists. *Cell*, 92(3), 291-294.
- Alonso, A., Sasin, J., Bottini, N., Friedberg, I., Friedberg, I., Osterman, A., . . . Mustelin, T. (2004). Protein tyrosine phosphatases in the human genome. *Cell*, 117(6), 699-711. doi: 10.1016/j.cell.2004.05.018
- Amarante-Mendes, G. P., Naekyung Kim, C., Liu, L., Huang, Y., Perkins, C. L., Green, D. R., & Bhalla, K. (1998). Bcr-Abl exerts its antiapoptotic effect against diverse apoptotic stimuli through blockage of mitochondrial release of cytochrome C and activation of caspase-3. *Blood*, 91(5), 1700-1705.
- Anderson, D., Koch, C. A., Grey, L., Ellis, C., Moran, M. F., & Pawson, T. (1990). Binding of SH2 domains of phospholipase C gamma 1, GAP, and Src to activated growth factor receptors. *Science*, 250(4983), 979-982.
- Araki, T., Nawa, H., & Neel, B. G. (2003). Tyrosyl phosphorylation of Shp2 is required for normal ERK activation in response to some, but not all, growth factors. *J Biol Chem*, 278(43), 41677-41684. doi: 10.1074/jbc.M306461200
- Arkin, M. R., Tang, Y., & Wells, J. A. (2014). Small-molecule inhibitors of protein-protein interactions: progressing toward the reality. *Chem Biol*, 21(9), 1102-1114. doi: 10.1016/j.chembiol.2014.09.001
- Bard-Chapeau, E. A., Li, S., Ding, J., Zhang, S. S., Zhu, H. H., Princen, F., . . . Feng, G. S. (2011). Ptpn11/Shp2 acts as a tumor suppressor in hepatocellular carcinogenesis. *Cancer Cell*, 19(5), 629-639. doi: 10.1016/j.ccr.2011.03.023
- Barford, D., & Neel, B. G. (1998). Revealing mechanisms for SH2 domain mediated regulation of the protein tyrosine phosphatase SHP-2. *Structure*, 6(3), 249-254.
- Batori, V., Koide, A., & Koide, S. (2002). Exploring the potential of the monobody scaffold: effects of loop elongation on the stability of a fibronectin type III domain. *Protein Eng*, 15(12), 1015-1020.
- Beck, A., Wurch, T., Bailly, C., & Corvaia, N. (2010). Strategies and challenges for the next generation of therapeutic antibodies. *Nat Rev Immunol*, 10(5), 345-352. doi: 10.1038/nri2747
- Bennett, A. M., Hausdorff, S. F., O'Reilly, A. M., Freeman, R. M., & Neel, B. G. (1996). Multiple requirements for SHPTP2 in epidermal growth factor-mediated cell cycle progression. *Mol Cell Biol*, 16(3), 1189-1202.



- Bennett, A. M., Tang, T. L., Sugimoto, S., Walsh, C. T., & Neel, B. G. (1994). Protein-tyrosine-phosphatase SHPTP2 couples platelet-derived growth factor receptor beta to Ras. *Proc Natl Acad Sci U S A*, *91*(15), 7335-7339.
- Bentires-Alj, M., Gil, S. G., Chan, R., Wang, Z. C., Wang, Y., Imanaka, N., . . . Gu, H. (2006). A role for the scaffolding adapter GAB2 in breast cancer. *Nat Med*, *12*(1), 114-121. doi: 10.1038/nm1341
- Bentires-Alj, M., Paez, J. G., David, F. S., Keilhack, H., Halmos, B., Naoki, K., . . . Neel, B. G. (2004). Activating mutations of the noonan syndrome-associated SHP2/PTPN11 gene in human solid tumors and adult acute myelogenous leukemia. *Cancer Res*, *64*(24), 8816-8820. doi: 10.1158/0008-5472.CAN-04-1923
- Bixby, D., & Talpaz, M. (2010). Seeking the causes and solutions to imatinib-resistance in chronic myeloid leukemia. *Leukemia : official journal of the Leukemia Society of America, Leukemia Research Fund, UK*. doi: 10.1038/leu.2010.238
- Bloom, L., & Calabro, V. (2009). FN3: a new protein scaffold reaches the clinic. *Drug Discov Today*, *14*(19-20), 949-955. doi: 10.1016/j.drudis.2009.06.007
- Bolton-Gillespie, E., Schemionek, M., Klein, H. U., Flis, S., Hoser, G., Lange, T., . . . Skorski, T. (2013). Genomic instability may originate from imatinib-refractory chronic myeloid leukemia stem cells. *Blood*, *121*(20), 4175-4183. doi: 10.1182/blood-2012-11-466938
- Bonvini, E., DeBell, K. E., Veri, M. C., Graham, L., Stoica, B., Laborda, J., . . . Rellahan, B. L. (2003). On the mechanism coupling phospholipase Cgamma1 to the B- and T-cell antigen receptors. *Adv Enzyme Regul*, *43*, 245-269.
- Branford, S., Rudzki, Z., Walsh, S., Grigg, A., Arthur, C., Taylor, K., . . . Hughes, T. P. (2002). High frequency of point mutations clustered within the adenosine triphosphate-binding region of BCR/ABL in patients with chronic myeloid leukemia or Ph-positive acute lymphoblastic leukemia who develop imatinib (STI571) resistance. *Blood*, *99*(9), 3472-3475.
- Brasher, B. B., & Van Etten, R. A. (2000). c-Abl has high intrinsic tyrosine kinase activity that is stimulated by mutation of the src homology 3 domain and by autophosphorylation at two distinct regulatory tyrosines. *J Biol Chem*, *275*(45), 35631-35637.
- Brehme, M., Hantschel, O., Colinge, J., Kaupe, I., Planyavsky, M., Kocher, T., . . . Superti-Furga, G. (2009). Charting the molecular network of the drug target Bcr-Abl. *Proc Natl Acad Sci U S A*, *106*(18), 7414-7419. doi: 0900653106 [pii]  
10.1073/pnas.0900653106
- Brognaard, J., & Hunter, T. (2011). Protein kinase signaling networks in cancer. *Curr Opin Genet Dev*, *21*(1), 4-11. doi: 10.1016/j.gde.2010.10.012
- Brummer, T., Schmitz-Peiffer, C., & Daly, R. J. (2010). Docking proteins. *FEBS J*, *277*(21), 4356-4369. doi: 10.1111/j.1742-4658.2010.07865.x
- Brummer, T., Schramek, D., Hayes, V. M., Bennett, H. L., Caldon, C. E., Musgrove, E. A., & Daly, R. J. (2006). Increased proliferation and altered growth factor dependence of human mammary epithelial cells overexpressing the Gab2 docking protein. *J Biol Chem*, *281*(1), 626-637. doi: 10.1074/jbc.M509567200

- Buchdunger, E., Zimmermann, J., Mett, H., Meyer, T., Muller, M., Druker, B. J., & Lydon, N. B. (1996). Inhibition of the Abl protein-tyrosine kinase in vitro and in vivo by a 2-phenylaminopyrimidine derivative. *Cancer Res*, *56*(1), 100-104.
- Bunney, T. D., Esposito, D., Mas-Droux, C., Lamber, E., Baxendale, R. W., Martins, M., . . . Katan, M. (2012). Structural and functional integration of the PLCgamma interaction domains critical for regulatory mechanisms and signaling deregulation. *Structure*, *20*(12), 2062-2075. doi: 10.1016/j.str.2012.09.005
- Bunney, T. D., & Katan, M. (2011). PLC regulation: emerging pictures for molecular mechanisms. *Trends Biochem Sci*, *36*(2), 88-96. doi: 10.1016/j.tibs.2010.08.003
- Burckstummer, T., Bennett, K. L., Preradovic, A., Schutze, G., Hantschel, O., Superti-Furga, G., & Bauch, A. (2006). An efficient tandem affinity purification procedure for interaction proteomics in mammalian cells. *Nat Methods*, *3*(12), 1013-1019.
- Burke, B. A., & Carroll, M. (2010). BCR-ABL: a multi-faceted promoter of DNA mutation in chronic myelogenous leukemia. *Leukemia*, *24*(6), 1105-1112. doi: 10.1038/leu.2010.67
- Burns, J. C., Friedmann, T., Driever, W., Burrascano, M., & Yee, J. K. (1993). Vesicular stomatitis virus G glycoprotein pseudotyped retroviral vectors: concentration to very high titer and efficient gene transfer into mammalian and nonmammalian cells. *Proc Natl Acad Sci U S A*, *90*(17), 8033-8037.
- Caliceti, P., & Veronese, F. M. (2003). Pharmacokinetic and biodistribution properties of poly(ethylene glycol)-protein conjugates. *Adv Drug Deliv Rev*, *55*(10), 1261-1277.
- Capdeville, R., Buchdunger, E., Zimmermann, J., & Matter, A. (2002). Glivec (STI571, imatinib), a rationally developed, targeted anticancer drug. *Nat Rev Drug Discov*, *1*(7), 493-502.
- Carlesso, N., Frank, D. A., & Griffin, J. D. (1996). Tyrosyl phosphorylation and DNA binding activity of signal transducers and activators of transcription (STAT) proteins in hematopoietic cell lines transformed by Bcr/Abl. *J Exp Med*, *183*(3), 811-820.
- Chan, G., Kalaitzidis, D., & Neel, B. G. (2008). The tyrosine phosphatase Shp2 (PTPN11) in cancer. *Cancer Metastasis Rev*, *27*(2), 179-192. doi: 10.1007/s10555-008-9126-y
- Chan, W. W., Wise, S. C., Kaufman, M. D., Ahn, Y. M., Ensinger, C. L., Haack, T., . . . Flynn, D. L. (2011). Conformational control inhibition of the BCR-ABL1 tyrosine kinase, including the gatekeeper T315I mutant, by the switch-control inhibitor DCC-2036. *Cancer Cell*, *19*(4), 556-568. doi: 10.1016/j.ccr.2011.03.003
- Chen, J., Yu, W. M., Daino, H., Broxmeyer, H. E., Druker, B. J., & Qu, C. K. (2007). SHP-2 phosphatase is required for hematopoietic cell transformation by Bcr-Abl. *Blood*, *109*(2), 778-785. doi: blood-2006-04-019141 [pii] 10.1182/blood-2006-04-019141
- Cilloni, D., & Saglio, G. (2012). Molecular pathways: BCR-ABL. *Clin Cancer Res*, *18*(4), 930-937. doi: 10.1158/1078-0432.CCR-10-1613

- Cleghon, V., Feldmann, P., Ghiglione, C., Copeland, T. D., Perrimon, N., Hughes, D. A., & Morrison, D. K. (1998). Opposing actions of CSW and RasGAP modulate the strength of Torso RTK signaling in the *Drosophila* terminal pathway. *Mol Cell*, *2*(6), 719-727.
- Cohen, P., & Cohen, P. T. (1989). Protein phosphatases come of age. *J Biol Chem*, *264*(36), 21435-21438.
- Cole, M. D., & McMahon, S. B. (1999). The Myc oncoprotein: a critical evaluation of transactivation and target gene regulation. *Oncogene*, *18*(19), 2916-2924. doi: 10.1038/sj.onc.1202748
- Corbi-Verge, C., Marinelli, F., Zafra-Ruano, A., Ruiz-Sanz, J., Luque, I., & Faraldo-Gomez, J. D. (2013). Two-state dynamics of the SH3-SH2 tandem of Abl kinase and the allosteric role of the N-cap. *Proc Natl Acad Sci U S A*, *110*(36), E3372-3380. doi: 10.1073/pnas.1303966110
- Corbin, A. S., Agarwal, A., Loriaux, M., Cortes, J., Deininger, M. W., & Druker, B. J. (2010). Human chronic myeloid leukemia stem cells are insensitive to imatinib despite inhibition of BCR-ABL activity. *J Clin Invest*. doi: 10.1172/JCI35721
- Cortes, J. E., Kantarjian, H., Shah, N. P., Bixby, D., Mauro, M. J., Flinn, I., . . . Talpaz, M. (2012). Ponatinib in refractory Philadelphia chromosome-positive leukemias. *N Engl J Med*, *367*(22), 2075-2088. doi: 10.1056/NEJMoa1205127
- Cortes, J. E., Kantarjian, H. M., Brummendorf, T. H., Kim, D. W., Turkina, A. G., Shen, Z. X., . . . Gambacorti-Passerini, C. (2011). Safety and efficacy of bosutinib (SKI-606) in chronic phase Philadelphia chromosome-positive chronic myeloid leukemia patients with resistance or intolerance to imatinib. *Blood*, *118*(17), 4567-4576. doi: 10.1182/blood-2011-05-355594
- Cota, E., & Clarke, J. (2000). Folding of beta-sandwich proteins: three-state transition of a fibronectin type III module. *Protein Sci*, *9*(1), 112-120. doi: 10.1110/ps.9.1.112
- Cota, E., Steward, A., Fowler, S. B., & Clarke, J. (2001). The folding nucleus of a fibronectin type III domain is composed of core residues of the immunoglobulin-like fold. *J Mol Biol*, *305*(5), 1185-1194. doi: 10.1006/jmbi.2000.4378
- Cunnick, J. M., Meng, S., Ren, Y., Desponts, C., Wang, H. G., Djeu, J. Y., & Wu, J. (2002). Regulation of the mitogen-activated protein kinase signaling pathway by SHP2. *J Biol Chem*, *277*(11), 9498-9504. doi: 10.1074/jbc.M110547200
- Dance, M., Montagner, A., Salles, J. P., Yart, A., & Raynal, P. (2008). The molecular functions of Shp2 in the Ras/Mitogen-activated protein kinase (ERK1/2) pathway. *Cell Signal*, *20*(3), 453-459. doi: 10.1016/j.cellsig.2007.10.002
- Dechert, U., Adam, M., Harder, K. W., Clark-Lewis, I., & Jirik, F. (1994). Characterization of protein tyrosine phosphatase SH-PTP2. Study of phosphopeptide substrates and possible regulatory role of SH2 domains. *J Biol Chem*, *269*(8), 5602-5611.
- Deininger, M., Buchdunger, E., & Druker, B. J. (2005). The development of imatinib as a therapeutic agent for chronic myeloid leukemia. *Blood*, *105*(7), 2640-2653.

- Deininger, M. W., Goldman, J. M., & Melo, J. V. (2000). The molecular biology of chronic myeloid leukemia. *Blood*, *96*(10), 3343-3356.
- Deming, P. B., Schafer, Z. T., Tashker, J. S., Potts, M. B., Deshmukh, M., & Kornbluth, S. (2004). Bcr-Abl-mediated protection from apoptosis downstream of mitochondrial cytochrome c release. *Mol Cell Biol*, *24*(23), 10289-10299. doi: 10.1128/MCB.24.23.10289-10299.2004
- Diaz-Flores, E., Goldschmidt, H., Depeille, P., Ng, V., Akutagawa, J., Krisman, K., . . . Shannon, K. (2013). PLC-gamma and PI3K link cytokines to ERK activation in hematopoietic cells with normal and oncogenic Kras. *Sci Signal*, *6*(304), ra105. doi: 10.1126/scisignal.2004125
- Dickinson, C. D., Veerapandian, B., Dai, X. P., Hamlin, R. C., Xuong, N. H., Ruoslahti, E., & Ely, K. R. (1994). Crystal structure of the tenth type III cell adhesion module of human fibronectin. *J Mol Biol*, *236*(4), 1079-1092.
- Donato, N. J., Wu, J. Y., Stapley, J., Gallick, G., Lin, H., Arlinghaus, R., & Talpaz, M. (2003). BCR-ABL independence and LYN kinase overexpression in chronic myelogenous leukemia cells selected for resistance to STI571. *Blood*, *101*(2), 690-698.
- Dorey, K., Engen, J. R., Kretzschmar, J., Wilm, M., Neubauer, G., Schindler, T., & Superti-Furga, G. (2001). Phosphorylation and structure-based functional studies reveal a positive and a negative role for the activation loop of the c-Abl tyrosine kinase. *Oncogene*, *20*(56), 8075-8084.
- Druker, B. J., Sawyers, C. L., Kantarjian, H., Resta, D. J., Reese, S. F., Ford, J. M., . . . Talpaz, M. (2001). Activity of a specific inhibitor of the BCR-ABL tyrosine kinase in the blast crisis of chronic myeloid leukemia and acute lymphoblastic leukemia with the Philadelphia chromosome. *N Engl J Med*, *344*(14), 1038-1042.
- Druker, B. J., Talpaz, M., Resta, D. J., Peng, B., Buchdunger, E., Ford, J. M., . . . Sawyers, C. L. (2001). Efficacy and safety of a specific inhibitor of the BCR-ABL tyrosine kinase in chronic myeloid leukemia. *N Engl J Med*, *344*(14), 1031-1037.
- Druker, B. J., Tamura, S., Buchdunger, E., Ohno, S., Segal, G. M., Fanning, S., . . . Lydon, N. B. (1996). Effects of a selective inhibitor of the Abl tyrosine kinase on the growth of Bcr-Abl positive cells. *Nat Med*, *2*(5), 561-566.
- Eriksson, A., Nanberg, E., Ronnstrand, L., Engstrom, U., Hellman, U., Rupp, E., . . . Claesson-Welsh, L. (1995). Demonstration of functionally different interactions between phospholipase C-gamma and the two types of platelet-derived growth factor receptors. *J Biol Chem*, *270*(13), 7773-7781.
- Fang, Z. H., Dong, C. L., Chen, Z., Zhou, B., Liu, N., Lan, H. F., . . . Han, Z. C. (2009). Transcriptional regulation of survivin by c-Myc in BCR/ABL-transformed cells: implications in anti-leukaemic strategy. *J Cell Mol Med*, *13*(8B), 2039-2052. doi: 10.1111/j.1582-4934.2008.00549.x
- Feller, S. M. (2001). Crk family adaptors-signalling complex formation and biological roles. *Oncogene*, *20*(44), 6348-6371. doi: 10.1038/sj.onc.1204779
- Flynn, D. C. (2001). Adaptor proteins. *Oncogene*, *20*(44), 6270-6272. doi: 10.1038/sj.onc.1204769

- Frankfurt, O., & Licht, J. D. (2013). Ponatinib--a step forward in overcoming resistance in chronic myeloid leukemia. *Clin Cancer Res*, *19*(21), 5828-5834. doi: 10.1158/1078-0432.CCR-13-0258
- Futami, M., Zhu, Q. S., Whichard, Z. L., Xia, L., Ke, Y., Neel, B. G., . . . Corey, S. J. (2011). G-CSF receptor activation of the Src kinase Lyn is mediated by Gab2 recruitment of the Shp2 phosphatase. *Blood*, *118*(4), 1077-1086. doi: 10.1182/blood-2009-12-261636
- Gallego, O., Betts, M. J., Gvozdenovic-Jeremic, J., Maeda, K., Matetzki, C., Aguilar-Gurrieri, C., . . . Gavin, A. C. (2010). A systematic screen for protein-lipid interactions in *Saccharomyces cerevisiae*. *Mol Syst Biol*, *6*, 430. doi: 10.1038/msb.2010.87
- Gambacorti-Passerini, C., Piazza, R., & D'Incalci, M. (2003). Bcr-Abl mutations, resistance to imatinib, and imatinib plasma levels. *Blood*, *102*(5), 1933-1934; author reply 1934-1935.
- Gavin, A. C., Bosche, M., Krause, R., Grandi, P., Marzioch, M., Bauer, A., . . . Superti-Furga, G. (2002). Functional organization of the yeast proteome by systematic analysis of protein complexes. *Nature*, *415*(6868), 141-147.
- Gebauer, M., & Skerra, A. (2009). Engineered protein scaffolds as next-generation antibody therapeutics. *Curr Opin Chem Biol*, *13*(3), 245-255. doi: 10.1016/j.cbpa.2009.04.627
- Gilbreth, R. N., Esaki, K., Koide, A., Sidhu, S. S., & Koide, S. (2008). A dominant conformational role for amino acid diversity in minimalist protein-protein interfaces. *J Mol Biol*, *381*(2), 407-418. doi: 10.1016/j.jmb.2008.06.014
- Gilbreth, R. N., & Koide, S. (2012). Structural insights for engineering binding proteins based on non-antibody scaffolds. *Curr Opin Struct Biol*, *22*(4), 413-420. doi: 10.1016/j.sbi.2012.06.001
- Gishizky, M. L., Cortez, D., & Pendergast, A. M. (1995). Mutant forms of growth factor-binding protein-2 reverse BCR-ABL-induced transformation. *Proc Natl Acad Sci U S A*, *92*(24), 10889-10893.
- Glatter, T., Wepf, A., Aebersold, R., & Gstaiger, M. (2009). An integrated workflow for charting the human interaction proteome: insights into the PP2A system. *Mol Syst Biol*, *5*, 237. doi: 10.1038/msb.2008.75
- Goh, K. I., Cusick, M. E., Valle, D., Childs, B., Vidal, M., & Barabasi, A. L. (2007). The human disease network. *Proc Natl Acad Sci U S A*, *104*(21), 8685-8690. doi: 10.1073/pnas.0701361104
- Gorre, M. E., Mohammed, M., Ellwood, K., Hsu, N., Paquette, R., Rao, P. N., & Sawyers, C. L. (2001). Clinical resistance to STI-571 cancer therapy caused by BCR-ABL gene mutation or amplification. *Science*, *293*(5531), 876-880.
- Grebien, F., Hantschel, O., Wojcik, J., Kaupe, I., Kovacic, B., Wyrzucki, A. M., . . . Superti-Furga, G. (2011). Targeting the SH2-kinase interface in Bcr-Abl inhibits leukemogenesis. *Cell*, *147*(2), 306-319. doi: 10.1016/j.cell.2011.08.046
- Gresset, A., Hicks, S. N., Harden, T. K., & Sondek, J. (2010). Mechanism of phosphorylation-induced activation of phospholipase C-gamma isozymes. *J Biol Chem*, *285*(46), 35836-35847. doi: 10.1074/jbc.M110.166512



- Groffen, J., Stephenson, J. R., Heisterkamp, N., de Klein, A., Bartram, C. R., & Grosveld, G. (1984). Philadelphia chromosomal breakpoints are clustered within a limited region, bcr, on chromosome 22. *Cell*, *36*(1), 93-99.
- Gu, H., Maeda, H., Moon, J. J., Lord, J. D., Yoakim, M., Nelson, B. H., & Neel, B. G. (2000). New role for Shc in activation of the phosphatidylinositol 3-kinase/Akt pathway. *Mol Cell Biol*, *20*(19), 7109-7120.
- Gu, H., & Neel, B. G. (2003). The "Gab" in signal transduction. *Trends Cell Biol*, *13*(3), 122-130.
- Gu, H., Pratt, J. C., Burakoff, S. J., & Neel, B. G. (1998). Cloning of p97/Gab2, the major SHP2-binding protein in hematopoietic cells, reveals a novel pathway for cytokine-induced gene activation. *Mol Cell*, *2*(6), 729-740.
- Gu, H., Saito, K., Klamon, L. D., Shen, J., Fleming, T., Wang, Y., . . . Neel, B. G. (2001). Essential role for Gab2 in the allergic response. *Nature*, *412*(6843), 186-190. doi: 10.1038/35084076
- Halbach, S., Rigbolt, K. T., Wohrle, F. U., Diedrich, B., Gretzmeier, C., Brummer, T., & Dengjel, J. (2013). Alterations of Gab2 signalling complexes in imatinib and dasatinib treated chronic myeloid leukaemia cells. *Cell Commun Signal*, *11*(1), 30. doi: 10.1186/1478-811X-11-30
- Hamilton, A., Helgason, G. V., Schemionek, M., Zhang, B., Myssina, S., Allan, E. K., . . . Holyoake, T. L. (2012). Chronic myeloid leukemia stem cells are not dependent on Bcr-Abl kinase activity for their survival. *Blood*, *119*(6), 1501-1510. doi: 10.1182/blood-2010-12-326843
- Hantschel, O. (2012). Structure, regulation, signaling, and targeting of abl kinases in cancer. *Genes Cancer*, *3*(5-6), 436-446. doi: 10.1177/1947601912458584
- Hantschel, O., Grebien, F., & Superti-Furga, G. (2012). The growing arsenal of ATP-competitive and allosteric inhibitors of BCR-ABL. *Cancer Res*, *72*(19), 4890-4895. doi: 10.1158/0008-5472.CAN-12-1276
- Hantschel, O., Nagar, B., Guettler, S., Kretzschmar, J., Dorey, K., Kuriyan, J., & Superti-Furga, G. (2003). A Myristoyl/Phosphotyrosine Switch Regulates c-Abl. *Cell*, *112*(6), 845-857.
- Hantschel, O., Rix, U., & Superti-Furga, G. (2008). Target spectrum of the BCR-ABL inhibitors imatinib, nilotinib and dasatinib. *Leuk Lymphoma*, *49*(4), 615-619.
- Hantschel, O., & Superti-Furga, G. (2004). Regulation of the c-Abl and Bcr-Abl Tyrosine Kinases. *Nat Rev Mol Cell Biol*, *5*(1), 33-44.
- Hantschel, O., Warsch, W., Eckelhart, E., Kaupe, I., Grebien, F., Wagner, K. U., . . . Sexl, V. (2012). BCR-ABL uncouples canonical JAK2-STAT5 signaling in chronic myeloid leukemia. *Nat Chem Biol*, *8*(3), 285-293. doi: 10.1038/nchembio.775
- Hantschel, O., Wiesner, S., Guttler, T., Mackereth, C. D., Rix, L. L., Mikes, Z., . . . Superti-Furga, G. (2005). Structural basis for the cytoskeletal association of Bcr-Abl/c-Abl. *Mol Cell*, *19*(4), 461-473.
- Harnois, T., Constantin, B., Rioux, A., Grenioux, E., Kitzis, A., & Bourmeyster, N. (2003). Differential interaction and activation of Rho family GTPases by p210bcr-abl and p190bcr-abl. *Oncogene*, *22*(41), 6445-6454. doi: 10.1038/sj.onc.1206626
- Harrison, S. C. (2003). Variation on an Src-like Theme. *Cell*, *112*(6), 737-740.

- He, R., Zeng, L. F., He, Y., Zhang, S., & Zhang, Z. Y. (2013). Small molecule tools for functional interrogation of protein tyrosine phosphatases. *FEBS J*, *280*(2), 731-750. doi: 10.1111/j.1742-4658.2012.08718.x
- He, R. J., Yu, Z. H., Zhang, R. Y., & Zhang, Z. Y. (2014). Protein tyrosine phosphatases as potential therapeutic targets. *Acta Pharmacol Sin*, *35*(10), 1227-1246. doi: 10.1038/aps.2014.80
- Heisterkamp, N., Stephenson, J. R., Groffen, J., Hansen, P. F., de Klein, A., Bartram, C. R., & Grosveld, G. (1983). Localization of the c-ab1 oncogene adjacent to a translocation break point in chronic myelocytic leukaemia. *Nature*, *306*(5940), 239-242.
- Helgason, G. V., Karvela, M., & Holyoake, T. L. (2011). Kill one bird with two stones: potential efficacy of BCR-ABL and autophagy inhibition in CML. *Blood*, *118*(8), 2035-2043. doi: 10.1182/blood-2011-01-330621
- Hemmerlyckx, B., van Wijk, A., Reichert, A., Kaartinen, V., de Jong, R., Pattengale, P. K., . . . Heisterkamp, N. (2001). Crkl enhances leukemogenesis in BCR/ABL P190 transgenic mice. *Cancer Res*, *61*(4), 1398-1405.
- Hey, T., Fiedler, E., Rudolph, R., & Fiedler, M. (2005). Artificial, non-antibody binding proteins for pharmaceutical and industrial applications. *Trends Biotechnol*, *23*(10), 514-522. doi: 10.1016/j.tibtech.2005.07.007
- Hoelbl, A., Kovacic, B., Kerenyi, M. A., Simma, O., Warsch, W., Cui, Y., . . . Sexl, V. (2006). Clarifying the role of Stat5 in lymphoid development and Abelson-induced transformation. *Blood*, *107*(12), 4898-4906.
- Hoelbl, A., Schuster, C., Kovacic, B., Zhu, B., Wickre, M., Hoelzl, M. A., . . . Sexl, V. (2010). Stat5 is indispensable for the maintenance of bcr/abl-positive leukaemia. *EMBO Mol Med*, *2*(3), 98-110. doi: 10.1002/emmm.201000062
- Hof, P., Pluskey, S., Dhe-Paganon, S., Eck, M. J., & Shoelson, S. E. (1998). Crystal structure of the tyrosine phosphatase SHP-2. *Cell*, *92*(4), 441-450.
- Horita, M., Andreu, E. J., Benito, A., Arbona, C., Sanz, C., Benet, I., . . . Fernandez-Luna, J. L. (2000). Blockade of the Bcr-Abl kinase activity induces apoptosis of chronic myelogenous leukemia cells by suppressing signal transducer and activator of transcription 5-dependent expression of Bcl-xL. *J Exp Med*, *191*(6), 977-984.
- Huang, J., Koide, A., Makabe, K., & Koide, S. (2008). Design of protein function leaps by directed domain interface evolution. *Proc Natl Acad Sci U S A*, *105*(18), 6578-6583. doi: 10.1073/pnas.0801097105
- Huang, J., Makabe, K., Biancalana, M., Koide, A., & Koide, S. (2009). Structural basis for exquisite specificity of affinity clamps, synthetic binding proteins generated through directed domain-interface evolution. *J Mol Biol*, *392*(5), 1221-1231. doi: 10.1016/j.jmb.2009.07.067
- Hunter, T. (1995). Protein kinases and phosphatases: the yin and yang of protein phosphorylation and signaling. *Cell*, *80*(2), 225-236.
- Hunter, T. (2012). Why nature chose phosphate to modify proteins. *Philos Trans R Soc Lond B Biol Sci*, *367*(1602), 2513-2516. doi: 10.1098/rstb.2012.0013
- Ilaria, R. L., Jr., & Van Etten, R. A. (1996). P210 and P190(BCR/ABL) induce the tyrosine phosphorylation and DNA binding activity of multiple specific STAT family members. *J Biol Chem*, *271*(49), 31704-31710.



- Jackson, P., & Baltimore, D. (1989). N-terminal mutations activate the leukemogenic potential of the myristoylated form of c-abl. *EMBO J*, 8(2), 449-456.
- Jaeger, S., & Aloy, P. (2012). From protein interaction networks to novel therapeutic strategies. *IUBMB Life*, 64(6), 529-537. doi: 10.1002/iub.1040
- Jaiswal, S., Traver, D., Miyamoto, T., Akashi, K., Lagasse, E., & Weissman, I. L. (2003). Expression of BCR/ABL and BCL-2 in myeloid progenitors leads to myeloid leukemias. *Proc Natl Acad Sci U S A*, 100(17), 10002-10007. doi: 10.1073/pnas.1633833100
- Johansson, B., Fioretos, T., & Mitelman, F. (2002). Cytogenetic and molecular genetic evolution of chronic myeloid leukemia. *Acta Haematol*, 107(2), 76-94. doi: 46636
- Jones, N. P., & Katan, M. (2007). Role of phospholipase Cgamma1 in cell spreading requires association with a beta-Pix/GIT1-containing complex, leading to activation of Cdc42 and Rac1. *Mol Cell Biol*, 27(16), 5790-5805. doi: 10.1128/MCB.00778-07
- Kadamur, G., & Ross, E. M. (2013). Mammalian phospholipase C. *Annu Rev Physiol*, 75, 127-154. doi: 10.1146/annurev-physiol-030212-183750
- Kaplan, J. M., Mardon, G., Bishop, J. M., & Varmus, H. E. (1988). The first seven amino acids encoded by the v-src oncogene act as a myristylation signal: lysine 7 is a critical determinant. *Mol Cell Biol*, 8(6), 2435-2441.
- Karatan, E., Merguerian, M., Han, Z., Scholle, M. D., Koide, S., & Kay, B. K. (2004). Molecular recognition properties of FN3 monobodies that bind the Src SH3 domain. *Chem Biol*, 11(6), 835-844. doi: 10.1016/j.chembiol.2004.04.009
- Katan, M. (1998). Families of phosphoinositide-specific phospholipase C: structure and function. *Biochim Biophys Acta*, 1436(1-2), 5-17.
- Katan, M. (2005). New insights into the families of PLC enzymes: looking back and going forward. *Biochem J*, 391(Pt 3), e7-9. doi: 10.1042/BJ20051506
- Kavalerchik, E., Goff, D., & Jamieson, C. H. (2008). Chronic myeloid leukemia stem cells. *J Clin Oncol*, 26(17), 2911-2915. doi: 10.1200/JCO.2008.17.5745
- Ke, Y., Wu, D., Princen, F., Nguyen, T., Pang, Y., Lesperance, J., . . . Feng, G. S. (2007). Role of Gab2 in mammary tumorigenesis and metastasis. *Oncogene*, 26(34), 4951-4960. doi: 10.1038/sj.onc.1210315
- Keilhack, H., David, F. S., McGregor, M., Cantley, L. C., & Neel, B. G. (2005). Diverse biochemical properties of Shp2 mutants. Implications for disease phenotypes. *J Biol Chem*, 280(35), 30984-30993. doi: 10.1074/jbc.M504699200
- Kharas, M. G., Janes, M. R., Scarfone, V. M., Lilly, M. B., Knight, Z. A., Shokat, K. M., & Fruman, D. A. (2008). Ablation of PI3K blocks BCR-ABL leukemogenesis in mice, and a dual PI3K/mTOR inhibitor prevents expansion of human BCR-ABL+ leukemia cells. *J Clin Invest*, 118(9), 3038-3050. doi: 10.1172/JCI33337
- Kim, M. J., Chang, J. S., Park, S. K., Hwang, J. I., Ryu, S. H., & Suh, P. G. (2000). Direct interaction of SOS1 Ras exchange protein with the SH3 domain of phospholipase C-gamma1. *Biochemistry*, 39(29), 8674-8682.

- Kisseleva, T., Bhattacharya, S., Braunstein, J., & Schindler, C. W. (2002). Signaling through the JAK/STAT pathway, recent advances and future challenges. *Gene*, *285*(1-2), 1-24.
- Klinghoffer, R. A., & Kazlauskas, A. (1995). Identification of a putative Syp substrate, the PDGF beta receptor. *J Biol Chem*, *270*(38), 22208-22217.
- Koch, C. A., Anderson, D., Moran, M. F., Ellis, C., & Pawson, T. (1991). SH2 and SH3 domains: elements that control interactions of cytoplasmic signaling proteins. *Science*, *252*(5006), 668-674.
- Koide, A., Bailey, C. W., Huang, X., & Koide, S. (1998). The fibronectin type III domain as a scaffold for novel binding proteins. *J Mol Biol*, *284*(4), 1141-1151. doi: 10.1006/jmbi.1998.2238
- Koide, A., Gilbreth, R. N., Esaki, K., Tereshko, V., & Koide, S. (2007). High-affinity single-domain binding proteins with a binary-code interface. *Proc Natl Acad Sci U S A*, *104*(16), 6632-6637. doi: 0700149104 [pii] 10.1073/pnas.0700149104
- Koide, A., Jordan, M. R., Horner, S. R., Batori, V., & Koide, S. (2001). Stabilization of a fibronectin type III domain by the removal of unfavorable electrostatic interactions on the protein surface. *Biochemistry*, *40*(34), 10326-10333.
- Koide, A., Wojcik, J., Gilbreth, R. N., Hoey, R. J., & Koide, S. (2012). Teaching an old scaffold new tricks: monobodies constructed using alternative surfaces of the FN3 scaffold. *J Mol Biol*, *415*(2), 393-405. doi: 10.1016/j.jmb.2011.12.019
- Koide, S., & Huang, J. (2013). Generation of high-performance binding proteins for peptide motifs by affinity clamping. *Methods Enzymol*, *523*, 285-302. doi: 10.1016/B978-0-12-394292-0.00013-8
- Koide, S., Koide, A., & Lipovsek, D. (2012). Target-binding proteins based on the 10th human fibronectin type III domain ((1)(0)Fn3). *Methods Enzymol*, *503*, 135-156. doi: 10.1016/B978-0-12-396962-0.00006-9
- Konopka, J. B., Watanabe, S. M., & Witte, O. N. (1984). An alteration of the human c-abl protein in K562 leukemia cells unmasks associated tyrosine kinase activity. *Cell*, *37*(3), 1035-1042.
- Kossiakoff, A. A., & Koide, S. (2008). Understanding mechanisms governing protein-protein interactions from synthetic binding interfaces. *Curr Opin Struct Biol*, *18*(4), 499-506. doi: 10.1016/j.sbi.2008.06.004
- Krogan, N. J., Cagney, G., Yu, H., Zhong, G., Guo, X., Ignatchenko, A., . . . Greenblatt, J. F. (2006). Global landscape of protein complexes in the yeast *Saccharomyces cerevisiae*. *Nature*, *440*(7084), 637-643. doi: 10.1038/nature04670
- Kurzrock, R., Gutterman, J. U., & Talpaz, M. (1988). The molecular genetics of Philadelphia chromosome-positive leukemias. *N Engl J Med*, *319*(15), 990-998. doi: 10.1056/NEJM198810133191506
- Lamontanara, A. J., Gencer, E. B., Kuzyk, O., & Hantschel, O. (2013). Mechanisms of resistance to BCR-ABL and other kinase inhibitors. *Biochim Biophys Acta*, *1834*(7), 1449-1459. doi: 10.1016/j.bbapap.2012.12.009
- Larose, L., Gish, G., Shoelson, S., & Pawson, T. (1993). Identification of residues in the beta platelet-derived growth factor receptor that confer specificity for binding to phospholipase C-gamma 1. *Oncogene*, *8*(9), 2493-2499.
- Lattanzio, R., Marchisio, M., La Sorda, R., Tinari, N., Falasca, M., Alberti, S., . . . Cinbo. (2013). Overexpression of activated phospholipase Cgamma1 is a

- risk factor for distant metastases in T1-T2, N0 breast cancer patients undergoing adjuvant chemotherapy. *Int J Cancer*, 132(5), 1022-1031. doi: 10.1002/ijc.27751
- Lattanzio, R., Piantelli, M., & Falasca, M. (2013). Role of phospholipase C in cell invasion and metastasis. *Adv Biol Regul*, 53(3), 309-318. doi: 10.1016/j.jbior.2013.07.006
- Lee, C. H., Kominos, D., Jacques, S., Margolis, B., Schlessinger, J., Shoelson, S. E., & Kuriyan, J. (1994). Crystal structures of peptide complexes of the amino-terminal SH2 domain of the Syp tyrosine phosphatase. *Structure*, 2(5), 423-438.
- Lee, C. I., Kohn, D. B., Ekert, J. E., & Tarantal, A. F. (2004). Morphological analysis and lentiviral transduction of fetal monkey bone marrow-derived mesenchymal stem cells. *Mol Ther*, 9(1), 112-123.
- Lee, C. M., Iorno, N., Sierro, F., & Christ, D. (2007). Selection of human antibody fragments by phage display. *Nat Protoc*, 2(11), 3001-3008. doi: 10.1038/nprot.2007.448
- Legius, E., Schrandt-Stumpel, C., Schollen, E., Pulles-Heintzberger, C., Gewillig, M., & Fryns, J. P. (2002). PTPN11 mutations in LEOPARD syndrome. *J Med Genet*, 39(8), 571-574.
- Li, L., Modi, H., McDonald, T., Rossi, J., Yee, J. K., & Bhatia, R. (2011). A critical role for SHP2 in STAT5 activation and growth factor-mediated proliferation, survival, and differentiation of human CD34+ cells. *Blood*, 118(6), 1504-1515. doi: 10.1182/blood-2010-06-288910
- Liao, H. J., Kume, T., McKay, C., Xu, M. J., Ihle, J. N., & Carpenter, G. (2002). Absence of erythropoiesis and vasculogenesis in Plcg1-deficient mice. *J Biol Chem*, 277(11), 9335-9341. doi: 10.1074/jbc.M109955200
- Lipman, N. S., Jackson, L. R., Trudel, L. J., & Weis-Garcia, F. (2005). Monoclonal versus polyclonal antibodies: distinguishing characteristics, applications, and information resources. *ILAR J*, 46(3), 258-268.
- Liu, B. A., Jablonowski, K., Raina, M., Arce, M., Pawson, T., & Nash, P. D. (2006). The human and mouse complement of SH2 domain proteins-establishing the boundaries of phosphotyrosine signaling. *Mol Cell*, 22(6), 851-868. doi: 10.1016/j.molcel.2006.06.001
- Liu, Y., & Gray, N. S. (2006). Rational design of inhibitors that bind to inactive kinase conformations. *Nat Chem Biol*, 2(7), 358-364.
- Lopez-Otin, C., & Hunter, T. (2010). The regulatory crosstalk between kinases and proteases in cancer. *Nat Rev Cancer*, 10(4), 278-292. doi: 10.1038/nrc2823
- Lorenz, U. (2009). SHP-1 and SHP-2 in T cells: two phosphatases functioning at many levels. *Immunol Rev*, 228(1), 342-359. doi: 10.1111/j.1600-065X.2008.00760.x
- Lu, W., Gong, D., Bar-Sagi, D., & Cole, P. A. (2001). Site-specific incorporation of a phosphotyrosine mimetic reveals a role for tyrosine phosphorylation of SHP-2 in cell signaling. *Mol Cell*, 8(4), 759-769.
- Luo, J., Field, S. J., Lee, J. Y., Engelman, J. A., & Cantley, L. C. (2005). The p85 regulatory subunit of phosphoinositide 3-kinase down-regulates IRS-1 signaling via the formation of a sequestration complex. *J Cell Biol*, 170(3), 455-464. doi: 10.1083/jcb.200503088

- Lydon, N. (2009). Attacking cancer at its foundation. *Nat Med*, 15(10), 1153-1157. doi: 10.1038/nm1009-1153
- Maggon, K. (2007). Monoclonal antibody "gold rush". *Curr Med Chem*, 14(18), 1978-1987.
- Mahon, F. X., Deininger, M. W., Schultheis, B., Chabrol, J., Reiffers, J., Goldman, J. M., & Melo, J. V. (2000). Selection and characterization of BCR-ABL positive cell lines with differential sensitivity to the tyrosine kinase inhibitor STI571: diverse mechanisms of resistance. *Blood*, 96(3), 1070-1079.
- Margolis, B., Zilberstein, A., Franks, C., Felder, S., Kremer, S., Ullrich, A., . . . Schlessinger, J. (1990). Effect of phospholipase C-gamma overexpression on PDGF-induced second messengers and mitogenesis. *Science*, 248(4955), 607-610.
- Markova, B., Albers, C., Breitenbuecher, F., Melo, J. V., Brummendorf, T. H., Heidel, F., . . . Fischer, T. (2010). Novel pathway in Bcr-Abl signal transduction involves Akt-independent, PLC-gamma1-driven activation of mTOR/p70S6-kinase pathway. *Oncogene*, 29(5), 739-751. doi: 10.1038/onc.2009.374
- Mason, J. M., Morrison, D. J., Basson, M. A., & Licht, J. D. (2006). Sprouty proteins: multifaceted negative-feedback regulators of receptor tyrosine kinase signaling. *Trends Cell Biol*, 16(1), 45-54. doi: 10.1016/j.tcb.2005.11.004
- Mayer, B. J., Jackson, P. K., Van Etten, R. A., & Baltimore, D. (1992). Point mutations in the abl SH2 domain coordinately impair phosphotyrosine binding in vitro and transforming activity in vivo. *Mol Cell Biol*, 12(2), 609-618.
- McGahon, A., Bissonnette, R., Schmitt, M., Cotter, K. M., Green, D. R., & Cotter, T. G. (1994). BCR-ABL maintains resistance of chronic myelogenous leukemia cells to apoptotic cell death. *Blood*, 83(5), 1179-1187.
- McGahon, A. J., Cotter, T. G., & Green, D. R. (1994). The abl oncogene family and apoptosis. *Cell Death Differ*, 1(2), 77-83.
- McWhirter, J. R., Galasso, D. L., & Wang, J. Y. (1993). A coiled-coil oligomerization domain of Bcr is essential for the transforming function of Bcr-Abl oncoproteins. *Mol Cell Biol*, 13(12), 7587-7595.
- Melo, J. V., & Barnes, D. J. (2007). Chronic myeloid leukaemia as a model of disease evolution in human cancer. *Nat Rev Cancer*, 7(6), 441-453. doi: 10.1038/nrc2147
- Million, R. P., & Van Etten, R. A. (2000). The Grb2 binding site is required for the induction of chronic myeloid leukemia-like disease in mice by the Bcr/Abl tyrosine kinase. *Blood*, 96(2), 664-670.
- Mohi, M. G., & Neel, B. G. (2007). The role of Shp2 (PTPN11) in cancer. *Curr Opin Genet Dev*, 17(1), 23-30. doi: 10.1016/j.gde.2006.12.011
- Moran, M. F., Koch, C. A., Anderson, D., Ellis, C., England, L., Martin, G. S., & Pawson, T. (1990). Src homology region 2 domains direct protein-protein interactions in signal transduction. *Proc Natl Acad Sci U S A*, 87(21), 8622-8626.
- Moravcevic, K., Mendrola, J. M., Schmitz, K. R., Wang, Y. H., Slochower, D., Janmey, P. A., & Lemmon, M. A. (2010). Kinase associated-1 domains drive MARK/PAR1 kinases to membrane targets by binding acidic phospholipids. *Cell*, 143(6), 966-977. doi: 10.1016/j.cell.2010.11.028

- Muvarak, N., Nagaria, P., & Rassool, F. V. (2012). Genomic instability in chronic myeloid leukemia: targets for therapy? *Curr Hematol Malig Rep*, 7(2), 94-102. doi: 10.1007/s11899-012-0119-0
- Nagar, B., Bornmann, W. G., Pellicena, P., Schindler, T., Veach, D. R., Miller, W. T., . . . Kuriyan, J. (2002). Crystal Structures of the Kinase Domain of c-Abl in Complex with the Small Molecule Inhibitors PD173955 and Imatinib (STI-571). *Cancer Res*, 62(15), 4236-4243.
- Nagar, B., Hantschel, O., Seeliger, M., Davies, J. M., Weis, W. I., Superti-Furga, G., & Kuriyan, J. (2006). Organization of the SH3-SH2 unit in active and inactive forms of the c-Abl tyrosine kinase. *Mol Cell*, 21(6), 787-798. doi: 10.1016/j.molcel.2006.01.035
- Nagar, B., Hantschel, O., Young, M. A., Scheffzek, K., Veach, D., Bornmann, W., . . . Kuriyan, J. (2003). Structural Basis for the Autoinhibition of c-Abl Tyrosine Kinase. *Cell*, 112(6), 859-871.
- Neel, B. G., Gu, H., & Pao, L. (2003). The 'Shp'ing news: SH2 domain-containing tyrosine phosphatases in cell signaling. *Trends Biochem Sci*, 28(6), 284-293. doi: 10.1016/S0968-0004(03)00091-4
- Nero, T. L., Morton, C. J., Holien, J. K., Wielens, J., & Parker, M. W. (2014). Oncogenic protein interfaces: small molecules, big challenges. *Nat Rev Cancer*, 14(4), 248-262. doi: 10.1038/nrc3690
- Nishibe, S., Wahl, M. I., Hernandez-Sotomayor, S. M., Tonks, N. K., Rhee, S. G., & Carpenter, G. (1990). Increase of the catalytic activity of phospholipase C-gamma 1 by tyrosine phosphorylation. *Science*, 250(4985), 1253-1256.
- Nishida, K., & Hirano, T. (2003). The role of Gab family scaffolding adapter proteins in the signal transduction of cytokine and growth factor receptors. *Cancer Sci*, 94(12), 1029-1033.
- Notari, M., Neviani, P., Santhanam, R., Blaser, B. W., Chang, J. S., Galietta, A., . . . Perrotti, D. (2006). A MAPK/HNRPK pathway controls BCR/ABL oncogenic potential by regulating MYC mRNA translation. *Blood*, 107(6), 2507-2516. doi: 10.1182/blood-2005-09-3732
- Nowell, P. C. (2007). Discovery of the Philadelphia chromosome: a personal perspective. *J Clin Invest*, 117(8), 2033-2035. doi: 10.1172/JCI31771
- Nowell, P. C., & Hungerford, D. A. (1960). Minute Chromosome in Human Chronic Granulocytic Leukemia. *Science*, 132(3438), 1497-1497.
- Nuttall, S. D., & Walsh, R. B. (2008). Display scaffolds: protein engineering for novel therapeutics. *Curr Opin Pharmacol*, 8(5), 609-615. doi: 10.1016/j.coph.2008.06.007
- Nygren, P. A., & Skerra, A. (2004). Binding proteins from alternative scaffolds. *J Immunol Methods*, 290(1-2), 3-28. doi: 10.1016/j.jim.2004.04.006
- O'Hare, T., Eide, C. A., & Deininger, M. W. (2007). Bcr-Abl kinase domain mutations, drug resistance, and the road to a cure for chronic myeloid leukemia. *Blood*, 110(7), 2242-2249. doi: blood-2007-03-066936 [pii] 10.1182/blood-2007-03-066936
- O'Hare, T., Shakespeare, W. C., Zhu, X., Eide, C. A., Rivera, V. M., Wang, F., . . . Clackson, T. (2009). AP24534, a Pan-BCR-ABL Inhibitor for Chronic Myeloid Leukemia, Potently Inhibits the T315I Mutant and Overcomes Mutation-Based Resistance. *Cancer Cell*, 16(5), 401-412. doi: 10.1016/j.ccr.2009.09.028



- Obermeier, A., Tinhofer, I., Grunicke, H. H., & Ullrich, A. (1996). Transforming potentials of epidermal growth factor and nerve growth factor receptors inversely correlate with their phospholipase C gamma affinity and signal activation. *EMBO J*, *15*(1), 73-82.
- Olivieri, A., & Manzione, L. (2007). Dasatinib: a new step in molecular target therapy. *Ann Oncol*, *18 Suppl 6*, vi42-46. doi: 10.1093/annonc/mdm223
- Panjarian, S., Iacob, R. E., Chen, S., Engen, J. R., & Smithgall, T. E. (2013). Structure and dynamic regulation of Abl kinases. *J Biol Chem*, *288*(8), 5443-5450. doi: 10.1074/jbc.R112.438382
- Park, J. B., Lee, C. S., Jang, J. H., Ghim, J., Kim, Y. J., You, S., . . . Ryu, S. H. (2012). Phospholipase signalling networks in cancer. *Nat Rev Cancer*, *12*(11), 782-792. doi: 10.1038/nrc3379
- Pawson, T. (2004). Specificity in signal transduction: from phosphotyrosine-SH2 domain interactions to complex cellular systems. *Cell*, *116*(2), 191-203.
- Pawson, T., Gish, G. D., & Nash, P. (2001). SH2 domains, interaction modules and cellular wiring. *Trends Cell Biol*, *11*(12), 504-511.
- Pawson, T., & Scott, J. D. (1997). Signaling through scaffold, anchoring, and adaptor proteins. *Science*, *278*(5346), 2075-2080.
- Pelengaris, S., Khan, M., & Evan, G. (2002). c-MYC: more than just a matter of life and death. *Nat Rev Cancer*, *2*(10), 764-776. doi: 10.1038/nrc904
- Pendergast, A. M. (2002). The Abl family kinases: mechanisms of regulation and signaling. *Adv Cancer Res*, *85*, 51-100.
- Pendergast, A. M., Quilliam, L. A., Cripe, L. D., Bassing, C. H., Dai, Z., Li, N., . . . Gishizky, M. L. (1993). BCR-ABL-induced oncogenesis is mediated by direct interaction with the SH2 domain of the GRB-2 adaptor protein. *Cell*, *75*, 175-185.
- Peters, K. G., Marie, J., Wilson, E., Ives, H. E., Escobedo, J., Del Rosario, M., . . . Williams, L. T. (1992). Point mutation of an FGF receptor abolishes phosphatidylinositol turnover and Ca<sup>2+</sup> flux but not mitogenesis. *Nature*, *358*(6388), 678-681. doi: 10.1038/358678a0
- Piccolo, E., Innominato, P. F., Mariggio, M. A., Maffucci, T., Iacobelli, S., & Falasca, M. (2002). The mechanism involved in the regulation of phospholipase Cgamma1 activity in cell migration. *Oncogene*, *21*(42), 6520-6529. doi: 10.1038/sj.onc.1205821
- Piller, G. (2001). Leukaemia - a brief historical review from ancient times to 1950. *Br J Haematol*, *112*(2), 282-292.
- Plattner, R., Irvin, B. J., Guo, S., Blackburn, K., Kazlauskas, A., Abraham, R. T., . . . Pendergast, A. M. (2003). A new link between the c-Abl tyrosine kinase and phosphoinositide signalling through PLC-gamma1. *Nat Cell Biol*, *5*(4), 309-319.
- Plaxco, K. W., Spitzfaden, C., Campbell, I. D., & Dobson, C. M. (1996). Rapid refolding of a proline-rich all-beta-sheet fibronectin type III module. *Proc Natl Acad Sci U S A*, *93*(20), 10703-10706.
- Pluk, H., Dorey, K., & Superti-Furga, G. (2002). Autoinhibition of c-Abl. *Cell*, *108*(2), 247-259.
- Poole, A. W., & Jones, M. L. (2005). A SHPing tale: perspectives on the regulation of SHP-1 and SHP-2 tyrosine phosphatases by the C-terminal tail. *Cell Signal*, *17*(11), 1323-1332. doi: 10.1016/j.cellsig.2005.05.016

- Poulin, B., Sekiya, F., & Rhee, S. G. (2005). Intramolecular interaction between phosphorylated tyrosine-783 and the C-terminal Src homology 2 domain activates phospholipase C-gamma1. *Proc Natl Acad Sci U S A*, *102*(12), 4276-4281. doi: 10.1073/pnas.0409590102
- Puil, L., Liu, J., Gish, G., Mbamalu, G., Bowtell, D., Pelicci, P. G., . . . Pawson, T. (1994). Bcr-Abl oncoproteins bind directly to activators of the Ras signalling pathway. *EMBO J*, *13*(4), 764-773.
- Puttini, M., Coluccia, A. M., Boschelli, F., Cleris, L., Marchesi, E., Donella-Deana, A., . . . Gambacorti-Passerini, C. (2006). In vitro and in vivo activity of SKI-606, a novel Src-Abl inhibitor, against imatinib-resistant Bcr-Abl+ neoplastic cells. *Cancer Res*, *66*(23), 11314-11322. doi: 10.1158/0008-5472.CAN-06-1199
- Qin, J. Y., Zhang, L., Clift, K. L., Hular, I., Xiang, A. P., Ren, B. Z., & Lahn, B. T. (2010). Systematic comparison of constitutive promoters and the doxycycline-inducible promoter. *PLoS One*, *5*(5), e10611. doi: 10.1371/journal.pone.0010611
- Qiu, W., Wang, X., Romanov, V., Hutchinson, A., Lin, A., Ruzanov, M., . . . Chirgadze, N. Y. (2014). Structural insights into Noonan/LEOPARD syndrome-related mutants of protein-tyrosine phosphatase SHP2 (PTPN11). *BMC Struct Biol*, *14*, 10. doi: 10.1186/1472-6807-14-10
- Qu, C. K., Nguyen, S., Chen, J., & Feng, G. S. (2001). Requirement of Shp-2 tyrosine phosphatase in lymphoid and hematopoietic cell development. *Blood*, *97*(4), 911-914.
- Qu, C. K., Shi, Z. Q., Shen, R., Tsai, F. Y., Orkin, S. H., & Feng, G. S. (1997). A deletion mutation in the SH2-N domain of Shp-2 severely suppresses hematopoietic cell development. *Mol Cell Biol*, *17*(9), 5499-5507.
- Qu, C. K., Yu, W. M., Azzarelli, B., Cooper, S., Broxmeyer, H. E., & Feng, G. S. (1998). Biased suppression of hematopoiesis and multiple developmental defects in chimeric mice containing Shp-2 mutant cells. *Mol Cell Biol*, *18*(10), 6075-6082.
- Qu, C. K., Yu, W. M., Azzarelli, B., & Feng, G. S. (1999). Genetic evidence that Shp-2 tyrosine phosphatase is a signal enhancer of the epidermal growth factor receptor in mammals. *Proc Natl Acad Sci U S A*, *96*(15), 8528-8533.
- Quackenbush, R. C., Reuther, G. W., Miller, J. P., Courtney, K. D., Pear, W. S., & Pendergast, A. M. (2000). Analysis of the biologic properties of p230 Bcr-Abl reveals unique and overlapping properties with the oncogenic p185 and p210 Bcr-Abl tyrosine kinases. *Blood*, *95*(9), 2913-2921.
- Ramirez, P., & DiPersio, J. F. (2008). Therapy options in imatinib failures. *Oncologist*, *13*(4), 424-434. doi: 10.1634/theoncologist.2007-0170
- Regunathan, J., Chen, Y., Kutlesa, S., Dai, X., Bai, L., Wen, R., . . . Malarkannan, S. (2006). Differential and nonredundant roles of phospholipase Cgamma2 and phospholipase Cgamma1 in the terminal maturation of NK cells. *J Immunol*, *177*(8), 5365-5376.
- Ren, Y., Meng, S., Mei, L., Zhao, Z. J., Jove, R., & Wu, J. (2004). Roles of Gab1 and SHP2 in paxillin tyrosine dephosphorylation and Src activation in response to epidermal growth factor. *J Biol Chem*, *279*(9), 8497-8505. doi: 10.1074/jbc.M312575200



- Renshaw, M. W., Capozza, M. A., & Wang, J. Y. (1988). Differential expression of type-specific c-abl mRNAs in mouse tissues and cell lines. *Mol. Cell. Biol.*, *8*(10), 4547-4551.
- Rhee, S. G. (2001). Regulation of phosphoinositide-specific phospholipase C. *Annu Rev Biochem*, *70*, 281-312. doi: 10.1146/annurev.biochem.70.1.281
- Rix, U., Hantschel, O., Durnberger, G., Remsing Rix, L. L., Planyavsky, M., Fernbach, N. V., . . . Superti-Furga, G. (2007). Chemical proteomic profiles of the BCR-ABL inhibitors imatinib, nilotinib and dasatinib reveal novel kinase and non-kinase targets. *Blood*, *110*(12), 4055-4063.
- Roche-Lestienne, C., Soenen-Cornu, V., Gardel-Duflos, N., Lai, J. L., Philippe, N., Facon, T., . . . Preudhomme, C. (2002). Several types of mutations of the Abl gene can be found in chronic myeloid leukemia patients resistant to STI571, and they can pre-exist to the onset of treatment. *Blood*, *100*(3), 1014-1018.
- Rogers, G., Hoyle, M., Thompson Coon, J., Moxham, T., Liu, Z., Pitt, M., & Stein, K. (2012). Dasatinib and nilotinib for imatinib-resistant or -intolerant chronic myeloid leukaemia: a systematic review and economic evaluation. *Health Technol Assess*, *16*(22), 1-410. doi: 10.3310/hta16220
- Rowley, J. D. (1973). Letter: A new consistent chromosomal abnormality in chronic myelogenous leukaemia identified by quinacrine fluorescence and Giemsa staining. *Nature*, *243*(5405), 290-293.
- Rual, J. F., Venkatesan, K., Hao, T., Hirozane-Kishikawa, T., Dricot, A., Li, N., . . . Vidal, M. (2005). Towards a proteome-scale map of the human protein-protein interaction network. *Nature*, *437*(7062), 1173-1178. doi: 10.1038/nature04209
- Saglio, G., Kim, D.-W., Issaragrisil, S., le Coutre, P., Etienne, G., Lobo, C., . . . Investigators, E. (2010). Nilotinib versus imatinib for newly diagnosed chronic myeloid leukemia. *N Engl J Med*, *362*(24), 2251-2259. doi: 10.1056/NEJMoa0912614
- Sahay, S., Pannucci, N. L., Mahon, G. M., Rodriguez, P. L., Megjugorac, N. J., Kostenko, E. V., . . . Whitehead, I. P. (2008). The RhoGEF domain of p210 Bcr-Abl activates RhoA and is required for transformation. *Oncogene*, *27*(14), 2064-2071. doi: 10.1038/sj.onc.1210841
- Sala, G., Dituri, F., Raimondi, C., Previdi, S., Maffucci, T., Mazzoletti, M., . . . Falasca, M. (2008). Phospholipase Cgamma1 is required for metastasis development and progression. *Cancer Res*, *68*(24), 10187-10196. doi: 10.1158/0008-5472.CAN-08-1181
- Sanchez-Garcia, I., & Grutz, G. (1995). Tumorigenic activity of the BCR-ABL oncogenes is mediated by BCL2. *Proc Natl Acad Sci U S A*, *92*(12), 5287-5291.
- Sattler, M., & Griffin, J. D. (2003). Molecular mechanisms of transformation by the BCR-ABL oncogene. *Semin Hematol*, *40*(2 Suppl 2), 4-10.
- Sattler, M., Mohi, M. G., Pride, Y. B., Quinnan, L. R., Malouf, N. A., Podar, K., . . . Neel, B. G. (2002). Critical role for Gab2 in transformation by BCR/ABL. *Cancer Cell*, *1*(5), 479-492.
- Sattler, M., Salgia, R., Okuda, K., Uemura, N., Durstin, M. A., Pisick, E., . . . Griffin, J. D. (1996). The proto-oncogene product p120CBL and the adaptor proteins CRKL and c-CRK link c-ABL, p190BCR/ABL and p210BCR/ABL to the phosphatidylinositol-3' kinase pathway. *Oncogene*, *12*(4), 839-846.

- Sawyers, C. L. (1999). Chronic myeloid leukemia. *N Engl J Med*, *340*(17), 1330-1340.
- Sawyers, C. L., Callahan, W., & Witte, O. N. (1992). Dominant negative MYC blocks transformation by ABL oncogenes. *Cell*, *70*(6), 901-910.
- Schaller, M. D. (2001). Paxillin: a focal adhesion-associated adaptor protein. *Oncogene*, *20*(44), 6459-6472. doi: 10.1038/sj.onc.1204786
- Scherr, M., Chaturvedi, A., Battmer, K., Dallmann, I., Schultheis, B., Ganser, A., & Eder, M. (2006). Enhanced sensitivity to inhibition of SHP2, STAT5, and Gab2 expression in chronic myeloid leukemia (CML). *Blood*, *107*(8), 3279-3287. doi: 10.1182/blood-2005-08-3087
- Schindler, T., Bornmann, W., Pellicena, P., Miller, W. T., Clarkson, B., & Kuriyan, J. (2000). Structural mechanism for STI-571 inhibition of abelson tyrosine kinase. *Science*, *289*(5486), 1938-1942.
- Schwab, M. (1998). Amplification of oncogenes in human cancer cells. *Bioessays*, *20*(6), 473-479. doi: 10.1002/(SICI)1521-1878(199806)20:6<473::AID-BIES5>3.0.CO;2-N
- Sha, F., Gencer, E. B., Georgeon, S., Koide, A., Yasui, N., Koide, S., & Hantschel, O. (2013). Dissection of the BCR-ABL signaling network using highly specific monoclonal inhibitors to the SHP2 SH2 domains. *Proc Natl Acad Sci U S A*, *110*(37), 14924-14929. doi: 10.1073/pnas.1303640110
- Shah, N., Nicoll, J., Nagar, B., Gorre, M., Paquette, R., Kuriyan, J., & Sawyers, C. (2002). Multiple BCR-ABL kinase domain mutations confer polyclonal resistance to the tyrosine kinase inhibitor imatinib (STI571) in chronic phase and blast crisis chronic myeloid leukemia. *Cancer Cell*, *2*(2), 117-125.
- Shah, N. P., Tran, C., Lee, F. Y., Chen, P., Norris, D., & Sawyers, C. L. (2004). Overriding imatinib resistance with a novel ABL kinase inhibitor. *Science*, *305*(5682), 399-401.
- Sheng, Z., Ma, L., Sun, J. E., Zhu, L. J., & Green, M. R. (2011). BCR-ABL suppresses autophagy through ATF5-mediated regulation of mTOR transcription. *Blood*, *118*(10), 2840-2848. doi: 10.1182/blood-2010-12-322537
- Shepard, C. R., Kassis, J., Whaley, D. L., Kim, H. G., & Wells, A. (2007). PLC gamma contributes to metastasis of in situ-occurring mammary and prostate tumors. *Oncogene*, *26*(21), 3020-3026. doi: 10.1038/sj.onc.1210115
- Shtivelman, E., Lifshitz, B., Gale, R. P., & Canaani, E. (1985). Fused transcript of abl and bcr genes in chronic myelogenous leukaemia. *Nature*, *315*(6020), 550-554.
- Shuai, K., Halpern, J., ten Hoeve, J., Rao, X., & Sawyers, C. L. (1996). Constitutive activation of STAT5 by the BCR-ABL oncogene in chronic myelogenous leukemia. *Oncogene*, *13*(2), 247-254.
- Shuai, K., Horvath, C. M., Huang, L. H., Qureshi, S. A., Cowburn, D., & Darnell, J. E., Jr. (1994). Interferon activation of the transcription factor Stat91 involves dimerization through SH2-phosphotyrosyl peptide interactions. *Cell*, *76*(5), 821-828.
- Sidhu, S. S., & Koide, S. (2007). Phage display for engineering and analyzing protein interaction interfaces. *Curr Opin Struct Biol*, *17*(4), 481-487. doi: S0959-440X(07)00114-5 [pii] 10.1016/j.sbi.2007.08.007

- Skerra, A. (2000). Engineered protein scaffolds for molecular recognition. *J Mol Recognit*, 13(4), 167-187. doi: 10.1002/1099-1352(200007/08)13:4<167::AID-JMR502>3.0.CO;2-9
- Skerra, A. (2007). Alternative non-antibody scaffolds for molecular recognition. *Curr Opin Biotechnol*, 18(4), 295-304. doi: 10.1016/j.copbio.2007.04.010
- Skorski, T. (2002). Oncogenic tyrosine kinases and the DNA-damage response. *Nat Rev Cancer*, 2(5), 351-360. doi: 10.1038/nrc799
- Skorski, T., Bellacosa, A., Nieborowska-Skorska, M., Majewski, M., Martinez, R., Choi, J. K., . . . Calabretta, B. (1997). Transformation of hematopoietic cells by BCR/ABL requires activation of a PI-3k/Akt-dependent pathway. *EMBO J*, 16(20), 6151-6161. doi: 10.1093/emboj/16.20.6151
- Smith, J. M., & Mayer, B. J. (2002). Abl: mechanisms of regulation and activation. *Front Biosci*, 7, d31-42.
- Songyang, Z., Shoelson, S. E., McGlade, J., Olivier, P., Pawson, T., Bustelo, X. R., . . . et al. (1994). Specific motifs recognized by the SH2 domains of Csk, 3BP2, fps/fes, GRB-2, HCP, SHC, Syk, and Vav. *Mol Cell Biol*, 14(4), 2777-2785.
- Stelman, L. S., Pohnert, S. C., Shelton, J. G., Franklin, R. A., Bertrand, F. E., & McCubrey, J. A. (2004). JAK/STAT, Raf/MEK/ERK, PI3K/Akt and BCR-ABL in cell cycle progression and leukemogenesis. *Leukemia*, 18(2), 189-218.
- Stommel, J. M., Kimmelman, A. C., Ying, H., Nabioullin, R., Ponugoti, A. H., Wiedemeyer, R., . . . DePinho, R. A. (2007). Coactivation of receptor tyrosine kinases affects the response of tumor cells to targeted therapies. *Science*, 318(5848), 287-290. doi: 10.1126/science.1142946
- Suh, P. G., Park, J. I., Manzoli, L., Cocco, L., Peak, J. C., Katan, M., . . . Ryu, S. H. (2008). Multiple roles of phosphoinositide-specific phospholipase C isozymes. *BMB Rep*, 41(6), 415-434.
- Superti-Furga, G., & Courtneidge, S. A. (1995). Structure-function relationships in Src family and related protein tyrosine kinases. *Bioessays*, 17, 321-330.
- Superti-Furga, G., & Gonfloni, S. (1997). A crystal milestone: the structure of regulated Src. *Bioessays*, 19(6), 447-450.
- Taagepera, S., McDonald, D., Loeb, J. E., Whitaker, L. L., McElroy, A. K., Wang, J. Y., & Hope, T. J. (1998). Nuclear-cytoplasmic shuttling of C-ABL tyrosine kinase. *Proc Natl Acad Sci U S A*, 95(13), 7457-7462.
- Tangri, S., LiCalsi, C., Sidney, J., & Sette, A. (2002). Rationally engineered proteins or antibodies with absent or reduced immunogenicity. *Curr Med Chem*, 9(24), 2191-2199.
- Tartaglia, M., & Gelb, B. D. (2005). Germ-line and somatic PTPN11 mutations in human disease. *Eur J Med Genet*, 48(2), 81-96. doi: 10.1016/j.ejmg.2005.03.001
- Tartaglia, M., Mehler, E. L., Goldberg, R., Zampino, G., Brunner, H. G., Kremer, H., . . . Gelb, B. D. (2001). Mutations in PTPN11, encoding the protein tyrosine phosphatase SHP-2, cause Noonan syndrome. *Nat Genet*, 29(4), 465-468. doi: 10.1038/ng772
- Tartaglia, M., Niemeyer, C. M., Fragale, A., Song, X., Buechner, J., Jung, A., . . . Gelb, B. D. (2003). Somatic mutations in PTPN11 in juvenile myelomonocytic leukemia, myelodysplastic syndromes and acute myeloid leukemia. *Nat Genet*, 34(2), 148-150. doi: 10.1038/ng1156
- Teschendorf, C., Warrington, K. H., Jr., Siemann, D. W., & Muzyczka, N. (2002). Comparison of the EF-1 alpha and the CMV promoter for engineering

- stable tumor cell lines using recombinant adeno-associated virus. *Anticancer Res*, 22(6A), 3325-3330.
- Timmerman, I., Hoogenboezem, M., Bennett, A. M., Geerts, D., Hordijk, P. L., & van Buul, J. D. (2012). The tyrosine phosphatase SHP2 regulates recovery of endothelial adherens junctions through control of beta-catenin phosphorylation. *Mol Biol Cell*, 23(21), 4212-4225. doi: 10.1091/mbc.E12-01-0038
- Timsah, Z., Ahmed, Z., Lin, C. C., Melo, F. A., Stagg, L. J., Leonard, P. G., . . . Ladbury, J. E. (2014). Competition between Grb2 and Plcgamma1 for FGFR2 regulates basal phospholipase activity and invasion. *Nat Struct Mol Biol*, 21(2), 180-188. doi: 10.1038/nsmb.2752
- Tokarski, J. S., Newitt, J. A., Chang, C. Y., Cheng, J. D., Wittekind, M., Kiefer, S. E., . . . Klei, H. E. (2006). The structure of Dasatinib (BMS-354825) bound to activated ABL kinase domain elucidates its inhibitory activity against imatinib-resistant ABL mutants. *Cancer Res*, 66(11), 5790-5797.
- Tolcher, A. W., Sweeney, C. J., Papadopoulos, K., Patnaik, A., Chiorean, E. G., Mita, A. C., . . . Mita, M. (2011). Phase I and pharmacokinetic study of CT-322 (BMS-844203), a targeted Adnectin inhibitor of VEGFR-2 based on a domain of human fibronectin. *Clin Cancer Res*, 17(2), 363-371. doi: 10.1158/1078-0432.CCR-10-1411
- Turner, C. E. (2000). Paxillin interactions. *J Cell Sci*, 113 Pt 23, 4139-4140.
- Uemura, N., Salgia, R., Li, J. L., Pisick, E., Sattler, M., & Griffin, J. D. (1997). The BCR/ABL oncogene alters interaction of the adapter proteins CRKL and CRK with cellular proteins. *Leukemia*, 11(3), 376-385.
- Valius, M., Bazenet, C., & Kazlauskas, A. (1993). Tyrosines 1021 and 1009 are phosphorylation sites in the carboxy terminus of the platelet-derived growth factor receptor beta subunit and are required for binding of phospholipase C gamma and a 64-kilodalton protein, respectively. *Mol Cell Biol*, 13(1), 133-143.
- Van Etten, R. A. (1999). Cycling, stressed-out and nervous: cellular functions of c-Abl. *Trends Cell Biol*, 9(5), 179-186.
- von Bubnoff, N., Schneller, F., Peschel, C., & Duyster, J. (2002). BCR-ABL gene mutations in relation to clinical resistance of Philadelphia-chromosome-positive leukaemia to STI571: a prospective study. *Lancet*, 359(9305), 487-491. doi: 10.1016/S0140-6736(02)07679-1
- Wang, D., Feng, J., Wen, R., Marine, J. C., Sangster, M. Y., Parganas, E., . . . Ihle, J. N. (2000). Phospholipase Cgamma2 is essential in the functions of B cell and several Fc receptors. *Immunity*, 13(1), 25-35.
- Warsch, W., Kollmann, K., Eckelhart, E., Fajmann, S., Cerny-Reiterer, S., Hölbl, A., . . . Sexl, V. (2011). High STAT5 levels mediate imatinib resistance and indicate disease progression in chronic myeloid leukemia. *Blood*. doi: 10.1182/blood-2009-10-248211
- Weiner, L. M., Surana, R., & Wang, S. (2010). Monoclonal antibodies: versatile platforms for cancer immunotherapy. *Nat Rev Immunol*, 10(5), 317-327. doi: 10.1038/nri2744
- Weisberg, E., Manley, P., Mestan, J., Cowan-Jacob, S., Ray, A., & Griffin, J. D. (2006). AMN107 (nilotinib): a novel and selective inhibitor of BCR-ABL. *Br J Cancer*, 94(12), 1765-1769.

- Weisberg, E., Manley, P. W., Breitenstein, W., Bruggen, J., Cowan-Jacob, S. W., Ray, A., . . . Griffin, J. D. (2005). Characterization of AMN107, a selective inhibitor of native and mutant Bcr-Abl. *Cancer Cell*, 7(2), 129-141. doi: 10.1016/j.ccr.2005.01.007
- Weisberg, E., Manley, P. W., Cowan-Jacob, S. W., Hochhaus, A., & Griffin, J. D. (2007). Second generation inhibitors of BCR-ABL for the treatment of imatinib-resistant chronic myeloid leukaemia. *Nat Rev Cancer*, 7(5), 345-356.
- Wheadon, H., Paling, N. R., & Welham, M. J. (2002). Molecular interactions of SHP1 and SHP2 in IL-3-signalling. *Cell Signal*, 14(3), 219-229.
- Wiznerowicz, M., & Trono, D. (2003). Conditional suppression of cellular genes: lentivirus vector-mediated drug-inducible RNA interference. *J Virol*, 77(16), 8957-8961.
- Wöhrle, F. U., Daly, R. J., & Brummer, T. (2009). Function, regulation and pathological roles of the Gab/DOS docking proteins. *Cell Commun Signal*, 7, 22. doi: 10.1186/1478-811X-7-22
- Wohrle, F. U., Halbach, S., Aumann, K., Schwemmers, S., Braun, S., Auburger, P., . . . Brummer, T. (2013). Gab2 signaling in chronic myeloid leukemia cells confers resistance to multiple Bcr-Abl inhibitors. *Leukemia*, 27(1), 118-129. doi: 10.1038/leu.2012.222
- Wojcik, J., Hantschel, O., Grebien, F., Kaupe, I., Bennett, K. L., Barkinge, J., . . . Koide, S. (2010). A potent and highly specific FN3 monobody inhibitor of the Abl SH2 domain. *Nat Struct Mol Biol*, 17(4), 519-527. doi: 10.1038/nsmb.1793
- Wong, S., & Witte, O. N. (2004). The BCR-ABL Story: Bench to Bedside and Back. *Annu Rev Immunol*, 22, 247-306.
- Wood, A. J. (2006). A proposal for radical changes in the drug-approval process. *N Engl J Med*, 355(6), 618-623. doi: 10.1056/NEJMs055203
- Wu, J., Meng, F., Kong, L. Y., Peng, Z., Ying, Y., Bornmann, W. G., . . . Donato, N. J. (2008). Association between imatinib-resistant BCR-ABL mutation-negative leukemia and persistent activation of LYN kinase. *J Natl Cancer Inst*, 100(13), 926-939. doi: djn188 [pii]  
10.1093/jnci/djn188
- Wurch, T., Pierre, A., & Depil, S. (2012). Novel protein scaffolds as emerging therapeutic proteins: from discovery to clinical proof-of-concept. *Trends Biotechnol*, 30(11), 575-582. doi: 10.1016/j.tibtech.2012.07.006
- Xie, S., Lin, H., Sun, T., & Arlinghaus, R. B. (2002). Jak2 is involved in c-Myc induction by Bcr-Abl. *Oncogene*, 21(47), 7137-7146. doi: 10.1038/sj.onc.1205942
- Yamada, N., Makino, Y., Clark, R. A., Pearson, D. W., Mattei, M. G., Guenet, J. L., . . . et al. (1994). Human inositol 1,4,5-trisphosphate type-1 receptor, InsP3R1: structure, function, regulation of expression and chromosomal localization. *Biochem J*, 302 ( Pt 3), 781-790.
- Yasui, N., Findlay, G. M., Gish, G. D., Hsiung, M. S., Huang, J., Tucholska, M., . . . Koide, S. (2014). Directed network wiring identifies a key protein interaction in embryonic stem cell differentiation. *Mol Cell*, 54(6), 1034-1041. doi: 10.1016/j.molcel.2014.05.002
- Ye, D., Wolff, N., Li, L., Zhang, S., & Ilaria, R. L., Jr. (2006). STAT5 signaling is required for the efficient induction and maintenance of CML in mice. *Blood*, 107(12), 4917-4925.



- Young, M. A., Gonfloni, S., Superti-Furga, G., Roux, B., & Kuriyan, J. (2001). Dynamic coupling between the SH2 and SH3 domains of c-Src and Hck underlies their inactivation by C-terminal tyrosine phosphorylation. *Cell*, *105*(1), 115-126.
- Yu, H., Chen, J. K., Feng, S., Dalgarno, D. C., Brauer, A. W., & Schreiber, S. L. (1994). Structural basis for the binding of proline-rich peptides to SH3 domains. *Cell*, *76*(5), 933-945.
- Yu, W. M., Hawley, T. S., Hawley, R. G., & Qu, C. K. (2002). Role of the docking protein Gab2 in beta(1)-integrin signaling pathway-mediated hematopoietic cell adhesion and migration. *Blood*, *99*(7), 2351-2359.
- Zhang, S. Q., Yang, W., Kontaridis, M. I., Bivona, T. G., Wen, G., Araki, T., . . . Neel, B. G. (2004). Shp2 regulates SRC family kinase activity and Ras/Erk activation by controlling Csk recruitment. *Mol Cell*, *13*(3), 341-355.
- Zhang, W., & Liu, H. T. (2002). MAPK signal pathways in the regulation of cell proliferation in mammalian cells. *Cell Res*, *12*(1), 9-18. doi: 10.1038/sj.cr.7290105
- Zhao, X., Ghaffari, S., Lodish, H., Malashkevich, V. N., & Kim, P. S. (2002). Structure of the Bcr-Abl oncoprotein oligomerization domain. *Nat Struct Biol*, *7*, 117-120.
- Zheng, H., Alter, S., & Qu, C. K. (2009). SHP-2 tyrosine phosphatase in human diseases. *Int J Clin Exp Med*, *2*(1), 17-25.
- Zhou, X., & Agazie, Y. M. (2009). Molecular mechanism for SHP2 in promoting HER2-induced signaling and transformation. *J Biol Chem*, *284*(18), 12226-12234. doi: 10.1074/jbc.M900020200





# Curriculum Vitae

## Emel Başak GENCER AKCOK

*Nationality: Turkish*

*Marital Status: Married*

*Address: Rue de L'Ancienne Douane 2 1003 Lausanne /Switzerland*

*Telephone: +41 78 645 32 07*

*E-mail: ebasakgencer@hotmail.com*

### EDUCATION

---

- 2011 - 2015 :**      **Ph.D.** – Biotechnology and Bioengineering  
Ecole Polytechnique de Lausanne (EPFL) Lausanne,  
SWITZERLAND
- 2008 – 2010 :**      **M.Sc.** - Molecular Biology and Genetics  
Izmir Institute of Technology (IYTE), Izmir, TURKEY
- 2004 – 2008 :**      **B.Sc.** - Biochemistry Majored in Biotechnology  
Ege University, Faculty of Science, Izmir, TURKEY

### PROFESSIONAL SKILLS

---

**Cell culture:** mammalian cell culture, bacterial culture, proliferation assay, Apoptosis detection assay, plasmid transfection, FACS analysis

**Molecular biology:** cloning (conventional and Gateway system), site-directed mutagenesis, sequencing, quantitative PCR

**Biochemistry:** Western Blot, immunoprecipitation, Gel stainings (coomassie and silver staining), tandem affinity purifications from large-scale cell cultures

**Viral work:** retro- and lentivirus production and concentration, P2 work environment, transduction of human cells with virus (generation of stable cell lines)

### PUBLICATIONS

---

- 1) **Sha F\***, **Gencer EB\***, Georgeon S, Koide A, Yasui N, Koide S, Hantschel O. (2013) Dissection of the BCR-ABL signaling network using highly specific antibody inhibitors to the SHP2 SH2 domains. PNAS 110(37):14924-9
- 2) Lamontanara AJ, **Gencer EB**, Kuzyk O, Hantschel O. (2012) Mechanisms of resistance to BCR-ABL and other kinase inhibitors. Biochimica et Biophysica Acta S1570-9639(12)00289-0.
- 3) Camgoz A, **Gencer EB**, Ural AU, Baran Y. (2012) Mechanisms responsible for nilotinib resistance in human chronic myeloid leukemia cells and reversal of resistance, Leukemia and Lymphoma (doi:10.3109/10428194.2012.737919).

- 4) Camgoz A, **Gencer EB**, Ural AU, Avcu F, Baran Y. (2011) Roles of ceramide synthase and ceramide clearance genes in nilotinib-induced cell death in chronic myeloid leukemia cells. *Leukemia and Lymphoma* 52(8):1574-84.
- 5) **Gencer EB**, Ural AU, Avcu F, Baran Y. (2011) A novel mechanism of dasatinib-induced apoptosis in chronic myeloid leukemia; ceramide synthase and ceramide clearance genes. *Annals of Hematology* 90(11):1265-75.

## **LANGUAGES**

---

Turkish (Native), English (Fluent), French (Beginner)

## **COMPUTER SKILLS**

---

Basic Computer (MS Office Applications- Word, Excel, Powerpoint), Illustrator, Photoshop

## **AWARDS**

---

Young Participant Award of 2009 and 2010 by Turkish Society of Hematology

## **SEMINAR PRESENTATIONS**

---

**2009** : FEBS Advanced Course on "Lipid Signalling and Disease", Ortona, ITALY, **(oral presentation)**

**2011** : FEBS/EACR advanced lecture course, Molecular Mechanisms in Signal Transduction and Cancer, Spetses, GREECE, **(poster presentation)**

**2013** : FASEB SRC, Protein Kinases & Protein Phosphorylation, Niagara Falls, USA

**(poster presentation)**

## **RESEARCH EXPERIENCE & PROJECTS**

---

**Ph.D.** : Functional perturbation of the GAB2 Multiprotein complex by High Affinity SH2 Binding Monobodies in Chronic Myeloid Leukemia performed, showed, designed

**M.Sc.** : Increasing Chemosensitivity of Chronic Myeloid Leukemia Cells to Dasatinib by Targeting Bioactive Sphingolipids

## **REFERENCES**

---

Available upon request.